

Article

Effects of Long-Term Successive Rotations, Clear-Cutting and Stand Age of Prince Rupprecht's larch (*Larix principis-rupprechtii* Mayr) on Soil Quality

Kuangji Zhao ^{1,2}, Timothy J. Fahey ², Dong Liang ³, Zhongkui Jia ^{1,*} and Lvyi Ma ^{1,4}

¹ Key Laboratory for Silviculture and Conservation of the Ministry of Education, College of Forestry, Beijing Forestry University, Beijing 100083, China; zhaokuangji@gmail.com (K.Z.); maluyi@bjfu.edu.cn (L.M.)

² Department of Natural Resources, Cornell University, New York, NY 14853, USA; tjf5@cornell.edu

³ Beijing Hangtian Wanyuan Landscape Environment Greening Engineering Co., Ltd., Beijing 100076, China; deep_spring@163.com

⁴ National Energy R&D Center for Non-Food Biomass, Beijing Forestry University, Beijing 100083, China

* Correspondence: jiazk@bjfu.edu.cn

Received: 5 August 2019; Accepted: 8 October 2019; Published: 22 October 2019

Abstract: A decline in soil quality is a major factor contributing to the degradation of forest ecological function. Vegetation plays a vital role in maintaining soil quality; however, the influence of plantation length on soil quality remains unclear. In this study, we collected soil samples in Northern China using a space-for-time substitution method. Soil were collected from control grassland; a clear-cutting site; 16-year-old (young, first, and second generation), 28-year-old (immature, first, and second generation), and 44-year-old (mature, first generation) *Larix principis-rupprechtii* Mayr stands in May, July, and September 2016. We measured soil physical and chemical properties, microbial communities, and enzymatic activities. We selected soil bulk density, non-capillary porosity, volume humidity, soil organic carbon and activity of polyphenol oxidase to calculate a soil quality index (SQI) for each site. Our data indicated that clear-cutting greatly decreased soil quality of *Larix principis-rupprechtii* forests but returning the harvesting residues to the forest floor could reduce the negative impact of clear-cutting on soil quality. The soil quality improved significantly by prolonging the cultivation cycle and it took about 39 years for the first-generation forest to restore soil quality to the level of the control plot. Our study confirms that SQI provides a comprehensive measurement of soil quality with the identification of a minimum data set. Comparing SQI with other soil quality indicators would help us to optimize the method for assessing soil quality.

Keywords: soil quality; successive planting; generation; stand age; clear-cutting; *Larix principis-rupprechtii* Mayr

1. Introduction

Soil degradation is a global problem in the 21st century [1]. Declining soil quality leads to the disruption of normal ecosystem functions and a reduction in ecosystem services [2]. From 1950 to 2010, soil ecosystem services were degraded by 60% [3], and accelerated soil degradation was reported to globally affect around 33% of the earth's land surface [4]. One potential cause of soil degradation is plantation forestry since repeated harvest and successive replanting can result in the depletion of soil nutrients [5,6]. The high nutrient demands of some tree species [7,8] may eventually lead to a decrease in soil quality [9]. Therefore, to maintain the productivity of forests, urgent action is needed to assess the impact of successive cultivation of timber forests on soil quality.

The selection of soil quality indicators should be based on the comprehensive evaluation of soil functions and ecological services [10]. Some studies have evaluated soil quality with soil chemistry [11–13], in particular, soil organic carbon (SOC) and nitrogen content [14]. Some other works have assessed soil quality only in terms of biological properties, such as microarthropod communities, without regarding chemical or physical properties or both [15–17]. These studies only reflect the limited aspects of soil quality. Ideally, soil quality indicators should take physical properties, chemical properties, biological communities, enzyme activities, and the interactions among these indicators into account [18]. A more comprehensive and easy-to-understand soil quality index (SQI) has been proposed for quantifying the combined physical, chemical, and biological properties of soil and their response to soil management practices [19].

Soil quality and forest stand management can affect each other [20]. The impact of forest growth on soil quality has been extensively studied in fast-growing plantation forests [6]. However, soil quality changes in successive rotations have been rarely investigated in timber forests with long growth cycles. The contribution of soil quality to ecosystem services is closely linked to forest management activities. In some situations, forest management results in complex interactive effects on soil properties [21]. Many works have evaluated the effects of clear-cutting on soil quality [22–25]; however, few studies have reported the SQI approach by considering forest stand growth (stand age and forest generation), human management (afforestation and clear-cutting), afforestation-stand growth-timber harvest, continuous variation of forest land.

Larix principis-rupprechtii is one of the main afforestation species in China due to its wide ecological plasticity, rapid growth, high-quality wood products, and strong stress resistance. We explored the application of the SQI approach to evaluate the effects of forest plantation management on soil health in Northern China. We quantified a suite of soil properties and evaluated the SQI of a reference grassland and a series of *Larix principis-rupprechtii* forest plantations, including first-generation 16-year-old (young), 28-year-old (immature) and 44-year-old (mature) forests, a clear-cutting site, and second-generation 16-year-old (young) and 28-year-old (immature) forests. The changes in soil quality were investigated by measuring the physical and chemical properties, the microbial communities, and the extracellular enzyme activity of soil. We aimed to advise forest management planning to maintain soil health and sustainability. We expected (1) that the soil quality would improve with an increase in stand age; (2) that the soil quality would decline by the change of successive forest generations; and (3) that clear-cutting would decrease soil quality.

2. Materials and Methods

2.1. Study Area

This experiment was carried out in Saihanba National Forest Park (SNFP), Weichang Manchu and Mongolian Autonomous County, Hebei Province, China (E 116°51′–117°39′, N 42°02′–42°36′). The elevation of the study sites was from 1600 to 1800 m. The area has a semi-arid monsoon climate and is located in the cool temperate zone with a mean annual temperature of $-1.5\text{ }^{\circ}\text{C}$, a maximum annual temperature of $29.7\text{ }^{\circ}\text{C}$, and a minimum annual temperature of $-38.7\text{ }^{\circ}\text{C}$. The mean annual rainfall is 433 mm, concentrated from June to August. Study sites are characterized as mainly gray forest soils, predominantly consisting of sand, since about 65% of the soils are sand silt. The carbon (C): nitrogen (N) ratio is 8.9 ± 0.3 , and the soil parent materials are eluvium, saprolite, and alluvium; the thickness of the surface organic layer of each stand was about 3–8 cm [26]. *Larix principis-rupprechtii* is the dominant tree species in the coniferous forest belt of Northern China [27], and the plantation area accounts for 77.1% of the total plantation area in SNFP.

2.2. Experimental Design and Sampling

The experimental site was originally native grassland dominated by *Maianthemum bifolium* and *Saussurea japonica*. A reference grassland plot (abbreviated as CG) represented the sites on

which the forest plantations of *Larix principis* were established. The forest plantations included the first-generation 16-year-old (young, abbreviated as 1G-16YR), 28-year-old (immature, abbreviated as 1G-28YR), and 44-year-old (mature, abbreviated as 1G-44YR) stands; the second-generation 16-year-old (young, abbreviated as 2G-16YR) and 28-year-old (immature, abbreviated as 2G-28YR) stands; and a clear-cutting site (CC) where a mature, i.e., 44-year old, first-generation plantation was harvested in 45 years. The CG plot had never been planted with any trees and had no human disturbance. The 2G-16YR and 2G-28YR were plots where 3-year-old *Larix principis-rupprechtii* seedlings were planted after clear-cutting of mature plantations 13 and 25 years earlier respectively. The woodland was plowed the year before afforestation; in the year of afforestation, the woodland was excavated by a tree planting digger, and the seedlings were planted. The first five years after afforestation, workers used a mower to cut grass in the woodlands. After clear-cutting, we also employed a tracked grab wood machine to remove the timber from the woodland. Unfortunately, no 44-year-old second-generation stands were available in the SNFP. All the sites used in the present study were located in similar soil and landscape.

In May 2015, five 20 m × 20 m quadrats were established in a grid within each of the seven types of plots, totaling 35 plots. More information is provided in Table 1.

Table 1. Stand characteristics of *Larix principis-rupprechtii* plantations of seven types of plots.

| Samples | Aspect | Angle of the Slope (°) | Slope Position | Canopy Density | Age (YR) | Altitude (m) | Mean DBH (cm) | Mean Tree Height (m) |
|---------------------------|--------|------------------------|----------------|----------------|----------|--------------|---------------|----------------------|
| Control grassland | North | 1° | Above | - | - | 1657.50 | - | - |
| 1G-16YR | South | 3° | Below | 0.80 | 16 | 1666.20 | 8.80 | 9.40 |
| 1G-28YR | - | - | - | 0.50 | 28 | 1702.40 | 23.90 | 15.68 |
| 1G-44YR | North | 5° | Middle | 0.70 | 44 | 1712.00 | 35.50 | 20.50 |
| Clear-cutting forest land | - | - | - | - | - | 1672.00 | - | - |
| 2G-16YR | - | - | - | 0.90 | 16 | 1696.00 | 7.70 | 6.90 |
| 2G-28YR | South | 2° | Middle | 0.90 | 28 | 1692.20 | 11.00 | 9.60 |

Notes: DBH indicates the diameter at breast height.

In May, July, and September 2016, the soils from the top 0–10 cm, 10–20cm and 20–30 cm layers were collected from the study sites in one day. Ten soil cores were collected at randomly selected points from each plot with a 3.6-cm-diameter soil auger, and the samples from different depths at the same location were mixed together as a composite sample, thereby totaling ten composite samples. Stones and roots were removed from the soil samples by hand, and the samples were sieved through 2-mm sieves. Five soil samples were stored at 4 °C to analyze the soil microbial biomass and enzyme activity, and the remaining samples were oven-dried at 105 °C to reach a constant dry weight for chemical analysis.

2.3. Physical Analysis

Soil bulk density (SBD) was determined by the intact core method [28,29], and soil capillary porosity (CP) was subsequently calculated using Equation (1) [30]. Soil non-capillary porosity (NCP) was also assessed by employing Equation (2) [31]. Moreover, Equation (3) was utilized to quantify total soil porosity (TP) based on NCP and CP [32], and soil ventilation (SV) was measured by Equation (4); Equation (5) estimated volume humidity (VH). Soil water content (SWC) and saturated soil water content (SSWC) were also measured according to the gravimetric method [33]. Capillary water capacity (CWC) was characterized by the method of Rowell [34], and field capacity (FC) was analyzed using a pressure plate apparatus [35,36].

$$CP = CWC \times \frac{SBD}{v} \times 100 \quad (1)$$

$$NCP = \frac{SSWC - CWC}{SBD} \quad (2)$$

$$TP = NCP + CP \quad (3)$$

$$SV = VH - TP \quad (4)$$

$$VH = SWC \times SBD \quad (5)$$

where CP (%), CWC (%), SBD (g cm^{-3}), V (cm^3), and NCP (%) represent capillary porosity, capillary water capacity, the soil bulk density, the volume of the soil core, and non-capillary porosity, respectively; SSWC (%), TP (%), SV (%), VH (%), and SWC (%) stand for the saturated soil water content, the soil total porosity, the soil ventilation, volume humidity, and the soil water content, respectively.

2.4. Chemical Analysis

The soil pH was measured in deionized water by a Delta320 pH-meter using a slurry having a soil to water ratio of 2:5 (Mettler-Toledo Instruments, Shanghai Co., Ltd., Shanghai, China). The SOC was also evaluated using Walkley and Black wet oxidation method as outlined in Bao's work [37]. Moreover, the total nitrogen (TN) of the soil was digested by concentrated sulfuric acid (98% H_2SO_4), and the available phosphorus (AP) extracted from soil by employing hydrochloric acid-ammonium fluoride ($\text{HCl} + \text{NH}_4\text{F}$) was determined by AA3 HR AutoAnalyzer (Seal Analytical Ltd., Southampton, UK). The total potassium (TK) of the soil was extracted using concentrated sulfuric acid (98% H_2SO_4) and measured by Lumina3300 (Aurora Biomed Inc., Vancouver, BC, Canada).

2.5. Microbial Properties

Soil samples for soil microorganism analysis were passed through a 1-mm sieve and stored in a ziplock bag at 4 °C. The soil microbes were assessed using dilution plate counting [38], and five replicates were performed on each sample. Bacteria were cultured in a medium of beef-extracted peptone agar. Actinomycetes and fungi were respectively cultured using a modified Gaussian medium and Martin's agar medium; the culture temperature was 28 °C. The bacteria and actinomycetes were cultured for 3–5 days and the fungi were cultured for 5–7 days.

2.6. Soil Enzyme Activity

The activity of catalase and polyphenol oxidase (PPO) activities were measured by potassium permanganate titration and pyrogallol colorimetry according to Waldrop et al. [39]. Soil urease activity was also assessed by sodium phenol colorimetry according to Kandeler and Gerber [40].

2.7. Statistical Analysis

The SQI was calculated according to Andrews and Carroll [18], and three steps were involved in the elaboration of the quality index: (1) the identification of a minimum data set (MDS), (2) the assignment of a score to each indicator by linear scoring functions, and (3) the data integration into an index.

Three steps were used to identify the MDS. (1) Data screening: one-way analysis of variance (ANOVA) was performed on the physical, chemical, and biological properties and the enzyme activities of the soil. Then, the variables exhibiting significant differences among treatments ($p < 0.05$) were chosen for the next step. (2) Selection of representative variables: the principal component analysis (PCA, see Supplementary Material, Table S1) was performed on the variables chosen from step (1). Only the principal component (PC) explained greater than 5% and eigenvalues ≥ 1 were examined. Within each PC, only the factors weighted with absolute values within 10% of the highest weight were retained for the MDS. (3) Redundancy reduction: multivariate correlation coefficients were used to determine the strength of the relationships among the variables. Highly correlated variables (correlation coefficient > 0.70) were considered redundant and nominated to be eliminated from the data set. To choose variables within the well-correlated groups, we summed the absolute values of the correlation coefficients for these variables. It was assumed that the variable with the highest correlation sum represents the group best. Any uncorrelated, highly weighted variable was considered important and retained in the MDS.

Linear scoring was applied in this study following the approach of Andrews and Carroll [18]. The linear scoring function (Equation (6)) was used to convert the measured values to the scored values as follows [41]:

$$S_{ij} = \frac{V_{ij} - V_{imin}}{V_{imax} - V_{imin}} \tag{6}$$

where S_{ij} is the score of soil variable i of sample j , and V_{ij} represents the observed variable value of sample j ; V_{imax} and V_{imin} stand for the highest value of variable i and the lowest value of variable i , respectively. The scores of the indicators in the MDS (Table 2) were integrated into an SQI (Equation (7)) according to the work of Andrews et al. [42], as follows:

$$SQI = \sum_{i=1}^n (S_i \times Q(xi)) \tag{7}$$

where S_i is the score assigned to indicator i , and $Q(xi)$ denotes the scoring result of each soil quality factor; n represents the number of indicators included in the MDS.

Table 2. Soil quality indicator scores (mean \pm standard error) for the soil samples taken from the *Larix principis-rupprechtii* plantations.

| | CG | 1G-16YR | 1G-28YR | 1G-44YR | CC | 2G-16YR | 2G-28YR |
|-----|-------------------------------|-------------------------------|-------------------------------|------------------------------|-------------------------------|------------------------------|-------------------------------|
| SBD | 0.76 \pm 0.04 ^a | 0.29 \pm 0.04 ^c | 0.36 \pm 0.04 ^{bc} | 0.49 \pm 0.01 ^b | 0.48 \pm 0.04 ^b | 0.27 \pm 0.06 ^c | 0.28 \pm 0.04 ^c |
| NCP | 0.48 \pm 0.02 ^b | 0.25 \pm 0.11 ^b | 0.33 \pm 0.07 ^b | 0.75 \pm 0.11 ^a | 0.42 \pm 0.03 ^b | 0.37 \pm 0.06 ^b | 0.44 \pm 0.13 ^b |
| VH | 0.46 \pm 0.05 ^{cd} | 0.33 \pm 0.09 ^d | 0.59 \pm 0.03 ^{bc} | 0.67 \pm 0.03 ^b | 0.90 \pm 0.04 ^a | 0.33 \pm 0.03 ^d | 0.43 \pm 0.05 ^d |
| SOC | 0.24 \pm 0.04 ^c | 0.39 \pm 0.06 ^{bc} | 0.43 \pm 0.04 ^b | 0.71 \pm 0.09 ^a | 0.36 \pm 0.01 ^{bc} | 0.43 \pm 0.02 ^b | 0.47 \pm 0.02 ^b |
| PPO | 0.47 \pm 0.02 ^{bc} | 0.43 \pm 0.06 ^c | 0.58 \pm 0.09 ^{ab} | 0.63 \pm 0.02 ^a | 0.43 \pm 0.01 ^c | 0.25 \pm 0.02 ^d | 0.45 \pm 0.01 ^{bc} |

Notes: SBD: soil bulk density; NCP: non-capillary porosity; VH: volume humidity; SOC: soil organic carbon; and PPO: polyphenol oxidase. In rows, the values with different letters are significantly different ($p < 0.05$).

One-way analysis of variance (ANOVA) was utilized to judge the significant differences among the physical, chemical, and biological properties of the soil, among the enzyme activity of the soil, and among the SQI of these treatments for the seven types of the forest lands. First, Shapiro-Wilk test and Levene test were used to respectively verify the assumptions of the normality and homogeneity of variance of the data on each variable; Duncan test was then used for a multiple comparison analysis. All the statistics calculation was conducted using PASW Statistics 18 (IBM, Armonk, NY, USA) with the level of significance set at $p < 0.05$. A p -value smaller than 0.05 indicates that the possibility of assumption is greater than 95%, and a p -value less than 0.01 in the following denotes that the possibility of assumption is greater than 99%. All the figures were also generated using Origin 8 (Origin Lab, Northampton, MA, USA).

3. Results

3.1. Soil Physical Properties

3.1.1. Soil Bulk Density

As shown in Figure 1, SBD was significantly higher in CG plot (1.39 g cm⁻³) among the seven types of plots. After the initial afforestation, the sample SBD dropped significantly, i.e., the SBD of 1G-16YR was 1.12 g cm⁻³. The SBD of the first-generation forest was enhanced with an increase in stand age. The SBD of the mature forest wood (1.24 g cm⁻³) was also higher than that of the other stands. Moreover, there was no significant difference in SBD before and after clear-cutting. The SBD of the 2G-16YR plot (1.10 g cm⁻³) was significantly lower than that of CC plots. The SBD of the second-generation forest still rose with an increase in stand age, but the SBD of CC was significantly dropped by 11.85% compared to CG. In this study, the difference in the SBD of the soils of the seven types of plots was significant ($p < 0.01$).

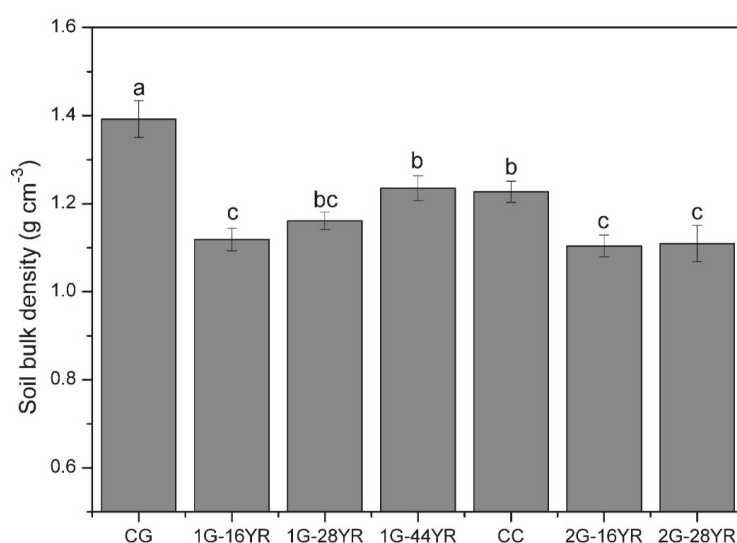


Figure 1. Soil bulk density in the successive *Larix principis-rupprechtii* plantations. CG indicated the control grassland; 1G-16YR indicated the 16-year 1st generation forest; 1G-28YR indicated the 28-year 1st generation forest; 1G-44YR indicated the 44-year 1st generation forest; CC indicated clear-cutting forest; 2G-16YR indicated the 16-year 2nd generation forest, and 2G-28YR indicated the 28-year 2nd generation forest. Soil bulk density (SBD) values with the same letter are not significantly different at $p < 0.05$. Error bars indicate the standard error; $n = 15$.

3.1.2. Soil Porosity

TP and NCP generally improved with a rise in stand age synchronously, and the values (60.73% and 11.99%) in 1G-44YR were higher compared to the other stand types (Figure 2). The TP of 1G-16YR was significantly increased by 9.62% compared with that of CG, but the NCP of 1G-16YR was 20.46% lower than that of CG. The TP and NCP of the samples in the plot were not significantly different before and after the second afforestation ($p > 0.05$). Caused by clear-cutting, NCP fell by 23.61% in the 1G-44YR plot. CP and SV also decreased with the increase of stand age. The values of forest CP (51.72%) and SV (43.61%) appeared in 1G-16YR were higher than those of the other stands. The CP and SV of 1G-16YR were 1.82% and 9.67% higher than that of CG, respectively, whereas the difference was not significant ($p < 0.05$). Also, the CP and SV of 2G-16YR significantly grew respectively by 2.63% and 106.62% compared to that of CC ($p < 0.01$); however, the SV of CC was significantly lower than that of CG by 49.77%. Except for CP ($p = 0.15$), the other soil porosity indicators were significantly different among the seven types of the plots ($p \leq 0.05$).

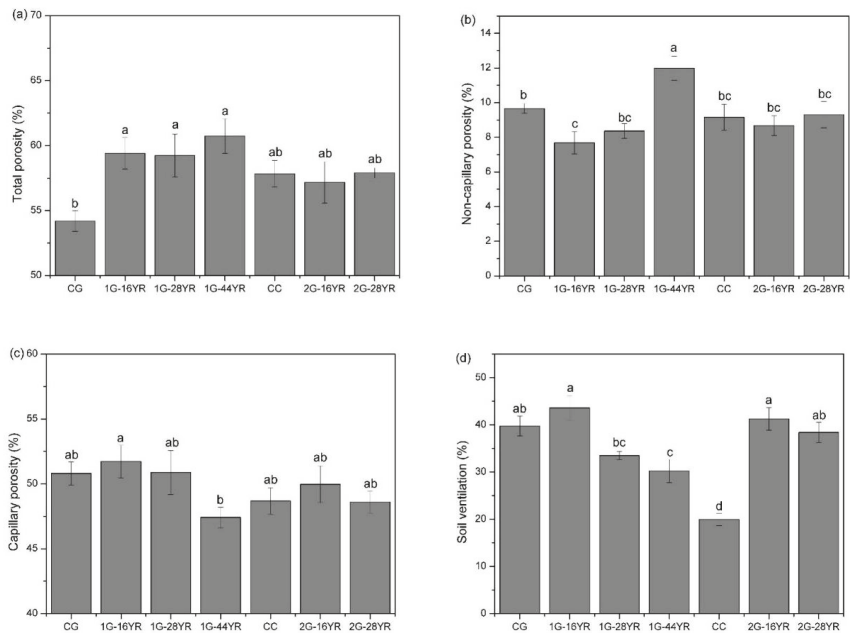


Figure 2. Soil porosity in the successive *Larix principis-rupprechtii* plantations. (a) Total porosity; (b) Non-capillary porosity; (c) Capillary porosity; (d) Soil ventilation. CG indicated the control grassland; 1G-16YR indicated the 16-year 1st generation forest; 1G-28YR indicated the 28-year 1st generation forest; 1G-44YR indicated the 44-year 1st generation forest; CC indicated clear-cutting forest; 2G-16YR indicated the 16-year 2nd generation forest, and 2G-28YR indicated the 28-year 2nd generation forest. Soil porosity values with the same letter are not significantly different at $p < 0.05$. Error bars indicate the standard error; $n = 15$.

3.1.3. Soil Water Content

The trend of SWC was the same as VH trend (Figure 3a,e). As stand age rises, a significant decline was seen in SWC and VH after afforestation, but an opposite trend was noticed after clear-cutting. SWC (30.97%) and VH (29.14%) in the CC plots were significantly higher than those of the other stands. The CWC and FC of the first-generation forest dropped with an increase in stand age. Nevertheless, no significant difference was seen in CWC and FC between the two stand ages of the second-generation forest. The values of CWC (46.39%) and FC (44.62%) appeared in 1G-16YR (Figure 3c,d) were higher compared to the other stand types, and CWC and FC were upgraded either by afforestation or by clear-cutting. The value of SSWC was significantly higher in 1G-16YR (49.97%) than in the CC plots (41.76%, Figure 3b). Compared with CG, SWC and VH significantly rose by 78.83% and 82.96% in the CC plots, respectively. Except for SSWC, the soil moisture indices were significantly different among the seven types of the plots ($p < 0.05$).

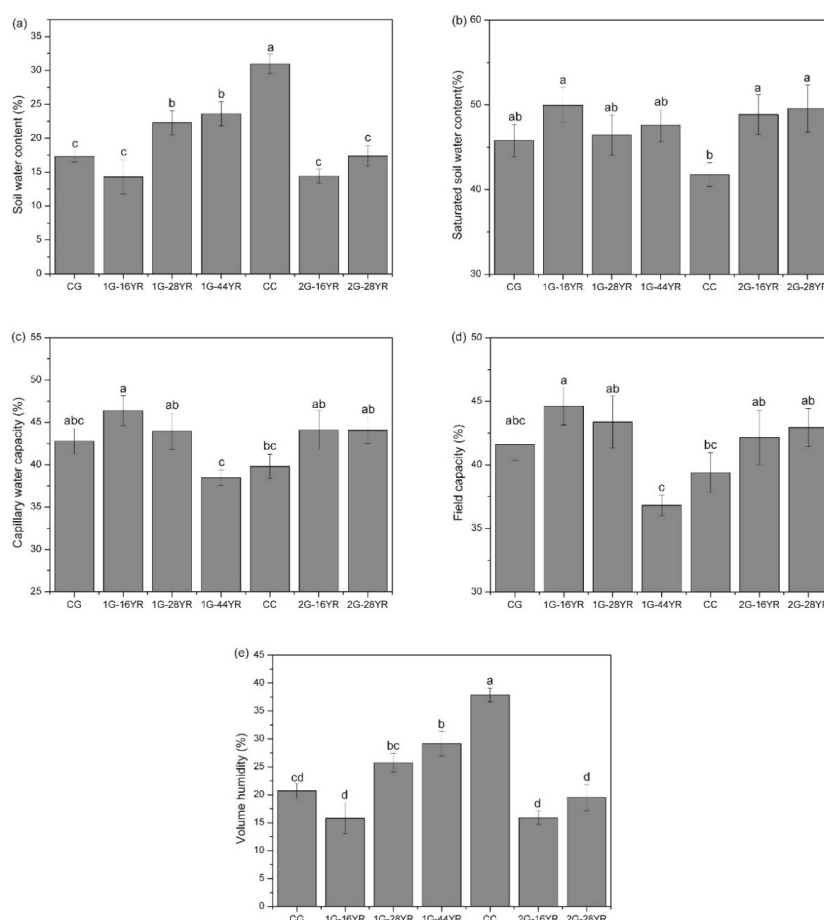


Figure 3. Water in soil in the successive *Larix principis-rupprechtii* plantations. (a) Soil water content; (b) Saturated soil water content; (c) Capillary water capacity; (d) Field capacity; (e) Volume humidity. CG indicated the control grassland; 1G-16YR indicated the 16-year 1st generation forest; 1G-28YR indicated the 28-year 1st generation forest; 1G-44YR indicated the 44-year 1st generation forest; CC indicated clear-cutting forest; 2G-16YR indicated the 16-year 2nd generation forest and 2G-28YR indicated the 28-year 2nd generation forest. Water in soil values with the same letter are not significantly different at $p < 0.05$. Error bars indicate the standard error; $n = 15$.

3.2. Soil Chemical Properties

3.2.1. Soil pH Value

The pH value of the second-generation forest was significantly higher than that of the first-generation forest (Figure 4); the acidity of the soil was lower in the CG plot (6.36), but the acidity of 1G-16YR (5.64) soil was higher compared to the other stand types. The pH value of the first-generation forest increased as the stand age rose, while the second-generation forest showed an opposite trend. The pH of clear-cut land was also reduced by 1.37%. Moreover, the pH of CC was significantly lower (9.59%) than that of CG. The pH difference among the plots was significant ($p < 0.01$).

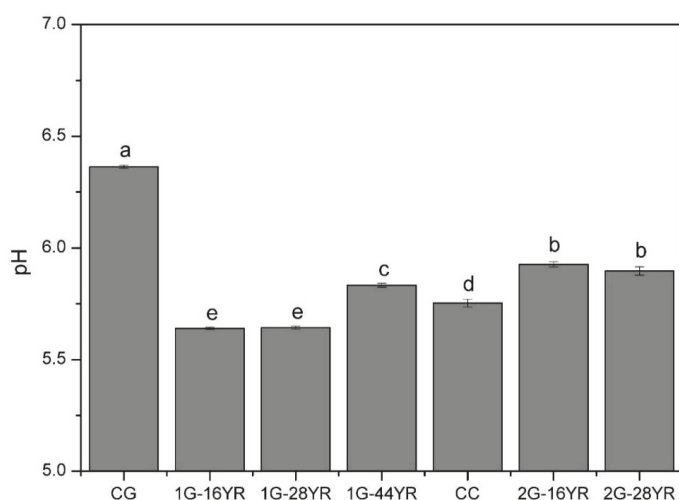


Figure 4. Soil pH value in the successive *Larix principis-rupprechtii* plantations. CG indicated the control grassland; 1G-16YR indicated the 16-year 1st generation forest; 1G-28YR indicated the 28-year 1st generation forest; 1G-44YR indicated the 44-year 1st generation forest; CC indicated clear-cutting forest; 2G-16YR indicated the 16-year 2nd generation forest and 2G-28YR indicated the 28-year 2nd generation forest. The pH value with the same letter is not significantly different at $p < 0.05$. Error bars indicate the standard error; $n = 15$.

3.2.2. Soil Nutrients

SOC, TN, and TK all were enhanced with an increase in stand age unanimously. After clear-cutting, SOC, TN, and TK were reduced by 44.44%, 29.85%, and 16.31%, respectively. Afforestation reduced TN and TK both in the CG plot and the CC plot but increased SOC. The value of SOC in 1G-44YR (84.27 g kg^{-1}) was significantly higher than that of the other stand types. In addition, the values of TN (3.90 g kg^{-1}) and TK (3.02 g kg^{-1}) of the CG plots were remarkably higher compared to the other stand types (Figure 5). However, the TN and TK values of the CC plot were considerably lower than those of CG plot by 44.97% and 23.65%, respectively. Except for AP, the indicators were markedly different among the seven types of plots ($p < 0.01$).

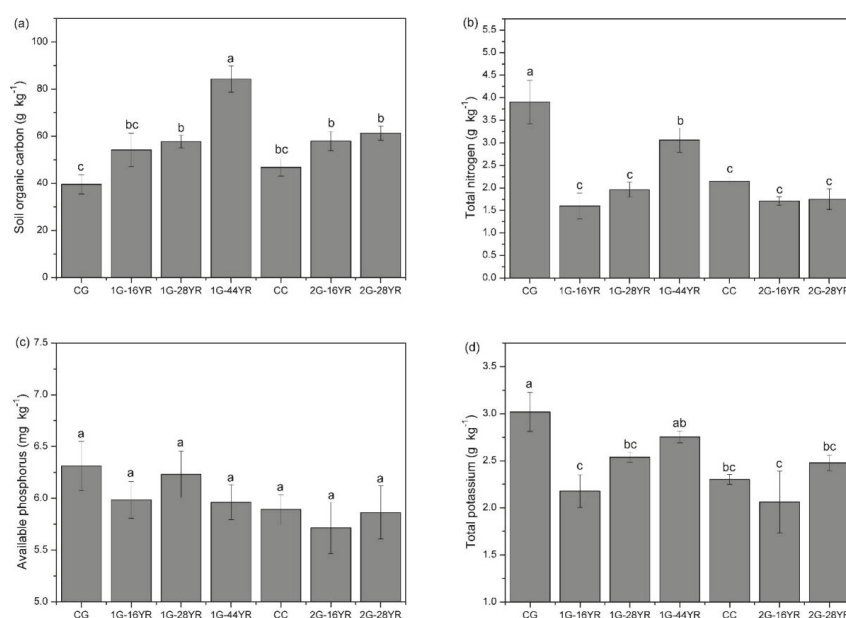


Figure 5. Soil nutrients in the successive *Larix principis-rupprechtii* plantations. (a) Soil organic carbon; (b) Total nitrogen; (c) Available phosphorus; (d) Total potassium. CG indicated the control grassland; 1G-16YR indicated the 16-year 1st generation forest; 1G-28YR indicated the 28-year 1st generation forest; 1G-44YR indicated the 44-year 1st generation forest; CC indicated clear-cutting forest; 2G-16YR indicated the 16-year 2nd generation forest and 2G-28YR indicated the 28-year 2nd generation forest. Soil nutrients with the same letter are not significantly different at $p < 0.05$. Error bars indicate the standard error; $n=15$.

3.3. Soil Biological Properties

3.3.1. Soil Microorganisms

As illustrated in Figure 6, bacteria, actinomycete, and fungi were promoted with the increased stand age. The value of bacteria in 1G-44YR ($60.87 \times 10^6 \text{ g}^{-1}$), the value of actinomycete in 2G-28YR ($11.70 \times 10^6 \text{ g}^{-1}$), and that of fungi in the CG plots ($11.83 \times 10^4 \text{ g}^{-1}$) were higher than their counterparts in the other types of stands. The bacteria of the first-generation forest land were significantly larger than those of the second-generation forest. The value of the bacteria of 1G-16YR was 2.27 times more than that of 2G-16YR, and the bacteria value of 1G-28YR was 1.69 times higher than that of 2G-28YR. Except for fungi ($p = 0.06$), the other indicators were noticeably different among the plots ($p < 0.05$).

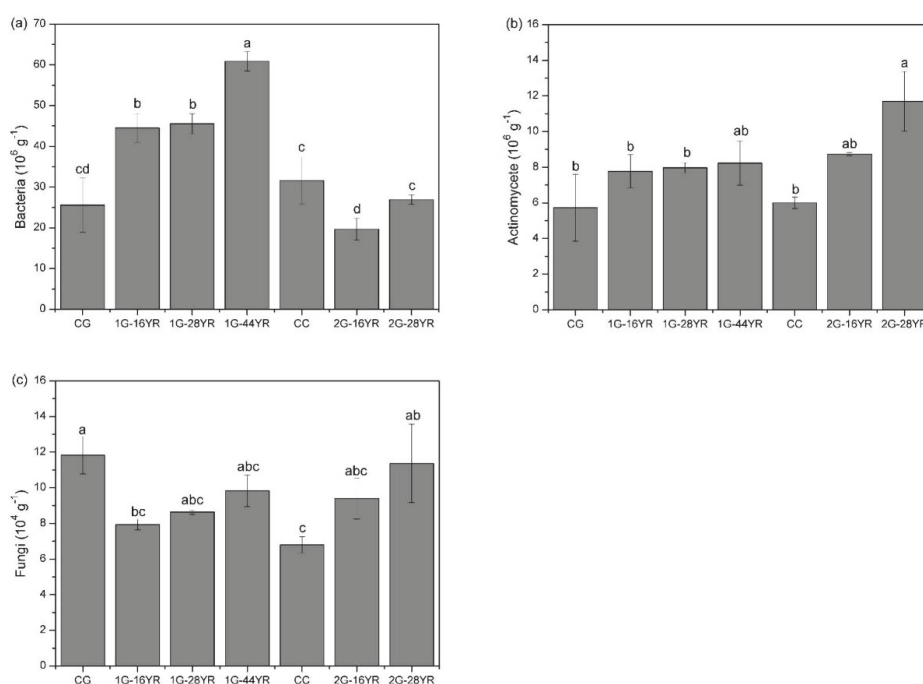


Figure 6. Soil microorganisms in the successive *Larix principis-rupprechtii* plantations. (a) Bacteria; (b) Actinomycete; (c) Fungi. CG indicated the control grassland; 1G-16YR indicated the 16-year 1st generation forest; 1G-28YR indicated the 28-year 1st generation forest; 1G-44YR indicated the 44-year 1st generation forest; CC indicated clear-cutting forest; 2G-16YR indicated the 16-year 2nd generation forest and 2G-28YR indicated the 28-year 2nd generation forest. Soil microorganisms with the same letter are not significantly different at $p < 0.05$. Error bars indicate the standard error; $n = 15$.

3.3.2. Soil Enzyme Activity

The activity of catalase, PPO, and urease was enhanced with the increase of stand age (Figure 7). The catalase value of the CG plot (0.62 mL g^{-1}) and the values of PPO and urease of the 1G-44YR plot (0.44×10^{-2} and 2.67 mg g^{-1}) were higher than those of the other plots. The PPO value of 2G-16YR was significantly decreased by 32.03% compared with that of the CC plot, while the PPO value was considerably reduced by 26.39% due to clear-cutting. Also, clear-cutting markedly dropped urease by 51.94%.

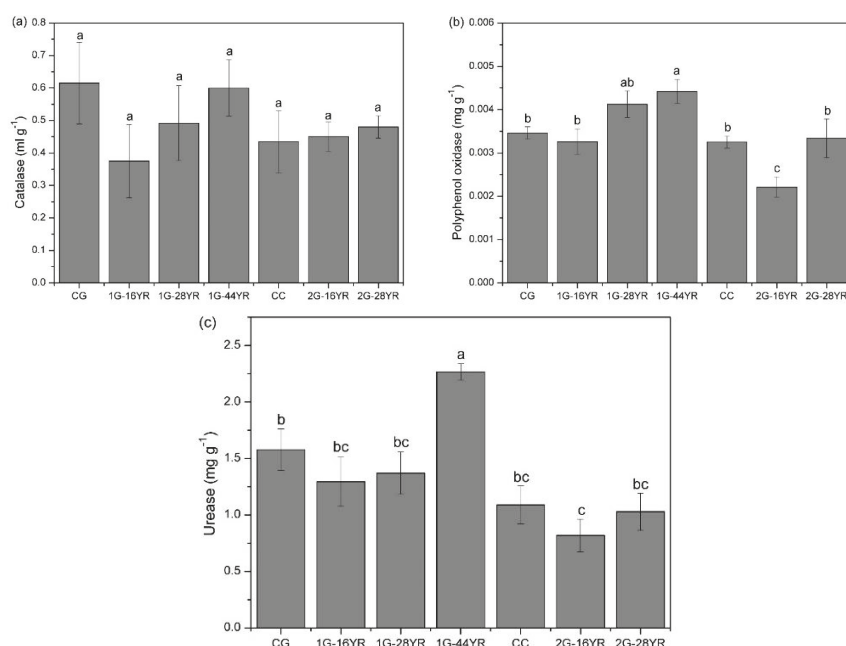


Figure 7. Soil enzyme activities in the successive *Larix principis-rupprechtii* plantations. (a) Catalase; (b) Polyphenol oxidase; (c) Urease. CG indicated the control grassland; 1G-16YR indicated the 16-year 1st generation forest; 1G-28YR indicated the 28-year 1st generation forest; 1G-44YR indicated the 44-year 1st generation forest; CC indicated clear-cutting forest; 2G-16YR indicated the 16-year 2nd generation forest and 2G-28YR indicated the 28-year 2nd generation forest. Soil enzyme activities with the same letter are not significantly different at $p < 0.05$. Error bars indicate the standard error; $n = 15$.

3.4. Soil Quality Index

Soil variables with significant differences among treatments included SBD, TP, NCP, SV, SWC, CWC, FC, VH, pH, SOC, TN, TK, bacteria, actinomycete, PPO, and urease. The first four PC's explained greater than 5% and eigenvalues ≥ 1 . The highly weighted variables under the four PC's were SBD, TN, SV, VH, bacteria, PPO, NCP and SOC (see Supplementary Material, Table S1). As illustrated in Figure 8 and Table S2, 1G-44YR had the greatest soil quality; NCP and SOC were not well correlated with the other variables and retained for the MDS. SBD and TN were remarkably correlated; SBD had a higher correlation sum, so it was retained for the MDS. SV and VH were negatively correlated to each other; VH was retained for the MDS by the higher correlation sum. Bacteria and PPO were noticeably correlated; PPO had a higher correlation sum and was retained for the MDS. The variables selected to remain in MDS are SBD, NCP, VH, SOC, and PPO, which are used to calculate SQI.

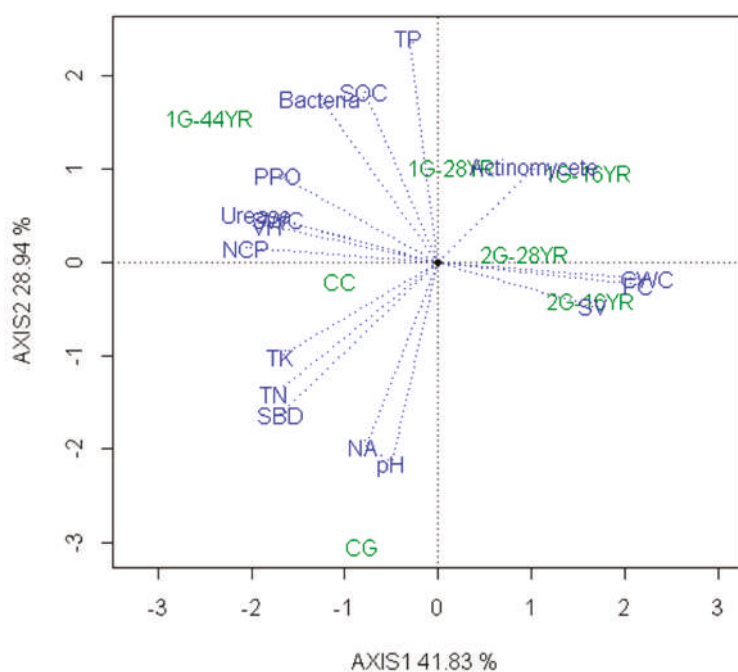


Figure 8. Biplots of soil variables and treatments in PC1 and PC2.

As depicted in Figure 9, the SQI of 1G-44YR (0.66) was significantly larger than that of the other stand types. The SQI of CG (0.47) and that of CC (0.51) were remarkably higher than that of 1G-16YR (0.34) and that of 2G-16YR (0.33) by 38.24% and 54.55%, respectively. After a stand incubation period (compare the 1G-16YR with the 2G-16YR), the SQI was decreased by 2.90%, but the improvement was not significant ($p < 0.05$).

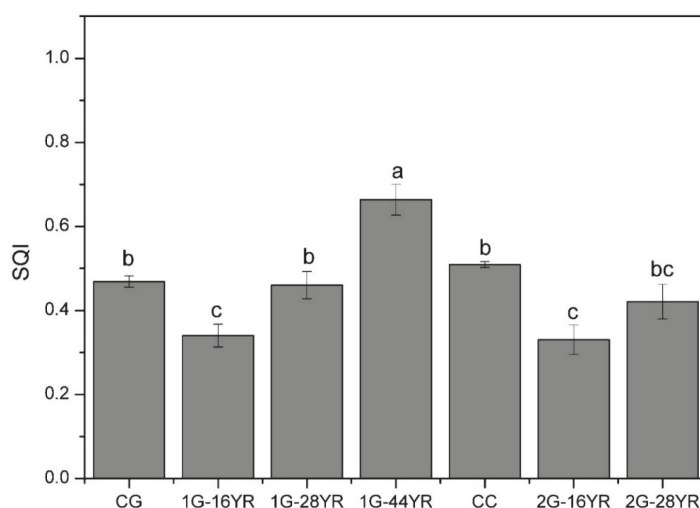


Figure 9. Soil quality index in the successive *Larix principis-rupprechtii* plantations. SQI: soil quality index; CG indicated the control grassland; 1G-16YR indicated the 16-year 1st generation forest; 1G-28YR indicated the 28-year 1st generation forest; 1G-44YR indicated the 44-year 1st generation forest; CC indicated clear-cutting forest; 2G-16YR indicated the 16-year 2nd generation forest and 2G-28YR indicated the 28-year 2nd generation forest. Soil quality indices with the same letter are not significantly different at $p < 0.05$. Error bars indicate the standard error; $n = 15$.

4. Discussion

4.1. Stand Age

Our observations supported our first hypothesis since all the indicators improved with an increase in stand age, except for TP, CP, SV, SSWC, CWC, FC, pH, AP, and catalase. The comprehensive analysis confirmed that the SQI was also significantly increased with an increased stand age. Furthermore, the results of this study are consistent with the work of Lima et al. [43], whereas they are contrary to the results of Zhang et al. [6]; this contrast is attributed to the lower temperature of the studied site, which consequently slowed down the decomposition of soil organic matter. Moreover, tree species are the main factors affecting microbial community activity and changing soil nutrient dynamics [44], and the pine needles of *Larix principis-rupprechtii* returns nutrients to the soil in the form of litter in the non-growth season. The growth rate of *Larix principis-rupprechtii* was slower and the demand for soil nutrients was relatively less. Thus, the cultivation of *Larix principis-rupprechtii* would improve soil quality. This study also stated that the average annual growth of the SQI from 28- to 44-year old was 1.27 times larger than that of the SQI from 16- to 28-year old (Figure 9). The older the forest stand is, the clearer the improvement of the soil quality is. It was speculated that the reason may be as follows: (1) The forest was gradually closed due to the increase of stand age; lower decomposition and soil disturbance reduction were found after the canopy closed [14,45,46]. Also, a high litter mass may contribute to the subsequent increase in SOC stocks in the older stands [47–49]. (2) During the early stages of plant life, nutrient absorption was kept at a high level, whereas litter production was at a low level. However, litter production increased, but nutrient absorption fell as the plant became older [50]. Therefore, extending the cultivation cycle of *Larix principis-rupprechtii* forests is beneficial to improving soil quality.

4.2. Forest Generation

The results also showed that indicators such as SWC, VH, bacteria and PPO dropped by the change of forest generation. According to the comprehensive analysis, increasing forest generation reduced the soil quality in the stand, but the difference was insignificant, which failed to support our second hypothesis. The results of this study are not consistent with the work of Zhang et al. [6] on the soil change of the third and fourth generations of *eucalyptus* forests. It was speculated that Zhang et al. [6] decreased the disturbance of soil afforestation activities by changing the reclamation method the after clear-cutting of the third-generation forest and fertilized forest land to supplement soil nutrients and improve soil quality. In the present study, plowing the forest (creating furrows and ridges) exposed the soil to air during afforestation. The exposure process promoted the loss of mineral components and reduced soil quality. In addition to afforestation activities, clear-cutting also accelerates the decomposition rate of SOC [51,52] and reduces SOC stocks, thereby causing a considerable decline in the soil quality in the forest land [27]. After clear-cutting, the cutting remains were not returned to the forest land, further resulting in a remarkable decrease in the soil quality of the forest land. However, the growth of the first-generation forests for more than 40 years has noticeably enhanced the soil quality. Therefore, an increase in the forest generation did not significantly reduce the soil quality of the forest land. Hence, the main reason for the decline of soil quality was artificial disturbance, including clear-cutting and afforestation. By returning harvesting residues and taking fertilizing measures, the negative effects of human disturbance, such as clear-cutting and afforestation, on the soil quality of forest lands would be reduced; delaying deforestation is also helpful in improving soil quality. Due to the long growth cycle of *Larix principis-rupprechtii* in Northern China, this study only focused on the first- and second-generation forests of *Larix principis-rupprechtii* in Northern China, and the influence of successive rotations on the soil quality should be continuously observed.

4.3. Clear-Cutting

Our observations demonstrated that a decline in the soil quality is caused by the reduction in porosity, microbial quantity except catalase, and the enzyme activity of soil with clear-cutting supporting the third hypothesis. Previous studies have shown that soil quality also declines due to human disturbance such as clear-cutting [6,53]. They are mutually validated by the present study. Deforestation negatively impacts on soil physical properties and leads to the loss of soil nutrients [23], coinciding with our results. Understorey vegetation also provides a better condition for microorganisms and alleviates rainfall-induced erosion and nutrient leaching [54]. After clear-cutting, dragging wood away and cutting residues could destroy the understorey vegetation and litter on soil and could expose a large number of aggregates of soil to air; thus, soil erosion and nutrient leaching occur after heavy rainfalls [55]. Erosion also damages soil structure and influences the circulation of elements, microbial populations, and organic compounds in soil [56,57]. While most litter and harvesting residues were not returned to the forest land, the return of forest nutrients mainly depends on the precipitation leaching and the decomposition of inorganic nutrients by roots, leading to the remarkable inhibition of nutrient cycle in the forest ecosystem and a marked reduction in the efficiency of nutrient cycle [58]. Clear-cutting causes the exposure of ridges to air, the decomposition of organic matter, and the massive loss of soil mineral elements (a maximum loss of N, C, and K+) [24,59–61], which in turn lowers the number of microorganisms and soil enzyme activity, thereby ultimately reducing the soil quality and making the soil more barren [22,25]. Therefore, clear-cutting causes exposure of soil to air and ultimately declines soil quality. In order to alleviate the negative effects of clear-cutting on soil quality, the use of heavy machinery should be minimized during the clear-cutting process, and the disturbance of human activities to forest soil should be lessened as well [62], especially the disturbance to forest soil during the removal of tree stumps. Returning the harvesting residues to the forest land is required to maintain the coverage of litter and understorey vegetation. Thus, the decomposition of the soil organic matters, the soil erosion, the changes in soil structure, and the loss of soil nutrients through drenching would be minimized.

4.4. Forest Cultivation Cycle and Soil Quality Recovery Time

From planting *Larix principis-rupprechtii* seedlings to harvesting wood as a cultivation cycle, the soil quality declined by 2.90% through a forest cultivation cycle. Soil quality declining problems such as exposure of soil to air and nutrient loss are caused by the distribution of land through planting trees. As the soil quality in the growing forests gradually recovers, the forests play a role in improving the soil quality. In this study, due to the use of heavy machinery in the harvesting process and failure to take measures such as returning the cutting leftovers, the forest soil quality was greatly reduced. The studies of Selvaraj et al. [52] also support our results. Since the soil quality gradually improved from 16-year-old to 44-year-old forest stands after planting *Larix principis-rupprechtii*, the change in the stand SQI (Figure 9) presumed that it would take about 39 years for the first-generation forest (calculated by regression analysis, see Supplementary Material, Table S3) and more than 28 years for the second-generation forest to restore soil quality. Therefore, in order to maintain the soil quality, the planting cycle of *Larix principis-rupprechtii* should be longer than 39 years.

SQI is a relatively novel method for soil quality assessment. In this research, five representative variables were selected among 24 soil variables to define the smallest data set, for SQI calculation. It provides a more intelligible and comprehensive measurement for soil quality. In future research, comparison SQI and other common indicators for soil quality evaluation would be expected for more accurate variables determining, to further optimize SQI calculation method.

5. Conclusions

The main findings of this study are as follows:

- (1) Extending the cultivation cycle of *Larix principis-rupprechtii* forest was beneficial to improving soil quality.
- (2) Increasing forest generation did not significantly reduce soil quality.
- (3) Clear-cutting could greatly decrease soil quality, and returning the harvesting residues to the forest land may reduce the negative impact of clear-cutting on soil quality.
- (4) In order to maintain soil health and achieve sustainable planting, the planting period of *Larix principis-rupprechtii* forests should be more than 39 years.
- (5) SQI provided a more intelligible and comprehensive measurement of soil quality with the identification of a minimum data set. Future studies should compare SQI with other soil quality indicators to further optimize SQI calculation method.

To better understand the impacts of successive *Larix principis-rupprechtii* planting on soil quality, more generations of *Larix principis-rupprechtii* plantations should be evaluated.

Supplementary Materials: The following are available online at <http://www.mdpi.com/1999-4907/10/10/932/s1>, Table S1: Results of the principal components analysis of soil variables, Table S2: Results of the correlation analysis of soil variables, Table S3: Standardized regression coefficients of the generalized linear models (GLMs) used to examine the effects of stand age on SQI for the first-generation *Larix principis-rupprechtii*.

Author Contributions: K.Z.: Data collection, data analysis, and manuscript writing. T.J.F.: Guide the revision of the manuscript. D.L.: Data collection, data analysis. Z.J.: Design of the study and supervision of the scientific experiments and data analysis. L.M.: Supervision of the scientific experiments.

Funding: This research was funded by National Natural Science Foundation of China (31870387) and China Scholarship Council.

Conflicts of Interest: The authors declare no conflicts of interest.

References

1. Lal, R. Restoring Soil Quality to Mitigate Soil Degradation. *Sustainability* **2015**, *7*, 5875–5895. [CrossRef]
2. Lal, R. Soil degradation as a reason for inadequate human nutrition. *Food Sec.* **2009**, *1*, 45–57. [CrossRef]
3. León, J.D.; Osorio, N.W. Role of Litter Turnover in Soil Quality in Tropical Degraded Lands of Colombia. *Sci. World J.* **2014**, *2014*, 693981. [CrossRef] [PubMed]

4. Bini, C. Soil: A precious natural resource. In *Conservation of Natural Resources*; Kudrow, N.J., Ed.; Nova Science Publishers: Hauppauge, NY, USA, 2009; pp. 1–48.
5. Yu, X.B.; Yang, G.Q.; Li, S.K. Study on the changes of soil properties in Eucalyptus plantation under continuous-planting practices. In *Studies on Longterm Productivity Management of Eucalyptus Plantation*; Yu, X.B., Ed.; China Forestry Publishing House: Beijing, China, 2000; pp. 94–103.
6. Zhang, K.; Zheng, H.; Chen, F.L.; Ouyang, Z.Y.; Wang, Y.; Wu, Y.F.; Lan, J.; Fu, M.; Xiang, X.W. Changes in Soil Quality after Converting Pinus to Eucalyptus Plantations in Southern China. *Solid Earth* **2015**, *6*, 115–123. [[CrossRef](#)]
7. LeBauer, D.S.; Treseder, K.K. Nitrogen Limitation of Net Primary Productivity in Terrestrial Ecosystems Is Globally Distributed. *Ecology* **2008**, *89*, 371–379. [[CrossRef](#)] [[PubMed](#)]
8. Laclau, J.P.; Ranger, J.; Goncalves, J.L.D.; Maquere, V.; Krusche, A.V.; M'Bou, A.T.; Nouvellon, Y.; Saint-Andre, L.; Bouillet, J.P.; Piccolo, M.D.; et al. Biogeochemical Cycles of Nutrients in Tropical Eucalyptus Plantations Main Features Shown by Intensive Monitoring in Congo and Brazil. *For. Ecol. Manag.* **2010**, *259*, 1771–1785. [[CrossRef](#)]
9. Yu, F.K.; Huang, X.H.; Wang, K.Q.; Duang, C.Q. An overview of ecological degradation and restoration of Eucalyptus plantations. *Chin. J. Eco-Agric.* **2009**, *17*, 393–398. [[CrossRef](#)]
10. Bünemann, E.K.; Bongiorno, G.; Bai, Z.; Creamer, R.E.; De Deyn, G.; de Goede, R.; Pulleman, M. Soil quality—A critical review. *Soil Biol. Biochem.* **2018**, *120*, 105–125. [[CrossRef](#)]
11. Garay, I.; Pellens, R.; Kindel, A.; Barros, E.; Franco, A.A. Evaluation of soil conditions in fast-growing plantations of Eucalyptus grandis and Acacia mangium in Brazil: A contribution to the study of sustainable land use. *Appl. Soil Ecol.* **2004**, *27*, 177–187. [[CrossRef](#)]
12. Muñoz-Rojas, M.; Jordán, A.; Zavala, L.M.; De la Rosa, D.; AbdElmabod, S.K.; Anaya-Romero, M. Organic carbon stocks in Mediterranean soil types under different land uses (Southern Spain). *Solid Earth* **2012**, *3*, 375–386. [[CrossRef](#)]
13. Parras-Alcántara, L.; Martín-Carrillo, M.; Lozano-García, B. Impacts of land use change in soil carbon and nitrogen in a Mediterranean agricultural area (Southern Spain). *Solid Earth* **2013**, *4*, 167–177. [[CrossRef](#)]
14. Zhang, Y.; Wei, Z.C.; Li, H.T.; Guo, F.T.; Wu, P.F.; Zhou, L.L.; Ma, X.Q. Biochemical quality and accumulation of soil organic matter in an age sequence of *Cunninghamia lanceolata* plantations in southern China. *J. Soils Sediments* **2017**, *17*, 2218–2229. [[CrossRef](#)]
15. Filip, Z. International approach to assessing soil quality by ecologically-related biological parameters. *Agric. Ecosyst. Environ.* **2002**, *88*, 169–174. [[CrossRef](#)]
16. Parisi, V.; Menta, C.; Gardi, C.; Jacomini, C.; Mozzanica, E. Microarthropod communities as a tool to assess soil quality and biodiversity: A new approach in Italy. *Agric. Ecosyst. Environ.* **2005**, *105*, 323–333. [[CrossRef](#)]
17. Ritz, K.; Black, H.I.J.; Campbell, C.D.; Harris, J.A.; Wood, C. Selecting biological indicators for monitoring soils: A framework for balancing scientific and technical opinion to assist policy development. *Ecol. Indic.* **2009**, *9*, 1212–1221. [[CrossRef](#)]
18. Andrews, S.S.; Carroll, C.R. Designing a soil quality assessment tool for sustainable agroecosystem management. *Ecol. Appl.* **2001**, *11*, 1573–1585. [[CrossRef](#)]
19. Zornoza, R.; Acosta, J.A.; Bastida, F.; Domínguez, S.G.; Toledo, D.M.; Faz, A. Identification of sensitive indicators to assess the interrelationship between soil quality, management practices and human health. *Soil* **2015**, *1*, 173–185. [[CrossRef](#)]
20. Gruba, P.; Socha, J.; Pietrzykowski, M.; Pasichnyk, D. Tree species affects the concentration of total mercury (Hg) in forest soils: Evidence from a forest soil inventory in Poland. *Sci. Total Environ.* **2019**, *647*, 141–148. [[CrossRef](#)]
21. Bouma, J.; Van Ittersum, M.K.; Stoorvogel, J.J.; Batjes, N.H.; Droogers, P.; Pulleman, M.M. Soil capability: Exploring the functional potentials of soils. *Glob. Soil Secur.* **2017**, 27–44. [[CrossRef](#)]
22. Weis, W.; Huber, C.; Gattlein, A. Regeneration of mature Norway spruce stands: Early effects of selective cutting and clear cutting on seepage water quality and soil fertility. *Sci. World J.* **2001**, *1*, 493–499. [[CrossRef](#)]
23. Zhou, X.N.; Zhou, Y.; Zhou, C.J.; Wu, Z.L.; Zheng, L.F.; Hu, X.S.; Chen, H.X.; Gan, J.B. Effects of Cutting Intensity on Soil Physical and Chemical Properties in a Mixed Natural Forest in Southeastern China. *Forests* **2015**, *6*, 4495–4509. [[CrossRef](#)]
24. Aleksandrowicz-Trzcinska, M.; Drozdowski, S.; Zybura, H. Effect of Mechanical Site Preparation on Features of the Soil in a Clear-Cut Area. *Sylvan* **2018**, *162*, 648–657.

25. Hume, A.M.; Chen, H.Y.H.; Taylor, A.R. Intensive Forest Harvesting Increases Susceptibility of Northern Forest Soils to Carbon, Nitrogen and Phosphorus Loss. *J. Appl. Ecol.* **2018**, *55*, 246–255. [[CrossRef](#)]
26. Zhao, K.J.; Zheng, M.X.; Fahey, T.J.; Jia, Z.K.; Ma, Y.L. Vertical gradients and seasonal variations in the stem CO₂ efflux of *Larix principis-rupprechtii* Mayr. *Agric. For. Meteorol.* **2018**, *262*, 71–80. [[CrossRef](#)]
27. Yao, Y.T.; Zhang, J.Z.; Hu, J.F. *Larix Principis-Rupprechtii*; Agricultural Science and Technology Press of China: Beijing, China, 2013.
28. McKenzie, N.; Coughlan, K.; Cresswell, H. *Soil Physical Measurement and Interpretation for Land Evaluation*; Csiro Publishing: Collingwood, Australia, 2002; Volume 5.
29. Wu, G.L.; Yang, Z.; Cui, Z.; Liu, Y.; Fang, N.F.; Shi, Z.H. Mixed artificial grasslands with more roots improved mine soil infiltration capacity. *J. Hydrol.* **2016**, *535*, 54–60. [[CrossRef](#)]
30. Jiao, F.; Wen, Z.M.; An, S.S. Changes in soil properties across a chronosequence of vegetation restoration on the Loess Plateau of China. *Catena* **2011**, *86*, 110–116. [[CrossRef](#)]
31. Huang, C.Y. *Soil Science*; China Agriculture Press: Beijing, China, 2003; pp. 89–92.
32. Hardie, M.; Clothier, B.; Bound, S.; Oliver, G.; Close, D. Does Biochar Influence Soil Physical Properties and Soil Water Availability? *Plant Soil* **2014**, *376*, 347–361. [[CrossRef](#)]
33. Clark, M.D.; Gilmour, J.T. The effect of temperature on decomposition at optimum and saturated soil water contents. *Soil Sci. Soc. Am. J.* **1983**, *47*, 927–929. [[CrossRef](#)]
34. Rowell, D.L. *Soil Science: Methods and Applications*; Routledge: London, UK, 2014.
35. Cassel, D.K.; Nielsen, D.R. Field capacity and available water capacity. In *Methods of Soil Analysis. Part 1*, 2nd ed.; Klute, A., Ed.; Agron. Monogr. 9. ASA and SSSA: Madison, WI, USA, 1986; pp. 901–926.
36. Givi, J.; Prasher, S.O.; Patel, R.M. Evaluation of pedotransfer functions in predicting the soil water contents at field capacity and wilting point. *Agric. Water Manag.* **2004**, *70*, 83–96. [[CrossRef](#)]
37. Bao, S.D. *Soil Agro-Chemical Analysis*; China Agriculture Press: Beijing, China, 2000.
38. Chen, H.K. *Soil Microbiology*; Shanghai Science and Technology Press: Shanghai, China, 1981; pp. 44–45.
39. Waldrop, M.P.; Balser, T.C.; Firestone, M.K. Linking microbial community composition to function in a tropical soil. *Soil Biol. Biochem.* **2000**, *32*, 1837–1846. [[CrossRef](#)]
40. Kandeler, E.; Gerber, H. Short-term assay of soil urease activity using colorimetric determination of ammonium. *Biol. Fertil. Soils* **1988**, *6*, 68–72. [[CrossRef](#)]
41. Zheng, H.; Ouyang, Z.Y.; Wang, X.K.; Miao, H.; Zhao, T.Q.; Peng, T.B. How different reforestation approaches affect red soil properties in Southern China. *Land Degrad. Dev.* **2005**, *16*, 387–396. [[CrossRef](#)]
42. Andrews, S.S.; Karlen, D.L.; Mitchell, J.P. A comparison of soil quality indexing methods for vegetable production systems in Northern California. *Agric. Ecosyst. Environ.* **2002**, *90*, 25–45. [[CrossRef](#)]
43. Lima, A.M.; Silva, I.R.; Neves, J.C.; Novais, R.F.; Barros, N.F.; Mendonça, E.S.; Leite, F.P. Soil organic carbon dynamics following afforestation of degraded pastures with eucalyptus in southeastern Brazil. *For. Ecol. Manag.* **2006**, *235*, 219–231. [[CrossRef](#)]
44. Lucas-Borja, M.E.; Hedo, J.; Cerdá, A.; Candel-Pérez, D.; Viñegra, B. Unravelling the importance of forest age stand and forest structure driving microbiological soil properties, enzymatic activities and soil nutrients content in Mediterranean Spanish black pine (*Pinus nigra* Ar. ssp. *salzmannii*) Forest. *Sci. Total Environ.* **2016**, *562*, 145–154. [[CrossRef](#)]
45. Mao, R.; Zeng, D.H.; Hu, Y.L.; Li, L.J.; Yang, D. Soil organic carbon and nitrogen stocks in an age-sequence of poplar stands planted on marginal agricultural land in Northeast China. *Plant Soil* **2010**, *332*, 277–287. [[CrossRef](#)]
46. Cheng, J.; Lee, X.; Theng, B.K.; Zhang, L.; Fang, B.; Li, F. Biomass accumulation and carbon sequestration in an age-sequence of *Zanthoxylum bungeanum* plantations under the Grain for Green Program in karst regions, Guizhou province. *Agric. For. Meteorol.* **2015**, *203*, 88–95. [[CrossRef](#)]
47. Zhou, G.Y.; Liu, S.G.; Li, Z.; Zhang, D.Q.; Tang, X.L.; Zhou, C.Y.; Yan, J.H.; Mo, J.M. Old-Growth Forests Can Accumulate Carbon in Soils. *Science* **2006**, *314*, 1417. [[CrossRef](#)]
48. Luyssaert, S.; Schulze, E.D.; Börner, A.; Knohl, A.; Hessenmoller, D.; Law, B.E.; Ciais, P.; Grace, J. Old-growth forests as global carbon sinks. *Nature* **2008**, *455*, 213–215. [[CrossRef](#)]
49. Chen, G.S.; Yang, Z.J.; Gao, R.; Xie, J.S.; Guo, J.F.; Huang, Z.Q.; Yang, Y.S. Carbon Storage in a Chronosequence of Chinese Fir Plantations in Southern China. *For. Ecol. Manag.* **2013**, *300*, 68–76. [[CrossRef](#)]

50. Xu, D.P. An approach to nutrient balance in tropical and south subtropical short rotation plantations. In *Studies on Long-Term Productivity Management of Eucalyptus Plantation*; Yu, X.B., Ed.; China Forestry Publishing House: Beijing, China, 2000; pp. 27–35.
51. Diochon, A.C.; Kellman, L. Physical fractionation of soil organic matter: Destabilization of deep soil carbon following harvesting of a temperate coniferous forest. *J. Geophys. Res. Biogeosci.* **2009**, *114*, G01016. [[CrossRef](#)]
52. Selvaraj, S.; Duraisamy, V.; Huang, Z.J.; Guo, F.T.; Ma, X.Q. Influence of Long-Term Successive Rotations and Stand Age of Chinese Fir (*Cunninghamia lanceolata*) Plantations on Soil Properties. *Geoderma* **2017**, *306*, 127–134. [[CrossRef](#)]
53. Jennings, T.N.; Smith, J.E.; Cromack, K.; Sulzman, E.W.; McKay, D.; Caldwell, B.A.; Beldin, S.I. Impact of postfire logging on soil bacterial and fungal communities and soil biogeochemistry in a mixed-conifer forest in central Oregon. *Plant Soil* **2012**, *350*, 393–411. [[CrossRef](#)]
54. Yu, X.B.; Chen, Q.B.; Wang, S.M.; Mo, X.Y. Research on land degradation in forest plantation and preventive strategies. In *Studies on Long-Term Productivity Management of Eucalyptus Plantation*; Yu, X.B., Ed.; China Forestry Publishing House: Beijing, China, 2000; pp. 1–7.
55. Zhang, X.; Kirschbaum, M.U.F.; Hou, Z.; Guo, Z. Carbon stock changes in successive rotations of Chinese fir (*Cunninghamia lanceolata* (Lamb.) Hook.) plantations. *For. Ecol. Manag.* **2004**, *202*, 131–147. [[CrossRef](#)]
56. Kibblewhite, M.G.; Ritz, K.; Swift, M.J. Soil health in agricultural systems. *Philos. Trans. R. Soc. Lond. Ser. B* **2008**, *363*, 685–701. [[CrossRef](#)]
57. Brussaard, L. Ecosystem services provided by the soil biota. In *Soil Ecology and Ecosystem Services*; Wall, D.H., Bardgett, R.D., Behan-Pelletier, V., Herrick, J.E., Jones, H., Ritz, K., Six, J., Strong, D.R., van der Putten, W.H., Eds.; Oxford University Press: Oxford, UK, 2012; pp. 45–58.
58. Zinn, Y.L.; Resck, D.V.; da Silva, J.E. Soil organic carbon as affected by afforestation with Eucalyptus and Pinus in the Cerrado region of Brazil. *For. Ecol. Manag.* **2002**, *166*, 285–294. [[CrossRef](#)]
59. Nave, L.E.; Vance, E.D.; Swanston, C.W.; Curtis, P.S. Harvest impacts on soil carbon storage in temperate forests. *For. Ecol. Manag.* **2010**, *259*, 857–866. [[CrossRef](#)]
60. Achat, D.L.; Deleuze, C.; Landmann, G.; Pousse, N.; Ranger, J.; Augusto, L. Quantifying consequences of removing harvesting residues on forest soils and tree growth—A meta-analysis. *For. Ecol. Manag.* **2015**, *348*, 124–141. [[CrossRef](#)]
61. Thiffault, E.; Hannam, K.D.; Pare, D.; Titus, B.D.; Hazlett, P.W.; Maynard, D.G.; Brais, S. Effects of forest biomass harvesting on soil productivity in boreal and temperate forests—A review. *Environ. Rev.* **2011**, *19*, 278–309. [[CrossRef](#)]
62. Cambi, M.; Grigolato, S.; Neri, F.; Picchio, R.; Marchi, E. Effects of forwarder operation on soil physical characteristics: A case study in the Italian alps. *Croat. J. For. Eng.* **2016**, *37*, 233–239.



© 2019 by the authors. Licensee MDPI, Basel, Switzerland. This article is an open access article distributed under the terms and conditions of the Creative Commons Attribution (CC BY) license (<http://creativecommons.org/licenses/by/4.0/>).

Article

Conversion of Natural Evergreen Broadleaved Forests Decreases Soil Organic Carbon but Increases the Relative Contribution of Microbial Residue in Subtropical China

Liuming Yang ^{1,2}, Silu Chen ^{1,2}, Yan Li ^{1,2}, Quancheng Wang ^{1,2}, Xiaojian Zhong ^{1,2}, Zhijie Yang ^{1,2}, Chengfang Lin ^{1,2,*} and Yusheng Yang ^{1,2}

¹ School of Geographical Science, Fujian Normal University, Fuzhou 350007, China; yanglm2007@aliyun.com (L.Y.); pydesj@163.com (S.C.); 15705956185@163.com (Y.L.); wangquancheng0304@126.com (Q.W.); xj.zhong@fjnu.edu.cn (X.Z.); zhijieyang@fjnu.edu.cn (Z.Y.); geoyys@fjnu.edu.cn (Y.Y.)

² Key Laboratory for Subtropical Mountain Ecology, School of Geographical Sciences, Fujian Normal University, Fuzhou 350007, China

* Correspondence: tonylcf99@fjnu.edu.cn; Tel.: +86-0591-83483731; Fax: +86-0591-83465379

Received: 27 April 2019; Accepted: 28 May 2019; Published: 29 May 2019

Abstract: It has been recognized that land use change affects soil organic carbon (SOC) dynamics and the associated microbial turnover. However, the contribution of microbial residue to SOC storage remains largely unknown in land use change processes. To this end, we adopted a “space for time” approach to examine the dynamics of SOC and amino sugars, which was a biomarker of microbial residue C, in different natural forest conversions. Three typical converted forests were selected: an assisted natural regeneration (ANR) and two coniferous plantations of *Cunninghamia lanceolata* (Lamb.) Hook (Chinese fir) and *Pinus massoniana* Lamb. (pine) each. All of these were developed at the same time after the harvest of an old natural forest and they were used to evaluate the effects of forest conversions with contrasting anthropogenic disturbance on SOC and microbial residue C, along with the natural forest. Natural forest conversion led to an approximately 42% decrease in SOC for ANR with low anthropogenic disturbance, 60% for the Chinese fir plantation, and 64% for the pine plantation. In contrast, the natural forest conversion led to a 32% decrease in the total amino sugars (TAS) for ANR, 43% for the Chinese fir plantation, and 54% for the pine plantation at a soil depth of 0–10 cm. The ratios of TAS to SOC were significantly increased following natural forest conversion, with the highest ratio being observed in the Chinese fir plantation, whereas the ratios of glucosamine to muramic acid (GluN/MurA) were significantly decreased in the two plantations, but not in ANR. The contents of SOC, individual amino sugar, or TAS, and GluN/MurA ratios were consistently higher at a soil depth of 0–10 cm than at 10–20 cm for all of the experimental forests. Redundancy analysis showed that microbial residue C was significantly correlated with SOC, and both were positively correlated with fine root biomass, annual litterfall, and soil available phosphorus. Taken together, our findings demonstrated that microbial residue C accumulation varied with SOC and litter input, and played a more important role in SOC storage following forest conversion to plantations with higher anthropogenic disturbance.

Keywords: soil organic carbon; soil microbial residue; forest conversion; natural forest; assisted natural regeneration; plantation

1. Introduction

The decomposition, transformation, and stabilization of soil organic carbon (SOC) are the consequence of microbial growth and activity, which is a process that is associated with proliferation, metabolism, and mortality of microorganisms. More and more attention has been paid to microbial residue in recent studies, which demonstrated that senesced microbial biomass may play a much greater role in the stabilization of soil C pools than that previously considered [1–4]. It is critical to elucidate the response of soil microbial residue to global change, as well as the underlying mechanisms driving its transformation, to better understand global biogeochemical cycles and improve current global C cycle models [5,6]. There are a number of studies exploring the effects of global change on soil microbial residue. For example, Zhang et al. reported land use effects on amino sugars in soil particle size fractions [7]. Liang and Balser observed that warming and N deposition reduced microbial residue contribution to the soil C pool [8]. To the best of our knowledge, studies investigating the effects of forest conversion on microbial residue contribution to soil C sequestration are lacking.

Space for time substitution is still used as a reasonable method to evaluate the legacy of forest conversion on ecosystem properties. In general, the reestablished forests, such as plantation forests, are taken as experimental units and adjacent native forest as a reference. The forest conversions are usually subjected to different management coupled with anthropogenic disturbances of various intensity, which alter the structure of the forest ecosystem [9–11]. Consequently, changes in forest structure and management practices likely lead to the alteration, not only of input rates and organic matter decomposability, but also of soil moisture and temperature regimes [12,13]. The adaptation of soil microbial abundance, community composition, and activity following these changes can shift the soil biogeochemical cycling processes regulated by microorganisms [14,15], eventually affecting the contribution of microbial residue C to the soil C pool [16].

It is difficult to establish the correlation between living microbial biomass and long-term SOC sequestration [17] or to directly measure C that is bound in microbial residues. Alternatively, amino sugars, which are important microbial residue biomarkers in soil [18,19], can represent the legacy of microbial-derived constituents and be used to estimate the contribution of dead microbial cells to soil organic C pools [20,21]. Glucosamine (GluN), muramic acid (MurA), galactosamine (GalN), and mannosamine (ManN) are the most important amino sugars in soils [22,23]. GluN is predominantly derived from the chitin of fungal cell walls and it is also found in bacterial peptidoglycan [18,24]. MurA is solely derived from bacterial cell walls [19,24]. GalN is generally considered to originate from bacteria [19]. The concentration and ratios of the above amino sugars can be used to evaluate the microbial (bacterial versus fungal) contribution to soil C sequestration [18,20,23,25].

Subtropical forests provide an important contribution to global terrestrial ecosystem C storage [26,27]. In southern China, the majority of natural forests were cleared by the late 1970s and first converted into two coniferous plantations, Chinese fir (*Cunninghamia lanceolata* (Lamb.) Hook) and pine (*Pinus massoniana* Lamb.), to satisfy the high demand for timber, fuel, and other forest products due to rapid human population growth. The conversion not only has a profound effect on the ecosystem C budget [11,28,29], but it also leads to other ecological consequences, such as a loss in species diversity [30–33] and soil erosion [34]. As an alternative to conversion to plantations, forests with assisted natural regeneration (ANR) have been introduced to China for more than five decades [35,36], with the goal of protecting and nurturing mother trees and their seedlings that are inherently present in the area, rather than the establishment of entirely new forest plantations [37]. Our previous study showed that, when compared to monoculture plantations, ANR significantly increased the plant biomass and diversity, and more effectively promoted ecosystem services, including the mitigation of runoff and soil erosion, and the exportation of dissolved organic C [34]. However, the effects of forest conversions on these forest types with various intensities of anthropogenic disturbance to soil C dynamics, and, in particular, that of microbial residue, have rarely been assessed and compared.

In the present study, an ANR forest and two dominant plantations (Chinese fir and pine) with contrasting intensity of anthropogenic disturbance were selected to examine the effects of forest

conversions on the dynamics of soil microbial residues. All of the selected forests were developed from a natural forest clearing in subtropical China, with similar soil properties and forest age. Following the conversion of native forest to plantations or ANR forests, different litter inputs exhibited a remarkable influence on the response of bacterial and fungal groups [38], which possibly resulted in distinct microbial residue retention patterns and different microbial functions during SOC accumulation [39,40]. We hypothesize that (1) soil amino sugar concentrations are lower in all of the converted forests than the native forest, with the lowest concentration in one of the two plantations. Mature and undisturbed ecosystems have a higher ratio of K-strategists to r-strategists than did young and disturbed ecosystems, according to the theory of Odum on ecosystem succession and disturbance [41,42]. Furthermore, a recent meta-analysis showed that converted forests consistently shifted from fungal to bacterial dominance with increasing land degradation [43]. Thus, we hypothesize that (2) natural forest conversion leads to a decrease of fungal relative to the bacterial residue C ratios, and these ratios, in descending order, will be as follows: native forest > ANR > plantations. Previous studies showed that labile C fractions were sensitive indicators of SOC dynamics that resulted from forest conversion [44], whereas microbial residue C was incorporated into the recalcitrant C pool [6], which may not respond equally to environmental change, as does the total soil C. Therefore, we hypothesize that (3) forest conversions increase the ratios of TAS (total amino sugars) to total SOC, with highest ratio in one of the two plantations, because of the entirely new forest establishment, resulting in rapid loss of labile C fractions, whereas a lower ratio than the plantations will occur in the ANR forest.

2. Materials and Methods

2.1. Site Description

This study was conducted in the Chenda Observation Study Site (26°19′55″ N, 117°36′53″ E, 300 m a.s.l.) of Sanming Forest Ecosystem and Global Change Research Station in Fujian Province, China. This study site borders the Daiyun Mountains on the southeast and the Wuyi Mountains on the northwest. A typical maritime subtropical monsoon climate characterizes the study site. The mean annual temperature (MAT) is 19.1 °C with low temperatures occurring in January and high temperatures occurring in July. The mean annual relative humidity is 81% and the mean annual precipitation (MAP) is 1750 mm. Approximately 75% of the total precipitation occurs from March to August. The mean annual potential evapotranspiration is 1585 mm. The soil at the study site is formed from granite and is classified as red soil according to the China soil classification system and it is equivalent to Ultisol in the USDA Soil Taxonomy [45]. Soil texture in the natural forest is sandy with sand (2–0.05 mm), silt (0.05–0.002 mm), and clay (<0.002 mm), being 16.4%, 37.3%, and 46.3%, respectively, which does not significantly change after forest conversions. The soil depth exceeds 1.0 m.

The natural forest represents an old-growth, evergreen broadleaved *Castanopsis carlesii* (Hemsl.) forest in mid-subtropical China, which has been protected for more than 200 years, according to the record of local forest management department and it is characterized with high biodiversity, widespread old trees, snags, and downed wood. In addition to *Castanopsis carlesii*, the overstory contained other tree species, such as *Castanopsis kawakamii* Hayata, *Schima superba* Gardner & Champ., *Litsea subcoriacea* Y.C. Yang & P.H. Huang, and *Elaeocarpus decipiens* Hemsl. Two types of regeneration were adopted following the deforestation of the natural *Castanopsis carlesii* forests in 1975. One was natural regeneration, in which only the overstory was harvested and the understory and harvest residue remained. The other was to reestablish entirely new plantations following the forest being clear-cut, slashed, and burned. In 1976, the soil was prepared by digging holes. Afterwards, one-year-old seedlings of *C. lanceolata* or *P. massoniana* were planted at 3000 trees per hectare. The plantations were managed with similar practices, such as weeding and fertilization during the first three years and thinning twice between 10 and 15-years-old. The distances between the selected experimental forests fell within 1 km. Table 1 presents the general characteristics of the forests.

Table 1. Forest characteristics in a natural forest of *Castanopsis carlesii* (Hemsl.) (NF), assisted natural regeneration (ANR) and two plantation forests of *Cunninghamia lanceolata* (Lamb.) Hook (Chinese fir, CF) and *Pinus massoniana* Lamb. (PM).

| Variable | NF | ANR | CF | PM |
|--|------|------|------|------|
| Altitude (m) | 315 | 315 | 301 | 303 |
| Slope (°) | 35 | 28 | 30 | 35 |
| Canopy coverage (%) | 89 | 90 | 65 | 70 |
| Mean tree height (m) | 11.9 | 10.8 | 18.2 | 18.4 |
| Mean tree diameter at breast height (cm) | 20.0 | 14.3 | 15.6 | 16.3 |
| Stand density (stem ha ⁻¹) | 1955 | 3788 | 2858 | 1500 |

2.2. Soil Sampling, Litterfall, and Fine Root Biomass Measurements

Three replicate plots (20 m × 50 m) were set up for each forest type, and the distance between plots was kept at 20 m to assess the effects of forest conversion on microbial residue. Soil samples (0–10 cm and 10–20 soil layer) were collected in April 2017; 15 cores (5 cm in diameter) were randomly collected from each plot in a plastic bag as a composite sample. After removing the stones, pebbles, roots, and large pieces of plant residues, the soil was ground and sieved (<2 mm sieve), and then combined, homogenized, and divided into three subsamples. The first samples were kept at 4 °C for the determination of soil enzyme activity and microbial biomass. The second samples were kept at −20 °C and they were freeze-dried at −80 °C, and then ground to pass through a 0.149 mm sieve for the determination of amino sugar. The third soil samples were air dried for analysis of soil physical and chemical properties. Five rectangle litter traps (0.5 m × 1.0 m) with 1 mm nylon mesh were randomly arranged about 0.25 m above the soil surface in each plot. Litterfall was semimonthly collected from October 2010 to September 2016 using the method that was described by Yang et al. [46]. For the fine root sampling, 15 soil cores were randomly taken in each plot with a soil corer (5 cm in diameter) in April of 2017. The thick roots (>2 mm) were carefully removed from the soil samples with forceps and then the soils were wet-sieved with a mesh size of 0.5 mm. The sieved soils were put into a beaker with deionized water at a temperature of 1 °C and repeatedly stirred to float the fine root segments to water surface for collection [47]. The fine roots were placed into an oven at a temperature of 65 °C for 48 h and then weighed.

2.3. Soil Analysis

Soil pH was measured with a soil:water ratio of 1:2.5. SOC and total N were determined while using a CN auto analyzer (Elementar Vario MAX, Germany). For nitrate and ammonium analyses, 5 g of fresh soil from each sample was extracted using a 2 mol/L KCl solution. The solutions were shaken for 40 min. and then filtered for nitrate and ammonium determination while using a continuous flow analyzer (SKALAR San++, Breda, The Netherlands). The soil cation exchange capacity (CEC) was assessed by the ammonium acetate extraction method at pH 7. The soil available phosphorus (P) was detected while using the ion exchange resin method that Sibbesen developed [48].

2.4. Determination of Soil Amino Sugars

Amino sugar content in soils was detected while using the method of Zhang and Amelung [22]. Briefly, the finely ground soil samples (containing approximately 0.3 mg N) were hydrolyzed with 10 mL 6 M HCl at 105 °C for 8 h, and 0.1 mL myo-inositol (internal standard) was added to the hydrolysate solution, which was filtered through a glass fiber membrane filter (0.45 diameter), dried using a rotary evaporator, re-dissolved with deionized water, and then transferred into a 50 mL Teflon tube. The pH of the sample solutions was adjusted to 6.6–6.8 with 1 M KOH and 0.01 M HCl and the samples were then centrifuged. After the solution was freeze-dried, 5 mL methanol was added to dissolve the residues, after which the methanol solution was transferred to a vial and dried with N₂ at

45 °C. Finally, 1 mL deionized water and 0.1 mL recovery standard (*N*-methylglucamine) were added to the residues and freeze-dried.

The freeze-dried residues were dissolved with 0.3 mL derivatization reagent containing 32 mg mL⁻¹ hydroxylamine hydrochloride and 40 mg mL⁻¹ 4-dimethylamino-pyridine in pyridine-methanol (4:1 *v/v*) were heated at 78 °C for 35 min. in a water bath. After cooling, 1 mL acetic anhydride was added and then reheated to 78 °C for 25 min. Next, 1.5 mL dichloromethane and 1 mL 1 M HCl were added to achieve liquid–liquid separation. After water phase removal, the organic phase was washed three times with 1 mL deionized water. The remaining organic phase was dried by N₂ gas at 45 °C. Finally, 0.2 mL ethyl acetate-hexane (1:1) was added to dissolve the derivative for final analysis. The amino sugar derivatives were separated using an Agilent 6890A gas chromatography (GC, Agilent Tech. Co. Ltd., USA) that was equipped with DB-1 fused silica column (25 m × 0.32 mm × 0.25 mm) with a flame ionization detector. The concentrations of individual amino sugars were quantified based on the internal standard myo-inositol.

2.5. Statistics

Each forest was considered as an experimental unit, and the data were averaged across the three plots from each forest. Due to using pseudo-replication in this study, all of the standard errors were pseudo-replication errors as were mean comparisons. Results must be carefully interpreted and only trends in the data by forest type can be discussed, with an appreciation of the problems of pseudo-replication.

Before analysis, all the variables were checked for normal distribution (Kolmogorov–Smirnov test) and homogeneity (Levene test). One-way ANOVA with Tukey's HSD test was performed to test for differences of litter mass, fine root biomass, soil physicochemical properties, and soil amino sugars among forests. Statistical significance was established at the 5% level, unless otherwise mentioned. Redundancy analysis (RDA) was applied to elucidate the relationships among total amino sugar (TAS), GluN, GalN, MurA, GluN/MurA, GluN/GalN, the proportion of total amino sugar to total C, and the corresponding soil environmental variables (total litterfall, fine root biomass, pH, soil organic C, total N, total P, soil texture) among different forest types. SPSS 18.0 (SPSS, Inc., Chicago, IL, USA) was used for all statistical analyses, except for RDA, which was performed while using CANOCO software for Windows 4.5 (Ithaca, NY, USA). Forward selection was based on Monte Carlo permutation ($n = 999$). Before RDA, we conducted forward selection of the environmental variables that were significantly correlated with variations of amino sugars while using the Monte Carlo permutation test ($p < 0.05$).

3. Results

3.1. Soil Properties

The SOC content was high in the natural forest (51.8 ± 3.0 mg g⁻¹). Following conversion of the natural forest, there was an approximately 42% reduction in SOC for the ANR forest (30.0 ± 2.7 mg g⁻¹), 60% for the Chinese fir plantation (20.9 ± 1.3 mg g⁻¹), and 64% for the pine plantation (18.6 ± 0.9 mg g⁻¹) at 0–10 cm soil layer, with over 50% reductions at the 10–20 cm soil layer for all the converted forests. Similarly, the soil N content was 2.75 ± 0.10 mg g⁻¹ at 0–10 cm soil layer in the natural forest, and there was an approximately 30% reduction in the ANR (1.91 ± 0.12 mg g⁻¹) and an approximately 50% decrease in the two plantations (1.13 ± 0.09 and 1.29 ± 0.07 mg g⁻¹ for the Chinese fir and pine plantations, respectively) after forest conversions, as well as more than a 50% decrease at the 10–20 cm soil layer for all of the converted forests (Table 2). Soil pH was increased for all of the converted forests (Table 2).

Table 2. Soil properties under four different forest types.

| Soil Property | 0–10 cm Layer | | | | 10–20 cm Layer | | | |
|---|----------------|---------------|---------------|----------------|----------------|----------------|---------------|----------------|
| | NF | ANR | PM | CF | NF | ANR | PM | CF |
| SOC (mg g ^{−1}) | 51.8 ± 3.0 A | 30.0 ± 2.7 B | 18.6 ± 0.9 C | 20.9 ± 1.3 BC | 27.0 ± 1.4 A | 12.7 ± 0.1 b | 10.7 ± 0.5 b | 11.7 ± 0.7 b |
| TN (mg g ^{−1}) | 2.75 ± 0.10 A | 1.91 ± 0.12 B | 1.13 ± 0.09 C | 1.29 ± 0.07 C | 1.47 ± 0.03 a | 1.06 ± 0.03 b | 0.75 ± 0.01 c | 0.86 ± 0.05 bc |
| C/N | 18.8 ± 0.6 A | 15.6 ± 0.4 B | 16.5 ± 1.1 BC | 16.2 ± 0.2 C | 18.3 ± 0.8 a | 12.0 ± 0.3 b | 14.3 ± 0.4 b | 13.7 ± 0.2 b |
| CEC (cmol kg ^{−1}) | 15.8 ± 1.7 A | 7.1 ± 1.2 B | 6.7 ± 0.6 B | 6.5 ± 0.5 B | 9.8 ± 0.4 a | 5.5 ± 0.2 b | 5.7 ± 0.3 b | 6.0 ± 0.2 b |
| pH | 4.08 ± 0.07 B | 4.44 ± 0.09 A | 4.47 ± 0.03 A | 4.52 ± 0.06 A | 4.10 ± 0.03 a | 4.28 ± 0.04 ab | 4.39 ± 0.02 b | 4.35 ± 0.02 b |
| NH ₄ ⁺ (mg kg ^{−1}) | 27.3 ± 0.8 A | 26.5 ± 4.7 A | 11.6 ± 0.9 B | 12.8 ± 1.0 B | 12.2 ± 0.2 a | 9.6 ± 0.8 b | 6.4 ± 0.1 b | 6.8 ± 0.2 b |
| NO ₃ [−] (mg kg ^{−1}) | 0.86 ± 0.09 BC | 1.98 ± 0.33 A | 0.26 ± 0.03 C | 1.38 ± 0.18 AB | 1.19 ± 0.04 a | 1.14 ± 0.06 a | 0.32 ± 0.03 c | 0.73 ± 0.05 b |
| Sand (2–0.05 mm, %) | 16.4 ± 2.7 A | 15.2 ± 3.1 A | 11.1 ± 0.3 A | 12.3 ± 0.2 A | 16.3 ± 1.1 a | 17.5 ± 3.0 a | 13.3 ± 0.5 b | 16.6 ± 0.5 a |
| Silt (0.05–0.002 mm, %) | 37.3 ± 1.9 A | 34.9 ± 1.9 A | 39.0 ± 1.6 A | 37.5 ± 1.2 A | 40.6 ± 1.8 a | 36.6 ± 1.8 a | 40.8 ± 1.2 a | 41.1 ± 0.2 a |
| Clay (<0.002 mm, %) | 46.3 ± 3.3 A | 50.0 ± 1.9 A | 50.0 ± 1.9 A | 50.3 ± 1.4 A | 43.1 ± 2.8 a | 45.8 ± 1.7 a | 45.8 ± 1.7 a | 42.4 ± 0.6 a |
| Available P (mg kg ^{−1}) | 5.47 ± 0.45 A | 6.55 ± 0.56 A | 2.57 ± 0.52 B | 3.46 ± 0.35 B | 1.10 ± 0.14 b | 1.96 ± 0.20 a | 1.17 ± 0.10 b | 1.22 ± 0.06 b |

The effects were significant at $p < 0.05$; different uppercase letters indicate significant differences at 0–10 cm among different forests, and different lowercase letters indicate significant differences at 10–20 cm among different forests. Values are means ± standard errors ($n = 3$). ANR: Assisted natural regeneration; CEC: cation exchange capacity; CF: Chinese fir forest; NF: Natural forest; PM: *Pinus massoniana* Lamb. forest; SOC: Soil organic carbon; TN: Total nitrogen.

The average annual litterfall from 2011 to 2016 was found to be the highest in the natural forest (8.04 Mg hm^{-2}), followed by the ANR forest (6.15 Mg hm^{-2}), pine plantation (5.03 Mg hm^{-2}), and Chinese fir (4.63 Mg hm^{-2}) plantation. The conversion of the natural forest led to a significant decrease in annual leaf litterfall in the pine and Chinese fir plantations, but not in the ANR, with the lowest annual litterfall observed in the Chinese fir plantation. Similarly, the conversion of the natural forest led to a significant decrease in fine root biomass at the 0–10 cm soil layer in all the converted forests, with the lowest biomass being observed in the pine plantation (Figure 1).

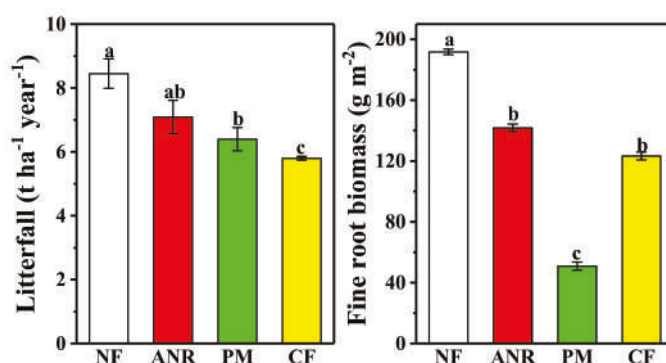


Figure 1. Litterfall and fine root biomass (0–10 cm) under different forest types; different lowercase letters indicate significant differences among the different forests. Values are means \pm standard errors ($n = 3$), Natural forest: NF; Natural regeneration forest: ANR; *Pinus massoniana* Lamb. forest: PM; Chinese fir forest: CF.

3.2. Concentrations of Amino Sugars in the Different Forests

Conversions of natural forest to either ANR forest or plantations led to significant decreases in the concentrations of GluN, MurA, and TAS at the 0–10 cm soil layers, whereas, for GalN, significant decreases were only observed in the pine plantation. The concentration of TAS was high in the natural forest (1850 mg kg^{-1}), which was reduced by 32% in the ANR forest (1250 mg kg^{-1}), by 43% in the Chinese fir plantation (1050 mg kg^{-1}), and by 54% in the pine plantation (850 mg kg^{-1}). All of the individual amino sugar and total amino sugar concentrations were significantly higher at the 0–10 cm than at the 10–20 cm soil layer for all forest types (Figure 2).

In the converted forests, there were significantly higher concentrations of GluN and TAS at the 0–10 cm soil layer in the ANR forest than in the pine plantation, but there were no significant differences in the concentrations of individual amino sugars or TAS at the 10–20 cm soil layers (Figure 2).

3.3. Amino Sugar Biomarker Ratios

Following the conversions of the natural forest, there was an approximately 20% decrease in the GluN/MurA ratios for the two plantations at the 0–10 cm soil layer, but there was no significant decrease at the 10–20 cm soil layer for all the converted forests (Figure 3).

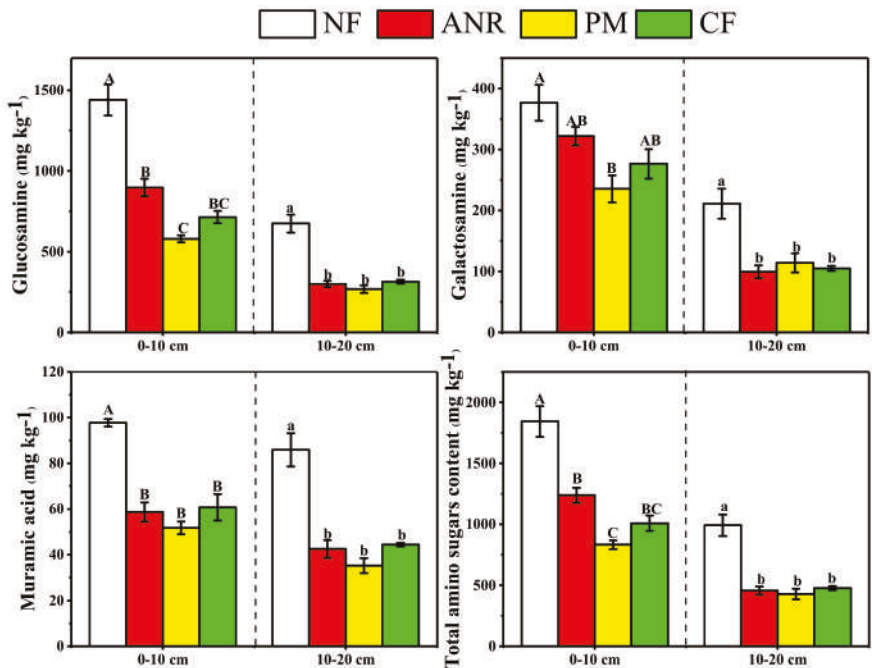


Figure 2. The concentration of soil amino sugars at different soil layers in different forest types; different uppercase letters indicate significant differences at 0–10 cm among the different forests, and different lowercase letters indicate significant differences at 10–20 cm among the different forests. Values are means \pm standard errors ($n = 3$), Natural forest: NF; Natural regeneration forest: ANR; *P. massoniana* forest: PM; Chinese fir forest: CF.

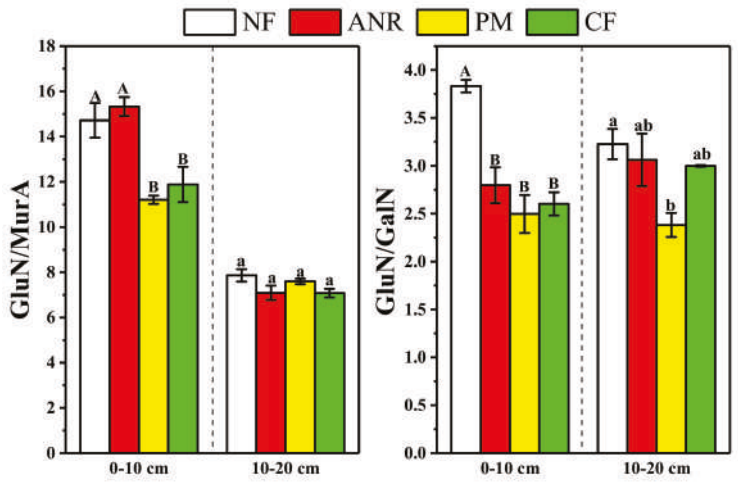


Figure 3. Ratios of glucosamine (GluN) to muramic acid (MurA) or to galactosamine (GalN) at different soil layers in different forest types; different uppercase letters indicate significant differences at 0–10 cm among the different forests, and different lowercase letters indicate significant differences at 10–20 cm among the different forests. Values are means \pm standard errors ($n = 3$), Natural forest: NF; Natural regeneration forest: ANR; *P. massoniana* forest: PM; Chinese fir forest: CF.

Conversions of the natural forest led to significant decreases in the GluN/GalN ratios for all of the converted forest types at the 0–10 cm soil layer. At the 10–20 cm soil layer, the natural forest conversion to pine plantation led to a significant decrease in the GluN/GalN ratio (Figure 3).

3.4. Ratios of TAS to SOC in the Different Forest Type

Conversions of the natural forest led to a significant increase in the ratios of TAS to SOC at the 0–10 cm soil layer, but there was no significant difference among the converted forests. No differences were observed in the ratios of TAS to SOC following conversions of the natural forest at the 10–20 cm soil layer, but there was a significantly higher ratio of TAS to SOC in the pine plantation than in the ANR (Figure 4).

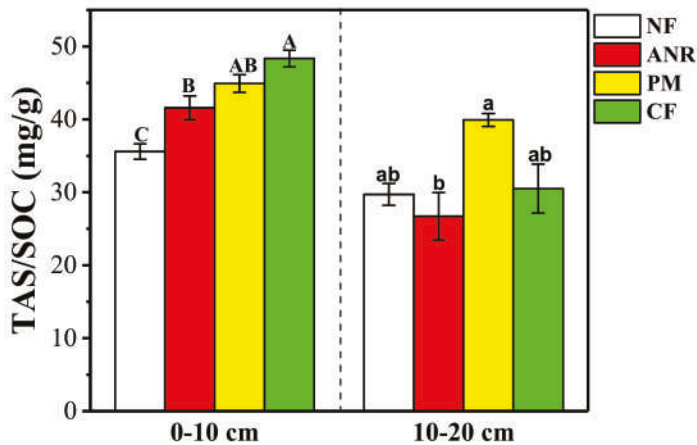


Figure 4. The proportion of total amino sugars to total soil organic carbon (TAS/SOC) in two soil layers under different forest types; different uppercase letters indicate significant differences at 0–10 cm among the different forests, and different lowercase letters indicate significant differences at 10–20 cm among the different forests. Values are means \pm standard errors ($n = 3$), Natural forest: NF; Natural regeneration forest: ANR; *P. massoniana* forest: PM; Chinese fir forest: CF.

3.5. Correlation between Amino Sugars and Soil Properties

Redundancy analysis indicated that the environmental factors explained 87.9% of the variance of soil amino sugars across four different forests, with axis 1 explaining 83.1% and axis 2 explaining 4.8% of the variance (Figure 5). The ordination biplot from RDA was clearly distinguished among the four forests. Forward selection of factors in the RDA ordinations revealed that variations in soil amino sugars were closely related to SOC, fine root biomass, litter fall, and available P.

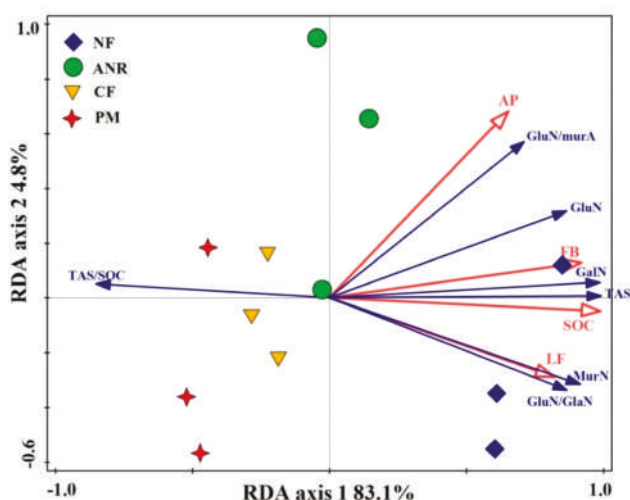


Figure 5. Correlations of soil amino sugar data to soil environmental factors determined by redundancy analysis (RDA). The amino sugar data included glucosamine (GluN), galactosamine (GalN), muramic acid (MurA), total amino sugar (TAS), ratios of glucosamine (GluN) to muramic acid, and proportion of total amino sugar to SOC (TAS/SOC). AP, available P; SOC, soil organic carbon; FB, fine root biomass, LF, litterfall; Natural forest: NF; Natural regeneration forest: ANR; *P. massoniana* forest: PM; Chinese fir forest: CF.

4. Discussion

4.1. Effects of Natural Forest Conversion on Concentrations of Soil Total C and Amino Sugars

Although a considerable disagreement remains regarding the effects of land-use change on soil C stocks [49], it is generally considered that the preservation of natural old-growth forests may be related to a much higher C sequestration than that by the promotion of forest regrowth in long-term C pools, in particular, in recalcitrant soil organic matter [50–52]. Our previous studies in the subtropics also showed a much higher soil C concentration in the older natural forest than in the secondary forests or plantations [44,53]. Consistent with this finding, in the present study, conversions of old natural forest result in over 40% decreases in soil C concentration in all of the converted forests (Table 1). Replacing old-growth forest by young stands will lead to massive soil C losses to the atmosphere, mainly by reducing the flux into a permanent pool of soil organic matter and by redistributing C between pools with different turnover times because of the disturbance effects of various intensities [54]. The converted forests had experienced several forest management disturbances before our experiment, and the present study showed that natural forest conversion has a profound effect on soil C stocks in the subtropical forest, which cannot be recovered to a pre-harvest level, even after over 40 years of forest regrowth.

We anticipate that forest conversion may affect not only the SOC dynamics, but also the variation of microbial residues, because microbial C residues are regarded as a significant contributor to SOC, owing to their relatively long residence time in soils [19,55–58]. As in hypothesis (1), we observed a generally significant reduction in the concentration of microbial residues, including GluN, GalN, MurA, and TAS, in the converted forests, with the lowest decrease of TAS being observed in the ANR forest and the highest decrease in the pine plantation (Figure 1). These results are consistent with the results of previous studies, which also show that land use and management substantially affected amino sugar concentrations [2,59,60]. High temperature and rainfall, steep slopes, and fragile soil characterize South China. Following natural forest conversion, increases in soil temperature and

erosion due to less forest cover in the initial forest regrowth generally led to accelerated SOC loss in the subtropics [44,61]. In particular, increased and intensive anthropogenic disturbance, such as slash burning and site preparation, contributed to higher SOC reduction in forest plantations [61]. Likewise, these aforementioned factors may also affect microbial residue accumulation in the different forest types, which the redundancy analysis that showed soil amino sugar concentrations were closely correlated with SOC and soil available P was confirmed (Figure 5). Most tropical and subtropical forests occur in highly weathered soil, where the available P is low [62,63]. The soil P availability could influence the activities, biomass, and compositions of soil microbial communities [64–66], which may also explain the amino sugar dynamics during the forest conversions.

Further, Liang et al. reported there was a tree species-specific effect on soil microbial residue accumulation in an old-growth forest ecosystem, with recalcitrant Eastern Hemlock litter making a relatively lower contribution of microbial residue to the total soil C [67]. When compared with the plantations, the ANR forest mostly consisted of broad leaf tree species, which, when compared to coniferous litter, could be conducive to microbial residue retention by increasing soil amino sugars [68]. Correlation analysis showed that soil amino sugar concentrations were positively correlated with fine root biomass and annual leaf litterfall (Figure 5). These factors could again explain the higher GluN, GalN, and TAS in the ANR forest than in the pine plantations (Figure 1). Unexpectedly, the absence of significant differences in all amino sugars was observed between the ANR forest and the Chinese fir plantation in the present study. This could result from the high fine root biomass in the Chinese fir plantations, mainly owing to a higher abundance of herbs and shrubs than those in other two converted forests [69]. The herbs and shrubs are ephemeral, which could lead to high input of fine root litter and eventually contribute to amino sugar accumulation.

The higher concentration of SOC in surface soil than in deeper soil may support more abundant microorganisms [70,71]. Thus, larger amounts of microbial residue accumulated at the 0–10 cm than at 10–20 cm soil depth in each forest that was observed in this study (Table 1). This was consistent with the results of previous studies [68,72,73].

4.2. Amino Sugar Biomarker Ratios

Ratios of GluN/MurA and GluN/GalN are normally used to indicate the contribution of fungal versus bacterial residues to SOC accumulation [20,23,25,57]. Land use change may affect the formation of microbial residues [7]. In this study, forest conversions resulted in dramatic declines in all of the examined amino sugars, including GluN, GalN, and MurA, but at different rates (Figure 1). The decrease of GluN/MurA ratios in the two plantations indicated a slower recovery of fungal communities relative to bacteria following natural forest conversion, which is in agreement with Hedlund et al., who argued that fungi, in particular, mycorrhizal fungi, may have less efficient dispersal and colonizing abilities after vegetation removal [74]. Among the converted forests, although there was no difference in TAS, different GluN/MurA ratios (Figure 2) may reflect the effect of land use intensification on amino sugar partition. Our finding of higher GluN/MurA ratios in the ANR forest indicated that slight anthropogenic disturbance is conducive to the accumulation of fungal derived microbial residue, which is in agreement with our hypothesis (2).

When compared to the 0–10 cm soil depth, at 10–20 cm, there was an approximately 40% decrease in GluN to MurA ratios (Figure 2). The reduction in fungal biomass and residues in subsoil might be related to the accumulation of less decomposed plant residues with an increasing depth. Moritz et al. [75] and Liang and Balser [17] observed similar decreases in the GluN to MurA ratio with depth. These decreases indicated that bacteria are more important in subsoil organic C turnover than are fungi. Fungi are aerobic organisms that typically utilize fresh litter as their preferred C source and generally successfully outcompete bacteria in the surface soils, particularly under acidic conditions [76]. With increasing depth, studies have typically shown a decrease in the relative abundance of fungi [70,75,77].

The absence of a difference in GluN/GalN rather than GluN/MurA ratios between the two soil depths was observed in this study (Figure 3), which is consistent with the result of Liang et al. [66] and

Moritz et al. [75]. Liang et al. argued that GluN/MurA and GluN/GalN indicated different aspects of the relative fungal to bacterial contribution or the relative retention times of various amino sugars in soil C dynamics [67].

4.3. Contribution of TAS to SOC in the Different Forest Types

Microbial residues are important constituents of SOC and they do not always change in the same pattern, as does the SOC dynamics [68]. Our previous studies showed a more pronounced loss of labile C than total SOC following the conversion of natural forest into plantations or secondary forests [44]. The present study shows a significant increase in the ratios of TAS to total SOC at the 0–10 cm soil depth in the converted forest, whereas no significant difference between the natural forest and converted forests occurred for the 10–20 cm soil depth (Figure 3). These results indicate the slower loss of microbial residue C than other soil C fractions following forest conversions, which suggests that microbial residue, as a refractory C, plays an important role in SOC storage, particularly in the surface 0–10 cm soil. Furthermore, lower increases of the TAS to total SOC ratio in the ANR forest than those in the two plantations may reflect that microbial residue is of greater importance in soil storage with the intensity of anthropogenic disturbance. Our findings support hypothesis (3), that forest conversions increase the ratios of microbial residue C to total C, with the highest increase in the two plantations.

We compared the effects of forest conversions that are based on the experiment of three replicate plots in each stand, which is not truly replicated. Therefore, our results should be cautiously interpreted because of an intrinsic error of pseudo-replication [78]. Furthermore, we should be critical of the scope of possible interpretation due to inevitable temporal and spatial heterogeneity derived from space for time substitution. It deserves special notice that all mean comparisons were expected to be a best-case scenario, because the error terms should be larger and mean separations should have a wider difference to allow for a true separation.

5. Conclusions

In the subtropics, natural forest conversions result in dramatic reductions, not only in SOC, but also in microbial residue C, which cannot be recovered, even after more than 40 years of forest regrowth. Microbial residue C accumulation varies with SOC and litter input constrained by forest management with various anthropogenic disturbances. As a recalcitrant C, microbial residue plays an important role in soil C storage following forest conversions. When comparing with tree plantations, natural forest conversion to the ANR forest had a significant effect in maintaining SOC, but not necessarily a significant effect on microbial residue accumulation.

Author Contributions: L.Y., C.L., X.Z. and Y.Y. designed the experiments; S.C., Y.L., Q.W. and L.Y. performed the experiments; C.L., L.Y., Y.Y. and Z.Y. analyzed the data, wrote and revised the paper.

Funding: The research was financially supported by the National Natural Science Foundation of China (No. 31770663, 31300523, 31130013, 31600433, and 31700545).

Acknowledgments: We are grateful to the two anonymous reviewers, whose comments help greatly improve this manuscript. Thanks also go to Jim Nelson for providing valuable comments and doing proofreading on the manuscript.

Conflicts of Interest: The authors declare no conflict of interest.

References

1. Liang, C.; Schimel, J.P.; Jastrow, J.D. The importance of anabolism in microbial control over soil carbon storage. *Nat. Microbiol.* **2017**, *2*, 17105. [[CrossRef](#)] [[PubMed](#)]
2. Ma, T.; Zhu, S.; Wang, Z.; Chen, D.; Dai, G.; Feng, B.; Su, X.; Hu, H.; Li, K.; Han, W.; et al. Divergent accumulation of microbial necromass and plant lignin components in grassland soils. *Nat. Commun.* **2018**, *9*, 3480. [[CrossRef](#)] [[PubMed](#)]
3. Liang, C.; Cheng, G.; Wixon, D.L.; Balser, T.C. An Absorbing Markov Chain approach to understanding the microbial role in soil carbon stabilization. *Biogeochemistry* **2011**, *106*, 303–309. [[CrossRef](#)]

4. Schimel, J.P.; Schaeffer, S.M. Microbial control over carbon cycling in soil. *Front. Microbiol.* **2012**, *3*, 1–11. [\[CrossRef\]](#)
5. Benner, R. Biosequestration of carbon by heterotrophic microorganisms. *Nat. Rev. Microbiol.* **2011**, *9*, 75. [\[CrossRef\]](#) [\[PubMed\]](#)
6. Liang, C.; Balser, T.C. Microbial production of recalcitrant organic matter in global soils: Implications for productivity and climate policy. *Nat. Rev. Microbiol.* **2011**, *9*, 75. [\[CrossRef\]](#)
7. Zhang, X.; Amelung, W.; Yuan, Y.; Samson-Liebig, S.; Brown, L.; Zech, W. Land-use effects on amino sugars in particle size fractions of an Argiudoll. *Appl. Soil Ecol.* **1999**, *11*, 271–275. [\[CrossRef\]](#)
8. Liang, C.; Balser, T.C. Warming and nitrogen deposition lessen microbial residue contribution to soil carbon pool. *Nat. Commun.* **2012**, *3*, 1222. [\[CrossRef\]](#)
9. Raich, J.W. Effects of Forest Conversion on the Carbon Budget of a Tropical Soil. *Biotropica* **1983**, *15*, 177–184.
10. Piquer-Rodríguez, M.; Torella, S.; Gavíer-Pizarro, G.; Volante, J.; Somma, D.; Ginzburg, R.; Kuemmerle, T. Effects of past and future land conversions on forest connectivity in the Argentine Chaco. *Landsc. Ecol.* **2015**, *30*, 817–833.
11. Jandl, R.; Lindner, M.; Vesterdal, L.; Bauwens, B.; Baritz, R.; Hagedorn, F.; Johnson, D.W.; Minkinen, K.; Byrne, K.A. How strongly can forest management influence soil carbon sequestration? *Geoderma* **2007**, *137*, 253–268. [\[CrossRef\]](#)
12. Post, W.M.; Kwon, K.C. Soil carbon sequestration and land-use change: processes and potential. *Chang. Boil.* **2000**, *6*, 317–327. [\[CrossRef\]](#)
13. Lal, R. Forest soils and carbon sequestration. *For. Ecol. Manag.* **2005**, *220*, 242–258. [\[CrossRef\]](#)
14. Schimel, J.; Balser, T.C.; Wallenstein, M. Microbial stress-response physiology and its implications for ecosystem function. *Ecology* **2007**, *88*, 1386–1394. [\[CrossRef\]](#) [\[PubMed\]](#)
15. Schimel, J. Microbial ecology: Linking omics to biogeochemistry. *Nat. Microbiol.* **2016**, *1*, 15028. [\[CrossRef\]](#) [\[PubMed\]](#)
16. Shao, P.; Liang, C.; Lynch, L.; Xie, H.; Bao, X. Reforestation accelerates soil organic carbon accumulation: Evidence from microbial biomarkers. *Soil Boil. Biochem.* **2019**, *131*, 182–190. [\[CrossRef\]](#)
17. Liang, C.; Balser, T.C. Preferential sequestration of microbial carbon in subsoils of a glacial-landscape toposequence, Dane County, WI, USA. *Geoderma* **2008**, *148*, 113–119. [\[CrossRef\]](#)
18. Joergensen, R.G. Amino sugars as specific indices for fungal and bacterial residues in soil. *Boil. Fertil. Soils* **2018**, *54*, 559–568. [\[CrossRef\]](#)
19. Amelung, W.; Miltner, A.; Zhang, X.; Zech, W. Fate of microbial residues during litter decomposition as affected by minerals. *Soil Sci.* **2001**, *166*, 598–606. [\[CrossRef\]](#)
20. Joergensen, R.G.; Wichern, F. Quantitative assessment of the fungal contribution to microbial tissue in soil. *Soil Boil. Biochem.* **2008**, *40*, 2977–2991. [\[CrossRef\]](#)
21. Reay, M.K.; Knowles, T.D.J.; Jones, D.L.; Evershed, R.P. Development of Alditol Acetate Derivatives for the Determination of ¹⁵N-Enriched Amino Sugars by Gas Chromatography–Combustion–Isotope Ratio Mass Spectrometry. *Anal. Chem.* **2019**, *91*, 3397–3404. [\[CrossRef\]](#)
22. Zhang, X.; Amelung, W. Gas chromatographic determination of muramic acid, glucosamine, mannosamine, and galactosamine in soils. *Soil Boil. Biochem.* **1996**, *28*, 1201–1206. [\[CrossRef\]](#)
23. Amelung, W.; Brodowski, S.; Sandhage-Hofmann, A.; Bol, R. Combining Biomarker with Stable Isotope Analyses for Assessing the Transformation and Turnover of Soil Organic Matter. *Adv. Agron.* **2008**, *100*, 155–250.
24. Parsons, J.W. Chemistry and Distribution of Amino Sugars in Soils and Soil Organisms. *Soil Biochem.* **1981**, *5*, 197–227.
25. Guggenberger, G.; Frey, S.D.; Six, J.; Paustian, K.; Elliott, E.T. Bacterial and Fungal Cell-Wall Residues in Conventional and No-Tillage Agroecosystems. *Soil Sci. Soc. J.* **1999**, *63*, 1188–1198. [\[CrossRef\]](#)
26. Pan, Y.; Birdsey, R.A.; Fang, J.; Houghton, R.; Kauppi, P.E.; Kurz, W.A.; Phillips, O.L.; Shvidenko, A.; Lewis, S.L.; Canadell, J.G.; et al. A Large and Persistent Carbon Sink in the World's Forests. *Science* **2011**, *333*, 988–993. [\[CrossRef\]](#) [\[PubMed\]](#)
27. Wang, Y.; Wang, H.; Xu, M.; Ma, Z.; Wang, Z.-L. Soil organic carbon stocks and CO₂ effluxes of native and exotic pine plantations in subtropical China. *CATENA* **2015**, *128*, 167–173. [\[CrossRef\]](#)

28. De Medeiros, E.V.; Duda, G.P.; Dos Santos, L.A.; de Sousa Lima, J.R.; de Almeida-Cort ez, J.S.; Hammecker, C.; Lardy, L.; Cournac, L. Soil organic carbon, microbial biomass and enzyme activities responses to natural regeneration in a tropical dry region in Northeast Brazil. *CATENA* **2017**, *151*, 137–146. [\[CrossRef\]](#)
29. Yang, Y.-S.; Chen, G.-S.; Guo, J.-F.; Xie, J.-S.; Wang, X.-G. Soil respiration and carbon balance in a subtropical native forest and two managed plantations. *Plant Ecol.* **2007**, *193*, 71–84. [\[CrossRef\]](#)
30. Murdiyarso, D.; Van Noordwijk, M.; Wasrin, U.R.; Tomich, T.P.; Gillison, A.N. Environmental benefits and sustainable land-use options in the Jambi transect, Sumatra. *J. Veg. Sci.* **2002**, *13*, 429–438. [\[CrossRef\]](#)
31. Yang, Y.S.; Guo, J.F.; Chen, G.S.; He, Z.M.; Xie, J.S. Effect of slash burning on nutrient removal and soil fertility in Chinese fir and evergreen broadleaved forests of mid-subtropical China. *Pedosphere* **2003**, *13*, 87–96.
32. Tian, D.; Yan, W.; Chen, X.; Deng, X.; Peng, Y.; Kang, W.; Peng, C. Variation in runoff with age of Chinese fir plantations in Central South China. *Hydrol. Process.* **2008**, *22*, 4870–4876. [\[CrossRef\]](#)
33. Chen, G.; Yang, Y.; Yang, Z.; Xie, J.; Guo, J.; Gao, R.; Yin, Y.; Robinson, D. Accelerated soil carbon turnover under tree plantations limits soil carbon storage. *Sci. Rep.* **2016**, *6*, 19693. [\[CrossRef\]](#)
34. Yang, Y.; Wang, L.; Yang, Z.; Xu, C.; Xie, J.; Chen, G.; Lin, C.; Guo, J.; Liu, X.; Xiong, D.; et al. Large Ecosystem service benefits of assisted natural regeneration. *J. Geophys. Res. Biogeosci.* **2018**, *123*, 676–687. [\[CrossRef\]](#)
35. Shono, K.; Cadaweng, E.A.; Durst, P.B. Application of Assisted Natural Regeneration to Restore Degraded Tropical Forestlands. *Restor. Ecol.* **2007**, *15*, 620–626. [\[CrossRef\]](#)
36. Chazdon, R.L.; Guariguata, M.R. Natural regeneration as a tool for large-scale forest restoration in the tropics: prospects and challenges. *Biotropica* **2016**, *48*, 716–730. [\[CrossRef\]](#)
37. Shoo, L.P.; Catterall, C.P. Stimulating Natural Regeneration of Tropical Forest on Degraded Land: Approaches, Outcomes, and Information Gaps. *Restor. Ecol.* **2013**, *21*, 670–677. [\[CrossRef\]](#)
38. Liu, L.; Gundersen, P.; Zhang, T.; Mo, J. Effects of phosphorus addition on soil microbial biomass and community composition in three forest types in tropical China. *Soil Biol. Biochem.* **2012**, *44*, 31–38. [\[CrossRef\]](#)
39. Tang, X.L.; Liu, S.G.; Zhou, G.Y.; Zhang, D.Q.; Zhou, C.Y. Soil-atmospheric exchange of CO₂, CH₄, and N₂O in three subtropical forest ecosystems in southern China. *Glob. Chang. Biol.* **2006**, *12*, 546–560. [\[CrossRef\]](#)
40. Wan, X.; Huang, Z.; He, Z.; Yu, Z.; Wang, M.; Davis, M.R.; Yang, Y. Soil C:N ratio is the major determinant of soil microbial community structure in subtropical coniferous and broadleaf forest plantations. *Plant Soil* **2015**, *387*, 103–116. [\[CrossRef\]](#)
41. Odum, E.P. The Strategy of Ecosystem Development. *Science* **1969**, *164*, 262–270. [\[CrossRef\]](#) [\[PubMed\]](#)
42. Odum, E.P. Trends Expected in Stressed Ecosystems. *BioScience* **1985**, *35*, 419–422. [\[CrossRef\]](#)
43. Zhou, Z.; Wang, C.; Luo, Y. Effects of forest degradation on microbial communities and soil carbon cycling: A global meta-analysis. *Glob. Ecol. Biogeogr.* **2018**, *27*, 110–124. [\[CrossRef\]](#)
44. Yang, Y.; Guo, J.; Chen, G.; Yin, Y.; Gao, R.; Lin, C. Effects of forest conversion on soil labile organic carbon fractions and aggregate stability in subtropical China. *Plant Soil* **2009**, *323*, 153–162. [\[CrossRef\]](#)
45. State Soil Survey Service of China (SSSSC). *China Soil*; China Agricultural Press: Beijing, China, 1998. (In Chinese)
46. Yang, Y.-S.; Chen, G.-S.; Lin, P.; Xie, J.-S.; Guo, J.-F. Fine root distribution, seasonal pattern and production in four plantations compared with a natural forest in Subtropical China. *Ann. For. Sci.* **2004**, *61*, 617–627. [\[CrossRef\]](#)
47. Liu, X.; Yang, Z.; Lin, C.; Giardina, C.P.; Xiong, D.; Lin, W.; Chen, S.; Xu, C.; Chen, G.; Xie, J.; et al. Will nitrogen deposition mitigate warming-increased soil respiration in a young subtropical plantation? *Agric. Meteorol.* **2017**, *246*, 78–85. [\[CrossRef\]](#)
48. Sibbesen, E. An investigation of the anion-exchange resin method for soil phosphate extraction. *Plant Soil* **1978**, *50*, 305–321. [\[CrossRef\]](#)
49. Powers, J.S.; Corre, M.D.; Twine, T.E.; Veldkamp, E. Geographic bias of field observations of soil carbon stocks with tropical land-use changes precludes spatial extrapolation. *Proc. Natl. Acad. Sci. USA* **2011**, *108*, 6318–6322. [\[CrossRef\]](#)
50. Luyssaert, S.; Schulze, E.D.; B rner, A.; Knohl, A.; Hessenm ller, D.; Law, B.E.; Ciais, P.; Grace, J. Old-growth forests as global carbon sinks. *Nature* **2008**, *455*, 213. [\[CrossRef\]](#)
51. Dybala, K.E.; Matzek, V.; Gardali, T.; Seavy, N.E. Carbon sequestration in riparian forests: A global synthesis and meta-analysis. *Glob. Chang. Biol.* **2019**, *25*, 57–67. [\[CrossRef\]](#)
52. Silver, W.L.; Kueppers, L.M.; Lugo, A.E.; Ostertag, R.; Matzek, V. Carbon sequestration and plant community dynamics following reforestation of tropical pasture. *Ecol. Appl.* **2004**, *14*, 1115–1127. [\[CrossRef\]](#)

53. Sheng, H.; Yang, Y.; Yang, Z.; Chen, G.; Xie, J.; Guo, J.; Zou, S. The dynamic response of soil respiration to land-use changes in subtropical China. *Glob. Chang. Boil.* **2010**, *16*, 1107–1121. [[CrossRef](#)]
54. Schulze, E.D.; Wirth, C.; Heimann, M. Climate change: Managing forests after Kyoto. *Science* **2000**, *289*, 2058–2059. [[CrossRef](#)] [[PubMed](#)]
55. Kiem, R.; Kögel-Knabner, I. Contribution of lignin and polysaccharides to the refractory carbon pool in C-depleted arable soils. *Soil Boil. Biochem.* **2003**, *35*, 101–118. [[CrossRef](#)]
56. Glaser, B.; Turrión, M.-B.; Alef, K. Amino sugars and muramic acid—biomarkers for soil microbial community structure analysis. *Soil Boil. Biochem.* **2004**, *36*, 399–407. [[CrossRef](#)]
57. Throckmorton, H.M.; Bird, J.A.; Monte, N.; Doane, T.; Firestone, M.K.; Horwath, W.R. The soil matrix increases microbial C stabilization in temperate and tropical forest soils. *Biogeochemistry* **2015**, *122*, 35–45. [[CrossRef](#)]
58. Keiluweit, M.; Wanzek, T.; Kleber, M.; Nico, P.; Fendorf, S. Anaerobic microsites have an unaccounted role in soil carbon stabilization. *Nat. Commun.* **2017**, *8*, 1771. [[CrossRef](#)] [[PubMed](#)]
59. Guan, Z.-H.; Li, X.G.; Wang, L.; Mou, X.M.; Kuzyakov, Y. Conversion of Tibetan grasslands to croplands decreases accumulation of microbially synthesized compounds in soil. *Soil Boil. Biochem.* **2018**, *123*, 10–20. [[CrossRef](#)]
60. Ye, G.; Lin, Y.; Kuzyakov, Y.; Liu, D.; Luo, J.; Lindsey, S.; Wang, W.; Fan, J.; Ding, W. Manure over crop residues increases soil organic matter but decreases microbial necromass relative contribution in upland Ultisols: Results of a 27-year field experiment. *Soil Biol. Biochem.* **2019**, *134*, 15–24. [[CrossRef](#)]
61. Chen, G.-S.; Yang, Y.-S.; Xie, J.-S.; Guo, J.-F.; Gao, R.; Qian, W. Conversion of a natural broad-leaved evergreen forest into pure plantation forests in a subtropical area: Effects on carbon storage. *Ann. For. Sci.* **2005**, *62*, 659–668. [[CrossRef](#)]
62. Li, J.; Li, Z.; Wang, F.; Zou, B.; Chen, Y.; Zhao, J.; Mo, Q.; Li, Y.; Li, X.; Xia, H. Effects of nitrogen and phosphorus addition on soil microbial community in a secondary tropical forest of China. *Biol. Fertil. Soils* **2015**, *51*, 207–215. [[CrossRef](#)]
63. Turner, B.L.; Brenes-Arguedas, T.; Condit, R. Pervasive phosphorus limitation of tree species but not communities in tropical forests. *Nature* **2018**, *555*, 367–370. [[CrossRef](#)] [[PubMed](#)]
64. Tang, X.; Placella, S.A.; Daydé, F.; Bernard, L.; Robin, A.; Journet, E.-P.; Justes, E.; Hinsinger, P. Phosphorus availability and microbial community in the rhizosphere of intercropped cereal and legume along a P-fertilizer gradient. *Plant Soil* **2016**, *407*, 119–134. [[CrossRef](#)]
65. Cleveland, C.C.; Townsend, A.R.; Schmidt, S.K. Phosphorus Limitation of microbial processes in moist tropical forests: Evidence from short-term laboratory incubations and field studies. *Ecosystems* **2002**, *5*, 680–691. [[CrossRef](#)]
66. Treseder, K.K.; Allen, M.F. Direct nitrogen and phosphorus limitation of arbuscular mycorrhizal fungi: a model and field test. *New Phytol.* **2002**, *155*, 507–515. [[CrossRef](#)]
67. Liang, C.; Fujinuma, R.; Wei, L.; Balser, T.C. Tree species-specific effects on soil microbial residues in an upper Michigan old-growth forest system. *Forestry* **2007**, *80*, 65–72. [[CrossRef](#)]
68. Shao, S.; Zhao, Y.; Zhang, W.; Hu, G.; Xie, H.; Yan, J.; Han, S.; He, H.; Zhang, X. Linkage of microbial residue dynamics with soil organic carbon accumulation during subtropical forest succession. *Soil Boil. Biochem.* **2017**, *114*, 114–120. [[CrossRef](#)]
69. Guo, J.; Yang, Z.; Lin, C.; Liu, X.; Chen, G.; Yang, Y. Conversion of a natural evergreen broadleaved forest into coniferous plantations in a subtropical area: effects on composition of soil microbial communities and soil respiration. *Boil. Fertil. Soils* **2016**, *52*, 799–809. [[CrossRef](#)]
70. Fierer, N.; Schimel, J.P.; Holden, P.A. Variations in microbial community composition through two soil depth profiles. *Soil Boil. Biochem.* **2003**, *35*, 167–176. [[CrossRef](#)]
71. Steenwerth, K.L.; Drenovsky, R.E.; Lambert, J.J.; Kluepfel, D.A.; Scow, K.M.; Smart, D.R. Soil morphology, depth and grapevine root frequency influence microbial communities in a Pinot noir vineyard. *Soil Boil. Biochem.* **2008**, *40*, 1330–1340. [[CrossRef](#)]
72. Zhang, B.; Liang, C.; He, H.; Zhang, X. Variations in Soil Microbial Communities and Residues Along an Altitude Gradient on the Northern Slope of Changbai Mountain, China. *PLoS ONE* **2013**, *8*, e66184. [[CrossRef](#)] [[PubMed](#)]

73. Sradnick, A.; Oltmanns, M.; Raupp, J.; Joergensen, R.G. Microbial residue indices down the soil profile after long-term addition of farmyard manure and mineral fertilizer to a sandy soil. *Geoderma* **2014**, *226*, 79–84. [\[CrossRef\]](#)
74. Hedlund, K.; Griffiths, B.; Christensen, S.; Scheu, S.; Setälä, H.; Tscharnkte, T.; Verhoef, H. Trophic interactions in changing landscapes: responses of soil food webs. *Basic Appl. Ecol.* **2004**, *5*, 495–503. [\[CrossRef\]](#)
75. Moritz, L.K.; Liang, C.; Wagai, R.; Kitayama, K.; Balser, T.C. Vertical distribution and pools of microbial residues in tropical forest soils formed from distinct parent materials. *Biogeochemistry* **2009**, *92*, 83–94. [\[CrossRef\]](#)
76. Turrión, M.B.; Glaser, B.; Zech, W. Effects of deforestation on contents and distribution of amino sugars within particle-size fractions of mountain soils. *Soil. Fertil. Soils* **2002**, *35*, 49–53. [\[CrossRef\]](#)
77. Taylor, J.P.; Wilson, B.; Mills, M.S.; Burns, R.G. Comparison of microbial numbers and enzymatic activities in surface soils and subsoils using various techniques. *Soil Biol. Biochem.* **2002**, *34*, 387–401. [\[CrossRef\]](#)
78. Hurlbert, S.H. Pseudoreplication and the Design of Ecological Field Experiments. *Ecol. Monogr.* **1984**, *54*, 187–211. [\[CrossRef\]](#)



© 2019 by the authors. Licensee MDPI, Basel, Switzerland. This article is an open access article distributed under the terms and conditions of the Creative Commons Attribution (CC BY) license (<http://creativecommons.org/licenses/by/4.0/>).

Article

Evaluation of Forest Conversion Effects on Soil Erosion, Soil Organic Carbon and Total Nitrogen Based on ^{137}Cs Tracer Technique

Xi Zhu ¹, Jie Lin ^{1,*}, Qiao Dai ¹, Yanying Xu ¹ and Haidong Li ²

¹ Co-Innovation Center for Sustainable Forestry in Southern China of Jiangsu Province, Key Laboratory of Soil and Water Conservation and Ecological Restoration of Jiangsu Province, Nanjing Forestry University, Nanjing 210037, China; 13913410166@163.com (X.Z.); D2313238461@163.com (Q.D.); xyy1414@163.com (Y.X.)

² Nanjing Institute of Environmental Sciences, Ministry of Ecology and Environment, Nanjing 210042, China; lhd@nies.org

* Correspondence: jielin@njfu.edu.cn

Received: 8 April 2019; Accepted: 13 May 2019; Published: 20 May 2019

Abstract: Soil erosion can affect the horizontal and the vertical distribution of soil carbon at the landscape scale. The ^{137}Cs tracer technique can overcome the shortcomings of traditional erosion research and has proven to be the best method to study soil erosion. To understand the responses of soil organic carbon and nitrogen to soil erosion and forest conversion in the development of slope economic forests in rocky mountain areas, three representative types of economic forests that were all formed after clear-cutting and afforestation on the basis of CBF (coniferous and broad-leaved mixed forests) were selected: CF (chestnut forests) with small human disturbance intensity, AF (apple forests), and HF (hawthorn forests) with high interference intensity. The results showed that all land use types have significantly eroded since 1950; the average annual loss of soil was 0.79 mm in the CBF, 2.31 mm in the AF, 1.84 mm in the HF, and 0.87 mm in the CF. The results indicated aggravation of soil erosion after the transformation of the CBF into an economic forest. The economic forest management reduced the average carbon storage and accelerated nutrient loss. The better vegetation coverage and litter coverage of CF made them stand out among the three economic forest varieties. Therefore, when developing economic forests, we should select species that can produce litter to ensure as much soil conservation as possible to reduce the risk of soil erosion.

Keywords: land use types; soil organic carbon; soil total nitrogen

1. Introduction

Forest ecosystems play a significant role in climate change mitigation by the uptake of a substantial portion of carbon dioxide (CO_2) from the atmosphere as well as their long-term deposition into biomass and soil [1,2]. Afforestation has proven to be an effective method for increasing C stocks [3–5]. However, the growth of the economy and the population drove up demand for forest products, facilitating forest conversion. Many studies showed that such forest conversion (i.e., forest-for-economic forest) may lead to soil erosion and other ecological problems [6,7]. Similarly, soil erosion—which is a worldwide problem with both social and environmental consequences—has proven to lead to lateral and vertical migration of nutrients [8].

The dynamic research on soil carbon and nitrogen storage and migration has attracted increasingly more scholars' attention worldwide [9–11]. In recent years, scholars have carried out extensive studies on the effects of soil erosion on soil organic carbon in sloping farmland [12–20]. However, few studies have been reported on soil erosion caused by forest transformation and the horizontal migration of soil nutrients. Therefore, it was necessary to systematically study how SOC (soil organic carbon) and TN (total nitrogen) respond to soil erosion after forest conversion.

China has the greatest area of forest plantations on a global scale, consisting of one fourth of the total plantation area [21]. Since the 1960s, the area of forests has rapidly increased to satisfy the ever-growing requirements for wood and other forest products in northeastern China, which has led to a series of serious ecological and environmental problems, such as soil erosion (especially water erosion) [22]. After transforming forests into economic forests, the structure of forests become uniform. Climate, biomass production, and plant distribution can also be totally changed [23–25]. Researchers have found reductions in soil C storage following forest conversion from natural forests to plantations [26,27]. In order to facilitate forest management, shrubs and weeds in forests are often removed. Such a change of vegetation cover can affect both the biological and the chemical properties of the soil, such as belowground C and nutrient storage [28]. Previous studies have also reported that water erosion is a pivotal process that can affect the horizontal migration and the redistribution of SOC and TN [29,30]. However, there have been few reports on how natural forest conversion into economic forests affects soil erosion, SOC, and TN. This is an important environmental issue that has not been well quantified.

Soil erosion caused by man-made, forced interference has received more and more attention [31–35]. Most of these studies made use of traditional RUSLE (revised universal soil loss equation) and evaluated large-scale changes in soil erosion intensity and spatial patterns by remote sensing and GIS. Traditional erosion research methods often miss information such as the soil erosion process and the land use change [36,37], while the ^{137}Cs tracer technology can overcome the shortcomings of traditional erosion research [38]. Under the background of global large-scale nuclear explosion tests in the 1950s and the 1970s, the ^{137}Cs tracer method was developed, and it has been widely used in soil erosion research at different spatial scales around the world since the 1990s [20,39]. This method has the characteristics of simplicity, high quantification degree, low research cost, and reliable results. It has been proven to be the best method to study soil erosion [40].

In this study, the goal was to explore the influence of forest conversion on soil erosion and carbon and nitrogen migration by using ^{137}Cs in order to provide a theoretical basis for the further rational utilization and protection of soil resources and to assist the in-depth study on the regional carbon and nitrogen balance. The specific goals were to answer the following questions: (a) How do the characteristics of soil thickness and nutrient change with forest conversion? (b) How does forest conversion affect the vertical distribution characteristics of soil organic carbon and total nitrogen after forest conversion? (c) How does the storage of SOC and TN change after forest conversion? (d) Through the comparison of the studied forest types, which is the best forest type for conversion? In order to assess how forest conversion into economic forests affects soil erosion as well as SOC and TN, this study chose the study area of the great Wu mountain valley. The basin is situated at the starting point of the Belt Road, Lianyungang, which was originally a coniferous and broad-leaved mixed forest (CBF). However, in the 1970s, the economic forest should have transformed in a short time.

2. Materials and Methods

2.1. Study Sites

Dawu Mountain (35°11' E, 118°50' N) is located in the northwest of Ganyu District, Lianyungang, Jiangsu province, Southeast China (Figure 1). It belongs to a warm-temperate maritime monsoon climate with four distinct seasons, an average annual temperature of 13.9 °C, an annual rainfall of 976.6 mm, a frost-free period of 216 days, and average annual sunshine of 2534 h. The soil is a subcategory of coarse-grained brown soil with more sand and gravel in the topsoil. The vegetation is a temperate deciduous broad-leaved forest area dominated by artificial forests, supplemented by a small amount of natural deciduous broad-leaved forests and evergreen coniferous forests, including secondary vegetation such as Masson pine, broad-leaved trees, and arborvitae, and economic trees such as hawthorn and chestnut. Most of the research area was originally planted on the open forestland at the end of the 20th century. By the beginning of the 21st century, part of the plantation forest was in

a state of natural regeneration, and some plantations were transformed into economic forests. In the experimental area, coniferous and broad-leaved mixed forests are the representative stand types of planted forests. The main tree species include *Pinus massoniana* Lamb., *Platycladus orientalis* (L.) Franco, sapling trees, and *Metasequoia glyptostroboides* Hu et W. C. Cheng, and there are herbs and humus layers under the forest. The hawthorn forest, the chestnut forest, and the apple forest are all economic forests that have been transformed by a mixed forest of coniferous and broad-leaved forest in which the surface of the chestnut forest is covered with litter, the surfaces of the hawthorn and the apple forests are exposed, and there are obvious artificial tilling traces. Basic information of different land use types was shown in Table 1.

In July 2016, field sampling was conducted to avoid the influence of topography, landforms, and elevation on the results of the study. Based on field surveys, the same parent material and relative geographical location were selected on the slope according to the principles of typicality and representativeness. According to the principles of typicality and representativeness, three sites, each of which has the same parent material and relatively centralized geographical location, were selected on the sloping land, including the HF (hawthorn forest), the AF (apple forest), the CF (chestnut forest), and the CBF. The three economic forests (HF, AF, and CF) were all formed after clear-cutting and afforestation on the basis of coniferous and broad-leaved mixed forests. The CBF was replanted after the replanting of the woodland. The forest age is approximately 10 years, and the slope is 10° – 15° , from which it can be assumed that the soil properties of all the plots were similar before the economic forest regeneration. The CBF is an artificial forest with no interference. The CF is an economic forest with less human interference intensity, while the HF and the AF are economic forests with greater interference intensity.



Figure 1. Location of the study site.

2.2. Sampling and Measuring Methods

Using the S-shaped sampling strategy, five sampling points in each sample were placed. The soil samples were collected by 0–10, 10–20, and 20–30 cm, and the same soil samples were mixed into three layered soil samples. At the same time, the soil samples were collected using a 100 cm³ standard ring knife. In order to determine the content of the nuclide in the soil, the whole sample of the 0–20 cm soil and the spaced 5 cm stratified sample were collected with the diameter of a 5 cm soil drill. After returning to the laboratory, the soil sample collected by the non-earth drills was naturally air-dried, and plant debris, small stones, and organisms were removed. Some of them were kept, as they were found along the natural cracks to form small clusters of approximately 1 cm³ to classify the aggregates. The other part was milled through a 2 mm sieve and was used for the determination of soil-related properties. After removing the stone weeds, the soil samples used for the determination of isotopes

were naturally air-dried after being ground through a 20-mesh sieve, dried in an oven at 105 °C to a constant weight, cooled to room temperature, and weighed with a precision of 0.001 g (ultimately weighing 300 g).

The physical and the chemical properties of the soil were measured according to the national standard. The soil bulk density was measured by the ring knife method. The pH was measured by an acidity meter. The total nitrogen, carbon, and nitrogen ratio and the ratio of carbon and hydrogen were measured by the element analyzer. The organic carbon content of the soil was oxidized with the potassium dichromate-external heating method. The mechanical composition was measured by a laser particle size analyzer (grading standard: 0.002, 0.05, and 2 mm). The specific surface area of the soil was analyzed using an ASAP2020 automatic surface area and pore size distribution analyzer (Micromeritics Instrument Corp, Atlanta, GA, USA). The soil water-soluble organic carbon was determined by weighing 5 g over a 2 mm screen soil in a 100 mL centrifuge tube, adding 25 mL of water, shaking, centrifuging, and taking the supernatant and filtering with a 0.45 µm microporous membrane to obtain the solution. At last, it was poured into a TOC (total organic carbon) sample tube and measured on a Shimadzu TOC-VCPH automatic analyzer [41]. The test of the nuclide ^{137}Cs used the background gamma spectrometer produced by the ORTEC Company (Dallas, TX, USA) of the United States and the C coaxial high pure germanium probe of the type GEM-40190 of the probe. The measurement time of each sample was 25,000 s, and the specific activity of the soil sample was calculated by a comparison with the standard source.

2.3. Calculation of the Soil ^{137}Cs

In this study, the top of Dawu Mountain was chosen as the background value point because there was no artificial activity on the top of the mountain, and the terrain was flat. The woodland structure is dominated by arbors, and the meadows are dominated by *Pinus massoniana*. Through the determination of two background value sampling points, the background value of ^{137}Cs was determined to be 1732.48 Bq/m². The ^{137}Cs content in soil was calculated using Formula (1).

$$CPI = \sum_{i=1}^n 1000 \times C_i \times Bd_i \times D_i \quad (1)$$

CPI is ^{137}Cs per unit area activity of the sampling point, Bq/m²; i is the sampling sequence number; n is the sampling layer number; 1000 is the unit correction factor; C_i is the specific activity of ^{137}Cs in the sampling layer i , Bq/kg; Bd_i is the soil bulk density of the sampling layer of layer i , g/cm³; D_i is the depth of sampling layer i , m.

The soil erosion modulus was calculated using the following models:

$$A(d) = A_{ref}(1 - e^{-\lambda d}) \quad (2)$$

$$h = -\frac{1}{(t - 1963)\lambda} \ln\left[1 - \frac{Y}{100}\right] \quad (3)$$

$$Y = 100(A_{ref} - A)/A_{ref} \quad (4)$$

$$E_R = 10000 \times h \times D \quad (5)$$

$A(d)$ is the total area activity of the soil above depth d , Bq/m²; A_{ref} is the ^{137}Cs area activity background value, Bq/m²; λ is the profile index of ^{137}Cs depth distribution, cm⁻¹. T is the sampling year; Y is the ^{137}Cs area activity of the measured relative background value reduction percentage, %; D is the soil bulk density, g/cm³; h is the erosion of years of erosion thickness, m/a; E_R is the soil erosion modulus, t/(km²·a).

2.4. Calculation the Storage and Loss of Soil Carbon and Nitrogen

The xth nutrient density per unit soil area is:

$$D_x = 0.01 \sum_{i=1}^n C_i \times d_i \times b_i \quad (6)$$

where D_x is the xth nutrient density (g/m^2); C_i is the xth nutrient content in the soil i layer (g/kg); b_i is the bulk density of the i layer soil (g/cm^3); d_i is the thickness of the i layer of soil (cm).

The absolute loss of the xth nutrient per unit area is:

$$L_X = 10 \times C_X \times D \times h \quad (7)$$

where L_X is the absolute loss of the xth nutrient (t/km^2); C_X is the xth nutrient content in the soil (g/kg); D is the soil bulk density (kg/m^3); h is the average annual loss of the soil thickness (m).

The relative loss rate of soil nutrient per unit area:

$$R = L_X / D_X \quad (8)$$

where R is the relative loss rate of the nth nutrient per unit area (%).

2.5. Data Processing and Analysis

Mean values were calculated for each of the variables, and one-way ANOVA was used to evaluate forest type and soil depth on the measured variables for pairwise comparison. The least significant difference (LSD) test was used for mean comparison of two forest types at the same soil depth and different soil depth in the same forest type at $p < 0.05$. The relationships between the ^{137}Cs and SOC or TN were evaluated by Pearson's correlation analysis. These statistical analyses were completed with the R language (Vienna University: Vienna, Austria) and SPSS 19.0. (SPSS Inc: Chicago, IL, USA). The graphics were plotted with Origin software (Publisher: city, country OriginLab: Northampton, MA, USA).

Table 1. Basic information of different land use types.

| Land Use Type | Forest Age (year) | LAI | Litter Thickness (mm) | Slope (°) | Aspect | pH | Soil Bulk Density/ g cm^{-3} | Sand/% | Silt/% | Clay/% |
|---------------|-------------------|-----|-----------------------|-----------|--------|-----------------|---------------------------------------|------------------|------------------|-----------------|
| HF | 11 | 2.1 | 0 | 15 | SE | 5.67 ± 0.27 | 1.42 ± 0.12 | 30.84 ± 5.05 | 65.00 ± 5.63 | 4.16 ± 0.36 |
| CF | 13 | 2.5 | 1.1 | 11 | SE | 5.95 ± 0.34 | 1.43 ± 0.05 | 31.57 ± 7.83 | 64.66 ± 6.66 | 3.77 ± 0.18 |
| AF | 10 | 2.2 | 0 | 13 | SE | 5.48 ± 0.26 | 1.47 ± 0.18 | 41.07 ± 8.65 | 56.63 ± 4.36 | 2.29 ± 0.23 |
| CBF | 25 | 3.2 | 1.3 | 13 | SE | 5.67 ± 0.27 | 1.44 ± 0.12 | 36.59 ± 7.53 | 60.21 ± 6.96 | 3.20 ± 0.41 |

Note: all data are expressed in mean \pm SE (standard error), which were calculated based on three samples. CBF: coniferous and broad-leaved mixed forest; HF: hawthorn forest; AF: apple forest; CF: chestnut forest; LAI: leaf area index.

3. Results

3.1. Characteristics of ^{137}Cs and Annual Erosion Modulus after Forest Conversion.

In comparison with the CBF, the specific activity of the ^{137}Cs decreased to 92%, 82%, and 36% at the 0–10 cm soil depth in AF, HF, and CF, respectively (Figure 2A). The CBF had the largest difference between the two soil layers, with the 0–10 cm layer 2.04 times that of the 10–20 cm layer. The specific activities of the ^{137}Cs in CH and CF were 1.28 and 1.06 times greater in 0–10 cm layer compared to the 10–20 cm layer, respectively. The results of the LSD analysis showed that, in the 0–10 cm soil layer, the average ^{137}Cs activity of the soil in CBF was significantly greater than that of the other three land use depths. In the 10–20 cm soil depth, the average ^{137}Cs specific activities in CBF and CF were significantly higher than those in HF and AF.

Compared with the background value, the ¹³⁷Cs content of all land use types was significantly lower than the background value of 1732.48 Bq·m². Among them, CBF decreased the least, which was 68.43% (Table 2). AF decreased the most by 96.50%. The annual soil erosion thickness for different land use types followed the order of AF (2.31 mm) > HF (1.84 mm) > CF (0.87 mm) > CBF (0.79 mm). In comparison with the CBF, the annual soil erosion thickness of AF and HF increased 192% and 133%, respectively (Figure 2B). Moreover, the annual soil erosion thickness significantly differed between the CBF and the economic forests (AF and HF). However, there was no significant difference between CBF and CF. The correlation analysis showed that the ¹³⁷Cs activity in the soil showed a significant positive correlation with the content of soil organic carbon and total nitrogen (*p* < 0.05) (Table 3).

Table 2. ¹³⁷Cs loss in different land use types.

| Land Use Types | Depth/cm | ¹³⁷ Cs Content/Bq·m ^{−2} | Percentage ¹³⁷ Cs Loss/% |
|----------------|----------|--|-------------------------------------|
| CBF | 0–20 | 546.92 | 68.4 |
| HF | 0–20 | 123.88 | 92.9 |
| AF | 0–20 | 60.60 | 96.5 |
| CF | 0–20 | 495.89 | 71.4 |

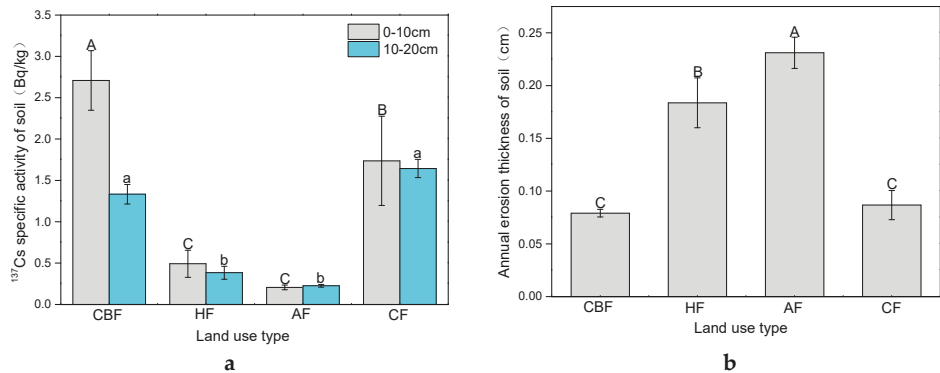


Figure 2. ¹³⁷Cs levels and the annual loss in soil depth under different land use types. Note: bars represent ± SE of the mean (*n* = 3). Different letters indicate significant differences in the same layer and different land use types (*p* < 0.05). (a) represents specific activity of soil ¹³⁷Cs in each layer with different land use types; (b) represents average annual loss thickness of soil in different land use types.

Table 3. Correlation between ¹³⁷Cs and soil chemical properties.

| | TN | TP | TK | SOC | DOC | C/N | C/H |
|------|---------|-------|-------|---------|------|--------|------|
| Cor. | 0.54 ** | −0.18 | −0.03 | 0.56 ** | 0.11 | 0.49 * | 0.40 |
| P | 0.006 | 0.39 | 0.99 | 0.005 | 0.60 | 0.02 | 0.05 |
| N | 24 | 24 | 24 | 24 | 24 | 24 | 24 |

TN: total nitrogen; TP: total phosphorus; TK: total kalium; SOC: soil organic carbon; DOC: dissolved organic carbon; C/N: carbon/ nitrogen; C/H: carbon/hydrogen. * Significant correlation was found at the level of $\alpha = 0.05$ and ** at the level of $\alpha = 0.01$.

3.2. SOC and TN Storage after Forest Conversion

The average SOC and TN storages in the CBF were 3.33 kg/m² and 0.36 kg/m², respectively, and the economic forest management reduced the SOC storage and the TN storage of the soil (Figure 3). In comparison with the CBF, the SOC storage and the TN storage in AF were the lowest, decreasing by 63.66% and 52.78%. The SOC (TN) storages in HF and CF decreased by 49.25% (38.89%) and 61.26% (50%), respectively. The results of the LSD analysis showed that the SOC and the TN storage in different

land use types did not change significantly with the soil layers. Among three economic forests, the SOC and the TN storage of the CF were significantly greater than those of the other three types of land use ($p < 0.05$). In the 20–30 cm soil layer, the SOC storage of the HF was significantly higher than that of the AF ($p < 0.05$). In the other two layers, there was no significant difference in the SOC storage of the three economic forests.

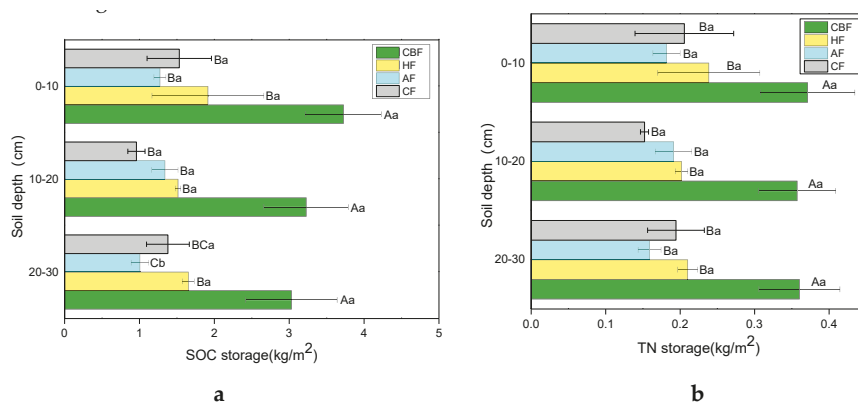


Figure 3. The TN and the SOC stocks under different land use types. Note: bars represent \pm SE of the mean ($n = 3$). Different capital letters indicate significant differences of different land use types in the same soil layer, and different lower-case letters indicate significant differences of different soil layers in the same land use types. (a,b) represent the reserves of organic carbon and nitrogen, respectively.

3.3. SOC and TN Losses after Forest Conversion

The annual loss of topsoil carbon in CBF was 41.37 t/km². HF had the most topsoil carbon loss, which was 50.78 t/km² (Figure 4A). The results of the LSD analysis showed that the annual loss of topsoil carbon in HF was significantly greater than that in CF. The annual loss of topsoil nitrogen in CBF was 2.95 t/km² (Figure 4B). The annual loss of topsoil nitrogen in HF, AF, and CF was 1.51, 1.42, and 0.61 that of CBF, respectively. The LSD analysis results showed that the annual loss of topsoil nitrogen of HF and AF was significantly greater than it was for CF ($p < 0.05$).

As shown in Figure 5A, the annual relative loss rate of SOC in the CBF was 0.41%. The economic forest construction increased the annual carbon soil relative loss rate. In comparison with the CBF, the AF was the largest, being 2.43 times that of the CBF. The annual relative churn rates of HF and CF were 2.36 and 1.49 times that of CBF, respectively. The results of the LSD analysis showed that the rates of the soil carbon loss per year in the soil of HF and AF were significantly greater than that in the CBF soil ($p < 0.05$).

The annual relative loss of TN in the CBF was 0.27%. The construction of economic forests increased the annual relative loss rate of TN. In comparison with the CBF, the AF loss was the largest—2.93 times that of CBF. The HF and the CF were 2.48 times and 1.19 times that of the CBF, respectively. The LSD analysis results showed that the annual rates of TN loss in the HF and the AF were significantly greater than those in the CF and the CBF ($p < 0.05$).

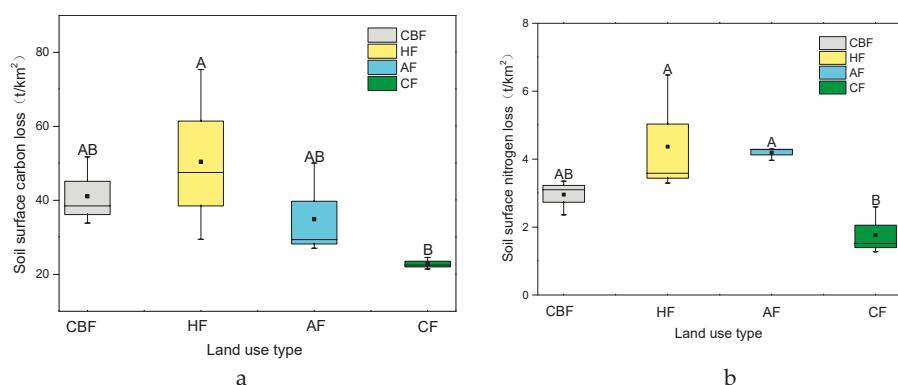


Figure 4. Soil surface carbon and nitrogen loss under different land use types. Note: the boxplot consists of five statistics: minimum, upper quartile, median, lower quartile, and maximum. The center of the boxplot is the median. Bars represent \pm SE of the mean ($n = 3$). Different capital letters indicate that the difference between different land use types of the same soil layer is significant. (a,b) represent the surface loss of carbon and nitrogen, respectively.

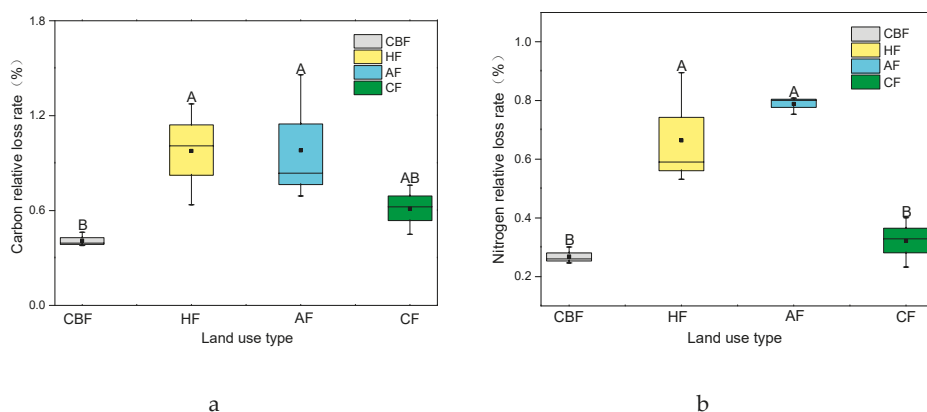


Figure 5. The carbon and nitrogen relative loss rates under different land use types. Note: the boxplot consists of five statistics: minimum, upper quartile, median, lower quartile, and maximum. The center of the boxplot is the median. Bars represent \pm SE of the mean ($n = 3$). Different capital letters indicate that the difference between different land use types of the same soil layer is significant. (a,b) represent the relative loss of carbon and nitrogen, respectively.

4. Discussion

4.1. Soil Erosion after Forest Conversion

The acquisition of the background value was the key to tracing soil erosion by nuclides [42,43]. The background value of ^{137}Cs can be obtained by the long-term monitoring of radioactive settlement, or it can be determined by selecting the correct reference points [44]. In this study, the background value of ^{137}Cs was 1732.48 Bq/m^2 . Similar research on the Yimeng mountain area showed that the background value was 1602 Bq/m^2 , which was close to this study [45]. In addition, according to the global simulated nuclear explosion ^{137}Cs background value model of Walling [46], the simulation background value of the study area was 1467 Bq/m^2 , which was roughly equivalent to the background value of this study area. This indicates that the measured background value was reliable. Compared

with the background value, all land use types underwent extremely serious soil erosion. It was reported that, in the Ganyu District of Liangyungang City, the high stone content in the soil made it more vulnerable to soil erosion. It has become a key area for soil erosion control [47–49].

The annual soil erosion thickness value of CBF was the lowest, which was 0.79 mm. The soil erosion moduli of AF, HF, and CF were all higher than CBF (Figure 2). The results indicated that CBF conversion to economic forests led to more severe soil erosion. As is shown in Table 1, compared with economic forests, CBF had the largest LAI (leaf area index), which indicated that CBF had high vegetation cover, which was consistent with previous studies. Binkley and Giardina [25] reported that, after being intercepted by canopy, the energy of raindrops was reduced to almost zero when they reached the soil. This explained why the thickness of soil loss in the CBF was the smallest. Among the three types of economic forests, the soil loss thickness of the CF was the smallest. CBF and CF had more litter cover on the surface than HF and AF. (Table 1). It has been reported that good litter cover reduces the ability of rain to wash the surface, which then reduces the loss of soil sediment [50–52]. We can further draw the conclusion that, when forests are converted into economic forests, it is necessary to select trees that can improve vegetation coverage and litter thickness so as to effectively reduce soil erosion. In this study, it was found that CF could better reduce soil erosion, which can be applied to the forestry construction in this area. However, in other areas, where environmental conditions may be different, the benefits of chestnut forests may not be realized. Therefore, more suitable tree species need to be selected according to local conditions. The potential benefits of chestnut forests observed in this study may depend more on the depth of litter in the study site. The abundance of litter depends not only on the defoliation but also on the management of forests in a variety of ways to maintain litter. Therefore, in addition to selecting suitable species for soil and water conservation, proper forest management is particularly important.

The annual soil erosion thickness was $AF > HF > CF > CBF$ (Figure 2 A). The change trend was the same as the specific surface area of soil (Figure 6). The BET (Brunner Emmett Teller method) specific surface area of the soils increased with the management of the economic forests. Among them, AF increased by 43.46%, while HF and CF increased by 20.09% and 5.61%, respectively. The specific surface area of soil is an important indicator of soil quality and an intuitive expression of land use at a micro-scale [53–55]. The specific surface area contains abundant information, such as material migration, tillage methods, parent material structure, and so on. An increase in the specific surface area of an economic forest can increase the soil porosity and the macroaggregate content. Therefore, both water holding capacity and anti-erosion ability of soil are weakened. This is consistent with the conclusions of our research. Conversion into economic forests and improper management will aggravate soil erosion.

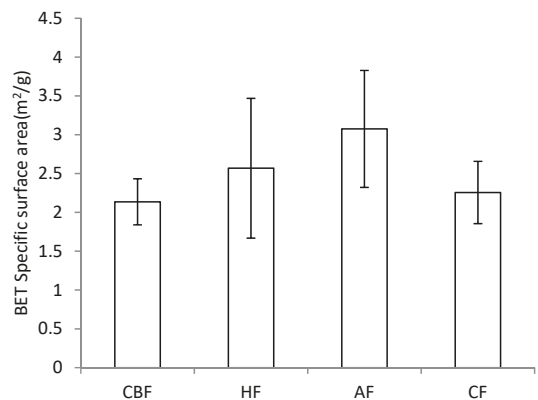


Figure 6. Soil pore structure under different land use patterns.

4.2. The Contact of Erosion and SOC and TN

The order of average SOC and TN storage was CBF > HF > CF > AF (Figure 3). This result indicated that the economic forest management reduced the SOC storage and the TN storage of the soil. It has been reported that the forest conversion can directly or indirectly affect many processes in the carbon–nitrogen biogeochemical cycle of ecosystems [55], such as changing the input and the degradation of organic matter and the physical protection of carbon and nitrogen by aggregates [56]. In addition, the SOC storage in the CBF decreased obviously as the soil layer deepened, which was consistent with the conclusions of related research done by Ma W et al. [7].

The results showed that the order of annual loss of SOC in the soil surface was HF > CBF > AF > CF (Figure 4). The reasons for this were two-fold. On one hand, erosion caused the absolute loss of nutrients. As was shown in Table 3, ^{137}Cs had a significant correlation with SOC. It was reported that the redistribution of soil carbon and nitrogen under soil erosion was generally divided into two aspects—lateral migration and vertical migration [57–59]. Water was the main cause of soil erosion, which was accompanied by the whole process of soil particle dispersion, migration, and deposition. Soil carbon and nitrogen, as important parts of the soil, were usually lost in both sediment-bound and runoff-dissolved states during erosion [60,61]. On the other hand, when the soil itself carried a high content of organic carbon, the absolute loss of nutrients was high. SOC content in CF and CBF was relatively rich in itself. When soil erosion was milder, there was a high absolute loss rate.

Compared with the absolute loss, the annual relative loss rate of soil carbon and nitrogen could better show the overall situation of soil carbon and nitrogen under different land use types, which was an effective index for characterizing the soil quality degradation [62]. The results showed that the relative loss rate of the CBF was significantly smaller than those of the AF and the HF, which were similar to the soil layer loss thickness distribution. This indicated that the soil carbon and the nitrogen loss in the AF and the HF were serious and should have been strengthened to reduce the soil erosion and the loss of nutrients as well as to improve the soil quality [63]. In addition, it was found that the rate of soil carbon loss per year under different land use types was obviously greater than that of soil nitrogen relative loss. This was consistent with relevant studies [64].

The correlation analysis showed that the ^{137}Cs activity in the soil showed a significant positive correlation with the content of soil organic carbon and total nitrogen (Table 3), which indicated that the contents of soil carbon and nitrogen under different land use modes in the area were closely related to soil erosion. This was consistent with earlier reports by Cheng J X et al. [65,66].

5. Conclusions and Deficiencies

The results showed that the conversion of coniferous broad-leaved mixed forests into the economic forests aggravated soil erosion. The average annual soil loss thickness of CBF was 0.79 mm, while those of AF, HF, and CF were 2.31 mm, 1.84 mm, and 0.87 mm, respectively. Economic forest management reduced the average carbon storage of soil, and the ranges from big to small were AF, CF, and HF by 63.66%, 61.26%, and 49.25%, respectively. The soil erosion process directly leads to the loss of soil carbon and nitrogen, which has a negative impact on the development of local agriculture and forestry. In the process of practical application, we should pay attention when forests are converted into economic forests, as it is necessary to select trees that can improve vegetation coverage and litter thickness in order to effectively reduce soil erosion. However, there are still some problems and shortcomings in this paper, such as the relative contribution rate of soil erosion and land use change to soil carbon and nitrogen loss, which could not be concluded from the existing data and will be more detailed in future experiments.

Author Contributions: Data interpretation, Y.X.; Data analysis, X.Z.; Manuscript drafting, X.Z.; Research design, Q.D.; Manuscript revision, J.L. Basic structure of this thesis, H.L.

Funding: This research was supported by National Natural Science Foundation of China (No. 31870600), Nation Key R&D program of China (2017YFC0505505), Priority Academic Program Development of Jiangsu Higher Education Institutions (PAPD).

Conflicts of Interest: The authors declare no conflict of interest.

References

1. Sun, Y.; Gu, L.; Dickinson, R.E.; Norby, R.J.; Pallardy, S.G.; Hoffman, F.M. Impact of mesophyll diffusion on estimated global land CO₂ fertilization. *Proc. Natl. Acad. Sci. USA* **2014**, *111*, 15774–15779. [[CrossRef](#)] [[PubMed](#)]
2. Tharammal, T.; Bala, G.; Narayanappa, D.; Nemani, R. Potential roles of CO₂ fertilization, nitrogen deposition, climate change, and land use and land cover change on the global terrestrial carbon uptake in the twenty-first century. *Clim. Dyn.* **2018**, *52*, 1–14. [[CrossRef](#)]
3. Li, D.; Niu, S.; Luo, Y. Global patterns of the dynamics of soil carbon and nitrogen stocks following afforestation: A meta-analysis. *New Phytol.* **2012**, *195*, 172–181. [[CrossRef](#)]
4. Vilén, T.; Cienciala, E.; Schelhaas, M.J.; Verkerk, P.J.; Lindner, M.; Peltola, H. Increasing carbon sinks in European forests: Effects of afforestation and changes in mean growing stock volume. *Forestry* **2016**, *89*, 82–90. [[CrossRef](#)]
5. Lebenya, R.M.; Huyssteen, C.W.V.; Preez, C.C.D. Change in soil organic carbon and nitrogen stocks eight years after conversion of sub-humid grassland to Pinus and Eucalyptus forestry. *Soil Res.* **2018**, *56*, 318. [[CrossRef](#)]
6. Jiang, W.; Yang, S.; Yang, X.; Ning, G. Negative impacts of afforestation and economic forestry on the Chinese Loess Plateau and proposed solutions. *Quat. Int.* **2016**, *399*, 165–173. [[CrossRef](#)]
7. Ma, W.; Li, Z.; Ding, K.; Huang, B.; Nie, X.; Lu, Y.; Xiao, H. Soil erosion, organic carbon and nitrogen dynamics in planted forests: A case study in a hilly catchment of Hunan Province, China. *Soil Tillage Res.* **2016**, *155*, 69–77. [[CrossRef](#)]
8. Gómez, J.A.; Campos, M.; Guzmán, G.; Castillollanque, F.; Vanwalleghem, T.; Lora, Á.; Giráldez, J.V. Soil erosion control, plant diversity, and arthropod communities under heterogeneous cover crops in an olive orchard. *Environ. Sci. Pollut. Res. Int.* **2017**, *25*, 1–13. [[CrossRef](#)]
9. Jian, S.; Li, J.; Ji, C.; Wang, G.; Mayes, M.A.; Dzantor, K.E.; Hui, D.; Luo, Y. Soil extracellular enzyme activities, soil carbon and nitrogen storage under nitrogen fertilization: A meta-analysis. *Soil Biol. Biochem.* **2016**, *101*, 32–43. [[CrossRef](#)]
10. Gentsch, N.; Mikutta, R.; Alves, R.J.E.; Barta, J.; Gittel, A.; Hugelius, G.; Kuhry, P.; Lashchinskiy, N.; Palmtag, J.; Richter, A. Storage and transformation of organic matter fractions in cryoturbated permafrost soils across the Siberian Arctic. *Biogeosciences* **2015**, *12*, 2697–2743. [[CrossRef](#)]
11. Murty, D.; Kirschbaum, M.U.F.; Mcmurtrie, R.E.; Mcgilvray, H. Does conversion of forest to agricultural land change soil carbon and nitrogen? a review of the literature. *Glob. Chang. Biol.* **2010**, *8*, 105–123. [[CrossRef](#)]
12. Fang, H.Y.; Sheng, M.L.; Sun, L.Y.; Cai, Q.G. [Using 137Cs and 210Pb(ex) to trace the impact of soil erosion on soil organic carbon at a slope farmland in the black soil region]. *Ying Yong Sheng Tai Xue Bao* **2013**, *24*, 1856–1862.
13. Nie, X.J.; Zhao, T.Q.; Qiao, X.N. Impacts of soil erosion on organic carbon and nutrient dynamics in an alpine grassland soil. *Soil Sci. Plant Nutr.* **2013**, *59*, 660–668. [[CrossRef](#)]
14. Zhao, P.; Sheng, L.; Wang, E.; Chen, X.; Deng, J.; Zhao, Y. Tillage erosion and its effect on spatial variations of soil organic carbon in the black soil region of China. *Soil Tillage Res.* **2018**, *178*, 72–81. [[CrossRef](#)]
15. Borrelli, P.; Paustian, K.; Panagos, P.; Jones, A.; Schütt, B.; Lugato, E. Effect of Good Agricultural and Environmental Conditions on erosion and soil organic carbon balance: A national case study. *Land Use Policy* **2016**, *50*, 408–421. [[CrossRef](#)]
16. Li, Y.; Zhang, Q.W.; Reicosky, D.C.; Lindstrom, M.J.; Bai, L.Y.; Li, L. Changes in soil organic carbon induced by tillage and erosion on a steep cultivated hillslope in the Chinese Loess Plateau from 1898–1954 and 1954–1998. *J. Geophys. Res. Biogeosci.* **2015**, *112*, 531–532. [[CrossRef](#)]
17. Maïga-Yaleu, S.; Guiguemde, I.; Yacouba, H.; Karambiri, H.; Ribolzi, O.; Bary, A.; Ouedraogo, R.; Chaplot, V. Soil crusting impact on soil organic carbon losses by water erosion. *Catena* **2013**, *107*, 26–34. [[CrossRef](#)]
18. Dialynas, Y.G.; Bastola, S.; Bras, R.L.; Marin-Spiotta, E.; Silver, W.L.; Arnone, E.; Noto, L.V. Impact of hydrologically driven hillslope erosion and landslide occurrence on soil organic carbon dynamics in tropical watersheds. *Water Resour. Res.* **2016**, *52*, 8895–8919. [[CrossRef](#)]

19. Janeau, J.L.; Gillard, L.C.; Grellier, S.; Jouquet, P.; Le, T.P.Q.; Luu, T.N.M.; Ngo, Q.A.; Orange, D.; Pham, D.R.; Tran, D.T. Soil erosion, dissolved organic carbon and nutrient losses under different land use systems in a small catchment in northern Vietnam. *Agric. Water Manag.* **2014**, *146*, 314–323. [\[CrossRef\]](#)
20. Zhang, J.H.; Wang, Y.; Li, F.C. Soil organic carbon and nitrogen losses due to soil erosion and cropping in a sloping terrace landscape. *Soil Res.* **2015**, *53*, 87–96. [\[CrossRef\]](#)
21. Rogowski, A.S.; Tamura, T. Movement of ¹³⁷Cs by Runoff, Erosion and Infiltration on the Alluvial Captina Silt Loam. *Health Phys.* **1963**, *11*, 1333–1340. [\[CrossRef\]](#)
22. Ge, F.L.; Zhang, J.H.; Su, Z.A.; Nie, X.J. Response of changes in soil nutrients to soil erosion on a purple soil of cultivated sloping land. *Acta Ecol. Sin.* **2007**, *27*, 459–463. [\[CrossRef\]](#)
23. Zhuang, J.Y.; Zhang, J.C.; Yang, Y.; Zhang, B.; Li, J. Effect of forest shelter-belt as a regional climate improver along the old course of the Yellow River, China. *Agrofor. Syst.* **2016**, *91*, 1–9. [\[CrossRef\]](#)
24. Hartanto, H.; Prabhu, R.; Ase, W.; Asdak, C. Factors affecting runoff and soil erosion: Plot-level soil loss monitoring for assessing sustainability of forest management. *For. Ecol. Manag.* **2003**, *180*, 361–374. [\[CrossRef\]](#)
25. Dan, B.; Giardina, C. Why do Tree Species Affect Soils? The Warp and Woof of Tree-soil Interactions. *Biogeochemistry* **1998**, *42*, 89–106.
26. Scott, N.A.; Tate, K.R.; Ross, D.J.; Parshotam, A. Processes influencing soil carbon storage following afforestation of pasture with *Pinus radiata* at different stocking densities in New Zealand. *Soil Res.* **2006**, *44*, 85–96. [\[CrossRef\]](#)
27. Lü, M.; Xie, J.; Chao, W.; Guo, J.; Wang, M.; Liu, X.; Chen, Y.; Chen, G.; Yang, Y. Forest conversion stimulated deep soil C losses and decreased C recalcitrance through priming effect in subtropical China. *Biol. Fertil. Soils* **2015**, *51*, 857–867. [\[CrossRef\]](#)
28. Lord, W.J.; Vlach, E. Responses of Peach Trees to Herbicides, Mulch, Mowing, and Cultivation. *Weed Sci.* **1973**, *21*, 227–229.
29. Zhang, X.; Li, Z.; Tang, Z.; Zeng, G.; Huang, J.; Guo, W.; Chen, X.; Hirsh, A. Effects of water erosion on the redistribution of soil organic carbon in the hilly red soil region of southern China. *Geomorphology* **2013**, *197*, 137–144. [\[CrossRef\]](#)
30. Wright, A.C. A model of the redistribution of disaggregated soil particles by rainsplash. *Earth Surf. Process. Landf.* **2010**, *12*, 583–596. [\[CrossRef\]](#)
31. Kateb, H.E.; Zhang, H.; Zhang, P.; Mosandl, R. Soil erosion and surface runoff on different vegetation covers and slope gradients: A field experiment in Southern Shaanxi Province, China. *Catena* **2013**, *105*, 1–10. [\[CrossRef\]](#)
32. Wei, L.; Zhang, B.; Wang, M. Effects of antecedent soil moisture on runoff and soil erosion in alley cropping systems. *Agric. Water Manag.* **2007**, *94*, 54–62. [\[CrossRef\]](#)
33. Zhang, Z.; Liu, S.; Dong, S. Ecological Security Assessment of Yuan River Watershed Based on Landscape Pattern and Soil Erosion. *Procedia Environ. Sci.* **2010**, *2*, 613–618. [\[CrossRef\]](#)
34. Vieira, D.C.S.; Fernández, C.; Vega, J.A.; Keizer, J.J. Does soil burn severity affect the post-fire runoff and interrill erosion response? A review based on meta-analysis of field rainfall simulation data. *J. Hydrol.* **2015**, *523*, 452–464. [\[CrossRef\]](#)
35. Klaminder, J.; Yoo, K.; Giesler, R. Soil carbon accumulation in the dry tundra: Important role played by precipitation. *J. Geophys. Res. Biogeosci.* **2009**, *114*, 126. [\[CrossRef\]](#)
36. Solaimani, K.; Modallaldoust, S.; Lotfi, S. Investigation of land use changes on soil erosion process using geographical information system. *Int. J. Environ. Sci. Technol.* **2009**, *6*, 415–424. [\[CrossRef\]](#)
37. Cotler, H.; Ortega-Larrocea, M.P. Effects of land use on soil erosion in a tropical dry forest ecosystem, Chamela watershed, Mexico. *Catena* **2006**, *65*, 107–117. [\[CrossRef\]](#)
38. Rodway-Dyer, S.J.; Walling, D.E. The use of ¹³⁷Cs to establish longer-term soil erosion rates on footpaths in the UK. *J. Environ. Manag.* **2010**, *91*, 1952–1962. [\[CrossRef\]](#) [\[PubMed\]](#)
39. Mabit, L.; Klik, A.; Benmansour, M.; Toloza, A.; Geisler, A.; Gerstmann, U.C. Assessment of erosion and deposition rates within an Austrian agricultural watershed by combining ¹³⁷Cs, ²¹⁰Pbex and conventional measurements. *Geoderma* **2009**, *150*, 231–239. [\[CrossRef\]](#)
40. Sheng, L.; Lobb, D.A.; Kachanoski, R.G.; Mcconkey, B.G. Comparing the use of the traditional and repeated-sampling-approach of the ¹³⁷Cs technique in soil erosion estimation. *Geoderma* **2011**, *160*, 324–335.

41. Zhang, G.; Weiliang, G.U.; Shulan, J.I.; Liu, Z.; Peng, Y.; Wang, Z. Preparation of polyelectrolyte multilayer membranes by dynamic layer-by-layer process for pervaporation separation of alcohol/water mixtures. *J. Membr. Sci.* **2006**, *280*, 727–733. [\[CrossRef\]](#)
42. Silva, J.; Mello, J.W.V.; Abrahão, W.A.P.; Fontes, M.P.F.; Junior, L.S.; Ferreira, V.P.; Taddei, M.H.T.; Rocha, O.F.; Gilkes, R.J.; Prakongkep, N. Multi-element background for trace elements and radionuclides in soil from Minas Gerais State, Brazil. In Proceedings of the 19th World Congress of Soil Science: Soil Solutions for a Changing World, Brisbane, Australia, 1–6 August 2010; Symposium 3.5.2 Risk Assessment and Risk Based Remediation 2010; pp. 40–43.
43. Gosman, A.; Blažiček, J. Study of the diffusion of trace elements and radionuclides in soils. *J. Radioanal. Nucl. Chem.* **1994**, *182*, 179–191. [\[CrossRef\]](#)
44. Lu, J.G.; Huang, Y.; Li, F.; Wang, L.; Li, S.; Hsia, Y. The investigation of ¹³⁷Cs and ⁹⁰Sr background radiation levels in soil and plant around Tianwan NPP, China. *J. Environ. Radioact.* **2006**, *90*, 89–99. [\[CrossRef\]](#)
45. Zhang, M.L.; Yang, H.; Xu, C.A.; Yang, J.D.; Liu, X.H. A preliminary study on soil erosion in Yimeng mountainous area using Cs tracer. *Acta Pedol. Sin.* **2010**, *47*, 408–414.
46. Walling, D.E.; He, Q.; Blake, W. Use of ⁷Be and ¹³⁷Cs measurements to document short- and medium-term rates of water-induced soil erosion on agricultural land. *Water Resour. Res.* **1999**, *35*, 3865–3874. [\[CrossRef\]](#)
47. Estifanos, A. Assessment Of Micro-Watershed Vulnerability For Soil Erosion In Ribb Watershed Using GIS And Remote Sensing. Ph.D. Thesis, Mekelle University, Mekelle, Ethiopia, 2014.
48. Jain, S.; Goel, M.K. Assessing the vulnerability to soil erosion of the Ukai Dam catchments using remote sensing and GIS. *Int. Assoc. Sci. Hydrol. Bull.* **2002**, *47*, 31–40. [\[CrossRef\]](#)
49. Zhao, Y.; Wang, E.; Cruse, R.M.; Chen, X. Characterization of seasonal freeze-thaw and potential impacts on soil erosion in northeast China. *Can. J. Soil Sci.* **2012**, *92*, 567–571. [\[CrossRef\]](#)
50. Clarke, P.J.; Prior, L.D.; French, B.J.; Vincent, B.; Knox, K.J.E.; Bowman, D.M.J.S. Using a rainforest-flame forest mosaic to test the hypothesis that leaf and litter fuel flammability is under natural selection. *Oecologia* **2014**, *176*, 1123–1133. [\[CrossRef\]](#)
51. Pan, C.; Wang, Q.; Ruan, X.; Li, Z. Biological Activity and Quantification of Potential Autotoxins from the Leaves of *Picea Schrenkiana*. *Chin. J. Plant Ecol.* **2009**, *27*, 245–262.
52. Pagel-Wieder, S.; Fischer, W.R. Short communication Estimation of the specific surface area of soil particles by adsorption of polyvinylalcohol in aqueous suspension. *J. Plant Nutr. Soil Sci.* **2015**, *164*, 441–443. [\[CrossRef\]](#)
53. Dolinar, B. Prediction of the soil-water characteristic curve based on the specific surface area of fine-grained soils. *Bull. Eng. Geol. Environ.* **2015**, *74*, 697–703. [\[CrossRef\]](#)
54. Dunjo, G.; Pardini, G.; Gispert, M. The role of land use-land cover on runoff generation and sediment yield at a microplot scale, in a small Mediterranean catchment. *J. Arid Environ.* **2004**, *57*, 239–256. [\[CrossRef\]](#)
55. Fang, Y.; Gundersen, P.; Vogt, R.D.; Koba, K.; Chen, F.; Xi, Y.C.; Yoh, M. Atmospheric deposition and leaching of nitrogen in Chinese forest ecosystems. *J. For. Res.* **2011**, *16*, 341–350. [\[CrossRef\]](#)
56. Koch, J.A.; Makeschin, F. Carbon and nitrogen dynamics in topsoils along forest conversion sequences in the Ore Mountains and the Saxonian lowland, Germany. *Eur. J. For. Res.* **2004**, *123*, 189–201. [\[CrossRef\]](#)
57. Wu, J.; Huang, J.; Liu, D.; Li, J.; Zhang, J.; Wang, H. Effect of 26 Years of Intensively Managed *Carya cathayensis* Stands on Soil Organic Carbon and Fertility. *Sci. World J.* **2014**, *2014*, 1–6.
58. Feng, W.; Zheng, S.; Jiang, J.; Xia, J.; Liang, J.; Zhou, J.; Luo, Y. Methodological uncertainty in estimating carbon turnover times of soil fractions. *Soil Biol. Biochem.* **2016**, *100*, 118–124. [\[CrossRef\]](#)
59. Guo, X.; Meng, M.; Zhang, J.; Chen, H.Y.H. Vegetation change impacts on soil organic carbon chemical composition in subtropical forests. *Sci. Rep.* **2016**, *6*, 29607. [\[CrossRef\]](#)
60. Chen, C.Y.; Hou, H.P.; Qiang, L.; Ping, Z.; Zhang, Z.Y.; Dong, Z.Q.; Ming, Z. Effects of planting density on photosynthetic characteristics and changes of carbon and nitrogen in leaf of different corn hybrids. *Acta Agron. Sin.* **2010**, *36*, 871–878. [\[CrossRef\]](#)
61. Abbasi, M.K.; Tahir, M.M.; Sabir, N.; Khurshid, M. Impact of the addition of different plant residues on nitrogen mineralization-immobilization turnover and carbon content of a soil incubated under laboratory conditions. *Solid Earth* **2015**, *6*, 197–205. [\[CrossRef\]](#)
62. Moldan, F.; Kjonaas, O.J.; Stuanes, A.O.; Wright, R.F. Increased nitrogen in runoff and soil following 13 years of experimentally increased nitrogen deposition to a coniferous-forested catchment at Gårdsjön, Sweden. *Environ. Pollut.* **2006**, *144*, 610–620. [\[CrossRef\]](#)

- 63. Wang, Y.; Fu, B.; Lü, Y.; Chen, L. Effects of vegetation restoration on soil organic carbon sequestration at multiple scales in semi-arid Loess Plateau, China. *Catena* **2011**, *85*, 58–66. [[CrossRef](#)]
- 64. Yuan, D.H.; Wang, Z.Q.; Chen, X.; Guo, X.B.; Zhang, R.L. Losses of nitrogen and phosphorus under different land use patterns in small red soil watershed. *Acta Ecol. Sin.* **2003**, *23*, 188–198.
- 65. Conant, R.T.; Paustian, K. Spatial variability of soil organic carbon in grasslands: Implications for detecting change at different scales. *Environ. Pollut.* **2002**, *116*, S127–S135. [[CrossRef](#)]
- 66. Dong, J.; Yang, D.Y.; Zhou, B.; Xu, Q.M. Study on Soil Erosion Rates in the Three Gorges Reservoir Area Using ^{137}Cs Tracing Method. *J. Soil Water Conserv.* **2006**, *20*, 1–5.



© 2019 by the authors. Licensee MDPI, Basel, Switzerland. This article is an open access article distributed under the terms and conditions of the Creative Commons Attribution (CC BY) license (<http://creativecommons.org/licenses/by/4.0/>).

Forest Soil Profile Inversion and Mixing Change the Vertical Stratification of Soil CO₂ Concentration without Altering Soil Surface CO₂ Flux

Xiaoling Wang ^{1,2}, Shenglei Fu ^{2,3}, Jianxiong Li ¹, Xiaoming Zou ⁴, Weixin Zhang ^{2,3}, Hanping Xia ², Yongbiao Lin ², Qian Tian ² and Lixia Zhou ^{2,*}

¹ Guangdong Key Laboratory of Animal Conservation and Resource Utilization, Guangdong Public Laboratory of Wild Animal Conservation and Utilization, Guangdong Institute of Applied Biological Resources, Guangzhou 510260, China; wangxl@giabr.gd.cn (X.W.); ljx196208@126.com (J.L.)

² Key Laboratory of Vegetation Restoration and Management of Degraded Ecosystems, South China Botanical Garden, Chinese Academy of Sciences, Guangzhou 510650, China; sfu@scbg.ac.cn (S.F.); weixinzhang@139.com (W.Z.); xiahanp@scbg.ac.cn (H.X.); linyb@scib.ac.cn (Y.L.); tianqian@scbg.ac.cn (Q.T.)

³ Key Laboratory of Geospatial Technology for the Middle and Lower Yellow River Regions (Henan University), Ministry of Education, College of Environment and Planning, Henan University, Kaifeng 475004, China

⁴ Department of Environmental Sciences, College of Natural Sciences, University of Puerto Rico, P.O. Box 70377, San Juan, PR 00936-8377, USA; xzou2015@163.com

* Correspondence: zhoulx@scbg.ac.cn; Tel.: +86-020-3725-2977

Received: 28 December 2018; Accepted: 19 February 2019; Published: 21 February 2019

Abstract: In order to gain more detailed knowledge of the CO₂ concentration gradient in forest soil profiles and to better understand the factors that control CO₂ concentration along forest soil profiles, we examined the soil surface CO₂ flux, soil properties and soil profile CO₂ concentration in upright (CK), inverted and mixed soil columns with a depth of 60 cm in two subtropical forests in China from May 2008 to December 2009. The results showed that: (1) The SOC (soil organic carbon), TN (total N) and microbial biomass were higher in the deeper layers in the inverted soil column, which was consistent with an increase in CO₂ concentration in the deeper soil layer. Furthermore, the biogeochemical properties were homogenous among soil layers in the mixed soil column. (2) CO₂ concentration in the soil profile increased with depth in CK while soil column inversion significantly intensified this vertical stratification as the most active layer (surface soil) was now at the bottom. The stratification of CO₂ concentration along the soil profile in the mixed soil column was similar to that in CK but it was not intensified after soil was mixed. (3) The soil surface CO₂ flux did not significantly change after the soil column was inverted. The surface CO₂ flux rate of the mixed soil column was higher compared to that of the inverted soil column but was not significantly different from CK. Our results indicated that the profile soil CO₂ production was jointly controlled by soil properties related to CO₂ production (e.g., SOC content and soil microbial biomass) and those related to gas diffusion (e.g., soil bulk density and gas molecular weight), but the soil surface CO₂ flux was mainly determined by soil surface temperature and may be affected by the intensity of soil disturbance.

Keywords: CO₂ production and diffusion; soil properties; CO₂ emission; surface soil layer

1. Introduction

An increase in atmospheric CO₂ concentration is considered to be one of the main causes for global warming [1,2]. As the largest terrestrial source and potential sink for CO₂, soil is particularly important in the global carbon cycle [3–7]. All CO₂ produced in the soil would be emitted through soil

surface efflux on a long-term basis [8]. The soil profile CO₂ concentration was reported to drive and accelerate this surface emission process [9] and therefore, this would influence the carbon balance of the forest. Some models estimated the soil CO₂ effluxes from the soil CO₂ concentration profiles [10–12]. Thus, we need to gain more detailed knowledge of the soil profile CO₂ concentration in order to better assess its contribution to soil surface CO₂ emission and global warming.

The majority of the forest soil CO₂ is produced in the surface layer since the majority of SOM (soil organic matter) and roots are distributed in the surface soil. However, the soil profile CO₂ concentration is high in the deep soil layer and low in the surface soil, which is the opposite to the production source layer [13]. Microbial biomass acts as both a source and sink for nutrients and participates in C, N and P transformation. Although it contributes less than 5% to SOM, it plays an active role in the soil C cycle [14]. The soil profile CO₂ concentration depends on both the processes of CO₂ production and diffusion. Studies have shown that soil CO₂ production and diffusion often has a strong and remarkable dependence on temperature and moisture [15–17]. It was also affected by soil properties, such as soil organic matter, total N (TN) and bulk density, root dynamics and microbial biomass [18,19]. However, there were limited studies focused on the relationship between the variation of soil properties and soil CO₂ concentration.

Agricultural practice, such as tillage, plays an important role in the storage and release of C within the terrestrial C cycle. The conventional intensive tillage was found to increase the emission of CO₂ by 16.0% in a subtropical rice farm [20]. Significantly greater CO₂ fluxes were also observed in subtropical paddy ecosystems after tillage operations [21]. Tillage disturbance does not occur as frequently as croplands in forests but during the process of restoring damaged ecosystems, tree planting and occasionally tillage are usual practices. Consequently, soil mixing is inevitable during ploughing.

In the present study, we manipulated a soil column experiment with upright, inverted and mixed soil columns in order to investigate the soil surface CO₂ flux, the distribution of CO₂ concentration in soil profiles and their influencing factors. The field site was a forest restoration ecosystem. We mixed the soil in “mixed” columns to identify the influence of “tillage” disturbance on soil CO₂. The purpose of our study was to examine the dependence of soil profile CO₂ concentration on soil properties in order to better understand the mechanism of the vertical stratification of soil profile CO₂ concentration and the relationship of soil profile CO₂ with soil surface CO₂ flux.

2. Materials and Methods

2.1. Study Area

The study was conducted over a 20-month period (from May 2008 to December 2009) in two subtropical plantation forests at the Heshan Hilly Land Interdisciplinary Experimental Station (112°50' E, 22°34' N), Guangdong Province, China. These selected forests included a coniferous forest (CF) mixed by *Pinus massoniana* Lamb, *Cunninghamia lanceolata* (Lamb) Hook and a broad-leaved forest (BF) dominated by *Schima wallichii* Choisy. The soil of the field site was an Orthic Acrisol [22] and the surface soil pH was about 4.0. The soil SOC (soil organic carbon) was 13.08 and 19.26 g kg^{−1} while the TN was 0.99 and 1.11 g kg^{−1} in CF and BF, respectively. The trees were about 25 years old when the current experiment started in 2008.

2.2. Experimental Design and Sample Analysis

A randomized block design with six replicates for each treatment was used in the soil column manipulation experiment. The soil column treatments were: (1) Upright soil column (CK); (2) inverted soil column (Inverted); and (3) mixed soil column (Mixed). The soil pillar was carefully dug and sheathed in the PVC (polyvinyl chloride) pipe to make a soil column cylinder. Each soil column had a diameter of 40 cm and a depth of 60 cm. In the upright and inverted soil columns, the soil pillar was undisturbed but in the mixed soil column, the topsoil and subsoil were thoroughly mixed. All soil columns were sealed at the bottom and placed back into the original location where the soil column

was manipulated. Each soil column was equipped with gas tubes and three-way stopcocks at depths of 20, 40 and 60 cm to sample soil CO₂ while a water tube was added at the bottom to sample the dissolved soil organic carbon and to avoid waterlog (Figure A1). Several holes with a diameter of 2 cm were made onto the wall of the PVC pipe to allow for the free exchange of soil air. All vegetation and litter fall were removed carefully from the soil surface of each soil column and were not present during the experiment period, which was achieved without disturbing the soil. All these manipulations were completed in May 2008.

We measured the soil surface CO₂ flux for each column once per month with the static chamber-gas chromatograph (GC) technique [23] from May 2008 to December 2009. PVC chamber with a diameter of 20 cm and a height of 20 cm was gently inserted 2 cm below the soil. Gas samples were collected four times at 10 min intervals from each soil column with 60 mL polypropylene syringes. Measurements were always made between 09:00 and 11:00 as suggested by Xu and Qi to represent the diurnal averages [19,24,25]. Soil CO₂ concentrations at depths of 20, 40 and 60 cm were sampled after the surface measurements and were determined using GC within 24 h. The soil temperature at depths of 5, 20, 40 and 60 cm was recorded every 0.5 h with an iButton DS1923 digital thermometer equipped in the soil column.

Gas flux was calculated based on the soil surface gas concentration change within the chamber over the measurement period, which was estimated as the slope of linear regression between concentration and time. It was expressed in the following equation [26]:

$$F = \frac{\Delta m}{\Delta t} \cdot D \frac{V}{A} = hD \frac{\Delta m}{\Delta t} \quad (1)$$

where F is the gas flux (mg m⁻² h⁻¹); h is the height of the chamber (m); D is the gas density in the chamber ($D = n/v = P/RT$, in mg m⁻³ where P is the air pressure; T is the temperature inside of the chamber and R is the air constant; $\Delta m/\Delta t$ denotes the linear slope of concentration changing with time over the measurement period.

The soil along the profiles was sampled in May and November both in 2008 and 2009. All soil samples were sieved with a 2 mm sieve before analysis. Soil water content (SWC) was measured by oven-drying for 48 h at 105 °C; SOC was determined by the dichromate oxidation method; soil TN was estimated by Kjeldahl digestion with UV spectrophotometric analysis [27]; and soil bulk density was determined by the intact soil core method. The soil microbial biomass and community structure was analyzed using the phospholipid fatty acids (PLFAs) method as described by Bossio and Scow [28]. Different PLFAs were considered to represent different groups of soil microorganisms. The abundance of individual fatty acids was calculated based on the 19:0 internal standard concentrations. Bacteria were identified by 10 PLFAs (i15:0, a15:0, 15:0, i16:0, 16: 1ω7, i17:0, a17:0, 17:0, cy17:0 and cy19:0) while 18:2ω6c and 18:1ω9c were used as the indicators of fungal biomass [29]. The ratio of fungal PLFAs to bacterial PLFAs was used to estimate the ratio of fungal to bacterial biomass (F/B) in soil [30]. The results of soil properties were the average of four measurements.

2.3. Statistical Analysis

A repeated measures analysis of variance (RM ANOVA) was performed to examine the monthly changes in CO₂ concentration and the soil surface CO₂ flux. Two-way ANOVA and LSD (least significant difference) tests were performed to compare the physicochemical and microbial traits among forest types and soil treatments. All statistics were performed using IBM SPSS Statistics 21 (IBM Corporation, New York, NY, USA) and SigmaPlot 12.5 (Systat Software Inc., San Jose, CA, USA).

3. Results

3.1. Precipitation and Air Temperature

The annual precipitation of the site was 1319.6 mm and 1525.6 mm while the average temperature was 21.60 °C and 22.49 °C in 2008 and 2009, respectively. The precipitation from May to September (high temperature period, monthly mean temperature >25 °C) in 2008 was 922.60 mm, which was significantly less than that in the same period in 2009 (1148.20 mm). The mean air temperature was 26.95 °C in this period in 2008, which was lower by 0.62 °C compared to 2009 (Figure A2). The mean soil temperature at a depth of 5 cm was 24.73 °C in CF in the study period, which was higher by 1.29 °C compared to BF.

3.2. Variation of Soil Profile CO₂ Concentration

Large variations of CO₂ concentration in soil profiles were observed both throughout time and with different depths in all treatments (Figure 1a–f). In general, the CO₂ concentration increased with depth, with the highest concentrations observed at a depth of 60 cm. CO₂ concentrations in soil profiles were quite different between the two years, with the peak accumulation having occurred in the high temperature period of the second year. The CO₂ concentration in the BF soil was higher than that in the CF soil.

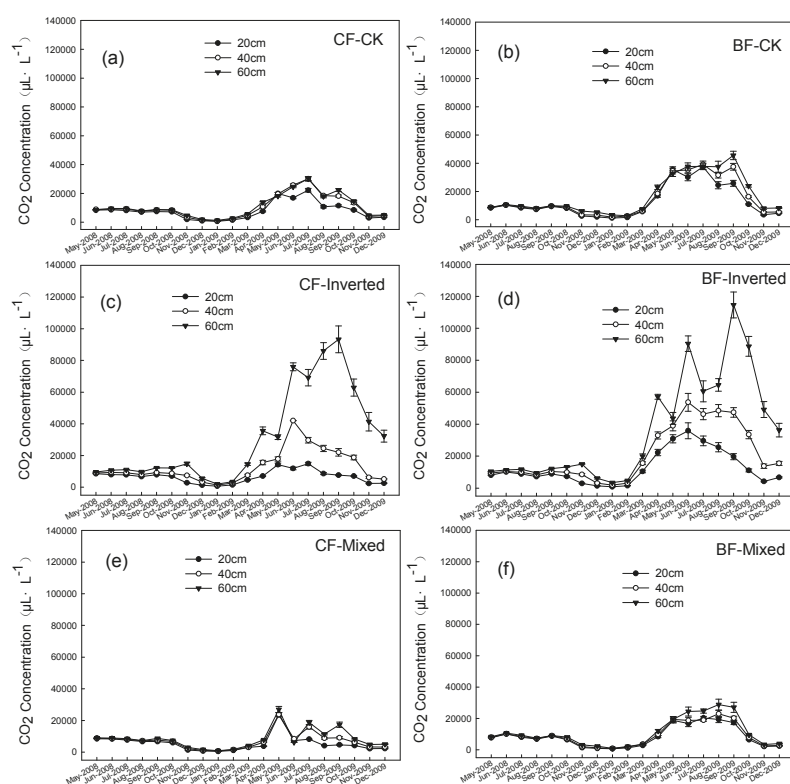


Figure 1. Seasonal variations of CO₂ concentration along soil profiles in a coniferous forest (CF) and a broad-leaved forest (BF). Different soil column treatments were: (a) CF-CK (upright soil column); (b) BF-CK; (c) CF-Inverted; (d) BF-Inverted; (e) CF-Mixed; and (f) BF-Mixed. Data are shown as means \pm SE, $n = 6$.

The average CO₂ concentration in CF at a depth of 60 cm was $1.1 \times 10^4 \mu\text{L}\cdot\text{L}^{-1}$, which was 39% higher than that in 20 cm. The CO₂ concentration in the inverted soil column at a depth of 60 cm reached $3.2 \times 10^4 \mu\text{L}\cdot\text{L}^{-1}$, which was about 4.8 times that of the 20 cm. In other words, the vertical stratification of CO₂ concentration in the soil profile was intensified in the inverted soil column compared to CK. In the mixed soil columns, the CO₂ concentration in each layer was lower than CK. Similar patterns were observed in BF, which showed that the inverted soil column intensified the stratification of CO₂ concentrations in soil profiles, while CO₂ concentrations in the “Mixed” soil column were lower than CK despite still maintaining its stratification.

3.3. Seasonal Variation of Soil Surface CO₂ Flux

Soil surface CO₂ flux rates varied significantly during the study period, with higher CO₂ flux rates observed during the summer both in BF and CF (Figure 2a,b). The repeated measures analyses of variance indicated a significant interaction between months and treatments ($p < 0.001$). The average soil surface CO₂ flux rates in CF were 185.69, 155.70 and 201.81 mg m⁻² h⁻¹ for the CK, inverted and mixed soil columns, respectively. In BF, the rates were 183.42, 159.95 and 197.70 mg m⁻² h⁻¹, respectively. The soil surface CO₂ flux rates of the inverted soil column were 13%–16% lower than CK while that of the “mixed” soil column were somewhat higher although these differences were not significant. However, soil surface CO₂ flux rates of the “mixed” soil column was significantly higher than that in the inverted soil column in BF ($p < 0.05$). Soil surface CO₂ flux rates from CF did not significantly differ from the rates measured in BF.

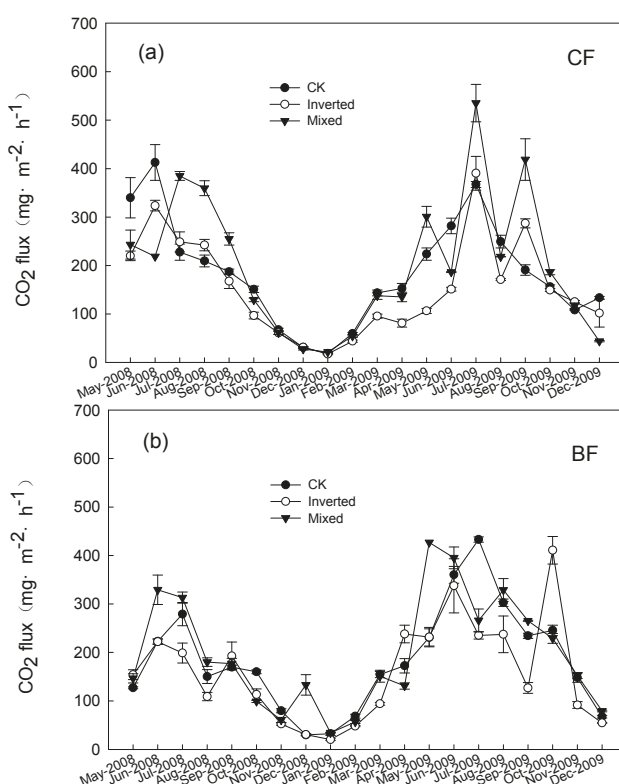


Figure 2. Fluxes of CO₂ in a coniferous forest (CF) (a) and a broad-leaved forest (BF) (b) in different soil column treatments: CK, inverted and mixed. Error bars represent standard errors of the mean ($n = 6$).

3.4. Soil Biogeochemical Properties in Different Columns

The SOC (at a depth of 0–20 cm) was significantly higher in the BF soil than in the CF soil ($p < 0.05$, Table 1). SWC, TN and bulk density did not differ between the two forests. In the upright soil column, the SOC and TN in the topsoil were significantly higher than in the subsoil ($p < 0.05$) while the soil bulk density was higher in the subsoil. Naturally, the opposite pattern was observed in the inverted soil column, which showed that SOC and TN were higher in “new subsoil” but soil bulk density was higher in the “new topsoil”. In the mixed soil column, all measured soil properties did not differ significantly among the three soil layers.

Table 1. Soil physical and chemical properties by depth and soil columns manipulation, including soil water content (SWC), total organic carbon (TOC), total nitrogen (TN) and bulk density. Error bars represent the standard errors of the mean ($n = 4$). Different letters represent significant differences (LSD test, $p < 0.05$).

| Forest Type | Treatments | Profile | SWC (%) | SOC (g·kg ⁻¹) | TN (mg·L ⁻¹) | Bulk Density (g·cm ⁻³) |
|-------------|------------|----------|---------------|---------------------------|--------------------------|------------------------------------|
| CF | CK | 0–20 cm | 19.66 ± 4.00a | 13.09 ± 2.74a | 1.17 ± 0.14a | 1.40 ± 0.05a |
| | | 20–40 cm | 18.95 ± 2.54a | 7.62 ± 2.21b | 0.83 ± 0.18b | 1.48 ± 0.06a |
| | Inverted | 40–60 cm | 19.93 ± 2.97a | 5.75 ± 1.45b | 0.70 ± 0.10b | 1.48 ± 0.08a |
| | | 0–20 cm | 19.08 ± 3.21a | 5.98 ± 1.00b | 0.66 ± 0.15b | 1.49 ± 0.02a |
| | | 20–40 cm | 20.04 ± 1.86a | 6.17 ± 1.76b | 0.71 ± 0.20b | 1.46 ± 0.11ab |
| | Mixed | 40–60 cm | 21.36 ± 2.58a | 10.12 ± 2.98a | 0.99 ± 0.20a | 1.35 ± 0.09b |
| | | 0–20 cm | 20.19 ± 2.63a | 10.89 ± 1.82a | 0.97 ± 0.18a | 1.31 ± 0.03a |
| | | 20–40 cm | 21.04 ± 2.67a | 9.25 ± 1.35a | 0.94 ± 0.16a | 1.30 ± 0.05a |
| | | 40–60 cm | 21.80 ± 1.53a | 9.42 ± 0.69a | 0.90 ± 0.16a | 1.28 ± 0.09a |
| BF | CK | 0–20 cm | 23.15 ± 1.82a | 17.25 ± 1.53a | 1.42 ± 0.41a | 1.39 ± 0.02b |
| | | 20–40 cm | 21.07 ± 2.15a | 6.97 ± 1.94b | 0.81 ± 0.29b | 1.55 ± 0.05a |
| | Inverted | 40–60 cm | 21.44 ± 1.60a | 4.76 ± 1.54b | 0.68 ± 0.33b | 1.48 ± 0.08a |
| | | 0–20 cm | 20.15 ± 1.82a | 5.51 ± 1.44b | 0.75 ± 0.41a | 1.39 ± 0.09a |
| | | 20–40 cm | 20.62 ± 2.51a | 5.31 ± 1.49b | 0.76 ± 0.31a | 1.48 ± 0.10a |
| | Mixed | 40–60 cm | 23.29 ± 1.83a | 12.79 ± 5.54a | 1.15 ± 0.29a | 1.39 ± 0.02a |
| | | 0–20 cm | 21.80 ± 2.31a | 9.43 ± 2.16a | 0.97 ± 0.33a | 1.32 ± 0.08a |
| | | 20–40 cm | 22.22 ± 1.57a | 9.18 ± 3.01a | 0.92 ± 0.21a | 1.35 ± 0.03a |
| | | 40–60 cm | 22.50 ± 3.93a | 8.33 ± 2.22a | 0.96 ± 0.40a | 1.32 ± 0.04a |

In the upright soil columns, the mean total soil microbial biomass (PLFA), fungal biomass, bacterial biomass and F/B ratio all decreased with depth both in CF and BF soil (Table 2). In the inverted soil column, bacterial biomass was higher in the “new subsoil” while fungal biomass was higher in the “new topsoil”. In the mixed soil column, the biogeochemical properties were homogenous among different soil layers.

Table 2. Soil microbial community characters in each soil layer over all manipulated soil columns. PLFA, total PLFA; Fun, fungi; Bac, Bacteria; F/B, the ratio of fungal to bacterial biomass. Error bars represent the standard errors of the mean ($n = 4$). Different letters represent significant differences (LSD test, $p < 0.05$).

| Forest Type | Treatments | Profile | PLFA (nmol·g ⁻¹) | Fun (mol%) | Bac (mol%) | F/B% |
|-------------|------------|----------|------------------------------|---------------|---------------|----------------|
| CF | CK | 0–20 cm | 6.34 ± 3.52a | 4.14 ± 1.34a | 28.64 ± 5.76a | 14.69 ± 4.23a |
| | | 20–40 cm | 4.07 ± 2.24a | 1.99 ± 0.98ab | 21.33 ± 8.61b | 10.75 ± 6.12a |
| | | 40–60 cm | 4.15 ± 2.30a | 1.53 ± 1.12b | 17.86 ± 4.93b | 8.89 ± 5.83a |
| | Inverted | 0–20 cm | 5.45 ± 2.66a | 3.52 ± 3.39a | 17.39 ± 3.31b | 19.64 ± 18.31a |
| | | 20–40 cm | 4.72 ± 2.25a | 1.18 ± 0.72a | 17.06 ± 3.36b | 7.34 ± 4.67b |
| | | 40–60 cm | 5.10 ± 1.90a | 2.94 ± 0.51a | 27.51 ± 6.05a | 11.18 ± 4.54a |
| | Mixed | 0–20 cm | 7.31 ± 4.60a | 5.01 ± 2.60a | 27.25 ± 3.00a | 17.43 ± 8.86a |
| | | 20–40 cm | 5.57 ± 2.73a | 3.21 ± 0.89a | 25.28 ± 3.84a | 12.09 ± 3.37a |
| | | 40–60 cm | 5.45 ± 1.77a | 2.76 ± 0.56a | 25.83 ± 2.10a | 10.19 ± 2.06a |

Table 2. Cont.

| Forest Type | Treatments | Profile | PLFA (nmol·g ^{−1}) | Fun (mol%) | Bac (mol%) | F/B% |
|-------------|------------|----------|------------------------------|--------------|---------------|---------------|
| BF | CK | 0–20 cm | 10.55 ± 1.92a | 3.35 ± 1.90a | 24.24 ± 6.24a | 13.04 ± 5.24a |
| | | 20–40 cm | 7.75 ± 1.94a | 2.05 ± 0.74a | 20.83 ± 3.85a | 9.79 ± 4.14a |
| | | 40–60 cm | 6.23 ± 1.05b | 0.98 ± 0.60a | 14.37 ± 3.15b | 7.32 ± 4.10a |
| | Inverted | 0–20 cm | 6.54 ± 1.55a | 3.71 ± 4.90a | 16.79 ± 3.93a | 8.46 ± 4.25a |
| | | 20–40 cm | 6.83 ± 2.49a | 1.39 ± 0.41a | 18.38 ± 3.64a | 8.81 ± 3.39a |
| | | 40–60 cm | 7.11 ± 0.96a | 1.74 ± 0.48a | 21.24 ± 1.06a | 8.93 ± 1.67a |
| | Mixed | 0–20 cm | 7.05 ± 2.27a | 2.21 ± 2.04a | 20.96 ± 4.47a | 9.88 ± 8.07a |
| | | 20–40 cm | 8.49 ± 2.37a | 1.44 ± 1.30a | 16.15 ± 6.37a | 8.19 ± 5.49a |
| | | 40–60 cm | 9.10 ± 3.08a | 1.32 ± 1.11a | 16.32 ± 4.66a | 7.93 ± 4.95a |

3.5. Correlations of Soil CO₂ Concentration and Temperature

The dependence of soil CO₂ concentration on temperature was strong and consistent in two forests in the CK and mixed soil columns (Figure 3a–f). The relationship was well fit by an exponential growth regression model (*p* < 0.001). The temperature explained 26%–76% of the variation in soil CO₂ concentration in the upright and mixed soil columns. In the inverted soil columns, this dependence was significantly weaker.

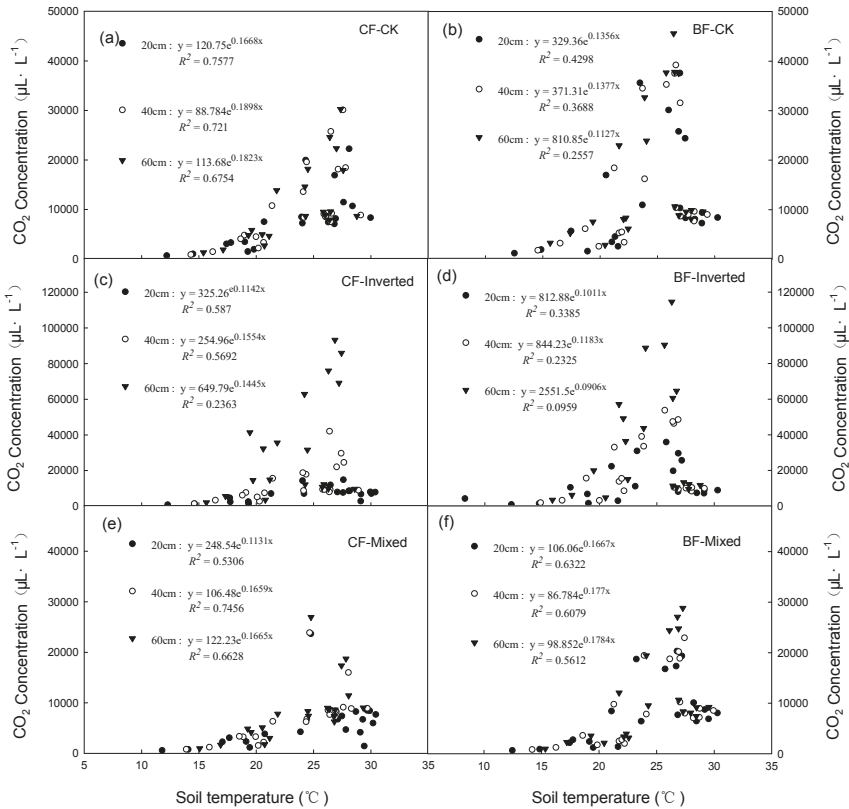


Figure 3. Relationship between soil profile CO₂ concentration and soil temperature. Different soil column treatments were: (a) CF-CK; (b) BF-CK; (c) CF-Inverted; (d) BF-Inverted; (e) CF-Mixed; and (f) BF-Mixed.

4. Discussion

4.1. Effects of Environment Variables on CO₂ Concentration in Soil Profiles and Soil Surface CO₂ Flux

In general, the soil CO₂ concentration was greater in the deeper soil layer regardless of the way that the soil columns were manipulated in the present study. We considered that this was mainly due to the difficulty of CO₂ diffusion within the soil profile to the atmosphere [15]. Studies have demonstrated that the molecular diffusion trait is the most important factor affecting CO₂ transportation within the soil profile. Furthermore, this was strongly dependent on soil porosity, which was closely related to soil moisture [9]. Rainfall could lead to an increase in soil moisture and a decrease in CO₂ diffusivity, which would subsequently result in CO₂ accumulation in soil and increase the CO₂ concentration in deep soil [16]. Our data also showed that CO₂ concentration in soil profiles increased with the seasonal temperature rise, which was probably due to an increase in soil microbial respiration with increasing temperature. This suggests that temperature is also a major factor that influences CO₂ concentration along the soil profile. The summer of 2009 was relatively hotter and wetter than the summer of 2008 during the study period, which resulted in a significantly higher CO₂ concentration in the summer of 2009 thus, verifying that temperature and moisture are major factors determining soil CO₂ concentration.

4.2. Soil Properties and Soil CO₂ Concentration Stratification

The inverted soil column was found to intensify the stratification of CO₂ concentration due to the replacement of the subsoil with the original topsoil. In this case, the SOC, TN and microbial biomass were higher in the deeper layer in the inverted soil column, which was consistent with an increase in CO₂ concentration in the deeper soil layer. SOC and TN provide energy and nutrients for microbial growth and thus, the CO₂ in the soil profiles mainly resulted from microbial activity. In addition, the higher soil bulk density in the “new topsoil” in the inverted soil column would have a negative effect on CO₂ emission from the soil since CO₂ diffusion within the soil profile depends on soil porosity, which is tied closely with soil bulk density.

As we observed, soil organic carbon, total nitrogen and microbial biomass were often higher in original topsoil and they coincided with higher CO₂ production. However, the soil CO₂ concentration was generally higher in the deeper soil layer. Furthermore, soil properties in the mixed soil columns did not differ significantly among soil layers but the CO₂ concentration along the soil profile showed a clear stratification. These results indicated that although CO₂ concentration was highly influenced by soil properties, it was the gravity that determined the vertical distribution of soil CO₂ concentration since the molecular weight of CO₂ is greater than air.

4.3. CO₂ Profile Concentration and its Relationship to Soil Surface CO₂ Flux

The surface CO₂ flux rates of the mixed soil column were 8%–9% higher than those in CK although these were not statistically significantly. This was much less than those in the croplands under conventional tillage [20,21]. Soil profile CO₂ is transported into the atmosphere primarily by diffusion and air turbulence at the forest soil surface, which could significantly impact the carbon balance of the forest ecosystem [31,32]. These important processes often occurred near the soil surface but had little effect on the subsoil CO₂ storage. Wiaux et al. [10] observed that approximately 90%–95% of the surface CO₂ fluxes originated from the top 10 cm of the soil profile. On one hand, the upward movement of CO₂ is a slow process limited by soil surface texture and turbulence. On the other hand, CO₂ has the tendency to sink down along the soil profile as the molecular weight of CO₂ is heavier than the average molecular weight of air [13].

In the present study, it is important to note that soil column inversion significantly intensified the vertical stratification of soil profile CO₂ concentration. However, this did not intensify soil surface CO₂ flux rate, which was even lower compared to CK. In contrast, soil column mixing increased the soil surface CO₂ flux to some extent (although this was not statistically significant). C content in BF

in the topsoil was 32% more than that in CF, while the soil surface CO₂ flux rates from BF were not significantly different from those in CF. These results suggested that CO₂ production was stimulated by the increased CO₂ production sources (SOC, TN and microbial communities) while surface soil CO₂ exchange could be altered by changing the soil texture (i.e., soil bulk density) and soil surface temperature (mean soil temperature at a depth of 5 cm was 1.29 °C higher in CF than in BF).

5. Conclusions

The soil profile CO₂ concentration appeared to be strongly affected by environmental factors (temperature and precipitation) and soil properties (SOC, TN, soil bulk density and microbial communities) in the current study. The surface CO₂ fluxes rates remained relatively stable when the CO₂ concentration in soil profile was increased to a significant extent. These results increased our understanding of the factors influencing CO₂ concentration in forest soil profile and the relationship of soil profile CO₂ with soil surface CO₂ flux. We concluded that the interaction of soil properties and environmental factors controlled the CO₂ production in the soil profile, but the soil surface CO₂ emission could be affected by the intensity of the disturbance or soil temperature variation. Although all CO₂ produced in the soil would be eventually emitted to the atmosphere through soil surface efflux on a long-term basis, CO₂ stored in the subsoil may be relatively stable in the deeper soil layers.

Author Contributions: Data curation, X.W. and Q.T.; formal analysis, X.W.; funding acquisition, J.L. and H.X.; investigation, X.W., Y.L. and Q.T.; project administration, S.F. and L.Z.; supervision, S.F.; writing—original draft, X.W.; writing—review and editing, X.Z. and W.Z.

Funding: This research was funded by the National Natural Science Foundation of China, grant numbers 41501268 and 30771704; and GDAS' Project of Science and Technology Development, grant number 2019GDASYL-0103060 and 2018GDASX-0107.

Acknowledgments: We thank Dima Chen for advice on the content and Xingquan Rao and Heshan Station for providing meteorological data. We thank Yanmei Xiong for improving the English of this manuscript. We are grateful to the editors and the three anonymous reviewers for helpful comments on the manuscript.

Conflicts of Interest: The authors declare no conflicts of interest.

Appendix A

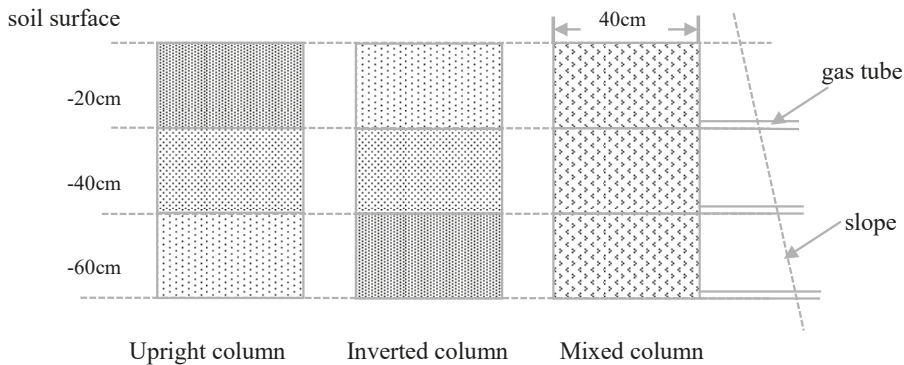


Figure A1. Diagram depicting soil column manipulation for field measurements of CO₂.

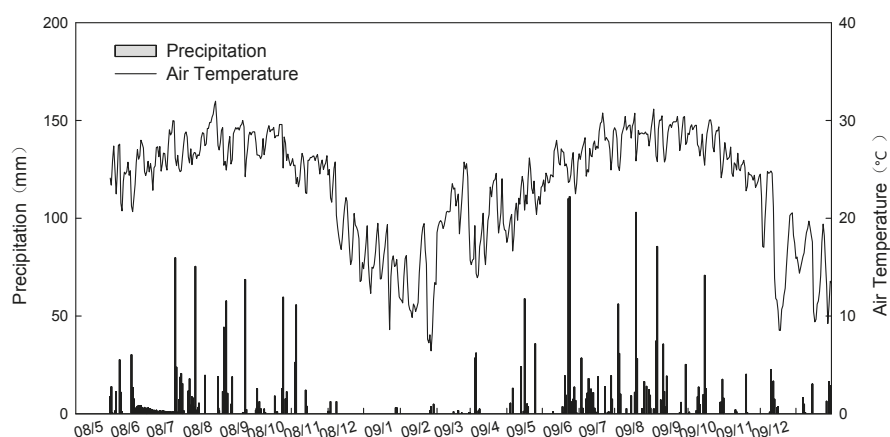


Figure A2. Precipitation and air temperature in Heshan station during the study period.

References

1. Houghton, J.T.; Meira-Filho, L.G.; Callander, B.A.; Harris, N. *Climate Change 1995: The Science of Climate Change*; Kathenberg, N., Maskell, K., Eds.; Cambridge University Press: New York, NY, USA, 1996.
2. Stocker, T.F.; Qin, D.; Plattner, G.K.; Tignor, M.; Allen, S.K.; Boschung, J.; Nauels, A.; Xia, Y. *Climate Change: The Physical Science Basis*; Bex, V., Midgley, P.M., Eds.; Cambridge University Press: New York, NY, USA, 2013.
3. Grüning, M.M.; Germeshausen, F.; Thies, C.; L.-M.-Arnold, A. Increased forest soil CO₂ and N₂O emissions during insect infestation. *Forests* **2018**, *9*, 612. [[CrossRef](#)]
4. Lee, S.; Yim, J.; Son, Y.; Son, Y.; Kim, R. Estimation of forest carbon stocks for national greenhouse gas inventory reporting in south Korea. *Forests* **2018**, *9*, 625. [[CrossRef](#)]
5. Schlesinger, W.H.; Andrews, J.A. Soil respiration and the global carbon cycle. *Biogeochemistry* **2000**, *48*, 7–20. [[CrossRef](#)]
6. Valentini, R.; Matteucci, G.; Dolman, A.J.; Schulze, E.D.; Rebmann, C.; Moors, E.J.; Granier, A.; Gross, P.; Jensen, N.O.; Pilegaard, K.; et al. Respiration as the main determinant of carbon balance in European forests. *Nature* **2000**, *404*, 861–865. [[CrossRef](#)] [[PubMed](#)]
7. Raich, J.W.; Schlesinger, W.H. The global carbon-dioxide flux in soil respiration and its relationship to vegetation and climate. *Tellus B* **1992**, *44*, 81–99. [[CrossRef](#)]
8. Maier, M.; Schack-Kirchner, H.; Hildebrand, E.E.; Schindler, D. Soil CO₂ efflux vs. soil respiration: Implications for flux models. *Agric. For. Meteorol.* **2011**, *151*, 1723–1730. [[CrossRef](#)]
9. Pihlatie, M.; Pumpanen, J.; Rinne, J.; Ilvesniemi, H.; Simojoki, A.; Hari, P.; Vesala, T. Gas concentration driven fluxes of nitrous oxide and carbon dioxide in boreal forest soil. *Tellus B* **2007**, *59*, 458–469. [[CrossRef](#)]
10. Wiaux, F.; Vanclooster, M.; Van-Oost, K. Vertical partitioning and controlling factors of gradient-based soil carbon dioxide fluxes in two contrasted soil profiles along a loamy hillslope. *Biogeosciences* **2015**, *12*, 4637–4649. [[CrossRef](#)]
11. Tang, J.W.; Baldocchi, D.D.; Qi, Y.; Xu, L.K. Assessing soil CO₂ efflux using continuous measurements of CO₂ profiles in soils with small solid-state sensors. *Agric. For. Meteorol.* **2003**, *118*, 207–220. [[CrossRef](#)]
12. Maier, M.; Schack-Kirchner, H. Reply to comment on “Using the gradient method to determine soil gas flux: A review”. *Agric. For. Meteorol.* **2014**, *197*, 256–257. [[CrossRef](#)]
13. Luo, Y.Q.; Zhou, X.H. Processes of CO₂ transport from soil to the atmosphere. In *Soil Respiration and the Environment*; Elsevier Inc.: Amsterdam, The Netherlands, 2006; pp. 61–76.
14. Hopkins, D.W.; Sparrow, A.D.; Shillam, L.L.; English, L.C.; Dennis, P.G.; Novis, P. Enzymatic activities and microbial communities in an antarctic dry valley soil: Responses to c and n supplementation. *Soil Biol. Biochem.* **2008**, *40*, 2130–2136. [[CrossRef](#)]
15. Risk, D.; Kellman, L.; Beltrami, H. Carbon dioxide in soil profiles: Production and temperature dependence. *Geophys. Res. Lett.* **2002**, *29*, 111–114. [[CrossRef](#)]

16. Jassal, R.; Black, A.; Novak, M.; Morgenstern, K.; Nestic, Z.; Gaumont-Guay, D. Relationship between soil CO₂ concentrations and forest-floor CO₂ effluxes. *Agric. For. Meteorol.* **2005**, *130*, 176–192. [\[CrossRef\]](#)
17. Albanito, F.; Saunders, M.; Jones, M.B. Automated diffusion chambers to monitor diurnal and seasonal dynamics of the soil CO₂ concentration profile. *Eur. J. Soil Sci.* **2009**, *60*, 507–514. [\[CrossRef\]](#)
18. Billings, S.A.; Richter, D.D.; Yarie, J. Soil carbon dioxide fluxes and profile concentrations in two boreal forests. *Can. J. For. Res.* **1998**, *28*, 1773–1783. [\[CrossRef\]](#)
19. Xu, M.; Qi, Y. Soil-surface CO₂ efflux and its spatial and temporal variations in a young ponderosa pine plantation in northern California. *Glob. Chang. Biol.* **2001**, *7*, 667–677. [\[CrossRef\]](#)
20. Zhang, Z.S.; Cao, C.G.; Guo, L.J.; Li, C.F. Emissions of CH₄ and CO₂ from paddy fields as affected by tillage practices and crop residues in central china. *Paddy Water Environ.* **2016**, *14*, 85–92. [\[CrossRef\]](#)
21. Li, C.F.; Kou, Z.K.; Yang, J.H.; Cai, M.L.; Wang, J.P.; Cao, C.G. Soil CO₂ fluxes from direct seeding rice fields under two tillage practices in central China. *Atmos. Environ.* **2010**, *44*, 2696–2704. [\[CrossRef\]](#)
22. FAO. *World Reference Base for Soil Resources 2006*; World Soil Resources Report; FAO: Rome, Italy, 2006; p. 103.
23. Wang, Y.S.; Wang, Y.H. Quick measurement of CH₄, CO₂ and N₂O emissions from a short-plant ecosystem. *Adv. Atmos. Sci.* **2003**, *20*, 842–844.
24. Larionova, A.A.; Rozonova, L.N.; Samoylov, T.I. Dynamics of gas exchange in the profile of a gray forest soil. *Sov. Soil Sci.* **1989**, *24*, 1359–1372.
25. Jian, J.S.; Steele, M.K.; Day, S.D.; Quinn, T.R.; Hodges, S.C. Measurement strategies to account for soil respiration temporal heterogeneity across diverse regions. *Soil Biol. Biochem.* **2018**, *125*, 167–177. [\[CrossRef\]](#)
26. Zhou, C.Y.; Zhou, G.Y.; Zhang, D.Q.; Wang, Y.H.; Liu, S.Z. CO₂ efflux from different forest soils and impact factors in Dinghu Mountain, China. *Sci. China Ser. D* **2005**, *48*, 198–206.
27. Liu, G. *Analysis of Soil Physical and Chemical Properties and Description of Soil Profiles*; China Standard: Beijing, China, 1996.
28. Bossio, D.A.; Scow, K.M. Impacts of carbon and flooding on soil microbial communities: Phospholipid fatty acid profiles and substrate utilization patterns. *Microb. Ecol.* **1998**, *35*, 265–278. [\[CrossRef\]](#) [\[PubMed\]](#)
29. Frostegard, A.; Baath, E. The use of phospholipid fatty acid analysis to estimate bacterial and fungal biomass in soil. *Biol. Fert. Soils* **1996**, *22*, 59–65. [\[CrossRef\]](#)
30. Baath, E.; Anderson, T.H. Comparison of soil fungal/bacterial ratios in a pH gradient using physiological and PLFA-based techniques. *Soil Biol. Biochem.* **2003**, *35*, 955–963. [\[CrossRef\]](#)
31. Massman, W.J.; Sommerfeld, R.A.; Mosier, A.R.; Zeller, K.F.; Hehn, T.J.; Rochelle, S.G. A model investigation of turbulence-driven pressure-pumping effects on the rate of diffusion of CO₂, N₂O and CH₄ through layered snow packs. *J. Geophys. Res.-Atmos.* **1997**, *102*, 18851–18863. [\[CrossRef\]](#)
32. Bowling, D.R.; Massman, W.J. Persistent wind-induced enhancement of diffusive CO₂ transport in a mountain forest snowpack. *J. Geophys. Res.-Biogeo.* **2011**, *116*, 352–370. [\[CrossRef\]](#)



© 2019 by the authors. Licensee MDPI, Basel, Switzerland. This article is an open access article distributed under the terms and conditions of the Creative Commons Attribution (CC BY) license (<http://creativecommons.org/licenses/by/4.0/>).

Methane Emission from Mangrove Wetland Soils Is Marginal but Can Be Stimulated Significantly by Anthropogenic Activities

Xiawan Zheng ^{1,2,3}, Jiemin Guo ^{3,4}, Weimin Song ^{1,5}, Jianxiang Feng ^{3,6} and Guanghui Lin ^{1,2,3,*}

¹ Ministry of Education Key Laboratory for Earth System Modeling, Department of Earth System Science, Tsinghua University, Beijing 100084, China; zhengxw16@mails.tsinghua.edu.cn (X.Z.); wmsong2005@163.com (W.S.)

² Joint Center for Global Change Studies, Beijing 100875, China

³ Graduate School at Shenzhen, Tsinghua University, Shenzhen 518055, China; jguo3@uwyo.edu (J.G.); weifeijx@163.com (J.F.)

⁴ Department of Botany, University of Wyoming, Laramie, WY 82071, USA

⁵ Yantai Institute of Coastal Zone Research, Chinese Academy of Science, Yantai 264006, China

⁶ School of Life Sciences, Sun Yat-sen University, Guangzhou 510275, China

* Correspondence: lingh@mail.tsinghua.edu.cn; Tel.: +86-010-62797230

Received: 21 October 2018; Accepted: 22 November 2018; Published: 27 November 2018

Abstract: Mangrove wetland soils have been considered as important sources for atmospheric CH₄, but the magnitude of CH₄ efflux in mangrove wetlands and its relative contribution to climate warming compared to CO₂ efflux remains controversial. In this study, we measured both CH₄ and CO₂ effluxes from mangrove soils during low or no tide periods at three tidal zones of two mangrove ecosystems in Southeastern China and collected CH₄ efflux data from literature for 24 sites of mangrove wetlands worldwide. The CH₄ efflux was highly variable among our field sites due to the heterogeneity of mangrove soil environments. On average, undisturbed mangrove sites have very low CH₄ efflux rates (ranging from 0.65 to 14.18 μmol m⁻² h⁻¹; median 2.57 μmol m⁻² h⁻¹), often less than 10% of the global warming potentials (GWP) caused by the soil CO₂ efflux from the same sites (ranging from 0.94 to 9.50 mmol m⁻² h⁻¹; median 3.67 mmol m⁻² h⁻¹), even after considering that CH₄ has 28 times more GWP over CO₂. Plant species, study site, tidal position, sampling time, and soil characteristics all had no significant effect on mangrove soil CH₄ efflux. Combining our field measurement results and literature data, we demonstrated that the CH₄ efflux from undisturbed mangrove soils was marginal in comparison with the CO₂ efflux in most cases, but nutrient inputs from anthropogenic activities including nutrient run-off and aquaculture activities significantly increased CH₄ efflux from mangrove soils. Therefore, CH₄ efflux from mangrove wetlands is strongly influenced by anthropogenic activities, and future inventories of CH₄ efflux from mangrove wetlands on a regional or global scale should consider this phenomenon.

Keywords: greenhouse gas emission; soil respiration; coastal wetlands; anthropogenic effect

1. Introduction

Global wetlands are considered as important carbon sinks for sequestering high amounts of carbon dioxide (CO₂) from the atmosphere and contain more than 30% of the world's organic carbon in the soils, despite accounting for only 5%–8% of the global terrestrial surface [1–3]. Mangrove wetlands could be key ecosystems in addressing climate regulation through their high productivity and effective carbon (C) sequestration rates [4–7]. The global carbon sequestration rate in mangrove wetlands is on average 174 g C m⁻² year⁻¹, corresponding to about 10%–15% of global coastal ocean carbon storage [8]. Organic-rich soils dominate in mangrove carbon storage, accounting for 49%–98% of

carbon stocks in mangrove wetlands [9,10]. However, the buried carbon may release back into the atmosphere as gaseous products such as CO₂ and methane (CH₄) [1]. Meanwhile, wetlands are also identified as major CH₄ sources for the atmosphere, emitting 177 to 284 Tg CH₄ year⁻¹, corresponding to approximately 40% of the total global CH₄ emission [11]. CH₄ has a global warming potential 28 times greater than that of CO₂ on a 100-year timescale and directly contributes to about 20% of recent climate warming, despite the fact its concentration is two orders of magnitude lower than that of CO₂ [12]. Thus, proper quantification of CH₄ efflux from mangrove wetlands is critical to evaluating its effect on climate warming mitigation. Additional knowledge of mangrove wetlands' CH₄ emission will further provide guidance on mangrove wetlands restoration efforts to mitigate atmospheric CO₂ increase.

CH₄ efflux from mangrove soils is generally identified to be low but highly variable [13–16]. The practice of mangrove carbon budget has shown that carbon burial, soil respiration, and soil CH₄ emission are 24 Tg C year⁻¹, 36 Tg C year⁻¹, and 2 Tg C year⁻¹, respectively [8], assuming a mangrove extent area of 138,000 km² [17]. Low CH₄ production and emission is mainly due to the presence of high sulfate in mangrove soil, which allows sulfate-reducing bacteria to outcompete CH₄-producing bacteria [18–20]. Additionally, mangrove ecosystems are inundated by periodic tides and receive nutrient input from anthropogenic activities, which provides an anaerobic environment and high availability of substrate for methanogenesis [21]. Recent studies reported a significant amount of CH₄ efflux from mangrove wetland soils [21–23] and claimed that the contribution of CH₄ efflux to climate warming was non-negligible in the estuarine mangrove wetlands, which could account for 9.3%–32.7% plant CO₂ sequestration [24]. Thus, considerable uncertainty still exists regarding the magnitude of mangrove soil CH₄ efflux and its contribution to climate warming, which requires further study.

The carbon stocks in mangrove wetlands of China play an essential role in global oceanic carbon cycling and differ among mangrove species in subtropical and tropical regions [25]. Large spatio-temporal variations in CH₄ efflux have been observed in mangrove soils [18,23,26]. Previous studies indicated that CH₄ efflux varied among different tidal positions, probably due to differences in soil temperature, salinity, and pH [27]. Temporal variation in CH₄ efflux could be explained by soil temperature, the position of the water table, and the availability of suitable substrate [23,28,29]. Meanwhile, mangrove wetlands in China are facing greater pollution pressure due to chemical discharge from aquaculture activity and sea-wall construction [30]. However, there are few studies that investigate human perturbations such as nutrient loading from aquaculture ponds on mangrove soil CH₄ efflux even though these activities can significantly change these factors [7,26].

In this study, we measured both soil CH₄ and CO₂ effluxes from mangrove wetland soils during low or no tide periods at three tidal zones of two mangrove ecosystems in Southeastern China and collected available CH₄ efflux data from literature for global mangrove wetlands. The aims of this study were to identify the magnitude of CH₄ efflux in mangrove wetlands with and without the influence of anthropogenic activities and to evaluate the relative contribution of CH₄ efflux over CO₂ efflux from mangrove wetland soils to climate warming.

2. Materials and Methods

2.1. Study Site Description

The study was conducted in two mangrove wetlands in Southeastern China, including Zhangjiang Estuary Mangrove National Natural Reserve (23°55'49" N, 117°24'54" E, abbreviated as the ZJ (Zhangjiang Estuary) site) and Qinglan Harbour Mangrove Provincial Natural Reserve (19°37'48" N, 110°46'12" E, abbreviated as the QL (Qinglan Harbour) site) (Figure 1).

ZJ site is located in an estuary of the Zhangjiang River, Yunxiao County, Fujian Province, China, with a subtropical marine monsoon climate. The monthly mean air temperature ranged from 13.5 °C in January to 28.9 °C in August, and the annual mean air temperature was 21.2 °C. Annual mean rainfall was 1714.5 mm, most of which occurred during the wet season from April to September.

Tides were semidiurnal, with an annual mean tidal-level variation of 2.32 m. The salinity of the seawater ranged from 12 to 26 ppt. The vegetation was dominated by *Kandelia obovata* Sheue, Liu & Yong (red mangrove), *Aegiceras corniculatum* (L.) Blanco (black mangrove), and *Avicennia marina* (Forssk.) Vierh. (grey mangrove), mixed with some other less common mangrove species such as *Bruguiera gymnorhiza* (L.) Savigny (black mangrove) and *Acanthus ilicifolius* L. (holy mangrove) [31].

QL site, situated in Wenchang County, Hainan Province, China, experienced a tropical monsoon climate. Annual mean air temperature was 23.9 °C, and the lowest monthly mean temperature was 18.3 °C in January. The annual precipitation was 1974 mm, of which more than 82% occurred during the wet season from May to October. Tides were semi-diurnal, and the tidal-level ranged from 0.01 m to 2.38 m, with the largest tidal-level variation of 2.07 m in one tidal cycle. The dominant mangrove species at QL site, which had the largest number of mangrove species in China, were *Bruguiera sexangula* (Lour.) Poir. (upriver orange mangrove), *Sonneratia caseolaris* (L.) Engl. (mangrove apple), *Lumnitzera racemosa* Willd. (tonga mangrove), *Ceriops tagal* (Pers.) C.B.Rob. (spurred mangrove), and *Rhizophora apiculata* Blume (red mangrove) communities [32,33].

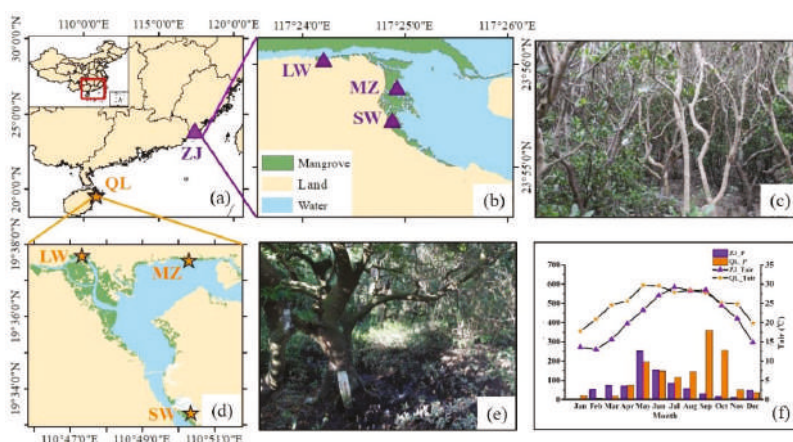


Figure 1. Map of sampling location and climatic conditions. (a) Geographical location of Zhangjiang Estuary (ZJ) and Qinglan Harbour (QL) mangrove wetlands. (b,c) Sampling sites and a typical scene from ZJ mangrove forest. (d,e) Sampling sites and a typical scene from QL mangrove forest. (f) Monthly precipitation (P, mm) and monthly air temperature (T, °C) from ZJ and QL mangrove wetlands. LW: landward zone, MZ: middle zone, and SW: seaward zone.

2.2. Measurements of Soil CH₄ and CO₂ Effluxes

Sampling campaigns were undertaken in July 2013 (represented wet season) and February 2014 (represented dry season) at ZJ site, and in August 2016 (represented wet season) and November 2017 (represented dry season) at QL site. For each sampling time, measurements were conducted in three tidal positions: landward zone (LW), middle zone (MZ), and seaward zone (SW), with the exception of SW at ZJ site during the dry season due to heavy rainfall making the site inaccessible. At each sampling position, four chambers were set up, and four replicated samples were collected on the same day at each site for a total of twelve samples. During low or no tide periods in the day time, we measured environmental variables and collected samples for laboratory analyses. The soil inundation and exposure duration were similar among three tidal positions and four replicates samples.

Gas effluxes from the soil were quantified through the standard static (closed) chamber technique [23]. Measurements were taken using PVC chambers (diameter 20 cm, length 15 cm, volume 4.50 L, and enclosing 0.025 m²). The open end of chamber was slightly inserted into the soil to a depth of 2–3 cm to ensure minimal lateral gas leakage. A controllable valve above the chamber was left open for 30 min prior to sampling, which is adequate to remove impacts of root disturbance caused by the

chamber insertion, and then the valve was closed during the whole measurements time. Deployment time was set at 2 h, with sampling at 0, 30, 60, 90, and 120 min intervals. Headspace gas was mixed carefully through the vent tube, and 8 mL gas samples were collected using a 50 mL gas-tight syringe equipped with a luer-lock valve (SGE Trajan Scientific and Medical Pty Ltd., Melbourne, Australia). Gas samples were then transferred into pre-evacuated gas sampling bags or vials for storage (Dalian Delin Gas Packing Inc., Dalian, Liaoning, China). The air temperature inside the chamber was measured simultaneously with the gas sampling.

All samples were transported to laboratory and analyzed within 24 h using an Agilent 7890A gas chromatograph (Agilent Technologies Inc., Wilmington, DE, USA) equipped with a flame ionization detector (FID) and a Poropak-Q column. The column and detector temperatures were set at 60 °C and 130 °C, respectively, with nitrogen as the carrier gas at a flow rate of 1200 mL s⁻¹. Standard curves were gained by injecting a series volume of pure CH₄ (99.992%) and CO₂ (99.999%) in high purity N₂ (99.999%, HKO Co Ltd., Hong Kong, China). The CH₄ and CO₂ concentrations were quantified by calculating the peak areas of samples against standards of similar concentration ranges. During the gas measurement, standard gas (40 mL L⁻¹ CH₄ and 2000 mL L⁻¹ CO₂) was analyzed every 10 samples to ensure data quality. Gas effluxes were calculated based on a linear least squares fit of the time series of gas concentrations. Data were accepted if the slope of the linear fit had a $R^2 > 0.80$.

2.3. Measurements of Environmental Factors

For each chamber measurement, soil cores (0–10 cm surface soil) were collected using a hand-held PVC tube after gas sampling. The soil samples were divided into two subsamples: fresh soil and air-dried soil. Soil moisture content was determined by oven-drying of 7 g fresh soil at 105 °C to a constant weight. Soil inorganic N (NH₄⁺-N and NO₃⁻-N) contents were extracted with 2 M KCl from fresh soil samples and then analyzed using a UV-2501PC UV-VIS spectrophotometer (Shimadzu Inc., Japan) [23]. While both NH₄⁺-N and NO₃⁻-N extraction methods require fresh soil samples, the samples from ZJ-SW during the wet season and ZJ-LW and ZJ-MZ during the dry season were dried before we could take any measurements. Air-dried soil was sieved through a 2 mm sieve. The pH and salinity were measured at a *w* (soil): *v* (water) of 1:5 and 1:2.5 soil slurry using an electrochemistry benchtop meter, Orion™ Versa Star Pro™ (Thermo Fisher Scientific Inc., Beverly, MA, USA). Soil total carbon content (TC), total nitrogen content (TN), and C:N ratio of air-dried soil were measured using the an elemental analyzer (Vario EL III, Elementar Analysensysteme GmbH Inc., Hanau, Germany). Analysis of soil characteristics all followed the standard methods described by Page et al. (1982), and data were expressed in term of 105 °C oven-dried weight.

2.4. Conversion to CO₂—Equivalent Efflux

The global warming potential for CH₄ was converted to CO₂ equivalents using a multiplier of 28 for 100-year timescale [34] to compare their global warming effects.

2.5. Collecting CH₄ Efflux Data from Literature

A total of 24 studies of CH₄ efflux from mangrove soil were reviewed (Table S2). These studies were selected because the same static chamber method was used as our study, which made the results comparable. We divided the mangrove wetlands into undisturbed and anthropogenic sites according to the eutrophic status of the chosen study sites (Table S3). Undisturbed sites are defined as not affected by nutrient input from anthropogenic activities involving agricultural, domestic, aquaculture, or other run-off from treatment plants as indicated by the reference's study site descriptions. Anthropogenic sites are those known to be influenced by activities described above.

2.6. Statistical Analysis

Two-way analysis of variance (ANOVA) was used to determine significance of differences between means of soil characteristics and effluxes of CH₄ and CO₂ among tidal positions and sampling time.

If the difference was significant at $p < 0.05$, a Post-hoc Turkey test was used to determine where the difference lay. All data were expressed as means \pm standard error (SE) with four replicates. Paired t -test was used to compare the differences in soil characteristics and effluxes of CH_4 and CO_2 among tropical and subtropical mangrove wetlands. Pearson correlation coefficient values (r) were calculated to determine the relationship between soil characteristics and CH_4 and CO_2 effluxes. All analysis processes were performed using SPSS 21.0 for Windows (SPSS Inc., Chicago, IL, USA).

3. Results

3.1. Soil CH_4 and CO_2 Effluxes

CH_4 efflux was highly variable among the sampling sites, for most sampling sites; CH_4 efflux was small and almost negligible, ranging from 0.65 ± 0.91 to $14.18 \pm 6.35 \mu\text{mol m}^{-2} \text{h}^{-1}$, while at the landward zone in Zhangjiang Estuary site (abbreviated as ZJLW) during the wet season, CH_4 efflux was about 10 times higher than the highest value found at other sites ($123.59 \pm 41.79 \mu\text{mol m}^{-2} \text{h}^{-1}$) (Figure 2a,b and Table S1). CO_2 efflux ranged from 0.94 ± 0.41 to $9.50 \pm 2.70 \text{ mmol m}^{-2} \text{h}^{-1}$, and the highest and lowest values were recorded at landward and seaward zones in Qinglan Harbour mangrove wetland during wet season (Figure 2c, Figure 2d and Table S1). No significant difference was found in soil CH_4 and CO_2 effluxes between ZJ and QL sites ($p = 0.173$ and $p = 0.111$).

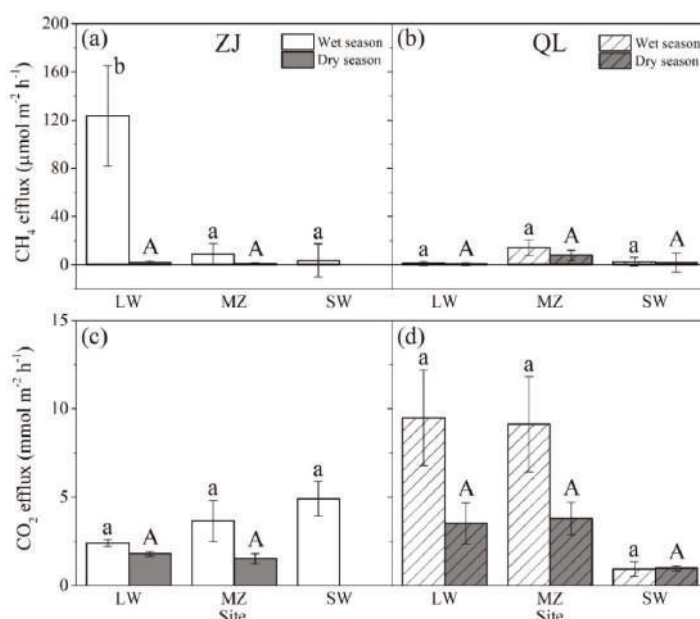


Figure 2. CH_4 and CO_2 effluxes from ZJ and QL mangrove soils. (a,b) Comparison of the mean soil CH_4 efflux among three tidal positions during wet and dry seasons at ZJ and QL site. (c,d) Comparison of the mean soil CO_2 efflux among three tidal positions during wet and dry seasons at ZJ and QL site. Error bars represent the standard error (SE) of the means ($n = 4$). Different letters indicate significant differences among tidal positions for each period (wet and dry seasons) according to analysis of variance (ANOVA) test (Turkey HSD test, $p < 0.05$). Site abbreviations were the same as Figure 1.

At ZJ site, CH_4 efflux ranged from 0.73 ± 0.73 to $123.59 \pm 41.79 \mu\text{mol m}^{-2} \text{h}^{-1}$ (Figure 2a), and significant differences in CH_4 efflux among tidal positions and sampling time were found ($p = 0.006$ and $p = 0.002$, respectively). The highest and lowest CH_4 values were recorded at landward zone during wet season and middle zone during dry season, respectively. Soil CH_4 efflux was higher

in wet season than that in the dry season at all sites. The CO_2 efflux ranged from 1.52 ± 0.29 to $4.91 \pm 0.98 \text{ mmol m}^{-2} \text{ h}^{-1}$ and did not differ significantly with tidal positions and seasons ($p = 0.160$ and $p = 0.108$) (Figure 2c).

At QL site, the value of soil CH_4 efflux ranged from 0.65 ± 0.91 to $14.18 \pm 6.35 \text{ } \mu\text{mol m}^{-2} \text{ h}^{-1}$ and showed no significant differences among different tidal positions and sampling time ($p > 0.05$) (Figure 2b). CH_4 efflux at the middle zone was the highest, followed by the CH_4 efflux at seaward zone. The CO_2 efflux ranged from 0.94 ± 0.41 to $9.50 \pm 2.70 \text{ mmol m}^{-2} \text{ h}^{-1}$ (Figure 2d) and changed with tidal position and sampling time significantly ($p = 0.045$ and $p = 0.042$, respectively). The lowest value of CO_2 efflux was measured at seaward zone, and highest CO_2 efflux was observed during wet season rather than dry season.

3.2. Soil Characteristics

Soil characteristics measured during wet and dry season at ZJ and QL sites are shown in Table 1. There were significant differences in soil temperature, pH, TC content, TN content, and C:N ratio among subtropical (ZJ site) and tropical (QL site) mangrove wetlands ($p < 0.05$). The mangrove soils had higher pH values (ranging from 6.62 ± 0.16 to 7.43 ± 0.14) at QL site than that at ZJ site (ranging from 5.46 ± 0.31 to 7.11 ± 0.03). Higher soil temperature, TC content, TN content, and C:N ratio were detected at QL site than at ZJ site ($p < 0.05$). Salinity and soil moisture content were not significantly different between QL site and ZJ site and were not significantly influenced by tidal positions and sampling time ($p > 0.05$).

At ZJ site, significantly higher soil temperatures were observed in the wet season rather than dry season ($p = 0.015$). Tidal position had significant effect on pH, TN content, and C:N ratio ($p < 0.05$). Lowest pH but highest TC content, TN content, and C:N ratio were observed in the middle zone ($p < 0.05$).

At QL site, both soil temperature and C:N ratio were significantly different between wet and dry season. Higher soil temperature and a lower C:N ratio were observed in wet season ($p < 0.05$). The pH value, NH_4^+ -N content, NO_3^- -N content, TN content, TC content, and C:N ratio were significantly affected by tidal position ($p < 0.05$). With an increase in tidal positions, salinity, pH value, and C:N ratio gradually increased, while the NH_4^+ -N content, NO_3^- -N content, TN content, and TC content gradually decreased.

Table 1. Key characteristics for mangrove soils at various study sites measured during wet and dry seasons.

| Mangrove Wetland | Season | Study Site | Species | T _{soil} | Salinity (ppt) | pH | Soil Moisture Content | NH ₄ ⁺ -N (ug g ⁻¹) | NO ₃ ⁻ -N (ug g ⁻¹) | TN (%) | TC (%) | C:N Ratio |
|------------------|------------|------------|---------|-------------------|----------------|---------------|-----------------------|---|---|--------------|----------------|----------------|
| ZJ | Wet season | LW | KO | 27.19 ± 0.19c | 2.07 ± 0.25a | 5.46 ± 0.31a | 0.85 ± 0.15a | 9.50 ± 0.92 | 0.14 ± 0.04 | 0.15 ± 0.03a | 1.82 ± 0.18a | 12.50 ± 1.07b |
| | | MZ | KO | 27.74 ± 0.05c | 5.70 ± 0.66ab | 7.11 ± 0.05c | 0.89 ± 0.23a | 9.09 ± 0.88 | 0.15 ± 0.05 | 0.15 ± 0.01a | 1.36 ± 0.01a | 9.25 ± 0.35a |
| | Dry season | SW | KO | 27.42 ± 0.09c | 7.70 ± 1.45ab | 6.82 ± 0.05ab | 1.04 ± 0.45a | | | 0.17 ± 0.01a | 1.96 ± 0.18a | 11.44 ± 0.65ab |
| | | LW | KO | 17.35 ± 0.19a | 9.00 ± 1.27b | 6.23 ± 0.10b | 0.75 ± 0.07a | 6.23 ± 0.10b | | 0.16 ± 0.02a | 1.98 ± 0.16a | 12.29 ± 0.47b |
| QL | Wet season | MZ | KO | 18.47 ± 0.09b | 15.55 ± 2.56c | 7.01 ± 0.14c | 0.81 ± 0.53a | | | 0.14 ± 0.01a | 1.49 ± 0.09a | 10.90 ± 0.31ab |
| | | SW | KO | | | | | | | | | |
| | Dry season | LW | BS, HL | 29.00D | 12.09 ± 1.37A | 6.81 ± 0.05AB | 1.85 ± 0.25B | 8.02 ± 0.90B | 4.31 ± 0.45B | 0.73 ± 0.10B | 11.48 ± 2.00AB | 15.44 ± 0.93A |
| | | MZ | BS, RA | 28.90D | 17.84 ± 5.91AB | 6.62 ± 0.16A | 0.56 ± 0.12A | 3.11 ± 0.55A | 1.28 ± 0.13A | 0.24 ± 0.05A | 4.01 ± 0.66AB | 17.03 ± 0.61A |
| ZJ | Wet season | SW | Mixed | 30.50E | 25.91 ± 4.22B | 6.85 ± 0.02AB | 0.51 ± 0.01A | 3.17 ± 0.13A | 1.63 ± 0.05A | 0.08 ± 0.01A | 4.48 ± 0.12AB | 57.81 ± 7.33B |
| | | LW | KO | 25.18 ± 0.07B | 11.12 ± 1.21A | 7.30 ± 0.11BC | 2.08 ± 0.39B | 8.14 ± 1.10B | 3.55 ± 0.35B | 0.79 ± 0.11B | 12.41 ± 2.58B | 15.10 ± 0.89A |
| | Dry season | MZ | KO | 23.34 ± 0.03A | 15.60 ± 0.67AB | 6.76 ± 0.16A | 0.60 ± 0.14A | 2.26 ± 0.75A | 1.42 ± 0.30A | 0.19 ± 0.05A | 3.52 ± 0.88A | 19.47 ± 0.74B |
| | | SW | KO | 25.45 ± 0.01C | 19.90 ± 0.30AB | 7.43 ± 0.14C | 0.44 ± 0.06A | 2.26 ± 0.33A | 1.31 ± 0.01A | 0.07 ± 0.01A | 4.75 ± 0.16AB | 74.26 ± 7.84C |

ZJ: Zhangjiang Estuary Mangrove National Natural Reserve; QL: Qinglan Harbour Mangrove Provincial Natural Reserve; LW: Landward zone; MZ: Middle zone; SW: Seaward zone; KO: *Kandelia chorata* Sheue, Liu & Yong (red mangrove) community; BS: *Bruguiera sexangula* (Lour.) Poit. (upriver orange mangrove) community; HL: *Heteria littoralis* Aiton (looking-glass mangrove) community; RA: *Rhizophora apiculata* Blume (red mangrove) community; Mixed: Mixed species community. Mean and standard error (SE) of four replicates are shown ($n = 4$). Different letters indicated significant differences among different sampling sites according to analysis of variance (ANOVA) test ($p < 0.05$).

3.3. The Relationship between Gas Effluxes and Soil Characteristics

Among soil characteristics measured in current study, soil temperature and pH were correlated with CO₂ efflux. The soil temperature had positive effect on CO₂ efflux ($p = 0.011$, $r = 0.342$), while pH had negative effect on it ($p < 0.001$, $r = -0.506$). No significant relationship among CH₄ efflux and any soil characteristics was recorded in this study.

4. Discussions

4.1. Magnitude of CH₄ Efflux from Mangrove Wetland Soils

Combining our data and literature data, we found CH₄ efflux from undisturbed mangrove wetlands was negligible but can be stimulated significantly by anthropogenic activities (Figure 3). The results from our direct field measurements indicated that low CH₄ efflux was recorded in undisturbed mangrove soils of Southeastern China, ranging from 0.65 ± 0.91 to $14.18 \pm 6.35 \mu\text{mol m}^{-2} \text{h}^{-1}$, which was consistent with the results found by others in nearby undisturbed mangrove areas [35–37]. The highest CH₄ efflux ($123.59 \pm 41.79 \mu\text{mol m}^{-2} \text{h}^{-1}$) was observed at landward zone in ZJ mangrove wetland, probably due to large and frequent discharge of freshwater as indicated by very low salinity at this site (as low as 2 ppt) (Table 1). This result was similar to the CH₄ efflux in the Jiulong River mangrove, which was also heavily influenced by human activities and positively correlated with NH₄⁺-N, organic carbon, and total Kjeldahl nitrogen [24]. Mangrove ecosystems are rich in carbon but nutrient-poor; in particular, they are limited by nitrogen and phosphorus [38]. Anthropogenic nutrient input improves microbial metabolic process, enhancing more emission of CH₄ efflux from soils into the atmosphere [39].

In addition, the CH₄ efflux data from literature for 24 sites of mangrove wetlands worldwide showed that mangroves affected by anthropogenic activities (ranging from 0.19 to $5168.62 \mu\text{mol m}^{-2} \text{h}^{-1}$ with the median values of $52.80 \mu\text{mol m}^{-2} \text{h}^{-1}$) had emission rates 14 times higher than those from undisturbed mangroves (ranging from -6.05 to $79.00 \mu\text{mol m}^{-2} \text{h}^{-1}$ with the median of $3.57 \mu\text{mol m}^{-2} \text{h}^{-1}$). These CH₄ efflux data revealed that the mangroves affected by anthropogenic activities made a greater contribution to climate warming rather than those undisturbed or not heavily disturbed mangrove forests. Anthropogenic activities cause significant increases in CH₄ emission, and if anthropogenic activities continue at the current pace without protective measures, these ecosystems could become potential major sources of CH₄ emission and decrease their ability to store carbon in the future [40]. The current study divided the mangrove wetlands into undisturbed and affected by anthropogenic activities based on whether the chosen study sites have involved agricultural, domestic, aquaculture, or other run-off from treatment plants in the references. Further research is needed to quantify the stimulation effect of nutrient input from anthropogenic activities on CH₄ emissions, combined with controlled experiments and microbial community analysis to model the extent of change.

4.2. Contribution of CH₄ Efflux from Mangrove Wetlands to Climate Warming

We calculated CH₄:CO₂ efflux ratio and CH₄:CO₂ warming effect ratio to evaluate the relative role of CH₄ efflux for warming potentials (Figure 4) among different tidal zones in two mangrove wetlands. The CH₄:CO₂ efflux ratio ranged from $-0.06\% \pm 0.32\%$ to $0.45\% \pm 0.57\%$ in most sampling sites except for the disturbed ZJLW site ($4.95\% \pm 1.46\%$). Considering CH₄ global warming potential in 100-year term, CH₄ accounted for $-0.63\% \pm 3.21\%$ to $4.54\% \pm 5.79\%$ of the warming effect, a relatively minor contributor to CO₂ equivalents, except at the ZJLW site, which was $50.37\% \pm 14.85\%$, making it a highly significant contributor. A higher CH₄:CO₂ warming effect ratio had been reported in the Jiulong River mangrove (10.30% to 48.35%) [24] and Futian mangrove (18.36% to 255.96%) [21] in South China, which received significant amounts of anthropogenic nutrient inputs. This reveals that the magnitude and contribution of CH₄ efflux from undisturbed mangrove soils to climate warming

was marginal in comparison with CO₂ efflux, but could be a potential major contributor to warming effect under the influence of anthropogenic activities.

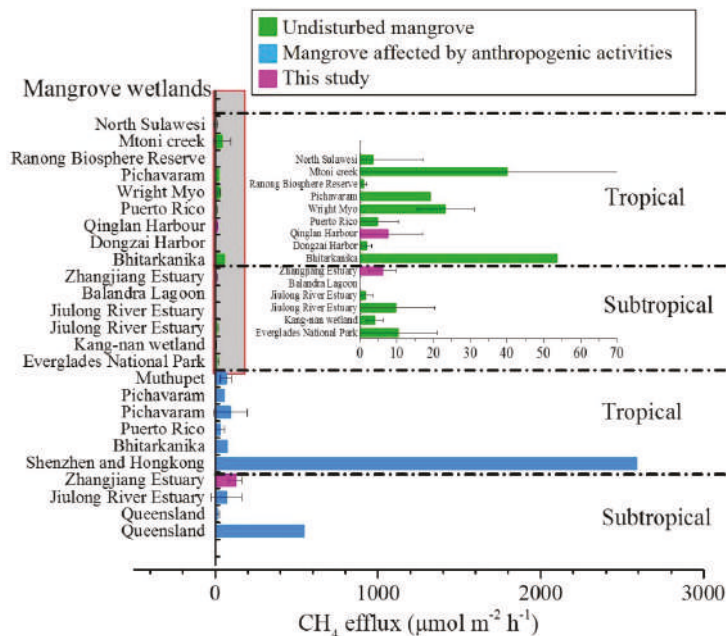


Figure 3. Comparison of CH₄ efflux from undisturbed mangrove wetlands and mangroves wetlands affected by anthropogenic activities. Detailed information on the literature sources of CH₄ efflux data is provided in Table S2. Nutrient concentrations and assignment of eutrophic status from mangrove wetlands are shown in Table S3.

In addition, the global median CH₄ efflux in mangrove wetlands (3.57 and 52.80 μmol m⁻² h⁻¹ for undisturbed mangroves and mangroves affected by anthropogenic activities, respectively) was negligible in contrast to other wetlands, such as freshwater wetlands (69.44 to 6944.44 μmol m⁻² h⁻¹) (Chmura et al., 2003), peatlands (31.39 to 59.93 μmol m⁻² h⁻¹) [41], and rice paddies (709.38 μmol m⁻² h⁻¹) [42]. This indicates that mangrove wetlands were not significant contributors to global wetland CH₄ budget compared with other wetlands. Recent studies have also found that mangrove soils acted as a net carbon sink after subtracting the effects of CH₄ emission from carbon sequestration [43]. Overall, mangrove wetlands should be restored and protected to mitigate climate warming without great concern for warming effect caused by CH₄ emission.

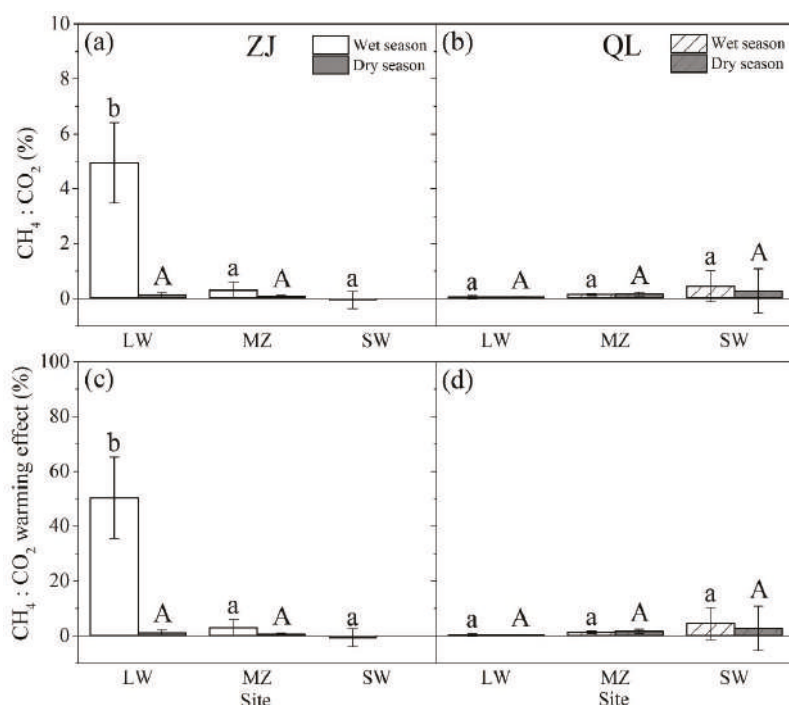


Figure 4. $\text{CH}_4 : \text{CO}_2$ effluxes ratio and $\text{CH}_4 : \text{CO}_2$ warming effect ratio from ZJ and QL mangrove wetlands. (a–b) Comparison of $\text{CH}_4 : \text{CO}_2$ effluxes ratio among three tidal positions during wet and dry seasons at ZJ and QL sites. (c–d) Comparison of $\text{CH}_4 : \text{CO}_2$ warming effect ratio among three tidal positions during wet and dry seasons at ZJ and QL site. Site abbreviations were the same as Figure 1.

5. Conclusions

The current study suggests that undisturbed mangrove soils were minor contributors to climate warming, but the CH_4 efflux from mangrove wetlands was significantly increased by nutrient inputs from anthropogenic activities including nutrient run-off and aquaculture activities. This phenomenon should be considered in order to better quantify the emission of CH_4 from regional or global mangrove wetlands and to evaluate the potential roles of constructed or restored mangrove wetlands for mitigating climate warming.

Supplementary Materials: The following are available online at <http://www.mdpi.com/1999-4907/9/12/738/s1>, Table S1: CH_4 and CO_2 effluxes from ZJ and QL mangrove wetlands; Table S2: summary of CH_4 efflux data as reported by authors or calculated from literature in other mangrove wetlands; and Table S3: nutrient concentrations and assignment of eutrophic status.

Author Contributions: G.L. conceived and designed the experiment. X.Z., J.G., W.S. and J.F. conducted the experiment and collected data. X.Z. and G.L. analyzed the data and wrote the initial draft of the manuscript. All authors contributed to the editing and revising of the final version of the manuscript. The authors approved the final version for publication and agree to be held accountable for the content therein.

Funding: This research described in this paper was supported financially by National Basic Research Program of China (973 Program); Ministry of Science and Technology, China (2013CB956601); Shenzhen Basic Research Discipline Layout Project, Shenzhen Science and Technology Innovation Committee, China (JCYJ20150529164918736); and the Ocean Open Public Fund Project, State Oceanic Administration, China (201305021).

Acknowledgments: We thank Jianzhang Chen for assistance in the elemental and Gas Chromatograph analyses, and Guangqiang Zheng, Jie Liang, Ziyao Yang and Jiacheng Lv for their assistances in field sampling and measurements. We thank Chris Feng for improving the English of this manuscript.

Conflicts of Interest: The authors declare no conflict of interest.

References

1. Mitsch, W.J.; Bernal, B.; Nahlik, A.M.; Mander, Ü.; Zhang, L.; Anderson, C.J.; Jørgensen, S.E.; Brix, H. Wetlands, carbon, and climate change. *Landsc. Ecol.* **2012**, *28*, 583–597. [[CrossRef](#)]
2. Sun, L.; Song, C.; Lafleur, P.M.; Miao, Y.; Wang, X.; Gong, C.; Qiao, T.; Yu, X.; Tan, W. Wetland-atmosphere methane exchange in Northeast China: A comparison of permafrost peatland and freshwater wetlands. *Agric. For. Meteorol.* **2017**, *249*, 239–249. [[CrossRef](#)]
3. Mitra, S.; Wassmann, R.; Vlek, P.L.G. An appraisal of global wetland area and its organic carbon stock. *Curr. Sci.* **2005**, *88*, 25–35.
4. McLeod, E.; Chmura, G.L.; Bouillon, S.; Salm, R.; Björk, M.; Duarte, C.M.; Lovelock, C.E.; Schlesinger, W.H.; Silliman, B.R. A blueprint for blue carbon: Toward an improved understanding of the role of vegetated coastal habitats in sequestering CO₂. *Front. Ecol. Environ.* **2011**, *9*, 552–560. [[CrossRef](#)]
5. Siteo, A.; Mandlate, L.; Guedes, B. Biomass and Carbon Stocks of Sofala Bay Mangrove Forests. *Forests* **2014**, *5*, 1967–1981. [[CrossRef](#)]
6. Cui, X.; Liang, J.; Lu, W.; Chen, H.; Liu, F.; Lin, G.; Xu, F.; Luo, Y.; Lin, G. Stronger ecosystem carbon sequestration potential of mangrove wetlands with respect to terrestrial forests in subtropical China. *Agric. For. Meteorol.* **2018**, *249*, 71–80. [[CrossRef](#)]
7. Lu, W.; Xiao, J.; Liu, F.; Zhang, Y.; Liu, C.; Lin, G. Contrasting ecosystem CO₂ fluxes of inland and coastal wetlands: A meta-analysis of eddy covariance data. *Glob. Chang. Biol.* **2017**, *23*, 1180–1198. [[CrossRef](#)] [[PubMed](#)]
8. Alongi, D.M. Carbon cycling and storage in mangrove forests. *Ann. Rev. Mar. Sci.* **2014**, *6*, 195–219. [[CrossRef](#)] [[PubMed](#)]
9. Benson, L.; Glass, L.; Jones, T.; Ravaoarinoroitsihoarana, L.; Rakotomahazo, C. Mangrove Carbon Stocks and Ecosystem Cover Dynamics in Southwest Madagascar and the Implications for Local Management. *Forests* **2017**, *8*, 190. [[CrossRef](#)]
10. Donato, D.C.; Kauffman, J.B.; Murdiyarso, D.; Kurnianto, S.; Stidham, M.; Kanninen, M. Mangroves among the most carbon-rich forests in the tropics. *Nat. Geosci.* **2011**, *4*, 293–297. [[CrossRef](#)]
11. Ciais, P.; Sabine, C.; Manyothers, I.; Patra, P.; Ciais, P.; Sabine, C.; Manyothers, I.; Patra, P. *Chapter 6: Carbon and Other Biogeochemical Cycles*; Cambridge University Press: Cambridge, UK, 2014.
12. Stocker, T.F.; Qin, D.; Plattner, G.-K.; Tignor, M.; Allen, S.K.; Boschung, J.; Nauels, A.; Xia, Y.; Bex, V.; Midgley, P.M. *Climate Change 2013: The Physical Science Basis. Contribution of Working Group I to the Fifth Assessment Report of the Intergovernmental Panel on Climate Change*; Cambridge University Press: Cambridge, UK; New York, NY, USA, 2013; pp. 465–570.
13. Harriss, R.C.; Sebach, D.I.; Bartlett, K.B.; Bartlett, D.S.; Crill, P.M. Sources of atmospheric methane in the south Florida environment. *Glob. Biogeochem. Cycle* **1988**, *2*, 231–243. [[CrossRef](#)]
14. Sotomayor, D.; Corredor, J.E.; Morell, J.M. Methane flux from mangrove sediments along the southwestern coast of Puerto Rico. *Estuaries* **1994**, *17*, 140–147. [[CrossRef](#)]
15. Kristensen, E. *Carbon Balance in Mangrove Sediments: The Driving Processes and Their Controls*; Gendai Toshō: Kanagawa, Japan, 2007; pp. 61–78.
16. Chen, G.C.; Ulumuddin, Y.I.; Pramudji, S.; Chen, S.Y.; Chen, B.; Ye, Y.; Ou, D.Y.; Ma, Z.Y.; Huang, H.; Wang, J.K. Rich soil carbon and nitrogen but low atmospheric greenhouse gas fluxes from North Sulawesi mangrove swamps in Indonesia. *Sci. Total Environ.* **2014**, *487*, 91–96. [[CrossRef](#)] [[PubMed](#)]
17. Giri, C.; Ochieng, E.; Tieszen, L.L.; Zhu, Z.; Singh, A.; Loveland, T.; Masek, J.; Duke, N. Status and distribution of mangrove forests of the world using earth observation satellite data. *Glob. Ecol. Biogeogr.* **2011**, *20*, 154–159. [[CrossRef](#)]
18. Biswas, H.; Mukhopadhyay, S.K.; Sen, S.; Jana, T.K. Spatial and temporal patterns of methane dynamics in the tropical mangrove dominated estuary, NE coast of Bay of Bengal, India. *J. Mar. Syst.* **2007**, *68*, 55–64. [[CrossRef](#)]
19. Segarra, K.E.A.; Comerford, C.; Slaughter, J.; Joye, S.B. Impact of electron acceptor availability on the anaerobic oxidation of methane in coastal freshwater and brackish wetland sediments. *Geochim. Cosmochim. Acta* **2013**, *115*, 15–30. [[CrossRef](#)]

20. Nobrega, G.N.; Ferreira, T.O.; Neto, M.S.; Queiroz, H.M.; Artur, A.G.; Mendonca, E.D.; Silva, E.D.; Otero, X.L. Edaphic factors controlling summer (rainy season) greenhouse gas emissions (CO₂ and CH₄) from semiarid mangrove soils (NE-Brazil). *Sci. Total Environ.* **2016**, *542*, 685–693. [[CrossRef](#)] [[PubMed](#)]
21. Chen, G.C.; Tam, N.F.Y.; Ye, Y. Summer fluxes of atmospheric greenhouse gases N₂O, CH₄ and CO₂ from mangrove soil in South China. *Sci. Total Environ.* **2010**, *408*, 2761–2767. [[CrossRef](#)] [[PubMed](#)]
22. Mukhopadhyay, S.; Biswas, H.; De, T.; Sen, B.; Sen, S.; Jana, T. Impact of Sundarban mangrove biosphere on the carbon dioxide and methane mixing ratios at the NE Coast of Bay of Bengal, India. *Atmos. Environ.* **2002**, *36*, 629–638. [[CrossRef](#)]
23. Allen, D.E.; Dalal, R.C.; Rennenberg, H.; Meyer, R.L.; Reeves, S.; Schmidt, S. Spatial and temporal variation of nitrous oxide and methane flux between subtropical mangrove sediments and the atmosphere. *Soil Biol. Biochem.* **2007**, *39*, 622–631. [[CrossRef](#)]
24. Chen, G.; Chen, B.; Yu, D.; Tam, N.F.Y.; Ye, Y.; Chen, S. Soil greenhouse gas emissions reduce the contribution of mangrove plants to the atmospheric cooling effect. *Environ. Res. Lett.* **2016**, *11*, 124019. [[CrossRef](#)]
25. Liu, H.; Ren, H.; Hui, D.; Wang, W.; Liao, B.; Cao, Q. Carbon stocks and potential carbon storage in the mangrove forests of China. *J. Environ. Manag.* **2014**, *133*, 86–93. [[CrossRef](#)] [[PubMed](#)]
26. Wang, H.T.; Liao, G.S.; D'Souza, M.; Yu, X.Q.; Yang, J.; Yang, X.R.; Zheng, T.L. Temporal and spatial variations of greenhouse gas fluxes from a tidal mangrove wetland in Southeast China. *Environ. Sci. Pollut. Res.* **2016**, *23*, 1873–1885. [[CrossRef](#)] [[PubMed](#)]
27. Chauhan, R.; Datta, A.; Ramanathan, A.L.; Adhya, T.K. Factors influencing spatio-temporal variation of methane and nitrous oxide emission from a tropical mangrove of eastern coast of India. *Atmos. Environ.* **2015**, *107*, 95–106. [[CrossRef](#)]
28. Walter, B.P.; Heimann, M. A process-based, climate-sensitive model to derive methane emissions from natural wetlands: Application to five wetland sites, sensitivity to model parameters, and climate. *Glob. Biogeochem. Cycle* **2000**, *14*, 745–765. [[CrossRef](#)]
29. Inubushi, K.; Furukawa, Y.; Hadi, A.; Purnomo, E.; Tsuruta, H. Seasonal changes of CO₂, CH₄ and N₂O fluxes in relation to land-use change in tropical peatlands located in coastal area of South Kalimantan. *Chemosphere* **2003**, *52*, 603–608. [[CrossRef](#)]
30. Zai-Wang, Z.; Xiang-Rong, X.; Yu-Xin, S.; Shen, Y.; Yong-Shan, C.; Jia-Xi, P. Heavy metal and organic contaminants in mangrove ecosystems of China: A review. *Environ. Sci. Pollut. Res. Int.* **2014**, *21*, 11938–11950.
31. Lin, P. *The Comprehensive Report of Science Investigation on the Natural Reserve of Mangrove Wetland of Zhangjiang Estuary in Fujian*; Xiamen University Press: Xiamen, China, 2001.
32. Ding, H.; Yao, S.; Chen, J. Authigenic pyrite formation and re-oxidation as an indicator of an unsteady-state redox sedimentary environment: Evidence from the intertidal mangrove sediments of Hainan Island, China. *Cont. Shelf Res.* **2014**, *78*, 85–99. [[CrossRef](#)]
33. Guo, Z.Z.; Guo, Y.; Wen, W.; Cao, M.; Guo, J.; Li, Z. Soil carbon sequestration and its relationship with soil pH in Qinglangang mangrove wetlands in Hainan island (in Chinese). *Sci. Silvae Sin.* **2014**, *50*, 8–15.
34. Myhre, G.; Shindell, D.; Bréon, F.-M.; Collins, W.; Fuglestedt, J.; Huang, J.; Koch, D.; Lamarque, J.-F.; Lee, D.; Mendoza, B. Anthropogenic and natural radiative forcing. *Clim. Chang.* **2013**, *423*, 658–740.
35. Lu, C.Y.; Wong, Y.S.; Tam, N.F.; Ye, Y.; Lin, P. Methane flux and production from sediments of a mangrove wetland on Hainan Island, China. *Mangroves Salt Marshes* **1999**, *3*, 41–49. [[CrossRef](#)]
36. Alongi, D.M.; Pfitzer, J.; Trott, L.A.; Tirendi, F.; Dixon, P.; Klumpp, D.W. Rapid sediment accumulation and microbial mineralization in forests of the mangrove *Kandelia candel* in the Jiulongjiang Estuary, China. *Estuar. Coast. Shelf Sci.* **2005**, *63*, 605–618. [[CrossRef](#)]
37. Chen, Y.P.; Chen, G.C.; Ye, Y. Coastal vegetation invasion increases greenhouse gas emission from wetland soils but also increases soil carbon accumulation. *Sci. Total Environ.* **2015**, *526*, 19–28. [[CrossRef](#)] [[PubMed](#)]
38. Alongi, D. Impact of Global Change on Nutrient Dynamics in Mangrove Forests. *Forests* **2018**, *9*, 596. [[CrossRef](#)]
39. Kreuzwieser, J.; Buchholz, J.; Rennenberg, H. Emission of Methane and Nitrous Oxide by Australian Mangrove Ecosystems. *Plant Biol.* **2003**, *5*, 423–431. [[CrossRef](#)]
40. Purvaja, R.; Ramesh, R. Natural and Anthropogenic Methane Emission from Coastal Wetlands of South India. *Environ. Manag.* **2001**, *27*, 547–557. [[CrossRef](#)]

41. Abdalla, M.; Hastings, A.; Truu, J.; Espenberg, M.; Mander, Ü.; Smith, P. Emissions of methane from northern peatlands: A review of management impacts and implications for future management options. *Ecol. Evolut.* **2016**, *6*, 7080–7102. [[CrossRef](#)] [[PubMed](#)]
42. Chen, H.; Zhu, Q.A.; Peng, C.H.; Wu, N.; Wang, Y.F.; Fang, X.Q.; Jiang, H.; Xiang, W.H.; Chang, J.; Deng, X.W.; et al. Methane emissions from rice paddies natural wetlands, lakes in China: Synthesis new estimate. *Glob. Chang. Biol.* **2013**, *19*, 19–32. [[CrossRef](#)] [[PubMed](#)]
43. Cabezas, A.; Mitsch, W.J.; MacDonnell, C.; Zhang, L.; Bydalek, F.; Lasso, A. Methane emissions from mangrove soils in hydrologically disturbed and reference mangrove tidal creeks in southwest Florida. *Ecol. Eng.* **2018**, *114*, 57–65. [[CrossRef](#)]



© 2018 by the authors. Licensee MDPI, Basel, Switzerland. This article is an open access article distributed under the terms and conditions of the Creative Commons Attribution (CC BY) license (<http://creativecommons.org/licenses/by/4.0/>).

Effect of Woodchips Biochar on Sensitivity to Temperature of Soil Greenhouse Gases Emissions

Irene Criscuoli ^{1,*}, Maurizio Ventura ¹, Andrea Sperotto ¹, Pietro Panzacchi ^{1,2} and Giustino Tonon ¹

¹ Faculty of Science and Technology, Free University of Bolzano/Bozen, Piazza Università, 5, 39100 Bolzano, Italy

² Centro di Ricerca per le Aree Interne e gli Appennini (ArIA), Università degli Studi del Molise, via Francesco De Sanctis 1, 86100 Campobasso, Italy

* Correspondence: irene.criscuoli@unibz.it; Tel.: +39-0471-017765

Received: 17 June 2019; Accepted: 14 July 2019; Published: 17 July 2019

Abstract: Research Highlights: Biochar is the carbonaceous product of pyrolysis or the gasification of biomass that is used as soil amendment to improve soil fertility and increase soil carbon stock. Biochar has been shown to increase, decrease, or have no effect on the emissions of greenhouse gases (GHG) from soil, depending on the specific soil and biochar characteristics. However, the temperature sensitivity of these gas emissions in biochar-amended soils is still poorly investigated. Background and Objectives: A pot experiment was set up to investigate the impact of woodchips biochar on the temperature sensitivity of the main GHG (CO₂, CH₄, and N₂O) emissions from soil. Materials and Methods: Nine pots (14 L volume) were filled with soil mixed with biochar at two application rates (0.021 kg of biochar/kg of soil and 0.042 kg of biochar/kg of soil) or with soil alone as the control (three pots per treatment). Pots were incubated in a growth chamber and the emissions of CO₂, CH₄, and N₂O were monitored for two weeks with a cavity ring-down gas analyzer connected to three closed dynamic chambers. The temperature in the chamber increased from 10 °C to 30 °C during the first week and decreased back to 10 °C during the second week, with a daily change of 5 °C. Soil water content was kept at 20% (w/w). Results: Biochar application did not significantly affect the temperature sensitivity of CO₂ and N₂O emissions. However, the sensitivity of CH₄ uptake from soil significantly decreased by the application of biochar, reducing the CH₄ soil consumption compared to the un-amended soil, especially at high soil temperatures. Basal CO₂ respiration at 10 °C was significantly higher in the highest biochar application rate compared to the control soil. Conclusions: These results confirmed that the magnitude and direction of the influence of biochar on temperature sensitivity of GHG emissions depend on the specific GHG considered. The biochar tested in this study did not affect soil N₂O emission and only marginally affected CO₂ emission in a wide range of soil temperatures. However, it showed a negative impact on soil CH₄ uptake, particularly at a high temperature, having important implications in a future warmer climate scenario and at higher application rates.

Keywords: CO₂; CH₄; N₂O; soil; biochar; sensitivity; temperature

1. Introduction

Forest management can contribute to climate change mitigation by allocating woody biomass to bioenergy production, thus displacing fossil fuel use [1]. Among the energy conversion processes that can utilize woody biomass as feedstock, pyrolysis and gasification are acknowledged to be promising technologies in terms of carbon (C) budget [2]. During pyrolysis and gasification, biomass is thermally degraded through heating (300–1200 °C) under the complete or partial exclusion of oxygen. The volatile components of biomass are therefore released in the form of syngas, that can be used to produce

thermal energy, electricity, or an oily fuel, and the leftover by-product of this process is charcoal [3]. In the last two decades, this C-rich, solid material has been proposed as a soil amendment with the name of biochar [4].

Due to its chemical structure, biochar is supposed to be particularly recalcitrant to soil degradation [5], even if estimations of its mean residence time vary from decades to millennia, depending on the starting feedstock, the production conditions, and the characteristics of the amended soil [6–8]. Biochar has been shown to improve soil characteristics and plant productivity in agricultural and forest ecosystems [9–13] as well as reduce nutrient losses from soil [14–16]. For these reasons, biochar has been proposed in forest restoration as a replacement to other forms of organic amendments and liming agents, particularly in degraded sites [9]. Applying biochar to forest soils may therefore contribute to mitigate climate change through the increase of soil C stock, improve soil characteristics, and allow at the same time the valorization of the woody biomass gasification chain, by turning what is now considered a waste into a resource.

However, little research has been conducted on biochar in forest ecosystems compared to agricultural crops [1,13,17] and most of the information on charcoal in forest ecosystems in the literature derives from studies on wildfires [18].

To evaluate the real climate change mitigation potential of biochar, its impact on greenhouse gases (GHG) emissions from soil has to be accounted. In fact, it is estimated that soil emissions of carbon dioxide (CO₂), methane (CH₄), and nitrous oxide (N₂O) represent 35%, 47%, and 53% of the total annual global emissions of these greenhouse gases (GHG), respectively [19,20]. Biochar has been shown to affect soil GHG emissions in different ways, depending on biochar and soil characteristics. For example, biochar application decreased [21], increased [22,23], or had no effect [24–26] on soil CO₂ emissions. Different results have also been obtained for CH₄. Biochar can in fact contribute to mitigate CH₄ emissions from flooded soils under anoxic conditions, while in non-flooded soils, especially if neutral or alkaline, biochar may decrease soil CH₄ uptake [27]. Finally, biochar has been shown to strongly reduce soil N₂O emissions in different situations, even if increases in emissions have been observed as well [28].

While different studies have examined the effect of biochar application on GHG soil emissions, only a few have evaluated the impact that specific environmental parameters exert on these emissions in biochar-amended soils. Soil temperature is known to be the most important driver of GHG fluxes from soil [20,29,30], as well as of biochar oxidation and decomposition [31]. However, the effect of temperature on GHG fluxes in biochar-amended soil has been poorly investigated. Understanding the role of temperature is fundamental to assessing the effect of biochar on GHG emissions in different climatic conditions and in the context of climate change.

The overall aim of this study was to assess the effect of biochar on temperature sensitivity and basal emission of soil GHG fluxes. In particular, soil CO₂, CH₄, and N₂O fluxes were measured in soils amended with woodchip biochar at two application rates and in un-amended (control) soils. During the experiment, the soil moisture was kept constant at 20% (w/w) in all treatments and the temperature ranged between 10 °C and 30 °C.

We hypothesized that the application of biochar could affect the sensitivity to temperature and the basal value of CO₂, N₂O, and CH₄ flux.

Our experimental results partially confirmed our hypothesis. In fact, biochar application did not affect the temperature sensitivity of CO₂ and N₂O fluxes, while it significantly reduced that of CH₄ flux. On the contrary, basal respiration significantly increased for CO₂ by biochar application.

2. Materials and Methods

2.1. Experimental Set Up and Soil and Biochar Characteristics

The soil used in the experiment was sampled near Merano (Bolzano Province, Northern Italy, 46°40′0.181″ N, 11°11′39.282″ E; about 600 m a.s.l.). The soil was sandy-loam soil (USDA classification),

with 64% sand, 29% silt, and 7% clay. The soil organic carbon (SOC) content was $2.4 \pm 0.8\%$ and soil pH was 6.4 ± 0.2 . The soil water content at field capacity, calculated using the SPAW model (USDA-ARS) was 20% (v/v). The soil was sieved to a 8 mm mesh size to remove stones and coarse organic matter fragments.

The biochar used in the experiment consisted of small particles (<5 mm) and was obtained from conifer woodchips, at approximately 500 °C, through fast pyrolysis (Record Immobiliare S.r.l., Lunano, Pesaro-Urbino, Italy). Biochar was characterized by a bulk density of 0.165 g cm^{-3} and C:N ratio of 151. A detailed physicochemical characterization of the biochar used in this experiment is provided in Table 1.

Table 1. Physicochemical characterization of the biochar used in the present work.

| Parameter | Unit | Value | Uncertainty |
|--------------------------|-------|-------|-------------|
| pH | - | 12.4 | ± 0.5 |
| Sieve fraction <5 mm | % | 100 | ± 10 |
| Sieve fraction <2 mm | % | 97 | ± 10 |
| Sieve fraction <0.5 mm | % | 70 | ± 7 |
| Max. water retention | % w/w | 86 | ± 7 |
| Ash (550 °C) | % | 31 | ± 3 |
| Total C | % | 58.9 | - |
| C from CaCO ₃ | % | 1.1 | - |
| Organic C | % | 57 | ± 5 |
| H:C molar ratio | - | 0.10 | ± 0.01 |
| Total N | % | 0.39 | ± 0.04 |
| Total P | % | 0.64 | |
| Total K | % | 3.5 | ± 0.5 |
| PAHs ¹ | mg/kg | <1 | |

¹ Polycyclic aromatic hydrocarbons.

B1 and B2 treatments were prepared by mixing biochar and the sieved soil at two rates: 0.021 kg of biochar kg⁻¹ of soil (dry weight) (B1), and 0.042 kg of biochar kg⁻¹ of soil (dry weight) (B2), respectively. The two mixing rates corresponded to field biochar application doses of 25 ton ha⁻¹ and 50 ton ha⁻¹, respectively, considering a field biochar incorporation depth of 20 cm and are in line with the biochar dosages used in the majority of previous studies in forest ecosystems [9]. Biochar and soil mixtures were then homogenized with a concrete mixer.

The experiment was set up in July 2018 in a growth chamber at the Laimburg research center for Agriculture and Forestry located in Auer/Ora (BZ), Northern Italy. A total of 9 pots (45 cm × 25 cm × 21 cm, 14 L volume) were filled with soil mixed with biochar or with un-amended soil as the control. A total of 3 replicates (pots) were prepared for each treatment. The pots were stored in the growth chamber for two weeks at 10 °C temperature. The temperature in the chamber was then increased from 10 °C to 30 °C during one week (first week of experiment), and from 30 °C back to 10 °C during the following week (second week of experiment), with an overnight change of 5 °C per day. The lowest temperature (10 °C) was chosen because it is a standard temperature used internationally to compare the soil respiration of different experimental sites or treatments, the so called basal soil respiration at 10 °C (R₁₀) [32]. The highest temperature (30 °C) was chosen because the maximum monthly temperature measured in Merano between 2011 and 2017 was on average 29.1 °C [33]. In order to isolate the effect of soil temperature, excluding any effect of soil humidity on soil GHG fluxes, soil moisture was kept constant at 20% (w/w) in all treatments. Soil water content at the beginning of the experiment was measured in each pot by collecting a soil subsample (~10 g of soil) and drying it for 24 h at 105 °C. The amount of water to be added daily to the soil was calculated as the difference between the actual weight of the pot and the theoretical weight if the soil moisture was equal to 20% (w/w).

2.2. Measurement of Soil GHG Fluxes

The emissions of GHG from the soil were measured by a gas analyzer CRDS (Picarro Inc., Santa Clara, CA, USA), connected to 3 closed dynamic chambers (eosAC Autochamber, Eosense Inc., Dartmouth, NS, Canada) operated by a multiplexer (eosMX, Eosense Inc., Dartmouth, NS, Canada). The chambers were installed on PVC (polymerizing vinyl chloride) collars (15.2 cm diameter, 7 cm height) inserted into the soil, 1 per pot, for 4 cm. Fluxes of CO₂ (μmol m⁻² s⁻¹), N₂O, and CH₄ (nmol m⁻² s⁻¹) were measured daily from the 3 experimental treatments by manually moving one chamber (leaving the collars on the soil) on the 3 pots of each treatment. The measurements on each pot lasted for 10 min. A valve delay of 66 s was set at the beginning and at the end of each measurement to account for the time needed to draw the air from the chamber, analyze the gas concentrations, and then recirculate the air sample back to the chamber through a tubing length of 30 m. During measurements, the soil temperature (°C) was measured at a 5 cm soil depth by a RT-1 Rugged Soil Temperature Sensor (Decagon Devices, Inc., Pullman, WA, USA).

2.3. Data Analysis

After the elimination of data associated with system malfunctioning, soil CO₂ flux (soil respiration) measured in the different treatments were related to soil temperature using the following exponential model:

$$F_s = R_{10} e^{b(T-10)} \quad (1)$$

where F_s is the soil CO₂ flux, T is the soil temperature (°C) at 5 cm depth, and R_{10} is the basal soil respiration, i.e., the value of F_s at the reference temperature of 10 °C. The model parameters R_{10} and b were estimated by nonlinear regression analysis. The apparent sensitivity of CO₂ flux to soil temperature was determined by the Q_{10} temperature coefficient as follows:

$$Q_{10} = e^{10b} \quad (2)$$

Fluxes of CH₄ and N₂O were related to soil temperature using a linear model:

$$F_s = R_{10} + b(T-10) \quad (3)$$

where F_s is the soil CH₄ or N₂O flux, T is the soil temperature (°C) at 5 cm depth, and R_{10} is the basal emission at 10 °C. Parameters R_{10} and b (slope of the regression line) are estimated by linear regression analysis.

For each gas, the linear regression models obtained in the different experimental treatments were then compared by Analysis of Covariance (ANCOVA) to analyze the effect of biochar on the sensitivity of GHG fluxes to temperature. Equation (1) was linearized with a log-transformation of CO₂ efflux data before analysis. At first the slopes of the linear regression model were compared and then only when the slopes were not significantly different, and the intercepts of the regression lines were also compared. In case ANCOVA highlighted significant differences, post-hoc individual comparisons were performed with the Tukey's HSD test. The homogeneity of variances was checked before analysis by plotting the residual vs. fitted values. When this condition was not fulfilled, a square root transformation was applied to the data before analysis. Statistical analysis was performed using the software R (version 3.4.2) [34].

3. Results

The highest CO₂ emission rates were observed in the biochar-treated soils (Figure 1). Biochar application did not significantly affect the Q_{10} value of CO₂ fluxes, while it significantly increased R_{10} of CO₂ when applied at the highest rate in comparison to the control (Figure 1 and Table 2).

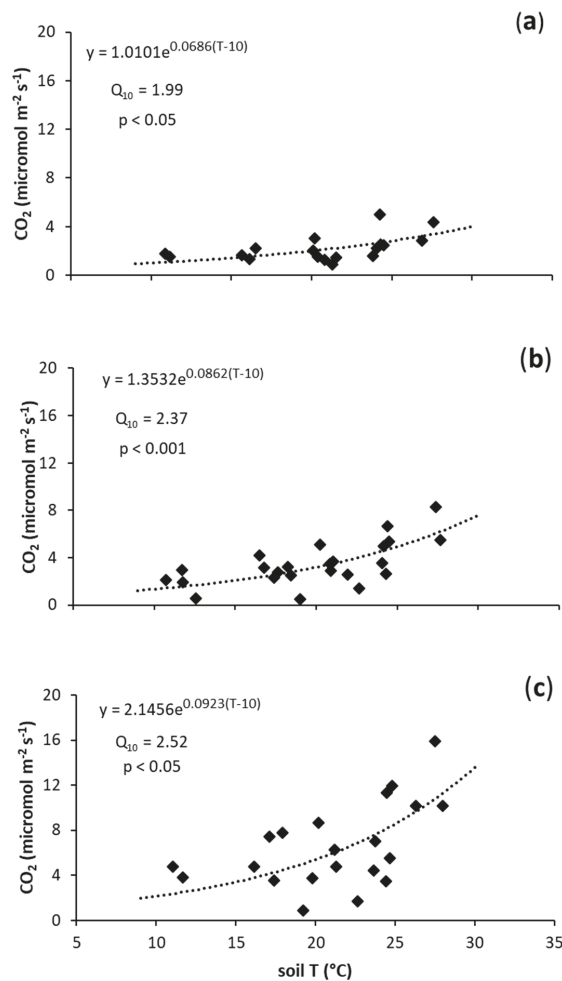


Figure 1. Relationship between CO₂ fluxes (μmol m⁻² s⁻¹) and soil temperature (°C) in: (a) N (control treatment); (b) B1 (0.021 kg of biochar/kg of soil); and (c) B2 (0.042 kg of biochar/kg of soil).

A negative CH₄ flux, i.e., a net CH₄ consumption in the soil, was observed in all treatments (Figure 2). The temperature sensitivity of soil CH₄ uptake significantly decreased following biochar application, showing a reduction in CH₄ uptake in biochar-amended soil in comparison to the control (Table 2). This effect was dependent on the biochar application rate and was particularly evident in the B2 treatment (Figure 2, Table 2). At this application rate, CH₄ flux was not significantly affected by soil temperature (slope: −0.0087) and its flux was always close to zero (Figure 2, Table 2).

Table 2. Results of Analysis of Covariance (ANCOVA) and the post-hoc Tukey test for a pairwise comparison of the slopes and intercepts of the linear models relating the fluxes of CO₂, CH₄, and N₂O to soil temperature (T, °C) in the treatments N (control), B1 (0.021 kg of biochar/kg of soil), and B2 (0.042 kg of biochar/kg of soil). Different letters indicate significant differences between model parameters determined for each soil treatment (*p* < 0.05) in the table.

| Model Parameters | | | | |
|-----------------------|---------|---|-----------------|----|
| | b | | R ₁₀ | |
| CO₂ | | | | |
| N | 0.0686 | a | 1.0101 | a |
| B1 | 0.0862 | a | 1.3532 | ab |
| B2 | 0.0923 | a | 2.1456 | b |
| CH₄ | | | | |
| N | −0.0378 | a | −1.2309 | a |
| B1 | −0.0389 | b | 0.0229 | a |
| B2 | −0.0087 | c | 0.1022 | a |
| N₂O | | | | |
| N | 0.0078 | a | −0.0066 | a |
| B1 | 0.0131 | a | −0.0141 | a |
| B2 | 0.0068 | a | 0.0262 | a |

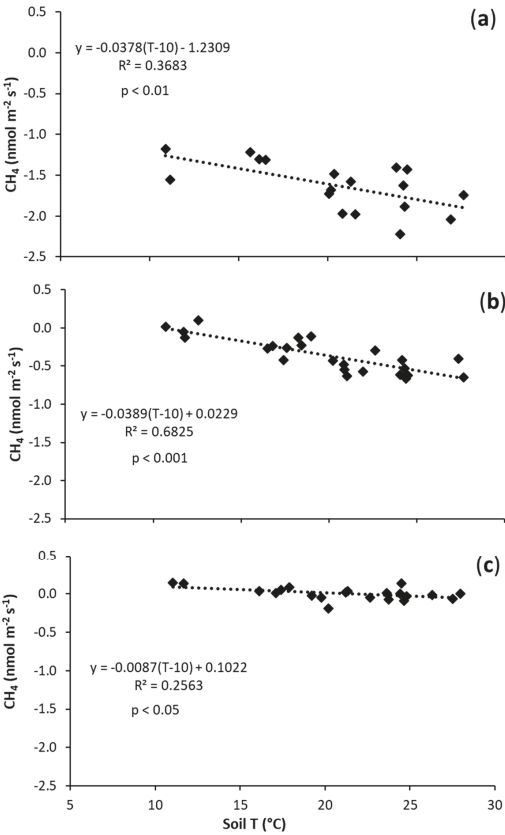


Figure 2. Relationship between CH₄ fluxes (nmol m^{−2} s^{−1}) and soil temperature (°C) in: (a) N (control treatment); (b) B1 (0.021 kg of biochar/kg of soil); and (c) B2 (0.042 kg of biochar/kg of soil).

The highest N₂O emissions from the soil were observed in the B1 treatment in comparison with control and B2, but the sensitivity of N₂O emissions from the soil, as well as the N₂O basal emission, were not significantly affected by the application of biochar (Figure 3, Table 2).

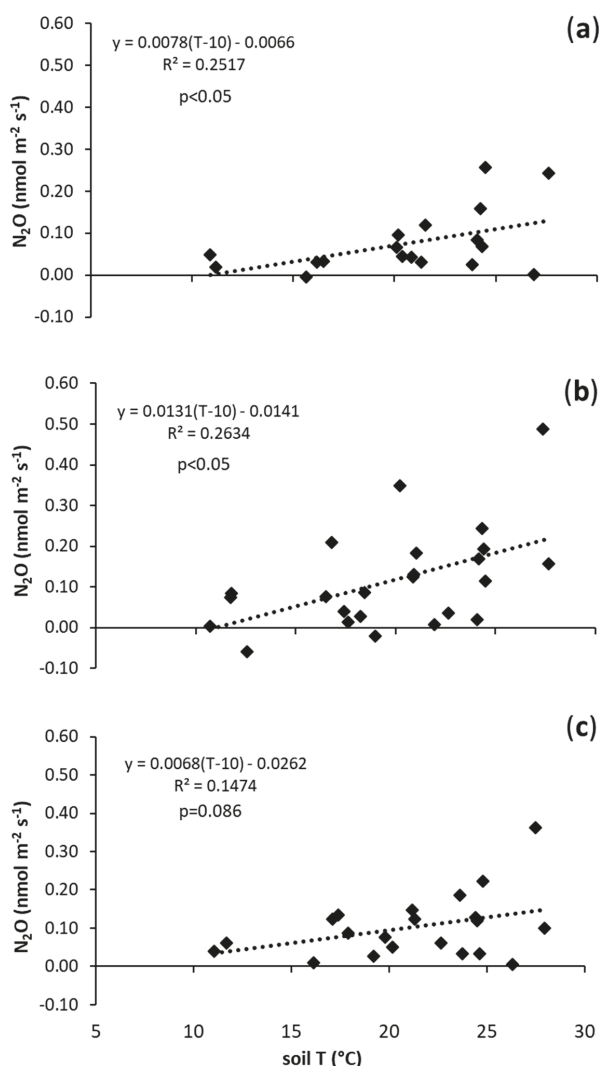


Figure 3. Relationship between N₂O fluxes (nmol m⁻² s⁻¹) and soil temperature (°C) in: (a) N (control treatment); (b) B1 (0.021 kg of biochar/kg of soil); and (c) B2 (0.042 kg of biochar/kg of soil).

4. Discussion

Soil temperature is known to be the most important driver of GHG fluxes from soil [20,29,30], as well as of biochar oxidation and decomposition [31]. The temperature sensitivity of GHG fluxes is therefore a key parameter to predict the impact that global warming will have on the flux of GHG [35,36].

In our experiment, we observed a positive exponential relationship between CO₂ fluxes and the temperature in biochar-amended soils. This relation was typically observed in forest and plantation

ecosystems [25,26,30,37,38]. The absence of a significant modification of the Q_{10} after the application of biochar (Figure 1, Table 2) was coherent with what was observed in previous studies with different biochars and application rates [26,37,39]. However, this result is inconsistent with other studies that reported a decrease [40–42] or an increase [25,43] to the temperature sensitivity of CO_2 emissions. These contrasting results derives from the complexity of the factors involved. In fact, the Q_{10} of biochar was expected to be higher than the less recalcitrant native soil organic matter (SOM) [44], but the sensitivity of CO_2 fluxes in biochar-amended soils also depends on the impact that biochar has on the Q_{10} of the native soil's organic matter [45]. Moreover, results can also change according to the incubation temperature range and soil type. More specifically, a smaller sensitivity was expected in soils with high clay, Fe, and Al oxides content as well as with an acidic pH [46].

In the present study, basal soil respiration increased significantly in the soil that was amended with biochar at a higher application rate. A R_{10} increase was found for heterotrophic respiration in different environments such as apple orchards [26] and the desert [47] after the application of biochar produced from wood and cotton straw, respectively. A significant increase in R_{10} for total soil respiration was also observed in soils amended with poultry litter biochar [48].

These results have been attributed to an increase of microbial biomass and/or activity [26,48]. The stimulation of soil microbes can derive from the decomposition of the labile fraction of biochar, consisting of bio-oils and condensation products [49–53]. However, the degradation of the more recalcitrant C compounds cannot be excluded [54]. This mechanism can be the main driver of the increased CO_2 efflux observed after biochar application in both agricultural and forest ecosystems [17,26]. Moreover, we cannot exclude that the increased CO_2 fluxes derive from an increased decomposition of the native soil's organic matter, the so-called priming effect (PE). In fact, a positive PE has been observed in several short term studies [55,56], especially in sandy soils [52], while in the long term, a protection of native organic matter from decomposition (negative PE) is generally observed in biochar-amended soils [23,57]. A boost in soil microbiota activity can also be due to a shift in soil properties such as soil aeration [58]. Biochar is characterized by a high porosity, which may have increased soil gas permeability and oxygen availability for soil microbes. Moreover, even if the soil water content was kept constant during the incubation experiment, the presence of biochar may have affected the availability of soil water by soil microorganisms. Biochar can in fact alter soil water potential [59,60], which is known to impact soil microbial population and activity [61].

Non-flooded soils in an oxic condition usually show a CH_4 -sink capacity [62], as CH_4 is oxidized by soil methanotrophic bacteria, and the rate of CH_4 oxidation depends on soil temperature [63]. This trend was also observed in the present study, as CH_4 consumption increased linearly with soil temperature (Figure 2). The decreased sensitivity to soil temperature of CH_4 flux in biochar-treated soil means that biochar decreased CH_4 consumption at a higher soil temperature, while at a lower soil temperature this effect was less pronounced. In their meta-analysis, Jeffery et al. [27] showed that the application of biochar from woody feedstock, produced at temperatures between 400 °C and 600 °C, decreases soil CH_4 uptake in non-flooded soils, especially in neutral or alkaline soil pH. Results of the present study are in line with these findings as our biochar was produced from wood chips at approximately 500 °C, and the soil water content was kept at 20%. Non-flooded upland soils contribute to approximately 15% of global CH_4 oxidation [64], therefore biochar application may decrease net CH_4 oxidation, reducing the climate change mitigation potential of these soils. However, few studies examined the sensitivity of CH_4 soil flux to temperature. Our study showed that the reduction of soil CH_4 uptake induced by biochar increased with soil temperature. This effect could therefore more pronounced under warmer climatic conditions and may worsen within the context of global warming. Moreover, the reduction of sensitivity to temperature for CH_4 was much more evident in the B2 treatment, which suggests not using high biochar application rates in order to preserve the soil CH_4 uptake capacity. However, a significant increase in soil CH_4 uptake [37,65] and sensitivity to temperature [37] was observed in some experiments in non-flooded soils, contradicting the results of

the present work and showing that the relation between biochar, soil, and CH₄ emissions is complex and hard to predict.

The mechanism behind the reduction of CH₄ oxidation might be a modification of the methanogenic/methanotrophic bacteria ratio in biochar-amended soils [66], and the release of chemicals with a toxic effect on the methanotrophic bacteria population, such as ethylene [67]. In addition, even if the soil water content was kept constant, biochar may have altered soil water potential and water availability for soil bacteria.

Soil N₂O emissions in the present work increased linearly with the temperature in all soil treatments and the application of biochar did not affect temperature sensitivity or basal soil N₂O emissions (Figure 3, Table 2). These results confirm a previous study by [68] but are in contrast with other studies, reporting a significant reduction of N₂O flux sensitivity to temperature, both in subtropical [37] and continental climate [69]. In a meta-analysis by Cayuela et al. [28], an average reduction of 54% in N₂O emissions has been reported in biochar-treated soils. In this case, the variability observed in the experimental results has been shown to depend on different characteristics of biochar (feedstock used, pyrolysis conditions, and C/N ratio) and soil. In particular, when biochar is applied to drained soils with a coarse texture, reduction in N₂O emissions has not been observed [28,70]. In our experiment, soil moisture was kept at a relatively low value, not exceeding the field capacity of the sandy-loam textured soil. In these conditions, it was likely that N₂O emission was not promoted and the effect of biochar was consequently not relevant.

In previous studies, an observed reduction of N₂O emissions from soils was explained by a toxic effect on soil microbes involved in N₂O production of Polycyclic aromatic hydrocarbons (PAHs) [71,72]. The PAHs content in the biochar used in this study was very low (Table 1) and therefore a toxic effect on soil biota was unlikely.

A decrease of soil N₂O emissions has also been associated with a shift in the soil's physical properties, such as a reduction in soil compaction [73]. This mechanism cannot have occurred in our experiment, as it was set up in controlled conditions and the soil was not subjected to compaction.

The reduction of N₂O emissions observed in previous studies has also been attributed to the sorption of reactive N on biochar surfaces and the reduction of its availability for N₂O emitting reactions. However, this mechanism is observed in case of biochar production at temperatures higher than 600 °C [74,75]. The absence of the biochar effect on the sensitivity to temperature of N₂O emission would suggest that biochar will not affect the emission of this powerful greenhouse gas in warmer climatic conditions.

It has to be considered that the short experimental duration of this study might limit the validity of the results to the first period after the application of biochar [76,77]. Therefore, these results may not be representative of the effect of biochar on long-term GHG emissions from soil in field application.

5. Conclusions

Before concluding if biochar application to soil is a forest management practice that is able to mitigate climate change, an evaluation of its effect on soil GHG emission is fundamental. The results of the present work show that biochar addition to soil did not significantly affect the sensitivity of CO₂ and N₂O fluxes, while it slightly increased the CO₂ basal soil respiration in case of a high application rate, indicating that biochar application would not affect the emission of these gases in warmer climatic conditions. However, the significant decrease of the temperature sensitivity of soil CH₄ uptake indicated that biochar can induce an important reduction of the soil CH₄ sink potential, in particular in a warmer environment, and this effect can become more relevant in a global warming scenario. Moreover, the reduction of sensitivity to temperature for CH₄ was much more evident in the case of the higher application rate, suggesting that high biochar dosages should be avoided in order to preserve the soil CH₄ uptake capacity.

The observed effects seem to depend on specific biochar characteristics (temperature of production, low content of PAHs) and soil characteristics (sandy-loam, drained soil). However, long-term field

studies are advisable in order to guarantee a thorough understanding of the impact of biochar on GHG emissions from soil.

Author Contributions: Conceptualization, G.T.; Methodology, G.T., M.V., and I.C.; validation, M.V., G.T., I.C., and P.P.; Formal analysis, I.C. and M.V.; Investigation, I.C., A.S.; Resources, I.C., P.P., A.S., and M.V.; Data Curation, I.C., A.S.; Writing—original draft preparation, I.C. and M.V.; Writing—review and editing, I.C., M.V., P.P., and G.T.; Visualization, I.C. and M.V.; Supervision, G.T.; Project administration, G.T.; Funding acquisition, G.T.

Funding: This research was funded by the Wood-Up project (Optimization of WOOD gasification chain in South Tyrol to produce bioenergy and other high-value green products to enhance soil fertility and mitigate climate change, EFRE-FESR 2014–2020, project number 1028), funded by the European Regional Development Fund of the European Union and the Autonomous Province of Bolzano/Bozen.

Acknowledgments: The authors would like to thank the Laimburg Research Center for the availability of the climatic chamber, and Christian Ceccon and Christian Grümer from the Free University of Bolzano for their support in soil sample preparation and analysis.

Conflicts of Interest: The authors declare no conflict of interest. The funders had no role in the design of the study, in the collection, analyses, or interpretation of data, in the writing of the manuscript, or in the decision to publish the results.

References

1. Cowie, A.; Barton, C.; Singh, B.; Ximenes, F.; Stone, C. Climate Change Impacts and Research Priorities for the Forestry Sector. In *DPI Priority Actions for Climate Change Workshop*; NSW Department of Primary Industries: Orange, NSW, Australia, 2007.
2. Lehmann, J. A Handful of Carbon. *Nature* **2007**, *447*, 143–144. [[CrossRef](#)] [[PubMed](#)]
3. Bridgwater, A.V. The Production of Biofuels and Renewable Chemicals by Fast Pyrolysis of Biomass. *Int. J. Glob. Energy Issues* **2007**, *27*, 160–203. [[CrossRef](#)]
4. Lehmann, J. Bio-Energy in the Black. *Front. Ecol. Environ.* **2007**, *5*, 381–387. [[CrossRef](#)]
5. Downie, A.; Munroe, P. Characteristics of Biochar—Physical and Structural Properties. In *Biochar for Environmental Management: Science, Technology and Implementation*; Lehmann, J., Joseph, S., Eds.; Earthscan: London, UK, 2009; pp. 13–29.
6. Lehmann, J.; Abiven, S.; Kleber, M.; Pan, G.; Singh, B.P.; Sohi, S.P.; Zimmerman, A.R. Persistence of Biochar in Soil. In *Biochar for Environmental Management: Science, Technology and Implementation*; Lehmann, J., Joseph, S., Eds.; Routledge: New York, NY, USA, 2015; pp. 235–282.
7. Criscuoli, I.; Alberti, G.; Baronti, S.; Favilli, F.; Martinez, C.; Calzolari, C.; Pusceddu, E.; Rumpel, C.; Viola, R.; Miglietta, F. Carbon Sequestration and Fertility after Centennial Time Scale Incorporation of Charcoal into Soil. *PLoS ONE* **2014**, *9*, e91114. [[CrossRef](#)] [[PubMed](#)]
8. Gurwick, N.P.; Moore, L.A.; Kelly, C.; Elias, P. A Systematic Review of Biochar Research, with a Focus on Its Stability in Situ and Its Promise as a Climate Mitigation Strategy. *PLoS ONE* **2013**, *8*, e75932. [[CrossRef](#)] [[PubMed](#)]
9. Thomas, S.C.; Gale, N. Biochar and Forest Restoration: A Review and Meta-Analysis of Tree Growth Responses. *New For.* **2015**, *46*, 931–946. [[CrossRef](#)]
10. Biederman, L.; Harpole, W.S. Biochar and Its Effects on Plant Productivity and Nutrient Cycling: A Meta-Analysis. *GCB Bioenergy* **2012**, *5*, 202–214. [[CrossRef](#)]
11. Liu, X.; Zhang, A.; Ji, C.; Joseph, S.; Bian, R.; Li, L.; Pan, G.; Paz-Ferreiro, J. Biochar's Effect on Crop Productivity and the Dependence on Experimental Conditions—A Meta-Analysis of Literature Data. *Plant Soil* **2013**, *373*, 583–594. [[CrossRef](#)]
12. Criscuoli, I.; Baronti, S.; Alberti, G.; Rumpel, C.; Giordan, M.; Camin, F.; Ziller, L.; Martinez, C.; Pusceddu, E.; Miglietta, F. Anthropogenic Charcoal-Rich Soils of the XIX Century Reveal That Biochar Leads to Enhanced Fertility and Fodder Quality of Alpine Grasslands. *Plant Soil* **2017**, *411*, 499–516. [[CrossRef](#)]
13. Li, Y.; Hu, S.; Chen, J.; Mueller, K.; Li, Y.; Fu, W.; Lin, Z.; Wang, H. Effects of Biochar Application in Forest Ecosystems on Soil Properties and Greenhouse Gas Emissions: A Review. *J. Soils Sediments* **2018**, *18*, 546–563. [[CrossRef](#)]
14. Ventura, M.; Sorrenti, G.; Panzacchi, P.; George, E.; Tonon, G. Biochar Reduces Short-Term Nitrate Leaching from a Horizon in an Apple Orchard. *J. Environ. Qual.* **2013**, *42*, 76–82. [[CrossRef](#)] [[PubMed](#)]

15. Major, J.; Steiner, C.; Downie, A.; Lehmann, J. Biochar Effects on Nutrient Leaching. In *Biochar for Environmental Management: Science, Technology and Implementation*; Lehmann, J., Joseph, S., Eds.; Routledge, Earthscan: New York, NY, USA, 2015; pp. 271–287.
16. Sorrenti, G.; Ventura, M.; Toselli, M. Effect of Biochar on Nutrient Retention and Nectarine Tree Performance: A Three-Year Field Trial. *J. Plant Nutr. Soil Sci.* **2016**, *179*, 1–11. [[CrossRef](#)]
17. Johnson, M.S.; Webster, C.; Jassal, R.S.; Hawthorne, I.; Black, T.A. Biochar Influences on Soil CO₂ and CH₄ Fluxes in Response to Wetting and Drying Cycles for a Forest Soil. *Sci. Rep.* **2017**, *7*, 6480. [[CrossRef](#)] [[PubMed](#)]
18. Stavi, I. Biochar Use in Forestry and Tree-Based Agro-Ecosystems for Increasing Climate Change Mitigation and Adaptation. *Int. J. Sustain. Dev. World Ecol.* **2013**, *20*, 166–181. [[CrossRef](#)]
19. Solomon, S.; Qin, D.; Manning, M.; Chen, Z.; Marquis, M.; Averyt, K.B.; Tignor, M.M.B.; Miller, H.L. *Climate Change 2007: The Physical Science Basis. Contribution of Working Group I to the Fourth Assessment Report of the Intergovernmental Panel on Climate Change*; Cambridge University Press: Cambridge, UK; New York, NY, USA, 2007.
20. Oertel, C.; Matschullat, J.; Zurba, K.; Zimmermann, F.; Erasmí, S. Greenhouse Gas Emissions from Soils—A Review. *Chemie der Erde—Geochemistry* **2016**, *76*, 327–352. [[CrossRef](#)]
21. Case, S.D.; McNamara, N.P.; Reay, D.S.; Whitaker, J. Can Biochar Reduce Soil Greenhouse Gas Emissions from a Miscanthus Bioenergy Crop? *GCB Bioenergy* **2014**, *6*, 76–89. [[CrossRef](#)]
22. Novak, J.M.; Busscher, W.J.; Watts, D.W.; Laird, D.A.; Ahmedna, M.A.; Niandou, M.A.S. Short-Term CO₂ Mineralization after Additions of Biochar and Switchgrass to a Typic Kandudult. *Geoderma* **2010**, *154*, 281–288. [[CrossRef](#)]
23. Ventura, M.; Alberti, G.; Panzacchi, P.; Delle Vedove, G.; Miglietta, F.; Tonon, G. Biochar Mineralization and Priming Effect on SOM Decomposition. Results from a Field Trial in a Short Rotation Coppice in Italy. In *EGU General Assembly Conference Abstracts*; EGU General Assembly: Vienna, Austria, 2016; Volume 18, p. 9109.
24. Scheer, C.; Grace, P.R.; Rowlings, D.W.; Kimber, S.; van Zwieten, L. Effect of Biochar Amendment on the Soil-Atmosphere Exchange of Greenhouse Gases from an Intensive Subtropical Pasture in Northern New South Wales, Australia. *Plant Soil* **2011**, *345*, 47–58. [[CrossRef](#)]
25. Wang, Z.; Li, Y.; Chang, S.X.; Zhang, J.; Jiang, P.; Zhou, G.; Shen, Z. Contrasting Effects of Bamboo Leaf and Its Biochar on Soil CO₂ Efflux and Labile Organic Carbon in an Intensively Managed Chinese Chestnut Plantation. *Biol. Fertil. Soils* **2014**, *50*, 1109–1119. [[CrossRef](#)]
26. Ventura, M.; Zhang, C.; Baldi, E.; Fornasier, F.; Sorrenti, G.; Panzacchi, P.; Tonon, G. Effect of Biochar Addition on Soil Respiration Partitioning and Root Dynamics in an Apple Orchard. *Eur. J. Soil Sci.* **2014**, *65*, 186–195. [[CrossRef](#)]
27. Jeffery, S.; Verheijen, F.G.A.; Kammann, C.; Abalos, D. Biochar Effects on Methane Emissions from Soils: A Meta-Analysis. *Soil Biol. Biochem.* **2016**, *101*, 251–258. [[CrossRef](#)]
28. Cayuela, M.L.; van Zwieten, L.; Singh, B.P.; Jeffery, S.; Roig, A.; Sánchez-Monedero, M.A. Biochar's Role in Mitigating Soil Nitrous Oxide Emissions: A Review and Meta-Analysis. *Agric. Ecosyst. Environ.* **2014**, *191*, 5–16. [[CrossRef](#)]
29. Reichstein, M.; Beer, C. Soil Respiration across Scales: The Importance of a Model-Data Integration Framework for Data Interpretation. *J. Plant Nutr. Soil Sci.* **2008**, *171*, 344–354. [[CrossRef](#)]
30. Shen, Y.; Zhu, L.; Cheng, H.; Yue, S.; Li, S. Effects of Biochar Application on CO₂ Emissions from a Cultivated Soil under Semiarid Climate Conditions in Northwest China. *Sustainability* **2017**, *9*, 1482. [[CrossRef](#)]
31. Nguyen, B.T.; Lehmann, J.; Hockaday, W.C.; Joseph, S.; Masiello, C.A. Temperature Sensitivity of Black Carbon Decomposition and Oxidation. *Environ. Sci. Technol.* **2010**, *44*, 3324–3331. [[CrossRef](#)] [[PubMed](#)]
32. Lloyd, J.; Taylor, A. On the Temperature Dependence of Soil Respiration. *Funct. Ecol.* **1994**, *8*, 315–323. [[CrossRef](#)]
33. Provincia Autonoma di Bolzano. Valori Medi Delle Temperature Massime e Minime—Merano/Quarazze cod. 23200MS. Available online: <http://www.provincia.bz.it/meteo/download/23200MS-TS-MeranoQuarazze-MeranGratsch.pdf> (accessed on 8 July 2019).
34. Ihaka, R.; Gentleman, R. R: A Language for Data Analysis and Graphics. *J. Comput. Graph. Stat.* **1996**, *5*, 299–314.

35. Luo, Y.; Wan, S.; Hui, D.; Wallace, L.L. Acclimatization of Soil Respiration to Warming in a Tall Grass Prairie. *Nature* **2001**, *413*, 622–625. [\[CrossRef\]](#)
36. Zhou, T.; Shi, P.; Hui, D.; Luo, Y. Global Pattern of Temperature Sensitivity of Soil Heterotrophic Respiration (Q₁₀) and Its Implications for Carbon-Climate Feedback. *J. Geophys. Res.* **2009**, *114*, 1–9. [\[CrossRef\]](#)
37. Lu, X.; Li, Y.; Wang, H.; Singh, B.P.; Hu, S.; Luo, Y.; Li, J.; Xiao, Y.; Cai, X.; Li, Y. Responses of Soil Greenhouse Gas Emissions to Different Application Rates of Biochar in a Subtropical Chinese Chestnut Plantation. *Agric. For. Meteorol.* **2019**, *271*, 168–179. [\[CrossRef\]](#)
38. Li, Y.; Li, Y.; Chang, S.X.; Yang, Y.; Fu, S.; Jiang, P.; Luo, Y.; Yang, M.; Chen, Z.; Hu, S.; et al. Biochar Reduces Soil Heterotrophic Respiration in a Subtropical Plantation through Increasing Soil Organic Carbon Recalcitrancy and Decreasing Carbon-Degrading Microbial Activity. *Soil Biol. Biochem.* **2018**, *122*, 173–185. [\[CrossRef\]](#)
39. Bamminger, C.; Poll, C.; Marhan, S. Offsetting Global Warming-Induced Elevated Greenhouse Gas Emissions from an Arable Soil by Biochar Application. *Glob. Chang. Biol.* **2018**, *24*, 318–334. [\[CrossRef\]](#) [\[PubMed\]](#)
40. Pei, J.; Zhuang, S.; Cui, J.; Li, J.; Li, B.; Wu, J.; Fang, C. Biochar Decreased the Temperature Sensitivity of Soil Carbon Decomposition in a Paddy Field. *Agric. Ecosyst. Environ.* **2017**, *249*, 156–164. [\[CrossRef\]](#)
41. Chen, J.; Sun, X.; Zheng, J.; Zhang, X.; Liu, X.; Bian, R.; Li, L.; Chneg, K.; Zheng, J.; Pan, G. Biochar Amendment Changes Temperature Sensitivity of Soil Respiration and Composition of Microbial Communities 3 Years after Incorporation in an Organic Carbon-Poor Dry Cropland Soil. *Biol. Fertil. Soils* **2018**, *54*, 175–188. [\[CrossRef\]](#)
42. He, X.; Du, Z.; Wang, Y.; Lu, N.; Zhang, Q. Sensitivity of Soil Respiration to Soil Temperature Decreased under Deep Biochar Amended Soils in Temperate Croplands. *Appl. Soil Ecol.* **2016**, *108*, 204–210. [\[CrossRef\]](#)
43. Zhou, G.; Zhou, X.; Zhang, T.; Du, Z.; He, Y.; Wang, X.; Shao, J.; Cao, Y.; Xue, S.; Wang, H.; et al. Biochar Increased Soil Respiration in Temperate Forests but Had No Effects in Subtropical Forests. *For. Ecol. Manage.* **2017**, *405*, 339–349. [\[CrossRef\]](#)
44. Conant, R.; Steinweg, J.; Haddix, M.; Paul, E.; Plante, A.; Six, J. Experimental Warming Shows That Decomposition Temperature Sensitivity Increases with Soil Organic Matter Recalcitrance. *Ecology* **2008**, *89*, 2384–2391. [\[CrossRef\]](#)
45. Fang, Y.; Singh, B.P.; Matta, P.; Cowie, A.L.; Van Zwieten, L. Temperature Sensitivity and Priming of Organic Matter with Different Stabilities in a Vertisol with Aged Biochar. *Soil Biol. Biochem.* **2017**, *115*, 346–356. [\[CrossRef\]](#)
46. Fang, Y.; Singh, B.P.; Singh, B. Temperature Sensitivity of Biochar and Native Carbon Mineralisation in Biochar-Amended Soils. *Agric. Ecosyst. Environ.* **2014**, *191*, 158–167. [\[CrossRef\]](#)
47. Liao, N.; Li, Q.; Zhang, W.; Zhou, G.; Ma, L.; Min, W.; Ye, J.; Hou, Z. Effects of Biochar on Soil Microbial Community Composition and Activity in Drip-Irrigated Desert Soil. *Eur. J. Soil Biol.* **2016**, *72*, 27–34. [\[CrossRef\]](#)
48. Mierzwa-Hersztek, M.; Klimkowicz-Pawlas, A.; Gondek, K. Influence of Poultry Litter and Poultry Litter Biochar on Soil Microbial Respiration and Nitrifying Bacteria Activity. *Waste Biomass Valorization* **2018**, *9*, 379–389. [\[CrossRef\]](#)
49. Kolb, S.E.; Fermanich, K.J.; Dornbush, M.E. Effect of Charcoal Quantity on Microbial Biomass and Activity in Temperate Soils. *Soil Sci. Soc. Am. J.* **2009**, *73*, 1173–1181. [\[CrossRef\]](#)
50. Zimmerman, A.R. Abiotic and Microbial Oxidation of Laboratory-Produced Black Carbon (Biochar). *Environ. Sci. Technol.* **2010**, *44*, 1295–1301. [\[CrossRef\]](#) [\[PubMed\]](#)
51. Kuzyakov, Y.; Bogomolova, I.; Glaser, B. Biochar Stability in Soil: Decomposition during Eight Years and Transformation as Assessed by Compound-Specific ¹⁴C Analysis. *Soil Biol. Biochem.* **2014**, *70*, 229–236. [\[CrossRef\]](#)
52. Wang, J.; Xiong, Z.; Kuzyakov, Y. Biochar Stability in Soil: Meta-Analysis of Decomposition and Priming Effects. *GCB Bioenergy* **2016**, *8*, 512–523. [\[CrossRef\]](#)
53. Ventura, M.; Alberti, G.; Panzacchi, P.; Delle Vedove, G.; Miglietta, F.; Tonon, G. Biochar Mineralization and Priming Effect in a Poplar Short Rotation Coppice from a 3-Year Field Experiment. *Biol. Fertil. Soils* **2019**, *55*, 67–78. [\[CrossRef\]](#)
54. Anderson, C.R.; Condon, L.M.; Clough, T.J.; Fiers, M.; Stewart, A.; Hill, R.A.; Sherlock, R.R. Biochar Induced Soil Microbial Community Change: Implications for Biogeochemical Cycling of Carbon, Nitrogen and Phosphorus. *Pedobiologia* **2011**, *54*, 309–320. [\[CrossRef\]](#)

55. Zimmerman, A.R.; Gao, B.; Ahn, M.Y. Positive and Negative Carbon Mineralization Priming Effects among a Variety of Biochar-Amended Soils. *Soil Biol. Biochem.* **2011**, *43*, 1169–1179. [\[CrossRef\]](#)
56. Maestrini, B.; Nannipieri, P.; Abiven, S. A Meta-Analysis on Pyrogenic Organic Matter Induced Priming Effect. *GCB Bioenergy* **2015**, *7*, 577–590. [\[CrossRef\]](#)
57. Fidel, R.B.; Laird, D.A.; Parkin, T.B. Impact of Six Lignocellulosic Biochars on C and N Dynamics of Two Contrasting Soils. *GCB Bioenergy* **2017**, *9*, 1279–1291. [\[CrossRef\]](#)
58. Zhou, Z.; Guo, C.; Meng, H. Temperature Sensitivity and Basal Rate of Soil Respiration and Their Determinants in Temperate Forests of North China. *PLoS ONE* **2013**, *8*, e81793. [\[CrossRef\]](#) [\[PubMed\]](#)
59. Laird, D.A.; Fleming, P.; Davis, D.D.; Horton, R.; Wang, B.; Karlen, D.L. Impact of Biochar Amendments on the Quality of a Typical Midwestern Agricultural Soil. *Geoderma* **2010**, *158*, 443–449. [\[CrossRef\]](#)
60. Novak, J.M.; Busscher, W.J.; Watts, D.W.; Amonette, J.E.; Ippolito, J.A.; Lima, I.M.; Gaskin, J.; Das, K.C.; Steiner, C.; Ahmedna, M.; et al. Biochars Impact on Soil-Moisture Storage in an Ultisol and Two Aridisols. *Soil Sci.* **2012**, *177*, 310–320. [\[CrossRef\]](#)
61. Sinegani, A.A.S.; Maghsoudi, J. The Effects of Water Potential on Some Microbial Populations and Decrease Kinetic of Organic Carbon in Soil Treated with Cow Manure under Laboratory Conditions. *J. Appl. Sci. Environ. Manag.* **2011**, *15*, 179–188. [\[CrossRef\]](#)
62. Suwanwaree, P.; Robertson, G.P. Methane Oxidation in Forest, Successional, and No-till Agricultural Ecosystems: Effects of Nitrogen and Soil Disturbance. *Soil Sci. Soc. Am. J.* **2005**, *69*, 1722–1729. [\[CrossRef\]](#)
63. Luo, G.J.; Kiese, R.; Wolf, B.; Butterbach-Bahl, K. Effects of Soil Temperature and Moisture on Methane Uptake and Nitrous Oxide Emissions across Three Different Ecosystem Types. *Biogeosciences* **2013**, *10*, 3205–3219. [\[CrossRef\]](#)
64. Powlson, D.S.; Goulding, K.W.T.; Willison, T.W.; Webster, C.P.; Hütsch, B.W. The Effect of Agriculture on Methane Oxidation in Soil. *Nutr. Cycl. Agroeco.* **1997**, *49*, 59–70. [\[CrossRef\]](#)
65. Karhu, K.; Mattila, T.; Bergström, I.; Regina, K. Biochar Addition to Agricultural Soil Increased CH₄ Uptake and Water Holding Capacity—Results from a Short-Term Pilot Field Study. *Agric. Ecosyst. Environ.* **2011**, *140*, 309–313. [\[CrossRef\]](#)
66. Feng, Y.; Xu, Y.; Yu, Y.; Xie, Z.; Lin, X. Mechanisms of Biochar Decreasing Methane Emission from Chinese Paddy Soils. *Soil Biol. Biochem.* **2012**, *46*, 80–88. [\[CrossRef\]](#)
67. Spokas, K.A.; Baker, J.M.; Reicosky, D.C. Ethylene: Potential Key for Biochar Amendment Impacts. *Plant Soil* **2010**, *333*, 443–452. [\[CrossRef\]](#)
68. Deem, L.M.; Yu, J.; Crow, S.E.; Deenik, J.; Penton, C.R. Biochar Increases Temperature Sensitivity of Soil Respiration and N₂O Flux. 2016. Available online: <https://biochar-us.org/presentation/biochar-increases-temperature-sensitivity-soil-respiration-and-n2o-flux> (accessed on 8 July 2019).
69. Chang, J.; Clay, D.E.; Clay, S.A.; Chintala, R.; Miller, J.M.; Schumacher, T. Biochar Reduced Nitrous Oxide and Carbon Dioxide Emissions from Soil with Different Water and Temperature Cycles. *Agron. Soils Environ. Qual.* **2016**, *108*, 2214–2221. [\[CrossRef\]](#)
70. Curtin, D.; Campbell, C.A.; Jilil, A. Effects of Acidity on Mineralization: PH-Dependence of Organic Matter Mineralization in Weakly Acidic Soils. *Soil Biol. Biochem.* **1998**, *30*, 57–64. [\[CrossRef\]](#)
71. Maliszewska-Kordybach, B.; Klimkowicz-Pawlas, A.; Smreczak, B.; Janusauskaite, D. Ecotoxic Effect of Phenanthrene on Nitrifying Bacteria in Soils of Different Properties. *J. Environ. Qual.* **2007**, *36*, 1635–1645. [\[CrossRef\]](#) [\[PubMed\]](#)
72. Guo, G.X.; Deng, H.; Qiao, M.; Yao, H.Y.; Zhu, Y.G. Effect of Long-Term Wastewater Irrigation on Potential Denitrification and Denitrifying Communities in Soils at the Watershed Scale. *Environ. Sci. Technol.* **2013**, *47*, 3105–3113. [\[CrossRef\]](#)
73. Rogovska, N.; Laird, D.; Cruse, R.; Fleming, P.; Parkin, T.; Meek, D. Impact of Biochar on Manure Carbon Stabilization and Greenhouse Gas Emissions. *Soil Sci. Soc. Am. J.* **2011**, *75*, 871–879. [\[CrossRef\]](#)
74. Clough, T.J.; Condon, L.M.; Kammann, C.; Müller, C. A Review of Biochar and Soil Nitrogen Dynamics. *Agronomy* **2013**, *3*, 275–293. [\[CrossRef\]](#)
75. Singh, B.P.; Hatton, B.; Balwant, S.; Cowie, A.L.; Kathuria, A. Influence of Biochars on Nitrous Oxide Emission and Nitrogen Leaching from Two Contrasting Soils. *J. Environ. Qual.* **2010**, *39*, 1224–1235. [\[CrossRef\]](#)
76. Fidel, R.; Laird, D.; Parkin, T. Effect of Biochar on Soil Greenhouse Gas Emissions at the Laboratory and Field Scales. *Soil Syst.* **2019**, *3*, 8. [\[CrossRef\]](#)

77. Spokas, K.A. Impact of Biochar Field Aging on Laboratory Greenhouse Gas Production Potentials. *GCB Bioenergy* **2013**, *5*, 165–176. [[CrossRef](#)]



© 2019 by the authors. Licensee MDPI, Basel, Switzerland. This article is an open access article distributed under the terms and conditions of the Creative Commons Attribution (CC BY) license (<http://creativecommons.org/licenses/by/4.0/>).

Biochar Is Comparable to Dicyandiamide in the Mitigation of Nitrous Oxide Emissions from *Camellia oleifera* Abel. Fields

Bangliang Deng ^{1,2}, Haifu Fang ¹, Ningfei Jiang ³, Weixun Feng ¹, Laicong Luo ¹, Jiawei Wang ¹, Hua Wang ⁴, Dongnan Hu ¹, Xiaomin Guo ¹ and Ling Zhang ^{1,*}

¹ Key Laboratory of Silviculture, College of Forestry, Jiangxi Agricultural University, Nanchang 330045, China; bangliangdeng@gmail.com (B.D.); fanghaifu11@163.com (H.F.); fw1754090341@126.com (W.F.); Luolaicong@126.com (L.L.); wjw_bjfu@163.com (J.W.); dnhu98@163.com (D.H.); gxmjxau@163.com (X.G.)

² Department of Plant Pathology, North Carolina State University, Raleigh, NC 27695, USA

³ Seed Management Station, Jiande Agricultural and Rural Bureau, Jiande 311600, China; jiangningfei2009@163.com

⁴ College of Land Resources and Environment, Jiangxi Agricultural University, Nanchang 330045, China; mengyiwanghua@sina.com

* Correspondence: lingzhang09@126.com; Tel.: +86-0791-8381-3243

Received: 25 October 2019; Accepted: 25 November 2019; Published: 27 November 2019

Abstract: *Research Highlights:* Intensive nitrogen (N) application for agricultural purposes has substantially increased soil nitrous oxide (N₂O) emissions. Agricultural soil has great potential in the reduction of N₂O emissions, and applications of biochar and nitrification inhibitors may be useful for mitigating agricultural soil N₂O emissions. *Background and Objectives:* *Camellia oleifera* Abel. is an important woody oil plant in China. However, intensive N input in *C. oleifera* silviculture has increased the risk of soil N₂O emissions. As an important greenhouse gas, N₂O is characterized by a global warming potential at a 100-year scale that is 265 times that of carbon dioxide. Thus, mitigation of soil N₂O emissions, especially fertilized soils, will be crucial for reducing climate change. *Materials and Methods:* Here, we conducted an in situ study over 12 months to examine the effects of *C. oleifera* fruit shell-derived biochar and dicyandiamide (DCD) on soil N₂O emissions from a *C. oleifera* field with intensive N application. *Results:* A three-fold increase of cumulative soil N₂O emissions was observed following N application. Cumulative N₂O emissions from the field with N fertilization were reduced by 36% and 44% with biochar and DCD, respectively. While N₂O emissions were slightly decreased by biochar, the decrease was comparable to that by DCD. *Conclusions:* Results indicated that biochar may mitigate soil N₂O emissions substantially and similarly to DCD under specific conditions. This result should be examined by prolonged and multi-site studies before it can be generalized to broader scales.

Keywords: biochar; *Camellia oleifera*; DCD; nitrification inhibitor; nitrous oxide

1. Introduction

Increased atmospheric greenhouse gases (GHGs) as a result of human activities contribute substantially to global warming. Nitrous oxide (N₂O) is an important component of GHGs [1] and is a dominant ozone-depleting substance [2]. Concentrations of atmospheric N₂O increased from 270 ppb in the 18th century to a new high at 329.9 ppb in 2017 [3]. Specifically, the global warming potential at a 100-year scale of N₂O is 265 times that of carbon dioxide [1]. Considering its important role in global warming, reduction of N₂O emissions is crucial for the mitigation of global climate change.

Soil is the largest source of N₂O emissions at 13 Tg N₂O-N year⁻¹. Human activities have contributed 7 Tg N₂O-N year⁻¹ thus far in the 21st century [4]. Intensive nitrogen (N) applications for

agricultural purposes have induced input of 79 Tg synthetic N and 7.4 Tg N of livestock manure per year [5,6]. Therefore, agricultural soil has large potential in the reduction of N_2O emissions and hence for the mitigation of global climate change.

Biochar and nitrification inhibitor applications are useful strategies for N_2O emission mitigation [7–10]. Biochar is produced by slow pyrolysis of organic matter under high temperatures and an anaerobic environment [11]. Biochar application reduced N_2O emissions caused by N fertilization by 33% [7]; this was ascribed to increased soil pH [12] or N immobilization [7]. In addition, 70% of N_2O emissions are emitted from microbial-driven nitrification and denitrification processes [4], which could be effectively inhibited by nitrification inhibitors. Nitrification inhibitors are a class of organic compounds that inhibit the activity of nitrifying nitrifiers, including synthetic nitrification inhibitors such as dicyandiamide (DCD), nitrapyrin, and 3, 4-dimethylpyrazole phosphate, and biological nitrification inhibitors such as methyl 3-(4-hydroxyphenyl) propionate [13] and brachialactone [14]. Nitrification inhibitors reduced N_2O emissions by 44% via inhibition of nitrifying nitrifiers [15]. As a commonly used nitrification inhibitor, DCD deactivates the activity of ammonium monooxygenase enzyme (a copper co-factor enzyme), and hence N_2O emissions [16].

Camellia oleifera Abel. is one of the world's four main woody edible oil crops, with a long cultivation history and wide cultivation area in subtropical China [17] due to the beneficial effects of its oil on human health [18]. *C. oleifera* is mainly cultivated in Typic Hapludult Ultisols (red soil) with lower soil fertility [17,19]. Therefore, intensive N input has been used to increase the yield of *C. oleifera* oil. However, large amounts of N input increase the risk of nitrate N (NO_3^- -N) leaching and gaseous N losses, such as N_2O emissions and ammonia volatilization [20,21]. While large amounts of *C. oleifera* fruit shells have been dumped without use, it might be an ideal feedstock for producing biochar for the mitigation of N_2O emissions [22].

Here, we conducted study using biochar derived from *C. oleifera* fruit shells and DCD to examine their effects in the mitigation of N_2O emissions from a *C. oleifera* field with intensive ammonium nitrate (NH_4NO_3) fertilization. We predicted that *C. oleifera* fruit shell-derived biochar or DCD may effectively mitigate soil N_2O emissions.

2. Materials and Methods

2.1. Study Site and Soil Collection

This study was conducted at a *C. oleifera* plantation covering 200 ha in Yongxiu county, Jiangxi province, China (29.16° N, 115.77° E) from 25 February 2017 to 16 March 2018. The *C. oleifera* plantation has been intensively managed more than 10 years, with each individual tree distributed 2 m or 3 m apart. Compound fertilizer with 14% N was applied at the rate of 300 mg plant⁻¹. In this region, there is a subtropical monsoon climate with a mean annual precipitation of 1561 mm and a mean annual air temperature of 17.5 °C (the monthly mean temperature ranges from 2.4 °C in January to 33.4 °C in July) (<http://www.worldclim.org>). Soil was classified as Typic Hapludult (red soil). Soil characteristics were obtained by collecting soil samples from 12 randomly selected sites and pooled together for measurement. The basic characteristics were as follows: bulk density, 1.42 g cm⁻³; pH, 4.45; total organic carbon (TOC), 11.06 g kg⁻¹; total N (TN), 1.18 g kg⁻¹; dissolved organic carbon (DOC), 0.28 g kg⁻¹; dissolved organic N (DON), 39.78 mg kg⁻¹; ammonium N (NH_4^+ -N), 4.52 mg kg⁻¹; NO_3^- -N, 1.37 mg kg⁻¹.

2.2. Experimental Design and Field Procedures

This study was conducted using a randomized design with four treatments (including Control, N only, N with Biochar, N with DCD) and four replications ($N = 16$, four soil amelioration treatment \times four replicates). Biochar was produced by pyrolyzing *C. oleifera* fruit shell at 450 °C without oxygen for 1 h and was applied at the rate of 500 g plant⁻¹ (equivalent to 10 t ha⁻¹). Biochar characteristics were: pH, 9.49; TOC, 743.89 g kg⁻¹; TN, 5.14 g kg⁻¹; DOC, 1.57 g kg⁻¹; DON, 14.28 mg kg⁻¹; NH_4^+ -N,

2.24 mg kg⁻¹; NO₃⁻-N, 2.65 mg kg⁻¹. DCD was applied by 2% (DCD/N) [22]. Two years before the study, the studied area was intensively managed but no fertilization was applied. In the study, N was applied by 20 g NH₄NO₃-N plant⁻¹ (equivalent to 400 kg NH₄NO₃-N ha⁻¹). Sixteen *C. oleifera* trees with similar size (mean ground diameter: 6.52 cm) were randomly selected and 0.5 m² plots were established under the crown of each plant for measurement of N₂O fluxes. Nitrogen, biochar, or DCD were thoroughly mixed and applied in all plots.

Static opaque chamber method was used for measurement of N₂O fluxes. Plastic collars with a groove (inner diameter = 16.7 cm, height = 10 cm, groove = 9 cm) were installed inside each plot. The collar groove was filled with water to seal the open-bottomed chamber (inner diameter = 19.5 cm, height = 80 cm) covered with foam and aluminum for minimizing temperature variation [23]. Gas samples were collected at minutes 0, 5, 10, and 15 min from chamber closing using a syringe, and were stored in aluminum foil gas sample bags before analysis.

Fluxes of N₂O were measured 21 times from 25 February, 2017 to 16 March, 2018 at days 4, 8, 12, 19, 26, 32, 46, 62, 77, 93, 111, 130, 140, 161, 175, 190, 210, 248, 287, 339, and 384. Air temperature, soil temperature, and moisture (10 cm depth) were monitored simultaneously when N₂O fluxes were measured. Meanwhile, soil NH₄⁺-N and NO₃⁻-N (0–20 cm layer) were measured nine times over the study on days 62, 93, 130, 161, 210, 248, 287, 339, and 384.

2.3. Analysis of Soil and Biochar Characteristics

Concentrations of soil and biochar NH₄⁺-N and NO₃⁻-N were extracted by 2 mol L⁻¹ KCl solution and measured by a discrete analyzer (Smartchem 200, Rome, Italy). Dissolved organic carbon and DON were extracted by 0.5 mol L⁻¹ K₂SO₄ and measured by element analyzer (Multi N/C 3100, Jena Germany). pH was measured by soil (1:2.5, w/w) or biochar (1:5, w/w) suspensions using pH meter and air-dried samples passed through 0.2-mm sieve (Mettler Toledo, Shanghai, China). Total organic carbon and TN were also analyzed by an element analyzer (Variomax CNS Analyzer, Elementar GmbH, Hanau, Germany) using samples passed through a 0.15-mm sieve.

2.4. Measurement of Soil N₂O Emission Rates and Cumulative Soil N₂O Emissions

Nitrous oxide concentration in each sample was determined using gas chromatograph (Agilent 7890B, Santa Clara, CA, USA). In situ measurements were conducted on sunny days with minimal partial pressure of water vapor. Nitrous oxide fluxes (F , µg m⁻² h⁻¹) were calculated by [23,24]:

$$F = P \times V \times \frac{\Delta c}{\Delta t} \times \frac{1}{RT} \times M \times \frac{1}{S} \quad (1)$$

where P stands for standard atmospheric pressure (Pa) (which should be adjusted if partial pressure of water vapor of chamber air taken into consideration [25]), V refers to the volume of chamber headspace (m³), $\Delta c/\Delta t$ means the rate of N₂O (ppb) concentration change with time based on linear regressions [26,27], R stands for universal gas constant (m³ mol⁻¹ K⁻¹), T is the absolute air temperature (K), M means the molecular mass of N₂O (g mol⁻¹), and S indicates the collar area (m²).

Cumulative soil N₂O emissions (E , µg m⁻²) were calculated by [28]:

$$E = \sum_{i=1}^n \frac{(F_i + F_{i+1})}{2} \times (t_{i+1} - t_i) \times 24 \quad (2)$$

where F indicates soil N₂O emission rates (µg m⁻² h⁻¹), i means the i th measurement, $(t_{i+1} - t_i)$ refers to the time span (days) between two measurements, and n means the total number of the measurements.

2.5. Statistical Analysis

One-way analysis of variance (ANOVA) was performed to examine dependence of cumulative N₂O emissions on N, biochar and DCD treatments. Repeated-measures ANOVA was used to examine

dependence of soil temperature, moisture, $\text{NH}_4^+\text{-N}$, $\text{NO}_3^-\text{-N}$ and N_2O emission rates on biochar and DCD treatments. Tukey's honestly significant difference (HSD) tests were used for identifying the significant differences among treatments in ANOVA. Follow-up contrasts were conducted for significant repeated-measures ANOVA results. Pairwise correlation analysis was applied to examine relationship between environment factor, inorganic N and soil N_2O emission rate. All statistical analyses were carried out using JMP 9.0. Software (Gary, NC, USA) at $\alpha = 0.05$.

3. Results

Application of N, biochar, or DCD significantly influenced soil N_2O emission rates ($F = 8.34$, $p = 0.0029$) and cumulative N_2O emissions ($F = 6.68$, $p = 0.0067$) compared to control from the *C. oleifera* field. No significant results were observed in soil temperature, moisture, $\text{NH}_4^+\text{-N}$, and $\text{NO}_3^-\text{-N}$ (Figures 1 and 2). Compared with N treatment, N + DCD ($F = 7.94$, $p = 0.0155$) or N + biochar ($F = 5.69$, $p = 0.0344$) treatments showed lower soil N_2O emission rates, but no significant differences were observed between N + DCD and N + biochar treatments ($F = 0.19$, $p = 0.67$; Figure 3). Overall, N, biochar, or DCD treatments significantly impacted soil N_2O emission rates over the 12-month study ($F = 10.11$, $p = 0.0013$; Figure 3).

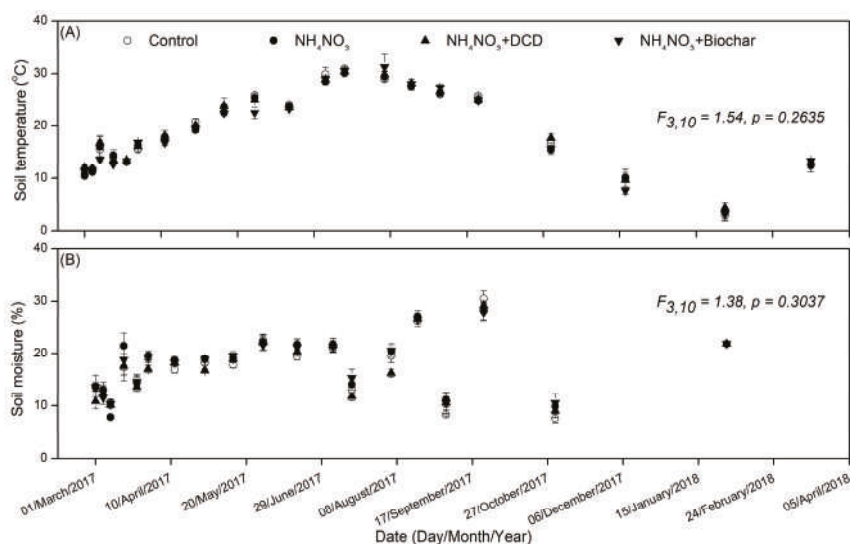


Figure 1. Soil (A) temperature and (B) moisture (mean \pm standard error) over the 12-month study in *Camellia oleifera* Abel. field with the N and mitigation treatments. Repeated-measure one-way analysis of variance results are shown. N: nitrogen; DCD: dicyandiamide; NH_4NO_3 : ammonium nitrate.

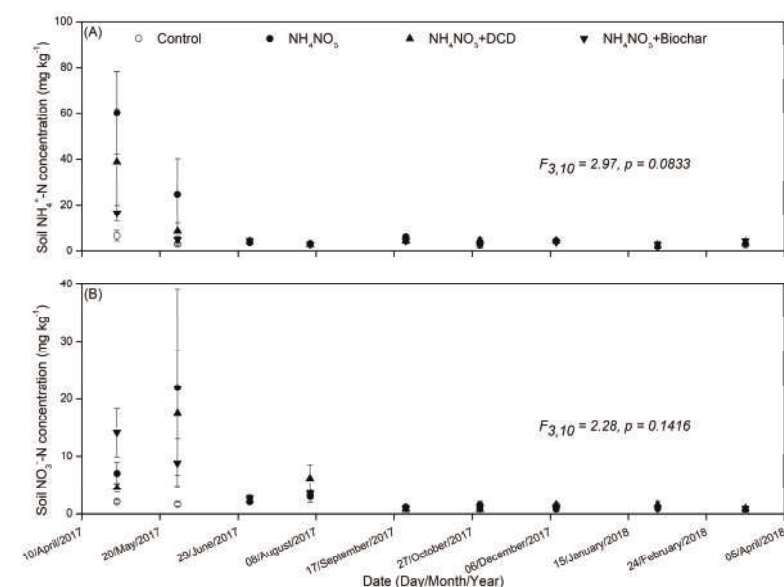


Figure 2. Soil inorganic N dynamics, including (A) NH_4^+ -N and (B) NO_3^- -N (mean \pm standard error), over the 12-month study in *Camellia oleifera* Abel. field with the N and mitigation treatments. Repeated-measure one-way analysis of variance results are shown. N: nitrogen; NH_4^+ -N: ammonium nitrogen; NO_3^- -N: nitrate nitrogen; DCD: dicyandiamide; NH_4NO_3 : ammonium nitrate.

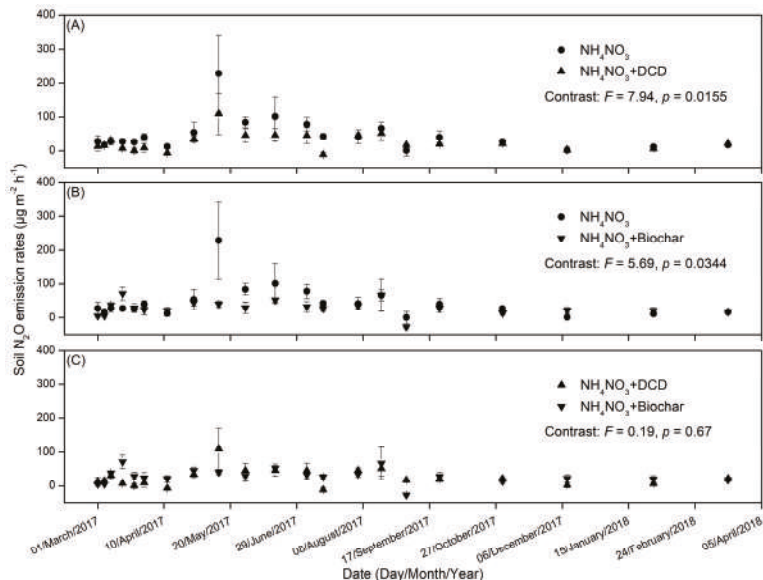


Figure 3. Soil N_2O emissions (mean \pm standard error) from soil with N, or N with DCD or biochar in a *Camellia oleifera* Abel. field. (A) NH_4NO_3 vs. NH_4NO_3 + DCD; (B) NH_4NO_3 vs. NH_4NO_3 + Biochar; (C) NH_4NO_3 + DCD vs. NH_4NO_3 + Biochar. Repeated-measure one-way analysis of variance and follow-up contrast results are shown. N: nitrogen; DCD: dicyandiamide; NH_4NO_3 : ammonium nitrate; N_2O : nitrous oxide.

Nitrogen treatment increased cumulative soil N₂O emissions (control vs. N, 92.14 ± 47.01 vs. 375.10 ± 60.30 mg m⁻², respectively). DCD reduced the increase of cumulative soil N₂O emissions caused by N addition, but no significant differences were observed between N + DCD and N + biochar treatments (Figure 4, N + DCD vs. N + biochar, 211.89 ± 35.88 vs. 238.34 ± 30.65 mg m⁻²). The soil N₂O emission rate positively correlated with soil temperature, moisture, NH₄⁺-N, and NO₃⁻-N (Table 1).

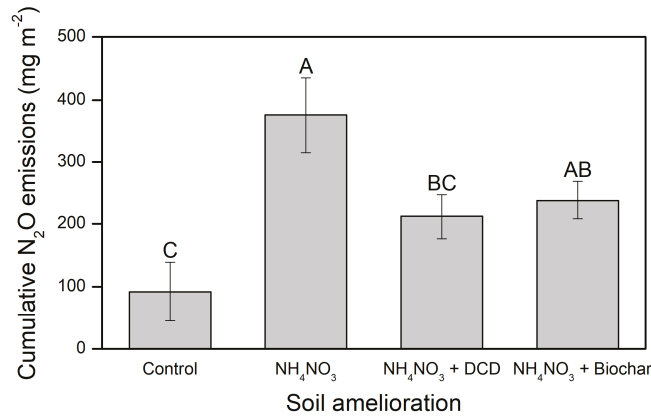


Figure 4. Cumulative soil N₂O emissions (mean ± SE) from the *Camellia oleifera* Abel. field as affected by N fertilization, DCD, or biochar treatments. Bars connected by the same letter are not significantly different in post-hoc tests at $\alpha = 0.05$. N: nitrogen; DCD: dicyandiamide; NH₄NO₃: ammonium nitrate; N₂O: nitrous oxide.

Table 1. Pairwise correlations among soil environmental factors, inorganic nitrogen and soil N₂O emission rate.

| Parameters | Soil Temperature | Soil Moisture | NH ₄ ⁺ -N | NO ₃ ⁻ -N |
|---------------------------------|------------------|---------------|---------------------------------|---------------------------------|
| Soil moisture | 0.275 *** | | | |
| NH ₄ ⁺ -N | 0.051 | −0.050 | | |
| NO ₃ ⁻ -N | 0.188 * | −0.003 | 0.414 *** | |
| N ₂ O | 0.216 *** | 0.201 *** | 0.285 *** | 0.221 ** |

*, $p < 0.05$; **, $p < 0.01$; ***, $p < 0.001$. NH₄⁺-N: ammonium nitrogen; NO₃⁻-N: nitrate nitrogen; N₂O: nitrous oxide.

4. Discussion

Nitrous oxide emitted from *C. oleifera* plantation was monitored over one year in situ study to investigate effects of biochar or DCD on soil N₂O emissions following application of N fertilization. Soil N₂O emission rates were decreased by biochar or DCD in fertilized soil and the decrease was comparable between two treatments (Figure 3). However, the cumulative soil N₂O emissions caused by NH₄NO₃ fertilization were reduced by DCD application to levels comparable to the control treatment (Figure 4).

4.1. Nitrogen Fertilization Stimulated Soil N₂O Emissions

Nitrogen fertilization stimulated cumulative soil N₂O emissions from *C. oleifera* plantation (Figure 4). N fertilization generally alters activities of N-transforming microorganisms via input of available N substrate [29], stimulating the processes of microbial-driven nitrification and denitrification and subsequent soil N₂O emissions [30,31]. In general, soil N₂O emissions were increased by N input with nonlinear responses [32]. Indeed, the soil N₂O emission rate was positively correlated with NH₄⁺-N and NO₃⁻-N (Table 1). Furthermore, intensive N fertilization, especially NH₄⁺-N fertilization, often results in soil acidification [33,34]. Changes in soil pH may regulate soil N₂O emissions via

altering the abundance and composition of N-transforming microorganisms [35–37]. For example, abundances of ammonia-oxidizing bacteria (AOB) were more sensitive to N addition than that of ammonia-oxidizing archaea (AOA) (+ 326% vs. + 27%) [35]. Soil acidification induced by intensive N fertilization results in a high ratio of $N_2O/(N_2O+N_2)$ in the previous study [38]. Therefore, N addition might alter the abundance and composition of AOB and AOA via acidifying soil, hence stimulating N_2O emissions.

In our study, positive correlations between N_2O emission rate and soil temperature or soil moisture were observed (Table 1). A previous study demonstrated that soil temperature and moisture can explain up to 86% variations of N_2O emissions [39]. Soil N_2O emissions varied with soil temperature in specific ranges [28,40], which may relate to different optimum temperatures of N-transforming microorganisms with or without N fertilization and different soil types [37,41]. Compared with soil temperature, soil moisture is the main factor impacting soil N_2O emissions. Consistently, soil N_2O emitted from a wheat–maize plantation showed a positive correlation with a soil water-filled pore space (WFPS) [42]. However, higher soil moisture with lower oxygen content was beneficial to denitrification [30,43] and potentially decrease soil N_2O emissions [44,45]. For example, WFPS at 67–76% was the optimum moisture environment for emitting N_2O [46]. Similarly, N_2O emitted from a rice–rapeseed rotation soil was higher in 60% WFPS than flooding in an incubation experiment [36]. Therefore, moisture effects of soil N_2O emissions may depend on soil type and present non-linear correlations.

4.2. Biochar Reduced Soil N_2O Emission Rates as Affected by N Fertilization

In fertilized soil, N_2O emission rates were significantly decreased and cumulative N_2O emissions were decreased by 36% by biochar (Figures 3B and 4), indicating biochar could be an ideal strategy for N_2O mitigations in *C. oleifera* plantations with N fertilization. Indeed, soil N_2O emissions with N fertilization were decreased 33% by biochar in a meta-analysis study [7]. Biochar-suppressed soil N_2O emissions may be relative, limiting the availability of NO_3^- -N to denitrifiers [47,48] or altering the N transformation process rather than limiting the availability of NH_4^+ -N or NO_3^- -N to N-transforming microorganisms [49]. In addition, biochar could also impose toxic effects on urease activity and subsequent generation of NH_4^+ -N by introducing polycyclic aromatic hydrocarbons, heavy metals, and free radicals into soil [50], which may suppress soil N_2O emissions via reducing the N substrate with respect to N-transforming microorganisms.

Biochar addition may suppress soil N_2O emissions by increasing soil pH [12]. The activity of N_2O -reductase was generally higher with higher soil pH [31]. Indeed, the pH of *C. oleifera* fruit shell-derived biochar was higher than that of the acid soil in *C. oleifera* plantations. While an acid soil improvement study showed that liming by dolomite addition could substantially mitigate N_2O emissions via increasing *nosZ* gene abundance [36,51], biochar application could also increase soil pH of the acid *C. oleifera* field soil, which might have also been accompanied by enhanced activities of N_2O -reducing enzymes and hence suppressed N_2O emissions. Moreover, the negative effects of biochar on N_2O emissions could also be induced by its buffer capacity rather than pH, in which biochar acted as “electron shuttle” and replaced NO_3^- as electron sink during denitrification [52]. However, the application of *C. oleifera* fruit shell-derived biochar stimulated N_2O emissions in a previous incubation study [22], which might have been caused by the short-term time scale of incubation study and further indicated the importance of in situ studies. Future studies are still needed for thoroughly understanding of *C. oleifera* fruit shell-derived biochar effects on N_2O emissions and its prolonged effects in mitigation of soil N_2O emissions.

4.3. DCD Reduced Soil N_2O Emissions as Affected by N Fertilization

Cumulative soil N_2O emissions were reduced 44% by DCD application in soil with N fertilization treatment (Figures 3A and 4), which indicated that the application of DCD is an effective strategy for mitigating soil N_2O emissions in *C. oleifera* plantations with intensive N fertilization. DCD has been proved to be effective in reducing average N_2O emission rates following NH_4NO_3 addition in a

previous study [22]. In agreement, DCD reduced soil N₂O emissions following (NH₄)₂SO₄ addition by suppressing *amoA* genes and stimulating *nosZ* genes [53]. Nitrification and denitrification are two main pathways producing N₂O [30,31,54]. Application of nitrification inhibitors can suppress soil N₂O emissions [15,16] by inhibiting the activity of ammonium monooxygenase enzyme involved in nitrification process [16]. Thereby, application of DCD generally decreases abundance of *amoA* genes and hence soil N₂O emissions.

4.4. Biochar and DCD Effects on Soil N₂O Emissions

While N fertilization significantly increased soil N₂O emissions compared with control treatment, DCD application decreased soil N₂O emissions to similar levels as control treatment (Figures 3A and 4). Even though biochar addition treatment did not significantly decrease N₂O emissions from soil with N, the slight decrease in cumulative N₂O emissions may potentially mitigate N₂O emissions in prolonged study, which should be examined in future studies. However, DCD application significantly decreased cumulative N₂O emissions and no significant difference was observed between control and DCD treatment (Figure 4), indicating DCD was effective in mitigation of N₂O emissions from *C. oleifera* field relative to biochar. No significant differences were observed between DCD and biochar treatments in their effects on N₂O emission rates (Figures 3C and 4), indicating biochar application could be considered as a potential mitigation strategy of soil N₂O. Similarly, both DCD and biochar reduced the yield-scaled N₂O following N fertilization, while biochar showed stronger effects than DCD in N₂O mitigation in a sweet corn field [55].

5. Conclusions

This study is the first in examining the effects of DCD and biochar derived from *C. oleifera* fruit shells on mitigation of soil N₂O emissions. Application of biochar and DCD showed comparable effects in mitigation of the N₂O emission rate in a *C. oleifera* field with intensive N fertilization practice, with biochar slightly decreasing and DCD significantly decreasing cumulative N₂O emissions. This might have implications for the disposal of dumped byproducts in management of *C. oleifera* and represent an ideal way to enhance both the economic and ecological benefits of the *C. oleifera* industry. If this pattern presents in other plantations, the combined effects of biochar and nitrification inhibitors on soil N₂O emissions should be focused upon in the future. However, the potential effects of biochar derived from *C. oleifera* fruit shell on cumulative N₂O emissions in prolonged studies and other kinds of ecosystems should be examined in future in order to provide guidance for intensive management of *C. oleifera* plantations and disposal of byproducts.

Author Contributions: Conceptualization, L.Z. and B.D.; methodology, L.Z. and B.D.; software, L.Z. and B.D.; validation, H.F., N.J., H.W., and D.H.; investigation, B.D., H.F., and N.J.; resources, L.Z. and X.G.; data curation, B.D., H.F., N.J., and J.W.; writing—original draft preparation, B.D.; writing—review and editing, L.Z., N.J., H.W., J.W., W.F., L.L., and X.G.; project administration, B.D., H.F., and L.Z.; funding acquisition, L.Z.

Funding: This research was funded by the National Natural Science Foundation of China, Grant Numbers 41967017 and 41501317, and the Jiangxi Education Department, Project Number GJJ160348. Bangliang Deng was supported by China Scholarship Council for study in the United States.

Acknowledgments: Thanks are given to Liya Zheng, Xiang Zheng, Qian Li, Xi Yuan, Shuli Wang, Xintong Xu, and Jianwei Wang for their help in laboratory and field work.

Conflicts of Interest: The authors have declared that no competing interests exist.

References

1. IPCC. *Synthesis Report, Climate Change 2014*; IPCC: Geneva, Switzerland, 2014; pp. 1–164.
2. Ravishankara, A.R.; Daniel, J.S.; Portmann, R.W. Nitrous oxide (N₂O): The dominant ozone-depleting substance emitted in the 21st century. *Science* **2009**, *326*, 123–125. [[CrossRef](#)] [[PubMed](#)]
3. WMO. *WMO Greenhouse Gas Bulletin: The State of Greenhouse Gases in the Atmosphere Based on Global Observations Through 2017*; Atmospheric Environment Research Division: Geneva, Switzerland, 2018; pp. 1–8.

4. Fowler, D.; Coyle, M.; Skiba, U.; Sutton, M.A.; Cape, J.N.; Reis, S.; Sheppard, L.J.; Jenkins, A.; Grizzetti, B.; Galloway, J.N.; et al. The global nitrogen cycle in the twenty-first century. *Philos. Trans. R. Soc. B Biol. Sci.* **2013**, *368*, 1–13. [\[CrossRef\]](#)
5. Gerber, J.S.; Carlson, K.M.; Makowski, D.; Mueller, N.D.; Garcia De Cortazar-Atauri, I.; Havlík, P.; Herrero, M.; Launay, M.; O'Connell, C.S.; Smith, P.; et al. Spatially explicit estimates of N₂O emissions from croplands suggest climate mitigation opportunities from improved fertilizer management. *Glob. Chang. Biol.* **2016**, *22*, 3383–3394. [\[CrossRef\]](#) [\[PubMed\]](#)
6. Carlson, K.M.; Gerber, J.S.; Mueller, N.D.; Herrero, M.; MacDonald, G.K.; Brauman, K.A.; Havlik, P.; Connell, C.S.; Johnson, J.A.; Saatchi, S.; et al. Greenhouse gas emissions intensity of global croplands. *Nat. Clim. Chang.* **2017**, *7*, 63–68. [\[CrossRef\]](#)
7. He, Y.; Zhou, X.; Jiang, L.; Li, M.; Du, Z.; Zhou, G.; Shao, J.; Wang, X.; Xu, Z.; Hosseini Bai, S.; et al. Effects of biochar application on soil greenhouse gas fluxes: A meta-analysis. *GCB Bioenergy* **2017**, *9*, 743–755. [\[CrossRef\]](#)
8. Gu, J.; Nie, H.; Guo, H.; Xu, H.; Gunnathorn, T. Nitrous oxide emissions from fruit orchards: A review. *Atmos. Environ.* **2019**, *201*, 166–172. [\[CrossRef\]](#)
9. Liu, Q.; Liu, B.; Zhang, Y.; Hu, T.; Lin, Z.; Liu, G.; Wang, X.; Ma, J.; Wang, H.; Jin, H.; et al. Biochar application as a tool to decrease soil nitrogen losses (NH₃ volatilization, N₂O emissions, and N leaching) from croplands: Options and mitigation strength in a global perspective. *Glob. Chang. Biol.* **2019**, *25*, 2077–2093. [\[CrossRef\]](#)
10. Shrestha, B.; Chang, S.; Bork, E.; Carlyle, C. Enrichment planting and soil amendments enhance carbon sequestration and reduce greenhouse gas emissions in agroforestry systems: A review. *Forests* **2018**, *9*, 369. [\[CrossRef\]](#)
11. Johannes, L.; Stephen, J. *Biochar for Environmental Management*; Routledge: New York, NY, USA, 2015; pp. 1–944.
12. Obia, A.; Cornelissen, G.; Mulder, J.; Dörsch, P. Effect of soil pH increase by biochar on NO, N₂O and N₂ production during denitrification in acid soils. *PLoS ONE* **2015**, *10*, 1–19. [\[CrossRef\]](#)
13. Zakir, H.A.; Subbarao, G.V.; Pearse, S.J.; Gopalakrishnan, S.; Ito, O.; Ishikawa, T.; Kawano, N.; Nakahara, K.; Yoshihashi, T.; Ono, H.; et al. Detection, isolation and characterization of a root-exuded compound, methyl 3-(4-hydroxyphenyl) propionate, responsible for biological nitrification inhibition by sorghum (*Sorghum bicolor*). *New Phytol.* **2008**, *180*, 442–451. [\[CrossRef\]](#)
14. Subbarao, G.V.; Nakahara, K.; Hurtado, M.P.; Ono, H.; Moreta, D.E.; Salcedo, A.F.; Yoshihashi, A.T.; Ishikawa, T.; Ishitani, M.; Ohnishi-Kameyama, M.; et al. Evidence for biological nitrification inhibition in *Brachiaria* pastures. *Proc. Natl. Acad. Sci. USA* **2009**, *106*, 17302–17307. [\[CrossRef\]](#) [\[PubMed\]](#)
15. Qiao, C.; Liu, L.; Hu, S.; Compton, J.E.; Greaver, T.L.; Li, Q. How inhibiting nitrification affects nitrogen cycle and reduces environmental impacts of anthropogenic nitrogen input. *Glob. Chang. Biol.* **2015**, *21*, 1249–1257. [\[CrossRef\]](#) [\[PubMed\]](#)
16. Ruser, R.; Schulz, R. The effect of nitrification inhibitors on the nitrous oxide (N₂O) release from agricultural soils—a review. *J. Plant Nutr. Soil Sci.* **2015**, *178*, 171–188. [\[CrossRef\]](#)
17. Liu, J.; Wu, L.; Chen, D.; Li, M.; Wei, C. Soil quality assessment of different *Camellia oleifera* stands in mid-subtropical China. *Appl. Soil Ecol.* **2017**, *113*, 29–35. [\[CrossRef\]](#)
18. Yuan, J.; Wang, C.; Chen, H.; Zhou, H.; Ye, J. Prediction of fatty acid composition in *Camellia oleifera* oil by near infrared transmittance spectroscopy (NITS). *Food Chem.* **2013**, *138*, 1657–1662. [\[CrossRef\]](#)
19. Liu, C.; Chen, L.; Tang, W.; Peng, S.; Li, M.; Deng, N.; Chen, Y. Predicting potential distribution and evaluating suitable soil condition of oil tea *Camellia* in China. *Forests* **2018**, *9*, 487. [\[CrossRef\]](#)
20. Martins, M.R.; Sant Anna, S.A.C.; Zaman, M.; Santos, R.C.; Monteiro, R.C.; Alves, B.J.R.; Jantalia, C.P.; Boddey, R.M.; Urquiaga, S. Strategies for the use of urease and nitrification inhibitors with urea: Impact on N₂O and NH₃ emissions, fertilizer-¹⁵N recovery and maize yield in a tropical soil. *Agric. Ecosyst. Environ.* **2017**, *247*, 54–62. [\[CrossRef\]](#)
21. Liu, S.; Lin, F.; Wu, S.; Ji, C.; Sun, Y.; Jin, Y.; Li, S.; Li, Z.; Zou, J. A meta-analysis of fertilizer-induced soil NO and combined NO+N₂O emissions. *Glob. Chang. Biol.* **2017**, *23*, 2520–2532. [\[CrossRef\]](#)
22. Deng, B.; Wang, S.; Xu, X.; Wang, H.; Hu, D.; Guo, X.; Shi, Q.; Siemann, E.; Zhang, L. Effects of biochar and dicyandiamide combination on nitrous oxide emissions from *Camellia oleifera* field soil. *Environ. Sci. Pollut. Res.* **2019**, *26*, 4070–4077. [\[CrossRef\]](#)

23. Zhang, L.; Wang, S.; Liu, S.; Liu, X.; Zou, J.; Siemann, E. Perennial forb invasions alter greenhouse gas balance between ecosystem and atmosphere in an annual grassland in China. *Sci. Total Environ.* **2018**, *642*, 781–788. [\[CrossRef\]](#)
24. Zhang, L.; Ma, X.; Wang, H.; Liu, S.; Siemann, E.; Zou, J. Soil respiration and litter decomposition increased following perennial forb invasion into an annual grassland. *Pedosphere* **2016**, *26*, 567–576. [\[CrossRef\]](#)
25. Carter, M.R.; Gregorich, E.G. *Soil Sampling and Methods of Analysis*; CRC Press: Boca Raton, IL, USA, 2007; pp. 1–1224.
26. Pärn, J.; Verhoeven, J.T.A.; Butterbach-Bahl, K.; Dise, N.B.; Ullah, S.; Aasa, A.; Egorov, S.; Espenberg, M.; Järveoja, J.; Jauhiainen, J.; et al. Nitrogen-rich organic soils under warm well-drained conditions are global nitrous oxide emission hotspots. *Nat. Commun.* **2018**, *9*, 1–8. [\[CrossRef\]](#)
27. Domeignoz-Horta, L.A.; Philippot, L.; Peyrard, C.; Bru, D.; Breuil, M.; Bizouard, F.; Justes, E.; Mary, B.; Léonard, J.; Spor, A. Peaks of in situ N₂O emissions are influenced by N₂O-producing and reducing microbial communities across arable soils. *Glob. Chang. Biol.* **2018**, *24*, 360–370. [\[CrossRef\]](#) [\[PubMed\]](#)
28. He, T.; Yuan, J.; Luo, J.; Wang, W.; Fan, J.; Liu, D.; Ding, W. Organic fertilizers have divergent effects on soil N₂O emissions. *Biol. Fertil. Soils* **2019**, *55*, 685–699. [\[CrossRef\]](#)
29. Lourenço, K.S.; Dimitrov, M.R.; Pijl, A.; Soares, J.R.; Do Carmo, J.B.; van Veen, J.A.; Cantarella, H.; Kuramae, E.E. Dominance of bacterial ammonium oxidizers and fungal denitrifiers in the complex nitrogen cycle pathways related to nitrous oxide emission. *GCB Bioenergy* **2018**, *10*, 645–660. [\[CrossRef\]](#)
30. Pauleta, S.R.; Dell Acqua, S.; Moura, I. Nitrous oxide reductase. *Coord. Chem. Rev.* **2013**, *257*, 332–349. [\[CrossRef\]](#)
31. Hu, H.; Chen, D.; He, J. Microbial regulation of terrestrial nitrous oxide formation: Understanding the biological pathways for prediction of emission rates. *FEMS Microbiol. Rev.* **2015**, *39*, 729–749. [\[CrossRef\]](#)
32. Shcherbak, I.; Millar, N.; Robertson, G.P. Global metaanalysis of the nonlinear response of soil nitrous oxide (N₂O) emissions to fertilizer nitrogen. *Proc. Natl. Acad. Sci. USA* **2014**, *111*, 9199–9204. [\[CrossRef\]](#)
33. Tian, D.; Niu, S. A global analysis of soil acidification caused by nitrogen addition. *Environ. Res. Lett.* **2015**, *10*, 24019. [\[CrossRef\]](#)
34. Matson, P.A.; McDowell, W.H.; Townsend, A.R.; Vitousek, P.M. The globalization of N deposition: Ecosystem consequences in tropical environments. *Biogeochemistry* **1999**, *46*, 67–83. [\[CrossRef\]](#)
35. Carey, C.J.; Dove, N.C.; Beman, J.M.; Hart, S.C.; Aronson, E.L. Meta-analysis reveals ammonia-oxidizing bacteria respond more strongly to nitrogen addition than ammonia-oxidizing archaea. *Soil Biol. Biochem.* **2016**, *99*, 158–166. [\[CrossRef\]](#)
36. Shaaban, M.; Wu, Y.; Khalid, M.S.; Peng, Q.; Xu, X.; Wu, L.; Younas, A.; Bashir, S.; Mo, Y.; Lin, S.; et al. Reduction in soil N₂O emissions by pH manipulation and enhanced *nosZ* gene transcription under different water regimes. *Environ. Pollut.* **2018**, *235*, 625–631. [\[CrossRef\]](#) [\[PubMed\]](#)
37. Blum, J.; Su, Q.; Ma, Y.; Valverde-Pérez, B.; Domingo-Félez, C.; Jensen, M.M.; Smets, B.F. The pH dependency of N-converting enzymatic processes, pathways and microbes: Effect on net N₂O production. *Environ. Microbiol.* **2018**, *20*, 1623–1640. [\[CrossRef\]](#) [\[PubMed\]](#)
38. Qu, Z.; Wang, J.; Almøy, T.; Bakken, L.R. Excessive use of nitrogen in Chinese agriculture results in high N₂O/(N₂O+N₂) product ratio of denitrification, primarily due to acidification of the soils. *Glob. Chang. Biol.* **2014**, *20*, 1685–1698. [\[CrossRef\]](#)
39. Schindlbacher, A. Effects of soil moisture and temperature on NO, NO₂, and N₂O emissions from European forest soils. *J. Geophys. Res.* **2004**, *109*, 1–12. [\[CrossRef\]](#)
40. Pinheiro, P.L.; Recous, S.; Dietrich, G.; Weiler, D.A.; Schu, A.L.; Bazzo, H.L.S.; Giacomini, S.J. N₂O emission increases with mulch mass in a fertilized sugarcane cropping system. *Biol. Fertil. Soils* **2019**, *55*, 511–523. [\[CrossRef\]](#)
41. Yin, C.; Fan, F.; Song, A.; Fan, X.; Ding, H.; Ran, W.; Qiu, H.; Liang, Y. The response patterns of community traits of N₂O emission-related functional guilds to temperature across different arable soils under inorganic fertilization. *Soil Biol. Biochem.* **2017**, *108*, 65–77. [\[CrossRef\]](#)
42. Chen, T.; Oenema, O.; Li, J.; Misselbrook, T.; Dong, W.; Qin, S.; Yuan, H.; Li, X.; Hu, C. Seasonal variations in N₂ and N₂O emissions from a wheat–maize cropping system. *Biol. Fertil. Soils* **2019**, *55*, 539–551. [\[CrossRef\]](#)
43. Quick, A.M.; Reeder, W.J.; Farrell, T.B.; Tonina, D.; Feris, K.P.; Benner, S.G. Nitrous oxide from streams and rivers: A review of primary biogeochemical pathways and environmental variables. *Earth-Sci. Rev.* **2019**, *191*, 224–262. [\[CrossRef\]](#)

44. Chen, H.; Mothapo, N.V.; Shi, W. Soil moisture and pH control relative contributions of fungi and bacteria to N₂O production. *Microb. Ecol.* **2015**, *69*, 180–191. [[CrossRef](#)]
45. Burgin, A.J.; Groffman, P.M. Soil O₂ controls denitrification rates and N₂O yield in a riparian wetland. *J. Geophys. Res. Biogeosci.* **2012**, *117*, 1–10. [[CrossRef](#)]
46. Chen, Z.; Ding, W.; Xu, Y.; Müller, C.; Yu, H.; Fan, J. Increased N₂O emissions during soil drying after waterlogging and spring thaw in a record wet year. *Soil Biol. Biochem.* **2016**, *101*, 152–164. [[CrossRef](#)]
47. Van Zwieten, L.; Singh, B.P.; Kimber, S.W.L.; Murphy, D.V.; Macdonald, L.M.; Rust, J.; Morris, S. An incubation study investigating the mechanisms that impact N₂O flux from soil following biochar application. *Agric. Ecosyst. Environ.* **2014**, *191*, 53–62. [[CrossRef](#)]
48. Case, S.D.C.; McNamara, N.P.; Reay, D.S.; Whitaker, J. The effect of biochar addition on N₂O and CO₂ emissions from a sandy loam soil - The role of soil aeration. *Soil Biol. Biochem.* **2012**, *51*, 125–134. [[CrossRef](#)]
49. Case, S.D.C.; McNamara, N.P.; Reay, D.S.; Stott, A.W.; Grant, H.K.; Whitaker, J. Biochar suppresses N₂O emissions while maintaining N availability in a sandy loam soil. *Soil Biol. Biochem.* **2015**, *81*, 178–185. [[CrossRef](#)]
50. Liu, Y.; Dai, Q.; Jin, X.; Dong, X.; Peng, J.; Wu, M.; Liang, N.; Pan, B.; Xing, B. Negative impacts of biochars on urease activity: High pH, heavy metals, polycyclic aromatic hydrocarbons, or free radicals? *Environ. Sci. Technol.* **2018**, *52*, 12740–12747. [[CrossRef](#)]
51. Shaaban, M.; Hu, R.; Wu, Y.; Younas, A.; Xu, X.; Sun, Z.; Jiang, Y.; Lin, S. Mitigation of N₂O emissions from urine treated acidic soils by liming. *Environ. Pollut.* **2019**, *225*, 113237. [[CrossRef](#)]
52. Cayuela, M.L.; Sánchez-Monedero, M.A.; Roig, A.; Hanley, K.; Enders, A.; Lehmann, J. Biochar and denitrification in soils: When, how much and why does biochar reduce N₂O emissions? *Sci. Rep.* **2013**, *3*, 1–7. [[CrossRef](#)]
53. Wang, Q.; Hu, H.W.; Shen, J.P.; Du, S.; Zhang, L.M.; He, J.Z.; Han, L.L. Effects of the nitrification inhibitor dicyandiamide (DCD) on N₂O emissions and the abundance of nitrifiers and denitrifiers in two contrasting agricultural soils. *J. Soils Sediments* **2017**, *17*, 1635–1643. [[CrossRef](#)]
54. Kuypers, M.M.M.; Marchant, H.K.; Kartal, B. The microbial nitrogen-cycling network. *Nat. Rev. Microbiol.* **2018**, *16*, 263–276. [[CrossRef](#)]
55. Yi, Q.; Tang, S.; Fan, X.; Zhang, M.; Pang, Y.; Huang, X.; Huang, Q. Effects of nitrogen application rate, nitrogen synergist and biochar on nitrous oxide emissions from vegetable field in south China. *PLoS ONE* **2017**, *12*, 1–15. [[CrossRef](#)]



© 2019 by the authors. Licensee MDPI, Basel, Switzerland. This article is an open access article distributed under the terms and conditions of the Creative Commons Attribution (CC BY) license (<http://creativecommons.org/licenses/by/4.0/>).

Estimation of Forest Carbon Stocks for National Greenhouse Gas Inventory Reporting in South Korea

Sun Jeoung Lee ^{1,3}, Jong Su Yim ¹, Yeong Mo Son ², Yowhan Son ³ and Raehyun Kim ^{4,*}

¹ Division of Forest Industry, National Institute of Forest Science, 57 Hoegi-ro, Seoul 02455, Korea; sunjlee1020@korea.kr (S.J.L.); yimjs@korea.kr (J.S.Y.)

² Division of Forest Welfare, National Institute of Forest Science, 57 Hoegi-ro, Seoul 02455, Korea; treelove@korea.kr

³ Department of Environmental Science and Ecological Engineering, Graduate School, Korea University, 145 Anam-ro, Seoul 02841, Korea; yson@korea.ac.kr

⁴ Division of Global Forestry, National Institute of Forest Science, 57 Hoegi-ro, Seoul 02455, Korea

* Correspondence: rhkim@korea.kr; Tel.: +82-2-961-2871

Received: 14 September 2018; Accepted: 5 October 2018; Published: 10 October 2018

Abstract: The development of country-specific emission factors in relation to the Agriculture, Forestry, and Other Land Use (AFOLU) sector has the potential to improve national greenhouse gas inventory systems. Forests are carbon sinks in the AFOLU that can play an important role in mitigating global climate change. According to the United Nations Framework Convention on Climate Change (UNFCCC), signatory countries must report forest carbon stocks, and the changes within them, using emission factors from the Intergovernmental Panel on Climate Change (IPCC) or from country-specific values. This study was conducted to estimate forests carbon stocks and to complement and improve the accuracy of national greenhouse gas inventory reporting in South Korea. We developed country-specific emissions factors and estimated carbon stocks and their changes using the different approaches and methods described by the IPCC (IPCC_{EF}: IPCC default emission factors, CS_{FT}: country-specific emission factors by forest type, and CS_{Sp}: country-specific emission factors by species). CS_{FT} returned a result for carbon stocks that was 1.2 times higher than the value using IPCC_{EF}. Using CS_{Sp}, CO₂ removal was estimated to be 60,648 Gg CO₂ per year with an uncertainty of 22%. Despite a reduction in total forest area, forests continued to store carbon and absorb CO₂, owing to differences in the carbon storage capacities of different forest types and tree species. The results of this study will aid estimations of carbon stock changes and CO₂ removal by forest type or species, and help to improve the completeness and accuracy of the national greenhouse gas inventory. Furthermore, our results provide important information for developing countries implementing Tier 2, the level national greenhouse gas inventory systems recommended by the IPCC.

Keywords: carbon stock changes; forest; greenhouse gas inventory; IPCC; South Korea

1. Introduction

According to the United Nations Framework Convention on Climate Change (UNFCCC), all parties are obligated to submit annual national greenhouse gas inventory reports for all emissions and removals, including those associated with the Agriculture, Forestry, and Other Land Use sector (AFOLU). Specifically, the Paris Agreement states that “parties shall account for their Nationally Determined Contributions (NDC)” [1]. The mitigation contributions of parties (included in the NDCs) should be accounted for in the context of the Paris Agreement and are expected to be based on greenhouse gas inventory reporting methodology.

All countries have made efforts to improve inventory reporting systems and tier levels given respective national circumstances, in accordance with the principles of Transparency,

Accuracy, Consistency, Comparability, and Completeness (TACCC) under the UNFCCC [1,2]. The Intergovernmental Panel on Climate Change (IPCC) guidelines provide three different tier levels for calculating the national greenhouse gas inventory, which relate to the activity data and emission factors in the AFOLU [2,3]. In general, using complementary data and moving to a methodology at higher tiers can improve the accuracy of the inventory and reduce uncertainty [2,3]. Most developing countries, including South Korea, have not been able to report on the carbon stocks from all carbon pools [4,5]. Estimating all carbon pools would represent a major improvement in completeness, which is linked to comparability and accuracy for national greenhouse gas inventory systems, and would also affect the greenhouse gas mitigation targets in NDC.

Dependent upon tree growth rate, forest ecosystems are able to remove CO₂ from the atmosphere; as such, they are the largest terrestrial carbon sink [6]. For this reason, Annex I countries under the UNFCCC should report the national emissions and removal of greenhouse gases associated with the forest sector in AFOLU [2,7]. To calculate greenhouse gas emissions and their removal, national forest inventories (NFIs) represent a key source of information [8]. Although relatively few countries carry out NFIs more frequently than every 5 or even 10 years, the national reports normally rely on projected quantities of carbon emissions and removal from forests and land use change for the reporting period [9,10].

Forests cover 64% of the total land area in South Korea, and they play an important role in the mitigation of greenhouse gases through carbon sequestration [11,12]. South Korean forests were a carbon source releasing carbon at a rate of 0.5 Tg C year^{−1} during 1954–1973; however, they have been acting as carbon sinks with a carbon sequestration rate of 12.6 Tg C year^{−1} since 1974 [12]. The annual carbon balance of South Korean forests from 1954 to 2012 was 8.3 Tg C year^{−1} [12]. Studies into forest carbon stocks have been also conducted to establish the greenhouse gas inventory system of the forestry sector in South Korea. The South Korean national greenhouse gas inventory system is based on country-specific emission factors and activity data from NFIs and on official statistics by forest type [5]. To complement the national greenhouse gas inventory system and improve its accuracy, a number of studies have focused on the emission factors in all carbon pools in South Korea [13–17]; a few case studies have also estimated total carbon stocks at the national scale using modeling [12].

Owing partly to a limited range of activity data, previous studies have focused on the above and belowground biomass in South Korean forests [5]. The purpose of this study was to develop country-specific emission factors and to examine the methodology in order to enhance the completeness and accuracy of national greenhouse gas inventory reporting using those factors.

2. Materials and Methods

2.1. Estimating Country-Specific Emission Factors

In order to develop country-specific emission factor for biomass, soil, and litter, we distributed the number of samples in proportion of growing stock by tree species (Figures S1 and S2). The major tree species of Korea were selected and sampled. Red pine (*Pinus densiflora* Siebold & Zucc.), Oak (*Quercus* spp.), and Larch (*Larix kaempferi* (Lamb.) Carrière) were sampled from all over the country; Hinoki-cypress (*Chamaecyparis obtuse* (Siebold & Zucc.) Endl.), Japanese cedar (*Cryptomeria japonica* (Thunb. ex L. f.) D. Don), Black pine (*Pinus thunbergii* Parl.), and other species that are distributed locally, were collected from relevant regions. The carbon emission factors of the carbon pools (biomass, soil, and litter) in Korean forests were estimated from 226 sampling plots during the 2007–2015 period; each sampling plot had an area of 20 × 20 m. In total, 16 tree species were sampled, representing about 77% of the total growing stock in South Korean forests. We measured the height and diameter at breast height of selected sample trees from each plot. These trees were then divided into branches, leaves, twigs, and roots, after which their respective fresh weights were measured. From the 226 sampling plots, we additionally selected 119 plots to estimate soil and litter carbon stocks for eight tree species across South Korea. Litter samples included humus, fallen leaves, and twigs (smaller than 10 cm in

diameter) [18]. Soil pits were dug at each sampling plot, and soil was sampled at depths of 0–10, 10–20, 20–30, and 30–50 cm [18]. Biomass, litter, and soil samples were brought to the laboratory for further analysis.

The dry mass of biomass and litter samples was measured after oven-drying at 85 °C at a constant weight. Soil samples from depths of 0–10 cm, 10–20 cm, 20–30 cm, and 30–50 cm were passed through a 2-mm sieve to remove coarse fragments and roots. Soil bulk density was estimated as the proportion of the dry mass of all mineral soils to the volume of the corer, while the coarse fragments content was estimated as the ratio between the dry mass of coarse fragments to mineral soils, both of which were based on the mass remaining after oven-drying at 105 °C. The carbon concentrations of the litter and mineral soil were determined using an elemental analyzer (vario Macro, Elementar Analysensysteme GmbH, Langenselbold, Germany). Biomass emission factors such as basic wood density (WD), biomass expansion factors (BEF), and the root to shoot ratio (R) were calculated using the dry mass, fresh mass, and volume. The WD was calculated as the ratio of dry-weight to fresh volume using the water displacement method [18]. The BEF was calculated as the ratio of aboveground biomass (stem, branches, leaves, and twigs) to the stem biomass. The R was calculated as the ratio of root biomass to aboveground biomass [18]. Litter carbon stocks (C ton/ha) were calculated using the dry mass multiplied by carbon concentration, and mineral soil carbon stocks (C ton/ha) were calculated as the sum of each soil depth multiplied by bulk density, coarse fragments content, and carbon concentration [18]. However, the country-specific emission factors for deadwood carbon stocks were calculated as the volume of the residences and tree mortality from the NFI data, multiplied by carbon conversion factors from previous studies in South Korea [19,20]. Uncertainty analysis was calculated using the error propagation equation from the IPCC guidelines [3];

$$\text{Uncertainty} = \frac{0.5 \times (95\%CI \text{ width})}{\mu} \times 100 \tag{1}$$

where *CI width* is the width of the 95% confidence interval and μ is the mean value following the IPCC methodology [3]. Emission factors of other coniferous forest and other deciduous forest except for deadwood carbon stocks were calculated by weighted average using the growing stock proportions in South Korean forest.

2.2. Estimating Carbon Stocks in Biomass, Soil, and Dead Organic Matter

We adopted three different approaches for estimating carbon stocks. The first approach (IPCC_{EF}) was applied according to IPCC default emission factors, where it is assumed that soil and dead organic matter do not change with forest management, forest type, or disturbance regime. The second approach (CS_{FT}) was applied according to country-specific emission factors in regard to forest type, while the third approach (CS_{SP}) was applied according to country-specific emission factors for tree species (Table 1).

Table 1. Three approaches for carbon stock estimation.

| Resolution | Forest Type | | Species |
|------------|--------------------|------------------|------------------|
| Approach | IPCC _{EF} | CS _{FT} | CS _{SP} |
| Biomass | E | E | E |
| Litter | NE | E | E |
| Soil | NE | E | E |
| Deadwood | NE | E | E |

IPCC_{EF}: Intergovernmental Panel on Climate Change (IPCC) default emission factors, CS_{FT}: country-specific emission factors by forest type, CS_{SP}: country-specific emission factors by species, E: estimated, NE: not estimated.

In the case of IPCC_{EF} and CS_{FT}, forest areas and growing stocks were taken from national greenhouse gas inventory reports [5], after which the carbon stocks in above and belowground biomass,

soil, litter, and deadwood were calculated using IPCC default emission factors for coniferous species (WD: 0.49, BEF: 1.30, and R: 0.32), deciduous species (WD: 0.58, BEF: 1.40, and R: 0.26), and carbon fraction (0.50) [3], along with country-specific emission factors developed by this study. If there was no country-specific emission factor by tree species, we applied emission factors of other coniferous or deciduous forests by tree species.

On the other hand, NFI data was used for CS_{SP} because official statistics for the growing stocks of tree species do not currently exist. The NFI provides data on merchantable growing stocks and the number of points for each tree species, while data on whole-tree biomass is needed to estimate biomass carbon pools. Specifically, we used data from the 5th and 6th NFI, which were conducted between 2006–2010 and 2011–2015, respectively, and included a nationally consistent sampling frame and plot design (Figure 1). In reference to the 6th NFI, 149 plots were not resampled at the original plots from the 5th NFI; however, 430 new plots were established for sampling. In order to estimate the area of forest types and tree species, we used the proportions of the sub-points in the specific stand for each species, multiplied by the known land area:

$$A_h = A \times p_h, (\text{where}, p_h = \frac{n_h}{n}) \quad (2)$$

where A_h is the total area by tree species; A is the forest area on the basis of the official statistics of the Korea Forest Service (KFS) and Greenhouse Gas Inventory and Research Center of Korea (GIR) [5,21,22]; p_h is the proportion of points that are of h ; n is the number of total points for forest types; n_h is the number of points for h ; and h is the tree species. The area of mixed forest was divided into ‘other coniferous’ and ‘other deciduous’ forests. The total growing stocks of each species was calculated using the growing stocks per ha and the species area, while the total growing stock was stratified by random sampling of each species.

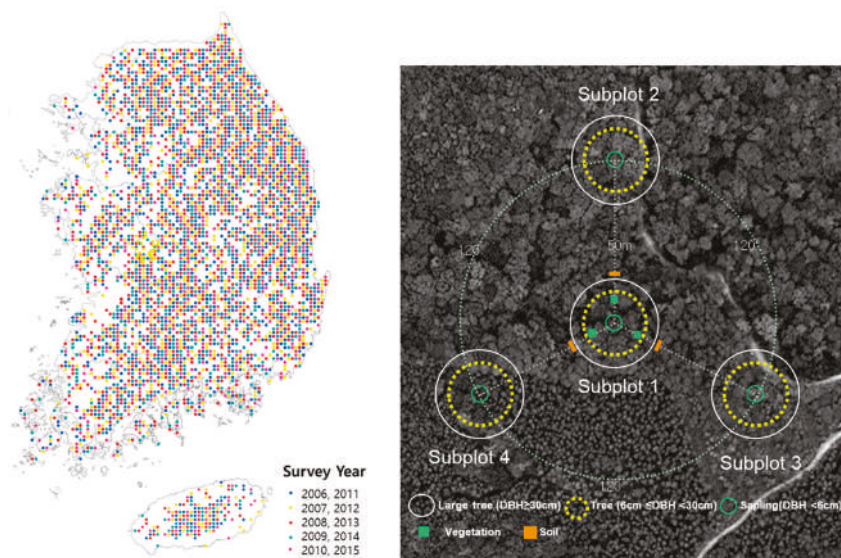


Figure 1. Permanent sample plots in the South Korean National Forest Inventory (NFI).

Total carbon stocks in biomass were calculated using area, growing stocks, biomass expansion factors, basic wood density, and the root to shoot ratio; total carbon stocks in soil and dead organic matter were calculated as the area multiplied by their carbon stocks (C ton/ha) developed by this study [3]. Annual changes in biomass, soil, and dead organic matter were estimated using the IPCC

stock changes method [3]. Specifically, the IPCC stipulates that the activity data for soil and dead organic matter have a transition period of 20 years [3]; in other words, the forest area for estimated carbon stocks should remain constant over a 20-year period. As the forest area in our study has decreased since 1970, we assumed that the forest area in the base year was equal to that of 20 years ago. Uncertainty was calculated using the error propagation equation in accordance with IPCC guidelines [3]. The uncertainty in tree growing stocks from official statistics assumes 0.05% from the previous study, while the uncertainty in IPCC default values is assumed to be 50% [3,11]. All statistical analyses were conducted using the proc GLM procedures of the SAS 9.4 software. And Tukey's HSD test was used to identify the significantly different means ($p < 0.05$).

3. Results

3.1. Estimation of Country-Specific Emission Factors

Emission factors for each carbon pool are shown in Tables 2 and 3. The biomass, calculated as basic wood density (WD, expressed in t dry matter/m³), ranged from 0.35 to 0.50 for coniferous species and from 0.46 to 0.83 for deciduous species. Deciduous species generally had higher basic wood density than coniferous species (Table 2). Basic wood density was highest for *Q. acuta*, a deciduous species, and lowest for *C. japonica*, a coniferous species (Table 2). Biomass expansion factors (BEF) ranged from 1.31 to 1.74 for coniferous species, and from 1.24 to 1.70 for deciduous species. The root to shoot ratio (R) ranged from 0.20 to 0.36 for coniferous species and from 0.19 to 0.48 for deciduous species (Table 2).

Coniferous species generally had higher litter carbon stocks than deciduous species ($P < 0.05$), while mineral soil carbon stocks were lower in coniferous forest than in deciduous forest ($P > 0.05$; Table 3). However, there was no difference in deadwood carbon stocks between coniferous forest and deciduous forest (Table 3).

Uncertainty in emission factors for biomass ranged from 2% to 12% for WD, 4% to 16% for BEF, and 6% to 33% for R, respectively. Uncertainty for carbon stocks in soil, litter, and deadwood ranged from 27% to 41%, 16% to 27%, and 8% to 1211%, respectively. Soil and dead organic matter had higher uncertainties than biomass; in particular, the uncertainty in deadwood had a large variation owing to lack of NFI sampling points for some tree species.

Table 2. Country-specific emission factors for biomass by tree species.

| Forest Type | Species | WD (t dry matter/m ³) | BEF | R |
|-------------------|-----------------------------------|--------------------------------------|----------------------------|----------------------------|
| Coniferous forest | <i>Chamaecyparis obtusa</i> | 0.43 (4%) ^{fg} | 1.35 (9%) ^{cd} | 0.20 (33%) ^e |
| | <i>Cryptomeria japonica</i> | 0.35 (4%) ^h | 1.31 (6%) ^{cd} | 0.23 (12%) ^{de} |
| | <i>Larix kaempferi</i> | 0.45 (6%) ^{efg} | 1.34 (8%) ^{cd} | 0.29 (15%) ^{bcde} |
| | <i>Pinus densiflora</i> (Gangwon) | 0.42 (12%) ^{fg} | 1.48 (12%) ^{abcd} | 0.26 (14%) ^{cde} |
| | <i>P. densiflora</i> (Jungbu) | 0.47 (4%) ^{efg} | 1.41 (6%) ^{bcd} | 0.25 (6%) ^{cde} |
| | <i>P. koraiensis</i> | 0.41 (6%) ^{hg} | 1.74 (13%) ^a | 0.28 (14%) ^{cde} |
| | <i>P. rigida</i> | 0.50 (4%) ^{de} | 1.33 (12%) ^{cd} | 0.36 (29%) ^{bcd} |
| | <i>P. thunbergii</i> | 0.48 (6%) ^{ef} | 1.52 (13%) ^{abcd} | 0.29 (19%) ^{bcde} |
| | Other coniferous forest | 0.46 (6%) | 1.43 (8%) | 0.27 (13%) |
| Deciduous forest | <i>Betula platyphylla</i> | 0.55 (4%) ^d | 1.30 (6%) ^{cd} | 0.29 (16%) ^{bcde} |
| | <i>Liriodendron tulipifera</i> | 0.46 (10%) ^{efg} | 1.24 (6%) ^d | 0.23 (27%) ^{de} |
| | <i>Quercus acuta</i> | 0.83 (5%) ^a | 1.70 (16%) ^{ab} | 0.19 (20%) ^e |
| | <i>Q. acutissima</i> | 0.72 (6%) ^b | 1.45 (6%) ^{abcd} | 0.31 (26%) ^{bcde} |
| | <i>Q. mongolica</i> | 0.66 (3%) ^{bc} | 1.60 (8%) ^{abc} | 0.39 (23%) ^{abc} |
| | <i>Q. serrata</i> | 0.66 (5%) ^{bc} | 1.55 (8%) ^{abcd} | 0.43 (21%) ^{ab} |
| | <i>Q. variabilis</i> | 0.72 (2%) ^b | 1.34 (4%) ^{cd} | 0.32 (15%) ^{bcde} |
| | <i>Robinia pseudoacacia</i> | 0.64 (11%) ^c | 1.47 (8%) ^{abcd} | 0.48 (17%) ^a |
| | Other deciduous forest | 0.68 (3%) | 1.51 (7%) | 0.36 (20%) |

WD: basic woody density, BEF: Biomass expansion factor, R: root to shoot ratio. Values with different letters indicate significant differences among tree species at $p < 0.05$ and with those in parenthesis representing uncertainty (%).

Table 3. Carbon stocks in soil and dead organic matter

| Forest Type | Species | Litter (C ton/ha) | Soil (C ton/ha) | Deadwood (C ton/ha) | |
|-------------------|--------------------------------------|--------------------------|--------------------|------------------------|-------------|
| | | | | 5th NFI | 6th NFI |
| Coniferous forest | <i>Chamaecyparis obtusa</i> | - | - | 1.59 (108%) | 3.26 (156%) |
| | <i>Cryptomeria japonica</i> | - | - | 4.37 (90%) | 3.50 (179%) |
| | <i>Larix kaempferi</i> | 7.01 (27%) ^{ab} | 46.71 (36%) | 2.98 (25%) | 2.63 (32%) |
| | <i>Pinus densiflora</i> (Gangwon) | 9.03 (16%) ^{ab} | 53.16 (41%) | 1.97 (20%) | 2.46 (28%) |
| | <i>P. densiflora</i> (Jungbu) | 11.85 (27%) ^a | 37.83 (28%) | 1.82 (14%) | 1.98 (12%) |
| | <i>P. koraiensis</i> | 7.36 (26%) ^{ab} | 37.77 (29%) | 2.78 (31%) | 1.51 (57%) |
| | <i>P. rigida</i> | 7.95 (25%) ^{ab} | 36.35 (40%) | 1.99 (24%) | 3.73 (37%) |
| | <i>P. thunbergii</i> | - | - | 2.18 (28%) | 1.94 (38%) |
| | Other coniferous forest | 11.25 (25%) | 38.75 (32%) | 2.11 (38%) | 1.90 (55%) |
| Deciduous forest | <i>Betula platyphylla</i> | - | - | 1.11 (290%) | 0.71 |
| | <i>Liriodendron tulipifera</i> | - | - | - | 0.13 |
| | <i>Quercus acuta</i> | - | - | 6.49 (1211%) | 0.19 |
| | <i>Q. acutissima</i> | 5.07 (19%) ^b | 64.30 (27%) | 1.55 (33%) | 1.27 (38%) |
| | <i>Q. mongolica</i> | 7.30 (20%) ^{ab} | 64.02 (34%) | 1.55 (15%) | 2.48 (21%) |
| | <i>Q. serrata</i> | - | - | 0.76 (41%) | 1.83 (37%) |
| | <i>Q. variabilis</i> | 6.49 (20%) ^{ab} | 57.09 (35%) | 1.43 (21%) | 1.56 (19%) |
| | <i>Robinia pseudoacacia</i> | - | - | 2.14 (50%) | 2.42 (37%) |
| | Other deciduous forest | 6.63 (20%) | 55.68 (33%) | 1.60 (11%) | 2.20 (8%) |

Values with different letters indicate significant differences among tree species at $p < 0.05$ with those in parenthesis representing uncertainty (%).

3.2. Estimation of Forest Area and Growing Stock by Tree Species

The estimated forest areas and growing stocks from the 5th NFI and 6th NFI are shown in Table 3. The estimated forest areas (1000 ha) in 2010 were 2581 for coniferous forest, 1865 mixed forest, and 1719 for deciduous forest; the estimated forest areas (1000 ha) for 2015 were 2339 for coniferous forest, 1706 for mixed forest, and 2029 for deciduous forest. Coniferous and mixed forests were converted to deciduous forest, with conversion rates of 9.36% and 8.53%, respectively. The conversion rate of forest area comprised of coniferous species was highest for *P. rigida*, followed by *P. densiflora* (Gangwon), and *L. kaempferi* (Table 3). The growing stock showed increases for all forest types, despite the reduction in forest area over the last five years. The estimated growing stock increased from 832 to 970 M m³ during the research period (2010–2015), while according to official statistics, South Korean forests increased from 800 to 925 M m³ during the same period (Table 4). The change in growing stock ranged from −6 M m³ (*P. rigida*) to 15 M m³ (*P. densiflora* [Jungbu]) for coniferous species, and from 0.07 M m³ (*Q. acuta*) to 62 M m³ (other deciduous forest) for deciduous species (Table 4).

Table 4. Estimated areas and growing stocks by tree species.

| Forest Type | Species | Area (1000 ha) | | Growing Stock (1000 m ³) | |
|-------------------|--------------------------------------|----------------|--------------|--------------------------------------|----------------|
| | | 2010 | 2015 | 2010 | 2015 |
| Coniferous forest | <i>Chamaecyparis obtusa</i> | 19 (0.2%) | 25 (0.3%) | 2377 ± 320 | 3898 ± 433 |
| | <i>Cryptomeria japonica</i> | 14 (0.2%) | 14 (0.2%) | 3680 ± 346 | 4850 ± 367 |
| | <i>Larix kaempferi</i> | 200 (2.5%) | 173 (2.1%) | 38,062 ± 1036 | 41,528 ± 1075 |
| | <i>Pinus densiflora</i> (Gangwon) | 363 (4.5%) | 312 (3.9%) | 62,836 ± 1244 | 62,316 ± 1271 |
| | <i>P. densiflora</i> (Jungbu) | 1315 (4.5%) | 1176 (14.5%) | 199,213 ± 2261 | 213,985 ± 2363 |
| | <i>P. koraiensis</i> | 126 (16.3%) | 116 (1.4%) | 16,844 ± 727 | 20,835 ± 841 |
| | <i>P. rigida</i> | 267 (1.6%) | 200 (2.5%) | 41,126 ± 1009 | 34,642 ± 946 |
| | <i>P. thunbergii</i> | 173 (3.3%) | 177 (2.2%) | 20,083 ± 870 | 25,959 ± 1072 |
| | Other coniferous forest | 104 (2.2%) | 146 (1.8%) | 12,649 ± 679 | 19,425 ± 958 |

Table 4. Cont.

| Forest Type | Species | Area (1000 ha) | | Growing Stock (1000 m ³) | |
|------------------|--------------------------------|----------------|--------------|--------------------------------------|----------------|
| | | 2010 | 2015 | 2010 | 2015 |
| Mixed forest | | 1865 (28.9%) | 1706 (29.1%) | 246,042 ± 2033 | 274,331 ± 2064 |
| Deciduous forest | <i>Betula platyphylla</i> | 6 (0.1%) | 6 (0.1%) | 160 ± 18 | 348 ± 34 |
| | <i>Liriodendron tulipifera</i> | - | 1 (0.0%) | - | 82 ± 32 |
| | <i>Quercus acuta</i> | 1 (0.0%) | 1 (0.0%) | 177 ± 27 | 244 ± 18 |
| | <i>Q. acutissima</i> | 66 (1.5%) | 78 (1.6%) | 6301 ± 281 | 9544 ± 346 |
| | <i>Q. mongolica</i> | 472 (10.7%) | 415 (8.6%) | 62,721 ± 698 | 64,431 ± 714 |
| | <i>Q. serrata</i> | 31 (0.7%) | 38 (0.8%) | 3248 ± 207 | 4783 ± 259 |
| | <i>Q. variabilis</i> | 221 (5.0%) | 235 (4.9%) | 32,085 ± 602 | 40,607 ± 685 |
| | <i>Robinia pseudoacacia</i> | 58 (1.3%) | 59 (1.2%) | 5306 ± 233 | 7254 ± 299 |
| | Other deciduous forest | 865 (19.6%) | 1196 (24.8%) | 78,913 ± 960 | 141,146 ± 1363 |
| Total | | 6165 (100%) | 6074 (100%) | 831,821 ± 3463 | 970,210 ± 3473 |

Values indicate the mean and standard error of stratified random sampling.

3.3. Estimation of Carbon Stocks and Their Changes in Biomass, Litter, Deadwood, and Soil

The estimated carbon stocks and their changes from 2010 to 2015 are shown in Figure 2. Applying IPCC default emission factors (IPCC_{EF}) demonstrated that carbon stocks increased by 57,363 Gg C (15.99%) from 2010 to 2015, with an increase of 15.55% in deciduous forests and 15.11% in coniferous forests (Figure 2). Our estimation of CO₂ removal was 42,067 Gg CO₂ per year, with an uncertainty of 35%. Furthermore, in applying IPCC default emission factors, we assumed that the soil and dead organic matter did not change [3]. Applying country-specific emission factors by forest type (CS_{FT}), total carbon stocks increased by 66,569 Gg C (8.47%) from 2010 to 2015, with increases of 15.48%, 0.13%, and 9.32% for biomass, soil, and deadwood, respectively, and a decrease of 3.65% for litter. Additionally, the estimation of CO₂ removal was 48,817 Gg CO₂ per year with an uncertainty of 17% (Figure 3); this CO₂ removal value was about 1.16 times that of IPCC_{EF}, which only estimates biomass using the IPCC default emission factors.

In terms of country-specific emission factors by tree species (CS_{SP}), total carbon stocks were increased by 82,702 Gg C (10.41%) from 2010 to 2015 (Figure 2). The carbon pools in biomass and dead wood increased by 19.20% and 14.67%, respectively, while those in litter and soil decreased by 3.17% and 0.21%, respectively. These results indicated a higher total carbon stock than CS_{FT}, despite the reduction of carbon stocks in litter and soil with CS_{SP}. The total carbon stocks of the tree species increased, with the exception of *P. densiflora* (Gangwon), *P. densiflora* (Jungbu), *P. rigida*, and *L. kaempferi* in coniferous forests, and *Q. mongolica* in deciduous forests. The CO₂ removal for CS_{SP} was 60,648 Gg CO₂, with an uncertainty of 22% (Figure 3). Estimated by species (CS_{SP}), CO₂ removal value was about 1.24 times greater than that estimated by forest type (CS_{FT}).

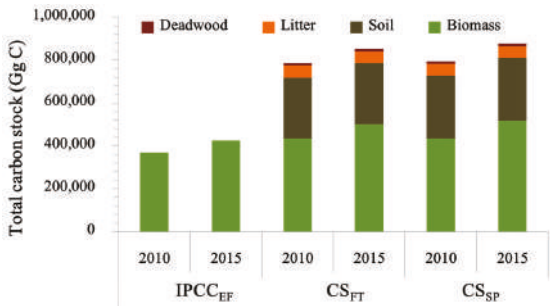


Figure 2. Total carbon stock in each approach. IPCC_{EF}: Intergovernmental Panel on Climate Change (IPCC) default emission factors, CS_{FT}: country-specific emission factors by forest type, CS_{SP}: country-specific emission factors by species.

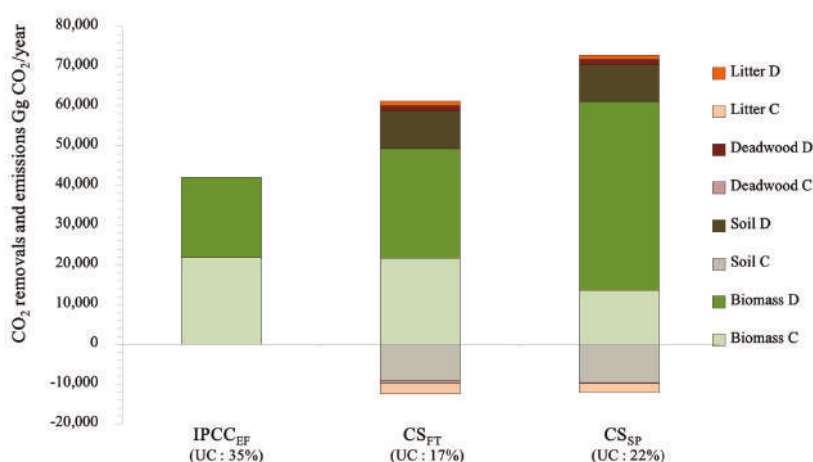


Figure 3. CO₂ removals (+) and emissions (−), and their uncertainty (UC) in each approach. C: coniferous forest, D: deciduous forest, IPCC_{EF}: Intergovernmental Panel on Climate Change (IPCC) default emission factors, CS_{FT}: country-specific emission factors by forest type, CS_{Sp}: country-specific emission factors by species.

4. Discussion

4.1. Development and Implications of Country-Specific Emission Factors

Using country-specific emission factors can complement other methods of national greenhouse gas inventory reporting and thereby offer improved accuracy. The IPCC [3] report a basic wood density (D) that ranges from 0.31 to 0.49 for coniferous species and 0.35 to 0.58 for deciduous species; however, our results yielded a basic wood density for deciduous forest that ranged from 0.46 to 0.83. Similarly, Kim et al. [23] found that the basic wood density of deciduous species ranged from 0.58 to 0.88 in Korean forests. Past studies have consistently found that basic wood density is higher in deciduous forests than in coniferous forests [3,23,24]. In the IPCC guidelines, the BEF ranges from 1.15 to 4.2 for coniferous species and from 1.15 to 3.2 for deciduous species in temperate regions. Although the IPCC and some other studies have found that BEF can depend on stand age and structure [3,24–26], we did not consider stand age in this study because other researchers have reported that BEF is not dependent upon stand age, but instead reflects stand density, which affects crown density [27,28]. Our results for R were also similar to those from previous studies at global and regional scales [3,23,28]. Additionally, the IPCC [3] report R ranges of 0.23–0.46 for coniferous species and 0.24–0.45 for deciduous species.

The IPCC guidelines do not stipulate default values in regard to the carbon stock of soil and dead organic matter, which do not change in the Tier 1 method; therefore, comparison with our results was not possible. The litter carbon stock was similar to the ranges indicated by previous studies focused on Korean forests; for example, Kim et al. [29] reported that the litter carbon stock (Mg C/ha) in Korean forests ranges from 6.7 to 8.5 for pine forests, 4.6 to 5.0 for oak forests, and 6.5 to 7.0 for larch forests [29]. Other studies have reported litter carbon stocks of 7.2 for coniferous forests and 4.8 for deciduous forests at the national scale [11], as litter carbon stocks are generally given to be higher for coniferous species than for deciduous species [11,29]. Furthermore, the literature shows that litter carbon stock is influenced by the varying composition and decomposition rates of different species [30,31]. Our study showed that litter carbon stock was highest for *P. densiflora* (Jungbu) in coniferous species. Moreover, we found that there was a large degree of variation between forests in terms of soil and deadwood carbon stocks. Another study focusing on *L. kaempferi* reported that carbon stocks (t C/ha) ranged from 45.43 to 165.48 in soil and from 0.1 to 3.4 in deadwood [32]; another study reported that soil carbon stocks were 83.2 t C/ha in deciduous forests and 59.1 t C/ha in coniferous

forests at the national scale [11]. Although there was a large degree of variation in the carbon stock values for soil and dead organic matter, our results are nevertheless within the range of results from previous studies. Furthermore, our results have been verified by GIR for the period 2013 to 2017, except for carbon stocks in deadwood, and this implies that the results are appropriate for use as country-specific emission factors in South Korea.

Most of the uncertainty levels for the emission factors of each carbon pool, except for deadwood, were estimated to be in the range of 10 to 40%, which is consistent with findings from previous studies [3,33]. The uncertainty levels for the deadwood were high in *Q. acuta* due to small sampling plots from NFI as *Q. acuta* occupied a small area in South Korea. In the EU, most countries use emission factors constructed from country-specific studies, although other countries continue to apply international studies or IPCC default emission factors. This trend is promising, as country-specific studies lead to more accurate estimations of carbon stocks in comparison with the use of IPCC default emission factors [34]. Additionally, it is difficult to estimate uncertainty when using IPCC default emission factors, due to the lack of statistical information. However, if country-specific emission factors are used, the uncertainty surrounding emission factors can be estimated. Therefore, it is considered good practice that countries use country-specific emission factors for national greenhouse gas inventory reporting [3].

4.2. Carbon Stocks and Their Changes for Use in National Greenhouse Gas Inventory Reporting

In this study, we estimated the carbon stocks in biomass, soil, litter, and deadwood for use in national greenhouse gas inventory reporting. The removal amount (expressed in Gg CO₂) varied from 42,067 to 60,648 per year, depending upon which of the three approaches was used. These results—specifically the increase of total carbon stocks in biomass and deadwood, which accounted for more than 50% of forest carbon storage—have shown that South Korean forests have stored carbon and absorbed CO₂. According to the NFI survey period, the age class was found to have increased [35], which would have affected the carbon stocks of biomass and deadwood, consistent with findings from studies based on forests in China and the US [36,37]. Large stocks of woody debris commonly occur in mature forests that have a large amount of living biomass [38]. However, forest age is also expected to affect the amount of woody debris at the local scale, and often a greater amount of woody debris is found in young growth stands than in other stands [39].

The CO₂ removal based on the CS_{FT} was about 1.16 times higher than that based on the IPCC_{EF}. The application of country-specific emission factors would reflect national circumstances [2] and improve accuracy over IPCC default emission factors, despite differences in previously reported CO₂ removal rates (48,507 Gg CO₂ per year) for forests [5]. These differences are due to the estimate of all carbon pools when estimating carbon stocks in Korean forests. We estimated soil and dead organic matter using the country-specific emission factors and NFI data as a way to improve the completeness of the national greenhouse gas inventory system for the forest sector. In terms of methodology, this difference might be due to using three year moving average data [2,3,5] in contrast to this study, which used single year data.

The application of country-specific emission factors for each species (CS_{SP}) yielded different results from the application of country-specific emission factors for forest type (CS_{FT}). These differences were reflected in changes of area for each species and differences in their carbon stocks from NFI data. In particular, the total growing stock for *P. rigida* has decreased during last five years, consistent with reporting that area of *P. rigida* has decreased owing to age [40]. The species also has high biomass emission factors, which would have an effect on the overall amount of CO₂ removal (Table 2).

According to the IPCC, the CS_{FT} and CS_{SP} approaches represent higher-level inventory reporting systems than the IPCC_{EF}, which lacks the accuracy and completeness of CS_{FT} and CS_{SP}. The CS_{FT} estimate reflects a simple difference between two forest types, whereas the CS_{SP} is based on several consecutive change estimates from permanent plots by species. The use of CS_{SP} would improve accuracy in regard to growing stock, as in the case of Finland [9]. Most EU countries could use their

NFIs, which provide information on aboveground biomass [34]. Aboveground biomass is derived from growing stock, which is collected by NFIs. Additionally, other carbon pools may also be based on the data collected in NFIs.

The CS approach has lower uncertainty than does the IPCC approach. While the CS_{SP} approach has higher uncertainty than does the CS_{FT} approach, the uncertainty is in regard to precision rather than accuracy [3,41]. The total uncertainty of net CO₂ removal was high owing to the high uncertainty of soil and dead organic matter despite the low uncertainty in biomass. The CS_{SP}, which appears to be a more complementary and accurate estimation method, includes the estimation of carbon stock changes by tree species. With increasing coverage of the inventory, there is increasing accuracy in terms of the estimated total greenhouse gas emissions, even though the precision of estimated net emissions might decrease [41].

In order to achieve accuracy and completeness, Annex I countries should also report CO₂ removals and emissions for all carbon pools using country-specific emission factors and models [9,42]. The results of this study are applicable to the improvement of greenhouse gas inventory systems in regard to domestic forests; furthermore, they provide information in regard to greenhouse gas inventory methodology to countries that do not yet have country-specific emission factors. However, it is also necessary to review the Tier 3-level reporting detailed in the UNFCCC report. In addition, an annual land-use change matrix should be established to improve the accounting of changes in carbon stocks for national greenhouse gas inventory systems.

5. Conclusions

The purpose of this study was to examine the methodology for enhancing the completeness and accuracy of national greenhouse gas inventory reporting using Korean forest survey data. The application of country-specific emission factors gave an estimated CO₂ removal value that was 1.2 times greater than for the IPCC default emission factors. In order to improve completeness and accuracy, we estimated CO₂ absorption by all carbon pools and each tree species, which gave a result of 60,648 Gg CO₂ per year with 22% uncertainty. Despite the reduction in total forest area, forests still store carbon and absorb CO₂ owing to differences in the carbon storage capacities of several species. Our results will aid in the development of South Korea's greenhouse gas inventory systems—or those of countries without country-specific emission factors—by improving the calculation of carbon stocks and CO₂ removal by species. However, it would be necessary to construct a land use change matrix, after which our study would be useful for the implementation of Tier 2-level national greenhouse gas inventory systems, as recommended by the IPCC.

Supplementary Materials: The following are available online at <http://www.mdpi.com/1999-4907/9/10/625/s1>, Figure S1: Location of studied sites for emission factor in biomass, soil, and litter by coniferous species; Figure S2: Location of studied sites for emission factor in biomass, soil, and litter by deciduous species.

Author Contributions: S.J.L., Y.M.S., Y.S., and R.K. conceived and designed the study; S.J.L., J.S.Y., and R.K. analyzed the data; S.J.L. and R.K. wrote the paper.

Funding: This research was funded by Korea Forest Service (Korea Forestry Promotion Institute), grant number (2017044C10-1819-BB01).

Acknowledgments: This study was carried out with support from the R&D Program for Forest Science Technology (Project No. 2017044C10-1819-BB01) provided by the Korea Forest Service (Korea Forestry Promotion Institute).

Conflicts of Interest: The authors declare no conflict of interest.

References

1. UNFCCC. The Paris Agreement. 2015. Available online: <https://unfccc.int/process-and-meetings/the-paris-agreement/the-paris-agreement> (accessed on 28 September 2018).
2. IPCC. *IPCC Guidelines for National Greenhouse Gas Inventory*; IPCC/IGES: Hayama, Japan, 2006.
3. IPCC. *Good Practice Guidance for Land Use, Land-Use Change and Forestry*; IPCC/IGES: Hayama, Japan, 2003.

4. FAO (Food and Agriculture organization). *Estimating Greenhouse Gas Emissions in Agriculture*; FAO: Rome, Italy, 2015.
5. GIR (Greenhouse Gas Inventory and Research Center of Korea). *National Greenhouse Gas Inventory Report 2017*; GIR: Seoul, Korea, 2017.
6. Pan, Y.; Birdsey, R.A.; Fang, J.; Houghton, R.; Kauppi, P.E.; Kurz, W.A.; Phillips, O.L.; Shvidenko, A.; Lewis, S.L.; Canadell, J.G.; et al. A large and persistent carbon sink in the world's forests. *Science* **2011**, *333*, 988–993. [CrossRef] [PubMed]
7. UNFCCC. COP 15 2009. Available online: https://unfccc.int/meetings/copenhagen_dec_2009/session/6262/php/view/decisions.php (accessed on 28 September 2018).
8. Baritz, R.; Strich, S. Forests and the national greenhouse gas inventory of Germany. *Biotechnol. Agron. Soc. Environ.* **2000**, *4*, 265–271.
9. Statistics Finland. *Greenhouse Gas Emissions in Finland 1990~2013*; Statistics Finland: Helsinki, Finland, 2015.
10. Federal Environment Agency. *Submission under the United Nations Framework Convention on Climate Change and the Kyoto Protocol 2015*; Federal Environment Agency: Dessau, Germany, 2015.
11. KFS (Korea Forest Service); Kofpi (Korea Forestry Promotion Institute). *Assessment of the Korea's Forest Resource*; Kofpi: Seoul, Korea, 2013.
12. Lee, J.; Yoon, T.K.; Han, S.; Kim, S.; Yi, M.J.; Park, G.S.; Kim, C.; Son, Y.M.; Kim, R.; Son, Y. Estimating the carbon dynamics of South Korean forests from 1954 to 2012. *Biogeoscience* **2014**, *11*, 4637–4650. [CrossRef]
13. Son, Y.M.; Kim, R.H.; Kang, J.T.; Lee, K.S.; Kim, S.W. A practical application and development of carbon emission factors. *J. Korean For. Soc.* **2014**, *103*, 593–598. [CrossRef]
14. Son, Y.M.; Kim, R.H.; Lee, K.H.; Pyo, J.K.; Kim, S.W.; Hwang, J.S.; Lee, S.J.; Park, H. *Carbon Emission Factors and Biomass Allometric Equations by Species in Korea*; KFRI: Seoul, Korea, 2014.
15. Lee, S.J.; Yim, J.S.; Kang, J.T.; Kim, R.; Son, Y.; Park, G.W.; Son, Y.M. Application and development of carbon emissions factors for deciduous species in Republic of Korea—*Robinia pseudoacacia*, *Betula platyphylla*, and *Liriodendron tulipifera*. *J. Clim. Chang. Res.* **2017**, *8*, 393–399. [CrossRef]
16. Pyo, J.K.; Son, Y.M.; Lee, K.H.; Kim, R.H.; Kim, Y.H.; Lee, Y.J. Estimating the uncertainty and validation of basic wood density for *Pinus densiflora* in Korea. *J. Korean For. Soc.* **2010**, *99*, 929–933.
17. Pyo, J.K.; Son, Y.M.; Jang, G.M.; Lee, Y.J. Uncertainty assessment of emission factors for *Pinus densiflora* using Monte Carlo simulation technique. *J. Korean For. Soc.* **2013**, *102*, 477–483. [CrossRef]
18. KFRI (Korea Forest Research Institute). *Survey Manual for Biomass and Soil Carbon*; KFRI: Seoul, Korea, 2010.
19. Yoon, T.K.; Chung, H.; Kim, R.H.; Noh, N.J.; Seo, K.W.; Lee, S.K.; Jo, W.; Son, Y. Coarse woody debris mass dynamics in temperate natural forests of Mt. Jumbong, Korea. *J. Ecol. Field Biol.* **2011**, *34*, 115–125. [CrossRef]
20. KFS (Korea Forest Service). *Improvement of Forest Carbon Accounting System for Post 2020 Climate Change Regime*; KFS: Daejeon, Korea, 2016.
21. KFS (Korea Forest Service). *Statistical Yearbook of Forest*; KFS: Daejeon, Korea, 2016.
22. KFS (Korea Forest Service). *Statistical Yearbook of Forest*; KFS: Daejeon, Korea, 2011.
23. Kim, H.; Kim, H.J.; Lee, K.H.; Son, Y.M.; Lee, K.S.; Lee, S.H. Biomass conversion factors for tree species and verification of applicability for national factors in Korea. *J. Korean Soc. Appl. Biol. Chem.* **2011**, *54*, 758–762. [CrossRef]
24. Lehtonen, A.; Mäkipää, R.; Heikkinen, J.; Sievänen, R.; Liski, J. Biomass expansion factor (BEFs) for Scots pine, Norway spruce and birch according to stand age for boreal forests. *For. Ecol. Manag.* **2004**, *188*, 211–224. [CrossRef]
25. Van Camp, N.; Walle, I.V.; Mertens, J.; De Neve, S.; Samson, R.; Lust, N.; Lemeur, R.; Boeckx, P.; Lootens, P.; Beheydt, D.; et al. Inventory-based carbon stock of Flemish forests: A comparison of European biomass expansion factors. *Ann. For. Sci.* **2004**, *61*, 677–682. [CrossRef]
26. Seo, Y.O.; Lee, Y.J.; Pyo, J.K.; Kim, R.; Son, Y.M.; Lee, K.H. Uncertainty analysis of stem density and biomass expansion factor for *Pinus rigida* in Korea. *J. Korean For. Soc.* **2011**, *100*, 149–153.
27. Kim, C.; Lee, K.S.; Son, Y.M.; Cho, H.S. Allometric equations and biomass expansion factors in and age-sequence of black pine (*Pinus thunbergii*) stands. *J. Korean For. Soc.* **2013**, *102*, 543–549. [CrossRef]
28. Noh, N.J.; Son, Y.; Kim, J.S.; Kim, R.; Seo, K.Y.; Seo, K.W.; Koo, J.W.; Kyung, J.H.; Park, I.H.; Lee, Y.J.; et al. A study on estimation of biomass, stem density and biomass expansion factor for stand age class of Japanese larch (*Larix leptolepis*) stands in Gapyeong area. *J. Korean For. Environ.* **2006**, *25*, 1–8.

29. Kim, S.; Kim, C.; Han, S.H.; Lee, S.T.; Son, Y. A multi-site approach toward assessing the effect of thinning on soil carbon contents across temperature pine, oak, and larch forests. *For. Ecol. Manag.* **2018**, *424*, 62–70. [\[CrossRef\]](#)
30. Berg, B. Litter decomposition and organic matter turn-over in northern forest soils. *For. Ecol. Manag.* **2000**, *133*, 13–22. [\[CrossRef\]](#)
31. Schulp, C.J.E.; Nabuurs, G.; Verburg, P.H.; Waal, R.W. Effect of tree species on carbon stocks in forest floor and mineral soil and implication for soil carbon inventories. *For. Ecol. Manag.* **2008**, *256*, 482–490. [\[CrossRef\]](#)
32. Ko, S. *Influence of Thinning on Carbon Storage in Soil, Forest Floor and Coarse Woody Debris of Larix kaempferi Stands in Korea*; Korea University: Seoul, Korea, 2013.
33. FAO (Food and Agriculture organization). *Global Forest Resource Assessment 2005*; FAO: Rome, Italy, 2006.
34. Cienciala, E.; Tomppo, E.; Snorrason, A.; Broadmeadow, M.; Colin, A.; Dunger, K.; Exnerova, Z.; Lasserre, B.; Petersson, H.; Privitzer, T.; et al. Preparing emission reporting from forests: Use of national forest inventories in European countries. *Silva Fennica* **2007**, *42*, 73–88. [\[CrossRef\]](#)
35. KFS (Korea Forest Service); Kofpi (Korea Forestry Promotion Institute). *Assessment of the Korea's Forest Resources*; Kofpi: Seoul, Korea, 2017.
36. Woodall, C.W.; Balters, B.F.; Oswalt, S.N.; Domke, G.M.; Toney, C.; Gray, A.N. Biomass and carbon attributes of downed woody materials in forests of the United States. *Forest. Ecol. Manag.* **2013**, *305*, 48–59. [\[CrossRef\]](#)
37. Zhu, J.; Hu, H.; Tao, S.; Chi, X.; Li, P.; Jiang, L.; Ji, C.; Zhu, J.; Tang, Z.; Pan, Y.; et al. Carbon stocks and changes of dead organic matter in China's forests. *Nat. Commun.* **2017**, *8*, 151. [\[CrossRef\]](#) [\[PubMed\]](#)
38. Smith, J.E.; Heath, L.S.; Skog, K.E.; Birdsey, R.A. *Methods of Calculating Forest Ecosystem and Harvested Carbon with Standard Estimates for Forests Types of the United State*; USDA: Newtown Square, PA, USA, 2006.
39. Coomes, D.A.; Allen, R.B. Effect of size, competition and altitude on tree growth. *J. Ecol.* **2007**, *95*, 1084–1097. [\[CrossRef\]](#)
40. Seo, Y.O.; Jung, S.C.; Lee, Y.J. Estimation of carbon storage for *Pinus rigida* stands in Muju. *Korean J. Environ. Ecol.* **2016**, *30*, 399–405. [\[CrossRef\]](#)
41. Monni, S.; Peltoniemi, M.; Palosuo, T.; Lehtonen, A.; Mäkipää, R.; Savolainen, I. Uncertainty of forest carbon stock changes—Implications to total uncertainty of GHG inventory of Finland. *Clim. Chang.* **2007**, *81*, 391–413. [\[CrossRef\]](#)
42. Swedish Environmental Protection Agency. *National Inventory Report 2015 Sweden*; Swedish Environmental Protection Agency: Stockholm, Sweden, 2015.



© 2018 by the authors. Licensee MDPI, Basel, Switzerland. This article is an open access article distributed under the terms and conditions of the Creative Commons Attribution (CC BY) license (<http://creativecommons.org/licenses/by/4.0/>).

MDPI
St. Alban-Anlage 66
4052 Basel
Switzerland
Tel. +41 61 683 77 34
Fax +41 61 302 89 18
www.mdpi.com

Forests Editorial Office
E-mail: forests@mdpi.com
www.mdpi.com/journal/forests



MDPI
St. Alban-Anlage 66
4052 Basel
Switzerland

Tel: +41 61 683 77 34
Fax: +41 61 302 89 18

www.mdpi.com



ISBN 978-3-03928-667-6